UNIVERSIDADE FEDERAL DO RIO GRANDE DO SUL
INSTITUTO DE CIÊNCIAS BÁSICAS DA SAÚDE
PROGRAMA DE PÓS-GRADUAÇÃO EM CIÊNCIAS BIOLÓGICAS: BIOQUÍMICA

Investigação do potencial terapêutico da doxazosina em modelos de gliomas *in vitro* e *in vivo*

MARIANA MAIER GAELZER

Porto Alegre
2017

UNIVERSIDADE FEDERAL DO RIO GRANDE DO SUL
INSTITUTO DE CIÊNCIAS BÁSICAS DA SAÚDE
PROGRAMA DE PÓS-GRADUAÇÃO EM CIÊNCIAS BIOLÓGICAS: BIOQUÍMICA

Investigação do potencial terapêutico da doxazosina em modelos de gliomas *in vitro* e *in vivo*

MARIANA MAIER GAELZER

Orientadora: Dra. Christianne G. Salbego

Tese apresentada ao curso de Pós-Graduação em Ciências Biológicas: Bioquímica da Universidade Federal do Rio Grande do sul, como requisito parcial à obtenção do grau de Doutor em Bioquímica.

Porto Alegre
2017

AGRADECIMENTOS

Agradeço a Deus, por ter me dado saúde, paciência e perseverança.

À minha orientadora, a Professora Dra. Christianne Salbego, obrigada pela oportunidade, pela liberdade intelectual, confiança e paciência. Agradeço-lhe não só pela orientação, mas pelo carinho e atenção durante esses anos.

Aos professores colaboradores: Professora Ana Battastini, Fabríco Simão, Leandra Campo, Guido Lenz, Ana Zeri, David Driemeier, Patrícia Setton, Vanina Usach, Cristiane Matté, obrigada pela oportunidade de aprender técnicas novas e pelos ensinamentos.

À Professora Dra. Fátima Guma, obrigada pelas colaborações em todos os trabalhos e por me proporcionar o aprendizado de novas técnicas.

Aos colegas de Laboratório, principalmente a Juliana Hoppe, obrigada pela convivência, ajuda e ensinamentos.

À Dra. Sílvia Resende, obrigada pela amizade e pelos ensinamentos de citometria.

À Doutoranda Bárbara P. Coelho e à minha bolsista, Alice Q. Hoffman, obrigada pela lealdade, intensa dedicação, esforço, pela doação, por saber me ouvir e, acima de tudo, pela amizade.

Às alunas Helena Flores e Mariana Santos, obrigada pela oportunidade de orientá-las e, assim, poder aprender também.

Aos funcionários, servidores e professores do Programa de Pós-Graduação em Ciências Biológicas: Bioquímica, obrigada por proporcionar-me um ambiente de trabalho adequado, através do qual pude concluir meus experimentos.

Por fim, agradeço a minha família por estarem sempre presentes, amo muito vocês!

SUMÁRIO

PARTE I

APRESENTAÇÃO..1

LISTA DE ABREVIATURAS..2

RESUMO...5

ABSTRACT..6

1. INTRODUÇÃO...7

1.1.Gliomas 8

1.2.Glioblastoma..10

1.2.1. Classificação (Glioblastomas – Análise Molecular)......................12

1.2.2 Origens do glioblastoma..15

1.3. Gliomas e Hipóxia...16

1.4. Gliomas e Mitocôndria...18

1.5. EGFR..20

1.6. Vias de sinalização alteradas em glioblastoma............................21

1.6.1. Via RTK/RAS e PI3K...22

1.6.1.1. Via da Ras...23

1.6.1.2. Via da PI3K..23

1.6.1.3. Via da p53..24

1.7. Apoptose..24

1.8. Diagnóstico e Terapêutica...25

1.9. Doxazosina...26

1.10. Fluorescência..28

1.11. Nanotecnologia aplicada a farmacologia.....................................29

2. OBJETIVOS 32

PARTE II

3. CAPÍTULO I

Artigo: Hypoxic and Reoxygenated Microenvironment: Stemness and Differentiation State in Glioblastoma…….…………………………………………………..…………….36

4. CAPÍTULO II

Artigo: Phosphatidylinositol 3-Kinase/Akt Pathway Inhibition by Doxazosin Promotes Glioblastoma Cells Death, Upregulation of p53 and Triggers Low Neurotoxicity………...49

5. CAPÍTULO III

Artigo: Mitochondrial biogenesis and apoptosis: doxazosin's targets in glioma…………68

6. CAPÍTULO IV

Artigo: Doxazosin's real-time autofluorescence on glioma cells: uptake, distribution and pathophysiological response………………………………………..………………...95

7. CAPÍTULO V

Artigo: Doxazosin targets EGFR and pretreatment with EGF potentiates the drug's antiglioma effects…………...……………………………………………………….…127

8. CAPÍTULO VI

Artigo: Doxazosin-loaded nanocapsules: possible *in vivo* and *in vitro* antiglioma agent……………………………………………………………………………………153

PARTE III

9. DISCUSSÃO……………………………………………………….……………188
10. CONCLUSÕES…………………………………………………………………200
11. PERSPECTIVAS………………………………………………………………203
12. REFERÊNCIAS BIBLIOGRÁFICAS……………………………….…………..205
13. ANEXO I
Lista de Figuras...220
14. ANEXO II
Normas de formatação de artigos da revista Oncotarget...222

APRESENTAÇÃO

Esta tese está organizada em seções dispostas da seguinte maneira: *Introdução*, *Objetivos*, *Capítulos* (I, II, III, IV, V e VI – referentes a artigos científicos), *Discussão*, *Conclusões*, *Perspectivas* e *Referências Bibliográficas*.

A seção *Introdução* apresenta o embasamento teórico que levou à formulação das propostas da Tese, as quais estão descritas na seção *Objetivos*.

A seção *Capítulos* contém os artigos científicos publicadas, submetidos ou em fase de preparação para submissão, os quais estão apresentados de acordo com os objetivos específicos. Esta seção também apresenta os materiais e métodos e as referências bibliográficas específicas de cada artigo e está dividida em *Capítulos I*, *II*, *III*, *IV*, *V* e *VI*. Os *Capítulos I a VI* foram realizados no Laboratório de Neuroproteção e Sinalização Celular – Departamento de Bioquímica (UFRGS), coordenado pela Profa. Dra. Christianne Gazzana Salbego; nos *Capítulos I*, *II* e *III* houve colaboração com o Departamento de Química Biológica da Universidade de Buenos Aires (UBA, Argentina), através da Profa. Dra. Patricia Setton-Avruj; no *Capítulo II* houve colaboração com o grupo do Prof. Dr. Carlos Alberto Saraiva Gonçalves do Departamento de Bioquímica da UFRGS; no *Capítulo III* houve colaboração com a Profa. Dra. Cristiane Matté do Departamento de Bioquímica da UFRGS; no *Capítulo IV* houve colaboração com a Dra. Ana Carolina Zeri do Laboratório Nacional de Biociências (CNPEM, Campinas, SP), com a Profa. Dra. Leandra Franciscato Campo do Departamento de Química da UFRGS e com a Profa. Dra. Fátima Guma do Departamento de Bioquímica da UFRGS; no *Capítulo V* houve colaboração com o Prof. Dr. David Dreiemeier do Setor de Patologia Veterinária da UFRGS, com a Profa. Dra. Denise Zancan do Departamento de Fisiologia da UFRGS e com a Profa. Dra. Ana O. Battastini do Departamento de Bioquímica da UFRGS.

A seção *Discussão* contém uma interpretação geral dos resultados obtidos nos diferentes artigos científicos. A seção *Conclusões* aborda as conclusões gerais obtidas na Tese. A seção *Perspectivas* aborda as possibilidades de desenvolvimento de projetos a partir dos resultados obtidos, dando continuidade a essa linha de pesquisa.

A seção *Referências Bibliográficas* lista as referências citadas na *Introdução* e *Discussão* da Tese.

LISTA DE ABREVIATURAS

ADM-1 – Adenomodulina-1

ADP - Adenosina difosfato

Akt/PKB - Proteína Cinase B (Protein Kinase B)

AMP - Adenosina monofosfato

ATP - Adenosina tri-fosfato

BHE - Barreira hemato-encefálica

CREB – Proteína de Ligação ao Elemento de Resposta ao AMP cíclico (cAMP Response Element Binding Protein)

CTT - Células tronco tumorais

DOX – Doxazosina

DOX-NC – Doxazosina nanoencapsulada

DR4/DR5 – Receptor de Morte 4/5 (Death Receptor 4/5)

EGF – Fator de Crescimento Endotelial (Endothelial Growth Factor)

EGFR - Receptor de Fator de Crescimento Endotelial (Endothelial Growth Factor Receptor)

ERBB – Oncogene de leucemia eritroblástica viral (erythroblastic leukemia viral oncogene)

EROs – Espécies reativas do Oxigênio

ERK – Cinase Regulada por Sinal Extracelular (Extracellular Signal-Regulated Kinase)

FAS – Receptor 6 da Superfamília de TNF (TNF superfamily receptor 6)

FDA – Administração de Alimentos e Medicamentos (Food and Drug Administration)

FOXO1 – Fator de Transcrição “forkhead homeobox O1” (Forkhead Homeobox Type O1)

GB - Glioblastoma

GB - Glioblastoma

GLUT-1 - Transportador tipo I de glicose

GSK-3β - Glicogênio Sintase Cinase-3 (Glycogen Synthase Kinase-3β)

HER – Receptor do Fator de Crescimento Epidermal Humano (Human Epidermal Growth Factor Receptor)

HIF - Fator induzível de hipóxia (Hypoxia Inducible Factor)

IDH – Isocitrato desidrogenase (isocitrate dehydrogenase)

IL – Interleucina

mAB – Anticorpo Monoclonal (Monoclonal Antibody)

MAPK - Proteína Cinase Ativada por Mitógenos (Mitogen-Activated Protein Kinase)

MDM2 – Double Minute murino 2 (Murine double minute 2)

MTIC - 5-(3-metiltriazeno-1-il)imidazol-4-carboxamida

mTORC – Complexo da Proteína Alvo da Rapamicina em Mamíferos (Mammalian Target of Rapamycin Complex)

OMS - Organização Mundial da Saúde

PDK1 - Cinase Dependente de Fosfoinositol (Phosphoinositide-dependent Kinase-1)

PGC-1α - Co-ativador-1 alfa do Receptor Ativado por Proliferador do Peroxissoma (Peroxisome proliferator-activated receptor gamma coactivator 1-alpha)

PI3K - Fosfatidilinositol 3-cinase (Phosphoinositide 3-kinase)

PIP2 - fosfatidilinositol-4,5-bifosfato

PIP3 - phosphatidilinositol-3,4,5-trisfosfato

PO – Privação de Oxigênio

PTEN - Homólogo Fosfatase e Tensina Deletado do Cromossomo 10 (Phosphatase and Tensin Homologue Deleted from Chromossome 10)

Raf – Proteína de Fibrossarcoma de Aceleração Rápida (Rapidly Accelerated Fibrosarcoma protein)

Ras – Vírus do Sarcoma de Rato (Rat sarcoma vírus)

Rb – Retinoblastoma

RTK – Receptores de tirosina cinases (Receptor Tyrosine Kinase)

TNFR - Receptor de Fator de Necrose Tumoral (Tumoral Necrosis Factor Receptor)

SF – Sem soro (Serum Free)

SNC - Sistema Nervoso Central

TCGA - The Cancer Genome Atlas

TERT: transcriptase reversa da telomerase (Telomerase Reverse Transcriptase)

TFAM – Fator de transcrição mitocondrial A (Mitochondrial transcription factor A)

TGF-α – Fator de Crescimento Tumoral alfa (Tumor Growth Factor alfa)

TKI – Inibidor de tirosina cinase (Tyrosine Kinase Inhibitor)

TMZ - Temozolomida

TNFα - Fator de necrose tumoral alfa (Tumoral Necrosis Factor alpha)

TRAIL - Ligante indutor de apoptose relacionado ao TNF (Tumor Necrosis Factor-Related Apoptosis-Inducing Ligand)

VEGF - Fator de Crescimento Endotelial Vascular (Vascular Endothelial Growth Factor)

wtEGFR - Receptor de Fator de Crescimento Endotelial “wild type” (wild type Endothelial Growth Factor Receptor)

RESUMO

Glioblastoma (GB) é o tumor cerebral humano mais frequente e maligno. O prognóstico dos pacientes com GB permanece alarmante, principalmente devido à baixa eficácia das estratégias terapêuticas atuais além da natureza invasiva desse tipo de câncer. Uma característica de tumores sólidos é apresentar áreas hipóxicas. Microambientes hipóxicos contribuem para a progressão do câncer, resistência ao tratamento e ao prognóstico ruim da doença. Dessa forma, neste trabalho, desenvolvemos um modelo *in vitro* que se aproxima ao microambiente hipóxico tumoral *in vivo*. Nossos resultados sugerem que a privação de oxigênio (PO) em combinação com ausência de soro forneceu um ambiente favorável à desdiferenciação das células C6 em células tronco tumorais (CTT). A doxazosina (DOX), um antihipertensivo utilizado na clínica, apresenta efeitos antitumorais em diversos tipos de câncer. Assim, avaliamos o efeito antitumoral da doxazosina em linhagens de glioma de rato (C6) e humano (U138-MG) e a toxicidade do fármaco em culturas primárias de astrócitos e culturas organotípicas de hipocampo. A doxazosina induziu morte celular nas linhagens de glioma e apresentou baixa neurotoxicidade. Além disso, o fármaco inibiu a via da PI3K/Akt e ativou GSK-3β e p53, resultando em indução de apoptose e parada no ciclo celular na fase G0/G1. Considerando a importância da mitocôndria na plasticidade de células tumorais e a resistência ao tratamento apresentada pelos GB, nós analisamos os efeitos da DOX nas interações entre núcleo e mitocôndrias. A DOX induziu biogênese mitocondrial e apoptose nas células C6 e diminuiu secreção de TNF-α. Ao analisar a estrutura química da DOX, encontramos diversas características que indicam que ela possui autofluorescência. Dessa forma, caracterizamos a autofluorescência da DOX em diversos meios. Observamos que há um padrão de distribuição do fármaco nas células C6: ele se encontra ao redor do núcleo e parece estar vesiculado. A superexpressão do receptor do fator de crescimento epidermal (EGFR) está relacionada às formas mais malignas e resistentes de GBs. Portanto, analisamos se a ação antiglioma da DOX está envolvida com EGFR. O tratamento com DOX foi capaz de diminuir os níveis de p-EGFR. O co-tratamento de DOX e AG1478 (inibidor de receptores de tirosina cinase) diminuiu a fosforilação de EGFR e causou necrose. Em vista disso, nossos resultados sugerem que o mecanismo de ação da DOX envolve sinalização de EGFR. Por fim, nós avaliamos os efeitos da DOX livre e nanoencapsulada (DOX-NC) em modelos *in vitro* e *in vivo* de glioma. Demonstramos que a DOX-NC induziu morte celular em linhagem de glioma em concentrações 100 vezes menores do que as que utilizamos para a DOX na sua forma livre. Além disso, analisamos o efeito da DOX-NC em culturas organotípicas de hipocampo e, da mesma maneira que o observado com a DOX, a DOX-NC demonstrou baixa toxicidade e diminuiu a área tumoral *in vivo*, sendo seletiva para células cancerosas. Nesta tese, alteramos o microambiente *in vitro* de células de glioma, avaliamos os efeitos antitumorais da doxazosina em sua forma livre e nanoencapsulada. Além disso, utilizamos modelos de glioma *in vitro* e *in vivo* e em diversos parâmetros celulares, descrevemos a autofluorescência do fármaco e também utilizamos essa característica para avaliar a captação e a distribuição da doxazosina em células de glioma. Nossos resultados contribuíram para aproximar os modelos de estudo com o que ocorre em gliomas *in vivo* e para evidenciar o potencial terapêutico da doxazosina como um agente antiglioma com baixa toxicidade neural e sistêmica.

ABSTRACT

Glioblastoma (GB) is the most frequent and malignant human brain tumor. The prognosis of patients with GB remains dismal, mainly due to the low effectiveness of current therapeutic strategies and the invasive nature of this type of cancer. A characteristic of solid tumors is the presence of hypoxic areas. Hypoxic microenvironments contribute to cancer progression, resistance to treatment, and poor prognosis of the disease. Thus, we developed an *in vitro* model that approximates the hypoxic tumor microenvironment found *in vivo*. Our results suggest that OD in combination with absence of serum provided an environment favorable to the dedifferentiation of C6 cells in cancer stem cells. Doxazosin (DOX), an antihypertensive used in the clinic, has antitumor effects in several types of cancer. Thus, we evaluated the antitumor effect of DOX on rat (C6) and human (U138-MG) glioma cell lines and drug toxicity in primary astrocyte cultures and organotypic hippocampal cultures. DOX induced cell death in glioma lines and showed low neurotoxicity. In addition, the drug inhibited the PI3K/Akt pathway and activated GSK-3β and p53, resulting in induction of apoptosis and cell cycle arrest in the G0/G1 phase. Considering the importance of mitochondria in the plasticity of tumor cells and the resistance to treatment presented by glioblastomas, we analyzed the effects of DOX the interactions between nucleus and mitochondria. DOX induced mitochondrial biogenesis and apoptosis in C6 cells, and decreased TNF-α secretion. When analyzing the chemical structure doxazosin, we find several characteristics that indicate that it has autofluorescence. Thus, we characterized the autofluorescence of DOX in several media. We observed that there is a pattern of distribution of the drug in the cell: it is around the nucleus and appears to be vesiculated. Overexpression of the Epidermal Growth Factor Receptor (EGFR) is related to the more malignant and resistant forms of GBs. Therefore, we analyzed whether the antiglioma action of DOX is involved with EGFR. DOX treatment was able to decrease p-EGFR levels. Co-treatment of DOX and AG1478 (a receptor tyrosine kinase inhibitor) decreased EGFR phosphorylation and caused necrosis. Thus, our results suggest that the mechanism of action of doxazosin involves EGFR signaling. We evaluated the effects of free and nanoencapsulated doxazosin (DOX-NC) in *in vitro* and *in vivo* models of glioma. We demonstrated that nanoencapsulated doxazosin (DOX-NC) induced cell death in a glioma line at concentrations 100 times lower than those used for doxazosin in its free form. In addition, we analyzed the effect of DOX-NC on organotypic hippocampal cultures and, in the same way as observed with DOX, DOX-NC demonstrated low toxicity and decreased tumor area *in vivo*, being selective for cancer cells. In this dissertation, we altered the *in vitro* microenvironment of glioma cells, we evaluated the antitumor effects of doxazosin in its free and nanoencapsulated form. In addition, we used glioma models *in vitro* and *in vivo* and analyzed several cellular parameters, we described the autofluorescence of the drug and also used this characteristic to evaluate the uptake and distribution of doxazosin in glioma cells. Our results have contributed to approximate the study models with what occurs in gliomas *in vivo* and to evidence the therapeutic potential of doxazosin as an antiglioma agent with low neural and systemic toxicity.

1. INTRODUÇÃO

1.1. Gliomas

A incidência de todos os tumores primários é estimada em 18,71 por 100.000 indivíduos por ano (Dolecek *et al.*, 2012). Cerca de 60% deles ocorrem nos quatro lobos cerebrais (Huse *et al.*, 2013).

Gliomas são os mais comuns dentre os tumores malignos do Sistema Nervoso Central (SNC). Representam mais de 30% de todos os tumores primários e 80% dos tumores malignos do SNC.

Os gliomas classificados, de acordo com a Organização Mundial da Saúde (OMS), de 2007, conforme três critérios principais: histopatológicos, grau de malignidade (variando de I à IV – quanto maior o grau mais maligno, tabela 1) e conforme a localização do tumor no cérebro (se são infra ou supra-tentoriais) (Huse *et al.*, 2011; Dolecek *et al.*, 2012; Lima *et al.*, 2012; Huse *et al.*, 2013).

Tabela 1: Classificação dos gliomas segundo os graus de malignidade.

Sistema de Estadiamento de Gliomas	
Grau	**Comentários**
Tumor Grau I (astrocitoma pilocítico, astrocitoma de célula gigante subependimal, subependimoma, ependimoma mixopapilar)	Tumor benigno, de crescimento lento; normalmente associado com sobrevivência a longo prazo; recorrência menos provável.
Tumor Grau II (astrocitoma, oligoastrocitoma, oligodendroglioma)	Hipercelularidade aumentada; sem mitose; sem proliferação vascular; sem necrose; pode recorrer como tumor de grau mais elevado.
Tumor Grau III (astrocitoma, oligoastrocitoma, oligodendroglioma)	Alta taxa de hipercelularidade; alta taxa de mitose; sem proliferação vascular; sem necrose; alta taxa de recorrência tumoral.
Tumor Grau IV (glioblastoma)	Taxa elevada de hipercelularidade; taxa elevada de mitose; presença de proliferação vascular; presença de necrose.

Adaptado de Eckley e Wargo, 2010 e de Louis et al., 2016.

Recentemente houve uma alteração na classificação dos gliomas de acordo com a OMS (Louis *et al.*, 2016) na qual foram adicionados parâmetros moleculares juntamente com a histologia para definir muitos dos tumores do SNC. A distribuição por histopatologia utilizada antes dessa atualização da OMS na classificação dos gliomas está ilustrada na Figura 1. Conforme Louis e colaboradores (2016), essa nova classificação com adição dos parâmetros moleculares é um estágio intermediário para a futura incorporação de dados moleculares objetivos na classificação de tumores do SNC (ainda encontra-se em estudo). Além disso, a nova classificação divide gliomas difusos em dois grandes grupos: os que possuem isocitrato desidrogenase (IDH) mutada ou selvagem (Fig. 2).

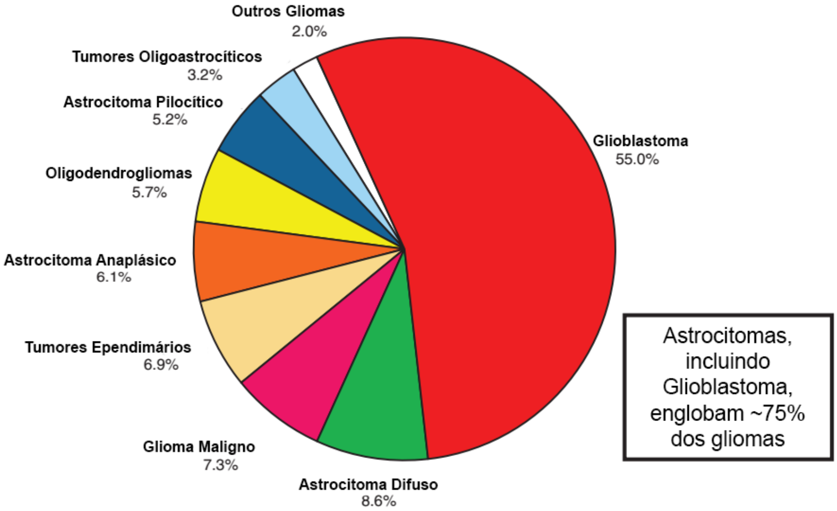

Figura 1: Classificação histológica dos tumores primários do SNC- Gliomas (N= 90,828). Adaptado de Dolecek *et al.*, 2012.

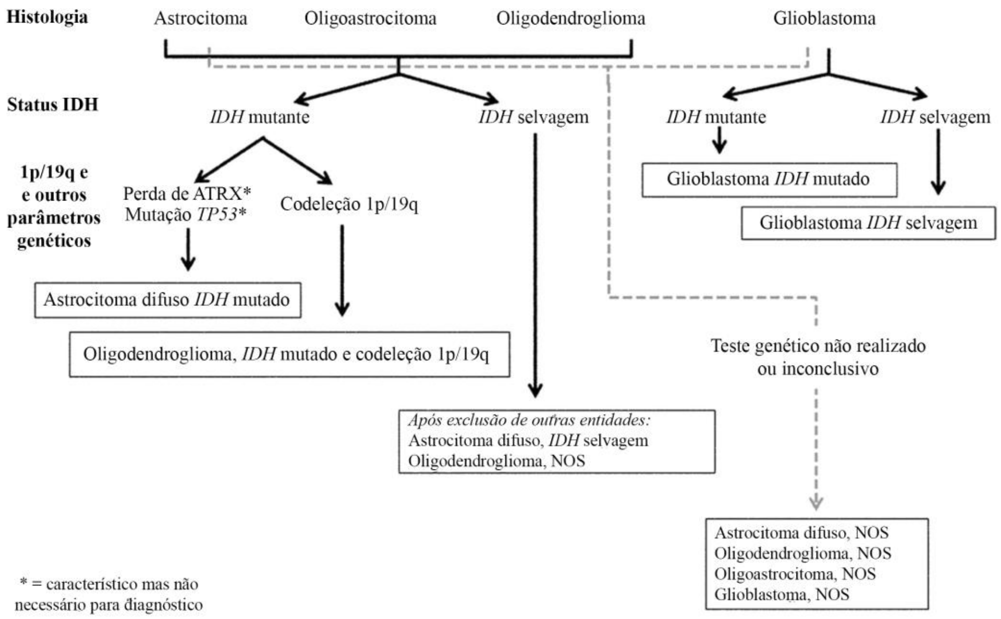
Histologia
Astrocitoma
Oligoastrocitoma
Oligodendroglioma
Glioblastoma
Status IDH
IDH mutante
IDH selvagem
IDH mutante
IDH selvagem
1p/19q e e outros parâmetros genéticos
Perda de ATRX*
Mutação TP53*
Codeleção 1p/19q
Glioblastoma IDH mutado
Glioblastoma IDH selvagem
Astrocitoma difuso IDH mutado
Oligodendroglioma, IDH mutado e codeleção 1p/19q
Teste genético não realizado ou inconclusivo
Após exclusão de outras entidades:
Astrocitoma difuso, IDH selvagem
Oligodendroglioma, NOS
Astrocitoma difuso, NOS
Oligodendroglioma, NOS
Oligoastrocitoma, NOS
Glioblastoma, NOS
* = característico mas não necessário para diagnóstico

Figura 2: Algoritmo de classificação de gliomas difusos de acordo com características histológicas e moleculares. NOS: não especificado (not otherwise specified). Adaptado de Louis *et al.*, 2016.

1.2. Glioblastoma

Como visto anteriormente, o glioblastoma é um subtipo de glioma. Esse tipo de câncer foi identificado primeiramente em 1863 pelo Dr. Rudolf Wirshow sendo classificado microscopicamente como um tumor de células com origem glial (Mackenzie, 1926). Dr. Walter Dandy removeu um hemisfério inteiro de dois pacientes em coma que tinham GB, e mesmo assim, eles vieram a falecer devido à doença, demonstrando o quão invasivo é esse tipo tumoral (Dandy, 1928).

O GB foi originalmente chamado de espongioblastoma multiforme, mas em 1926 o neuropatologista Dr. Percival Bailey e o neurocirurgião Dr. Harvey Cushingchamaram de glioblastoma multiforme (Mackenzie, 1926). O termo “multiforme”, designado por alguns pesquisadores, foi assim descrito pela primeira vez, pois observando esse tipo tumoral a partir de uma análise microscópica, eles apresentavam uma grande variabilidade histológica, bem como heterogeneidade molecular, o que acarretava, muitas vezes, em prognóstico ruim da doença (Bao *et al.*, 2006).

Estes tumores apresentam características de glioma de grau IV, como necrose endotelial, alta taxa proliferativa e elevada densidade de células atípicas (glioblastoma primário), podendo evoluir para um tumor de grau inferior (glioblastoma secundário). Essa classificação em primários ou secundários depende do processo gliomagênico e das vias de sinalização celular que se encontram alteradas nessas células tumorais (Wirsching e Weller, 2016).

Os GBs são os tumores cerebrais mais malignos e agressivos, compreendendo mais da metade de todos os gliomas. Constituem a segunda neoplasia maligna mais comum, representando 16% de todos os tumores primários cerebrais. Compreendem cerca de 3% de todos os tumores do SNC, diagnosticados na faixa de 0-19 anos de idade. São mais comuns em adultos e idosos. São 1,6 vezes mais comuns nos homens e a incidência é de duas a três vezes maior entre os brancos em comparação com negros ou outros grupos raciais (Dolecek *et al.*, 2012).

Os percentuais de sobrevivência dos indivíduos afetados por glioblastoma são baixos: menos de 5% dos pacientes sobrevivem cinco anos após o diagnóstico. Porém, tais estimativas são um pouco mais elevadas para um pequeno número de pacientes, que quando diagnosticados possuem idade inferior a 20 anos (Dolecek *et al.*, 2012).

Embora os glioblastomas possam ocorrer em todas as idades, inclusive na infância, normalmente é diagnosticado aos 55-64 anos (idade média do paciente). A faixa etária dos pacientes, o estadiamento do tumor, a ocorrência de déficits neurológicos, bem como a natureza infiltrativa deste tipo de câncer dificulta a remoção cirúrgica completa.

Os pacientes com GB exibem uma sobrevida média de apenas 14,6 meses após ressecção cirúrgica e tratamentos de rádio e quimioterapia adjuvantes (Ostrom *et al.*, 2015). A quimioterapia com temozolomida (TMZ), fármaco utilizado como terapia padrão para esse tipo tumoral, aumenta a sobrevivência dos pacientes em cerca de seis meses a um ano (Stupp *et al.*, 2005), dependendo do estadiamento do tumor. Mecanismos como desregulação de enzimas e proteínas transportadoras de membrana, aberrações genômicas e alterações da susceptibilidade a apoptose podem ser responsáveis pela alta incidência de quimio-resistência em pacientes com GB (Thakkar *et al.*, 2014; Ostrom *et al.*, 2015).

Alterações genéticas que são frequentes nos GBs incluem as mutações de perda de função ou silenciamento das proteínas p53, p16, Rb e PTEN e mutações de ganho de função como a amplificação do gene EGFR. Isso resulta em uma desregulação de vias de sinalização intracelulares que acabam levando a um aumento da proliferação, sobrevivência, invasão e angiogênese tecidual (Wechsler-Reya e Scott, 2001; Ghosh *et al.*, 2005; Huse *et al.*, 2013; Wirsching e Weller, 2016).

Não há causas subjacentes identificadas para a maioria dos gliomas malignos. Fatores epidemiológicos específicos, incluindo exposições ocupacionais, carcinógenos ambientais, alimentos que contenham compostos N-nitrosos, campos eletromagnéticos, têm sido associados a uma pequena proporção dos gliomas. Os dois únicos fatores estabelecidos em relação à causa de tumores cerebrais primários são a exposição a doses elevadas de radiação ionizante e mutações herdadas de genes, associados com síndromes raras. Podem ocorrer ainda, no desenvolvimento dos gliomas, polimorfismos em genes que afetam a desintoxicação, o reparo do DNA e a regulação do ciclo celular (Institute, 2016).

Aproximadamente 5% dos pacientes com glioblastoma maligno apresenta histórico familiar. Alguns desses casos estão associados com síndromes genéticas raras, como neurofibromatose tipo 1 e 2, e síndrome de Li-Fraumeni (Farrell e Plotkin, 2007).

1.2.1. Classificação (Glioblastomas – Análise Molecular)

Em relação à caracterização patogênica dos GB, durante anos não haviam sido divulgados grandes avanços. Com o desenvolvimento da genômica, alguns pesquisadores conseguiram comprovar através de análises moleculares a heterogeneidade vista não só na morfologia desse tipo tumoral, mas na expressão de proteínas desses tipos de câncer. Essa classificação dos GBs, através da catalogação dos perfis e a integralização de todo o espectro de anormalidades moleculares comuns, facilitou a identificação de subclasses moleculares em doenças aparentemente “uniformes”, graças ao uso da tecnologia de microarranjos de DNA (Parsons et al., 2008; Huse et al., 2011; Thakkar et al., 2014).

Como descrito acima, segundo a OMS (Louis *et al.*, 2016), os GBs são classificados em IDH mutados e IDH selvagens. A nova classificação, que ainda está em implementação, tmabém define as características principais desses dois grupos, conforme a Tabela 2.

Tabela 2. Principais características de glioblastomas IDH-selvagem e IDH-mutado

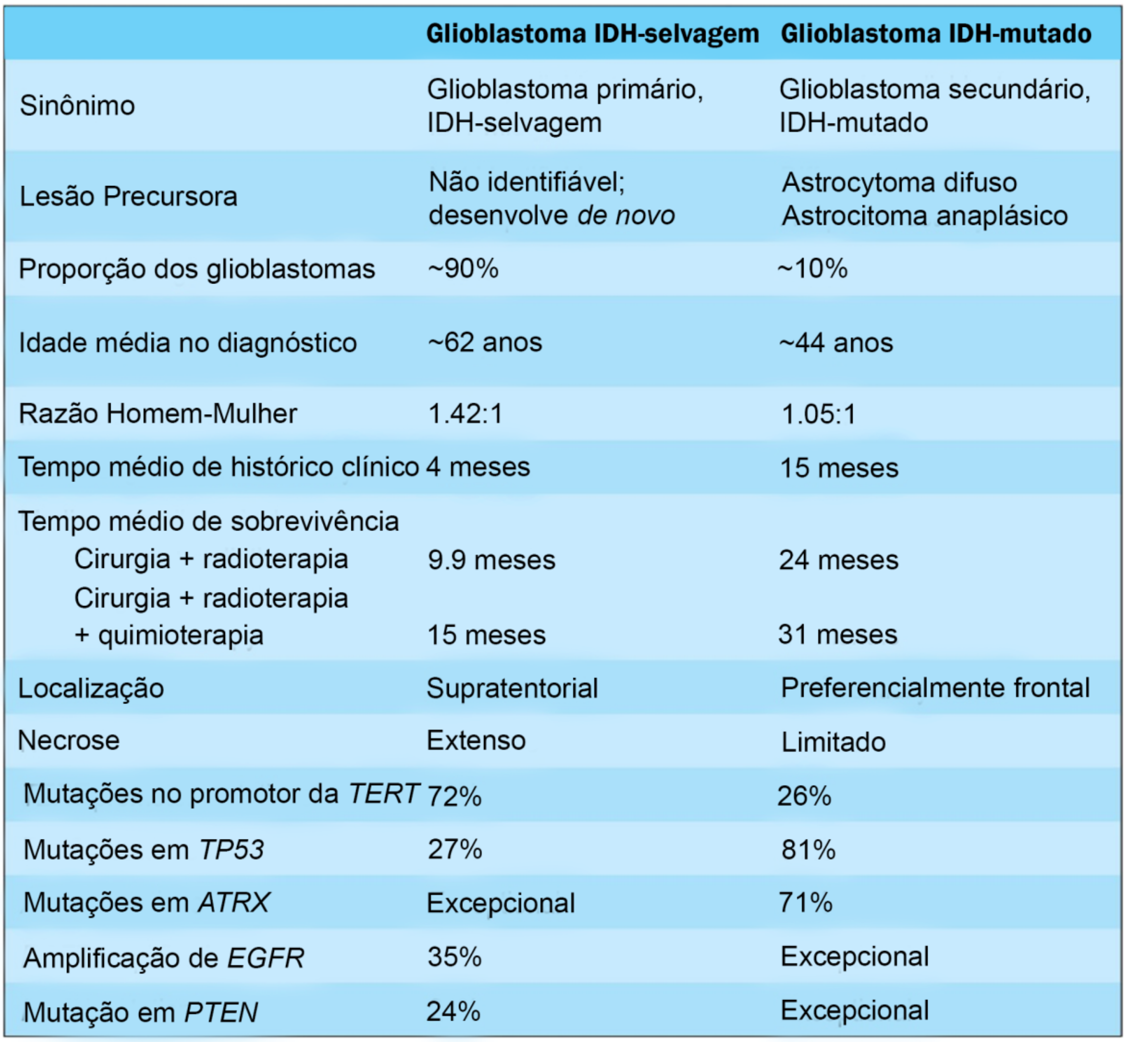

	Glioblastoma IDH-selvagem	**Glioblastoma IDH-mutado**
Sinônimo	Glioblastoma primário, IDH-selvagem	Glioblastoma secundário, IDH-mutado
Lesão Precursora	Não identifiável; desenvolve *de novo*	Astrocytoma difuso Astrocitoma anaplásico
Proporção dos glioblastomas	~90%	~10%
Idade média no diagnóstico	~62 anos	~44 anos
Razão Homem-Mulher	1.42:1	1.05:1
Tempo médio de histórico clínico	4 meses	15 meses
Tempo médio de sobrevivência		
Cirurgia + radioterapia	9.9 meses	24 meses
Cirurgia + radioterapia + quimioterapia	15 meses	31 meses
Localização	Supratentorial	Preferencialmente frontal
Necrose	Extenso	Limitado
Mutações no promotor da *TERT*	72%	26%
Mutações em *TP53*	27%	81%
Mutações em *ATRX*	Excepcional	71%
Amplificação de *EGFR*	35%	Excepcional
Mutação em *PTEN*	24%	Excepcional

Adaptado de Louis *et al.*, 2016.

Já os estudos iniciais em gliomas malignos demonstraram que as assinaturas transcricionais conseguem distinguir de maneira eficaz as subpopulações de GB, além de identificar vários tipos de genes cujos níveis de expressão podem estar correlacionados com o prognóstico (Fuller *et al.*, 1999; Sallinen *et al.*, 2000; Fuller *et al.*, 2002; Huse *et al.*, 2013).

O “Cancer Genome Atlas” (TCGA) é o instrumento de integração de dados de expressão e de perfis genéticos, que cataloga os padrões moleculares e integra todo o espectro de anormalidades vistas em GBs (Parsons *et al.*, 2008; Weinstein *et al.*, 2013). Esta avaliação explora as bases moleculares das distintas subclasses de GB, além de considerar a sua importância na patogênese da doença e no desenvolvimento terapêutico, os quais poderiam ser melhor avaliados por testes pré-clínicos e adequadamente concebidos nos ensaios clínicos.

De acordo com essas análises de expressão e de perfis genéticos, os glioblastomas são classificados em 4 subclasses moleculares: proneural, neural, clássica e mesenquimais (figura 3). Essas subclasses exibem correlações genômicas e de anormalidades epigenômicas definidas.

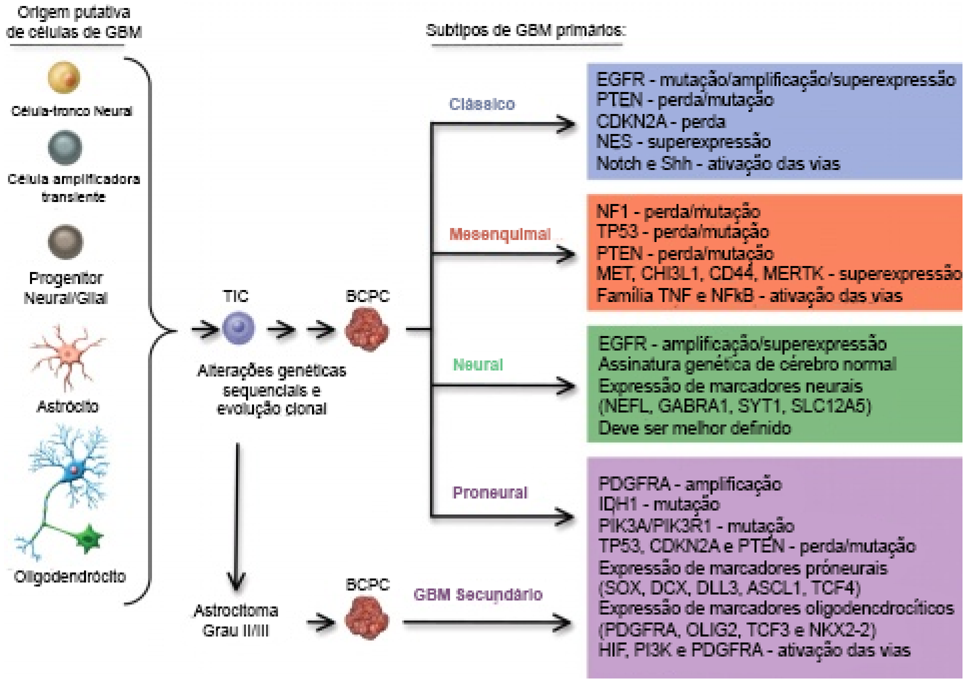
Origem putativa de células de GBM
Célula-tronco Neural
Célula amplificadora transiente
Progenitor Neural/Glial
Astrócito
Oligodendrócito
TIC
BCPC
Alterações genéticas sequenciais e evolução clonal
Astrocitoma Grau II/III
BCPC
GBM Secundário
Subtipos de GBM primários:
Clássico
EGFR - mutação/amplificação/superexpressão
PTEN - perda/mutação
CDKN2A - perda
NES - superexpressão
Notch e Shh - ativação das vias
Mesenquimal
NF1 - perda/mutação
TP53 - perda/mutação
PTEN - perda/mutação
MET, CHI3L1, CD44, MERTK - superexpressão
Família TNF e NFkB - ativação das vias
Neural
EGFR - amplificação/superexpressão
Assinatura genética de cérebro normal
Expressão de marcadores neurais
(NEFL, GABRA1, SYT1, SLC12A5)
Deve ser melhor definido
Proneural
PDGFRA - amplificação
IDH1 - mutação
PIK3A/PIK3R1 - mutação
TP53, CDKN2A e PTEN - perda/mutação
Expressão de marcadores próneurais
(SOX, DCX, DLL3, ASCL1, TCF4)
Expressão de marcadores oligodencdrocíticos
(PDGFRA, OLIG2, TCF3 e NKX2-2)
HIF, PI3K e PDGFRA - ativação das vias

Figura 3: Demonstra esquematicamente as alterações genéticas observadas na patogênese de diferentes subtipos de glioblastoma. Adaptado de Van Meir *et al.*, 2010.

A finalidade principal da subclassificação molecular dos GBs é delinear a biologia da tumorigênese e determinar os caminhos que levam a oncogênese e ao crescimento contínuo do tumor. A segunda meta é identificar as vulnerabilidades moleculares que podem servir de alvos terapêuticos, a fim de melhorar o controle dessa patologia e produzir melhores resultados aos pacientes.

A partir desses dados, três vias de controle de proliferação e de morte celular mostraram-se alteradas (McLendon *et al*., 2008):

(1) Via dos receptores Receptores de tirosina cinases/ Vírus do Sarcoma de Rato/Fosfatidilinositol 3-cinase (RTK/Ras/PI3K) alterada em 88% dos GB;

(2) Via da proteína p53 alterada em 87%;

(3) Via da proteína do retinoblastoma (Rb) alterada em 77% dos GB.

As vias 1 e 2 serão abordadas no item 1.6.

1.2.2 Origens do glioblastoma

As origens do GB versam por três hipóteses. A primeira e mais antiga confirma que são originados de células maduras (astrócito e/ou oligodendrócito) que sofreram diversas mutações em genes supressores tumorais e oncogenes, levando a desdiferenciação e ao desenvolvimento do tumor.

A segunda hipótese sustenta que tais tumores têm origem a partir de células progenitoras. As células progenitoras neurais adquirem mutações resultando em células com propriedades de tronco (Bao *et al.*, 2006; Eramo *et al.*, 2006; Visvader e Lindeman, 2008; Van Meir *et al.*, 2010).

A hipótese afirma que as células tronco neurais adultas (com um alto potencial proliferativo e de diferenciação) adquirem mutações transformando-se em tumorigênicas (figura 3, à esquera) (Dirks, 2006; Stiles e Rowitch, 2008). Esse último conceito de os glioblastomas apresentarem um 'pool' de células tumorais com propriedades tronco, responsáveis pela formação do tumor, originou o termo ‘células tronco tumorais’ (CTT).

A supressão espontânea da apoptose e desregulação da divisão celular constituem as propriedades mais críticas que uma célula somática adquire no decurso da sua transformação em neoplásica.

Existem pelo menos três razões que contribuem para a resistência dos glioblastomas à terapia:

(1) a massa tumoral muitas vezes pode estar localizada e invadir áreas cerebrais funcionais inacessíveis, impossibilitando a ressecção cirúrgica (tumores infiltrativos) sem que sejam afetadas as atividades motoras e/ou os processos cognitivos,

comprometendo de forma inequívoca a qualidade de vida do paciente (Sanai e Berger, 2008; Sanai *et al.*, 2008);

(2) os glioblastomas são caracterizados por apresentarem uma variedade de anormalidades genéticas. Esta heterogeneidade pode constituir um desafio terapêutico, porque as células que carregam anormalidades diferentes podem responder de forma diferente à terapia;

(3) a barreira hematoencefálica (BHE) protege o sistema nervoso central e evita que muitos quimioterápicos administrados sistemicamente tenham acesso ao local do tumor.

No intuito de compreender os mecanismos envolvidos na progressão dos glioblastomas, alguns pesquisadores identificaram uma população de CTTs com propriedades especiais, sendo denominadas de células tronco tumorais (CTTs) (Eramo *et al.*, 2006). Estas células possuem um papel crucial na iniciação e proliferação do tumor. Apesar de terem propriedades distintas das células tumorais, possuem a habilidade de se auto-renovar, diferenciar em vários tipos de células tumorais e sustentar o crescimento do tumor *in vivo* (Eramo *et al.*, 2006). São importantes, do ponto de vista clínico, devido a sua elevada resistência a rádio e quimioterapia. Essa descoberta explica a ineficácia da terapêutica atual (convencional), que está limitada às abordagens convencionais que visam eliminar a população de células neoplásicas em massa, não considerando as células remanecentes como as CTTs que conseguem regenerar o tumor (Smalley e Ashworth, 2003; Eramo *et al.*, 2006; Jordan *et al.*, 2006).

1.3. Gliomas e Hipóxia

Conforme exposto acima, glioblastomas são tumores que possuem uma alta taxa proliferativa, são muito infiltrativos e são capazes de promover angiogênse tecidual. Porém esse mecanismo de formação de novos vasos não supre totalmente a massa de células neoplásicas com nutrientes e aporte de oxigênio, o que favorece muitas vezes a formação de áreas hipóxicas (Joseph *et al.*, 2015). Esse fenômeno é comum em tumores sólidos (figura 4), onde a concentração de O_2 na massa tumoral varia de 2,5 a 5,3%, e pode chegar até abaixo de 0,1% em regiões necróticas, caracterizando um microambiente hipóxico (Keith e Simon, 2007; Persano *et al.*, 2013). As condições de normóxia para células humanas embrionárias ou adultas é em média 8% (57,6 mmHg) de Oxigênio molecular (O_2), geralmente variando entre 2,5 a 12% (14,4–64,8 mmHg) em tecidos cerebrais (Keith e Simon, 2007; Persano *et al.*, 2013).

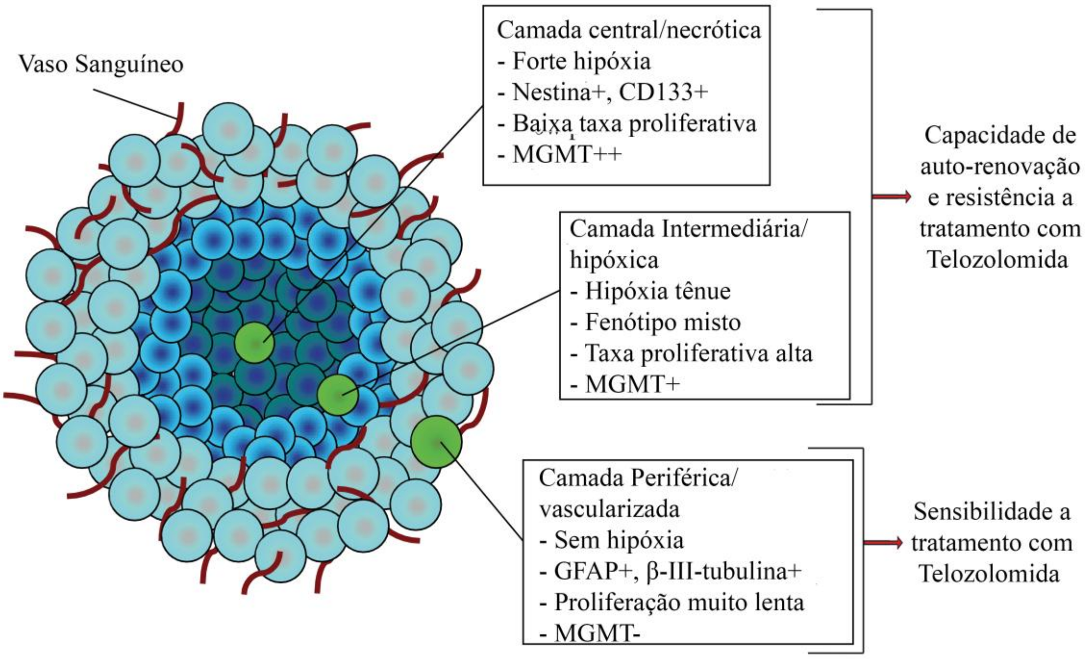
Vaso Sanguíneo
Camada central/necrótica
- Forte hipóxia
- Nestina+, CD133+
- Baixa taxa proliferativa
- MGMT++
Camada Intermediária/ hipóxica
- Hipóxia tênue
- Fenótipo misto
- Taxa proliferativa alta
- MGMT+
Camada Periférica/ vascularizada
- Sem hipóxia
- GFAP+, β-III-tubulina+
- Proliferação muito lenta
- MGMT-
Capacidade de auto-renovação e resistência a tratamento com Telozolomida
Sensibilidade a tratamento com Telozolomida

Figura 4: Características do microambiente hipóxico em glioblastoma. Adaptado de Persano *et al.*, 2011.

Microambientes hipóxicos contribuem para a progressão dos tumores através da ativação de programas transcricionais adaptativos que promovem a sobrevivência celular, motilidade e angiogênese (Keith e Simon, 2007). Além disso, evidências sugerem que a hipóxia induz a desdiferenciação de células tumorais maduras para CTT, responsáveis pelo crescimento tumoral e pela resistência a radio e quimioterapia (Soeda *et al.*, 2009; Persano *et al.*, 2011; Joseph *et al.*, 2015).

Os fatores induzíveis de hipóxia (HIFs) ativam a via apoptótica por meio da p53 em células tumorais e não-tumorais. GBs apresentam mutações de perda de função da p53; nestes, a apoptose induzida pela falta de O_2 é mediada por outras formas, sendo uma delas através da abertura do poro de transição de permeabilidade mitocondrial em uma via independente da p53 (Jakubovicz *et al.*, 1987; Lemasters *et al.*, 1997; Lemasters *et al.*, 1999).

Os HIFs não só sinalizam para a via apoptótica, mas principalmente são responsáveis pelas adaptações celulares frente à privação de O_2, através da transcrição de genes alvo. HIF-1α e HIF-2α compartilham alguns genes alvo, incluindo genes que codificam o fator de crescimento endotelial (VEGF), o transportador tipo I de glicose (GLUT-1) e a adrenomedulina-1 (ADM-1).

O VEGF pode estar associado com o aumento da massa e da progressão tumoral através da atuação em células endoteliais e também através de uma via de sinalização autócrina. Foi demonstrado que VEGF em tumores é responsável pela manutenção de um fenótipo característico de CTT (morfologia característica de células indiferenciadas) (Hamerlik *et al.*, 2012), pela proliferação celular (Knizetova *et al.*, 2008), pela invasão de células tumorais (Bachelder *et al.*, 2002) e por aumento de resistência a radio e quimioterapia (Eramo *et al.*, 2006).

Embora a secreção de VEGF e de outros fatores pró-angiogênicos em GBs leve a uma forte resposta angiogênica, a vasculatura tumoral resultante é anormal, exibindo vazamentos devido a uma elevada permeabilidade vascular, espessamentos focais de paredes vasculares e formação de glomerulóides originados de proliferação microvascular excessiva (Brat e Van Meir, 2001; Kaur *et al.*, 2005).

1.4. Gliomas e Mitocôndria

Alterações mitocondriais contribuem para a patogênese dos gliomas. As mitocôndrias apresentam alta mobilidade e plasticidade, constantemente alterando a sua forma. A distribuição e organização dessas organelas variam entre os diferentes tipos celulares. Cada mitocôndria é envolta por duas membranas altamente especializadas, com diferentes funções. Juntas, elas criam dois compartimentos mitocondriais distintos: a matriz e o espaço intermembrana (Alberts *et al.*, 2014).

A principal função da mitocondria é a geração de ATP por meio da oxidação do piruvato, proveniente principalmente da glicólise no citoplasma da célula. Os elétrons obtidos da oxidação do piruvato são carreados por $NADH.H^+$ e $FADH_2$ e combinados com O_2 pela cadeia respiratória presente na membrana mitocondrial interna. A grande quantidade de energia liberada é utilizada para encaminhar prótons contra seu gradiente de concentração através da membrana mitocondrial interna (para fora da matriz mitocondrial). Isso resulta em acúmulo de H^+ no espaço intermembrana, o qual então volta para a matriz por meio do complexo V da cadeia respiratória, gerando ATP (Nelson e Cox, 2012). A força que move os prótons para a mitocôndria (Δp) é uma combinação do potencial de membrana mitocondrial (Δψm) e o gradiente de pH mitocondrial (ΔpHm). Juntos, esses fatores ajudam a regular o controle mitocondrial sobre o metabolismo energético, homeostasia iônica na célula e morte celular.

Em relação aos glioblastomas, estes apresentam metabolismo dinâmico e o tumor passa por muitas adaptações para manter sua alta taxa proliferativa, o crescimento celular e garantir a sua sobrevivência frente a insultos ou em ambientes hostis (Ordys *et al.*, 2010). Essa plasticidade provém da heterogeneidade genética que as células apresentam (tipos de mutações e superexpressões) somada aos estímulos ambientais. Os quimioterápicos também podem induzir alterações metabólicas profundas nas células cancerosas, gerando resistência intrínseca à morte celular por apoptose (Yadava Phd, 2015).

As mitocôndrias têm um papel fundamental na regulação de todos esses processos, pois estão envolvidas na morte celular por apoptose (via intrínseca), na proliferação celular, no metabolismo energético e no equilíbrio de espécies reativas de oxigênio (EROs). Essa organela é responsável pelo metabolismo oxidativo na maioria das células, porém em gliomas a cadeia respiratória está comprometida e a produção de energia na sua maioria dá-se por via não oxidativa (via glicólise) (Ordys *et al.*, 2010).

Essa disfunção metabólica pode estar associada à estrutura tridimensional da cardiolipina, um fosfolipídio de membrana presente nas mitocôndrias (Schlame *et al.*, 2000). A cardiolipina em glioblastomas é sintetizada de forma errônea. Portanto, o complexo das proteínas da cadeia respiratória que se situam ancoradas na membrana também é afetado, gerando uma produção de ATP ineficiente (Kiebish *et al.*, 2008). Muitos trabalhos citam que a resistência intrínseca a apoptose nos gliomas pode estar associada à estrutura química alterada da cardiolipina, pois essas alterações comprometem a formação do poro de transição mitocondrial. Além disso, a inibição de apoptose, indução de angiogênese, invasão e metástase em células tumorais atualmente se atribui a mutações associadas ao DNA mitocondrial (Kiebish *et al.*, 2008; Ordys *et al.*, 2010).

No entanto, Yadava et al. (2015) avaliaram os mecanismos de diversos agentes terapêuticos em células cancerosas em relação a parâmetros mitocondriais e à morte apoptótica. Esse afirma que, após tratamento com quimioterápicos, ocorre biogênese mitocondrial independentemente da ativação das caspases 3 e 7 e que cada fármaco age de maneira diferente nesse contexto.

A biogênese mitocondrial e muitas funções da organela são reguladas por fatores de transcrição nucleares e coativadores, por exemplo, o fator de transcrição mitocondrial A (TFAM) e o co-ativador 1 alfa de receptor ativado por proliferadores de peroxissoma 1 gama (PGC-1α) (Scarpulla, 2008; Hock e Kralli, 2009). O PGC-1α serve como um elo entre eventos regulatórios nucleares e a maquinaria de transcrição da mitocôndria e o mesmo tem sido descrito como tendo um papel neuroprotetor por meio da indução da biogênese e função mitocondrial (Ventura-Clapier *et al.*, 2008).

1.5. EGFR

Alterações genéticas de RTKs, incluindo as do EGFR, têm um papel importante na resistência ao tratamento, no desenvolvimento e na progressão dos GB. A mutação mais comum associada ao glioma maligno é a amplificação do EGFR (também referido como ERBB1 ou HER1) com frequência de cerca de 50%. EGFR é um membro da superfamília HER de receptor tirosina cinases juntamente com ERBB2, ERBB3 e ERBB4 (Furnari *et al.*, 2015).

A estrutura de cada um dos membros compreende: um ectodomínio ligante-ligante com 2 regiões ricas em cisteína; uma única região transmembrana; e um domínio citoplasmático com ação enzimática tirosina cinase. Os ligantes responsáveis pela sua ativação incluem: EGF, TGF-α (Fator de Crescimento Transformador alfa), anfiregulina, betacelulina, dentre outros (Yewale *et al.*, 2013).

Enquanto inativo, o EGFR ocorre na membrana plasmática como um monômero. A ligação de uma molécula EGF ou outro ligante compatível (TGF-α, anfiregulina, betacelulina) em um monômero do receptor, induz mudanças conformacionais que permitem a interação entre dois monômeros de EGFR. A homo ou heterodimerização do receptor resulta em mais alterações conformacionais que ativam o domínio tirosina cinase intracelular. Isto resulta na autofosforilação da porção citoplasmática do receptor e indução da sinalização "downstream". A fosforilação das porções intracelulares desses receptores ativam rotas de sinalização como Ras-Cinase Regulada por Sinal Extracelular (ERK, Proteína Cinase Ativada por Mitógenos, MAPK) e PI3K/Akt, entre outras (Tebbutt *et al.*, 2013).

A dimerização, além de ativar a atividade das cinases na porção intracelular leva à formação de invaginações cobertas por clatrina na membrana. Essas invaginações formam vesículas endocíticas que se fusionam com endossomos iniciais. Moléculas de EGFR que estão presentes nesses compartimentos retornam à membrana plasmática (recicladas) ou são destinadas à degradação (Yewale *et al.*, 2013). Na ausência de ligante, EGFR está internalizado e possui meia-vida de 30 minutos sendo rapidamente reciclado e devolvido à membrana plasmática. A meia-vida metabólica de EGFR em linhagens celulares tumorais é de 20 h, isso significa que o mesmo receptor irá ciclar na via endocítica diversas vezes durante esse tempo (Hatanpaa *et al.*, 2010).

Em aproximadamente 50% dos tumores com amplificação de EGFR, pode ser detectado um mutante específico de EGFR (EGFRvIII, também conhecido como EGFR tipo III, de 2-7, ΔEGFR). A maioria dos GBs (54%) superexpressa a proteína EGFR "wild type" (wtEGFR) e 31% superexpressam tanto o wtEGFR como o EGFRvIII. O EGFRvIII é uma mutação deleção de wtEGFR, que remove os exons 2-7, resultando em uma deleção de 267 aminoácidos do domínio extracelular do receptor (Hatanpaa *et al.*, 2010). Desse modo, o EGFRvIII não possui a porção extracelular na qual o ligante se liga e esse receptor está constantemente ativo.

Em células saudáveis há cerca de $4x10^4$ a $1x10^5$ moléculas de EGFR presentes na membrana, enquanto células tumorais expressam mais de $2x10^6$ receptores por célula (Yewale *et al.*, 2013). Por essa razão, diversas alternativas terapêuticas para o câncer tem sido desenvolvidas visando o receptor EGFR como alvo.

Os agentes mais promissores são os anticorpos monoclonais (mAb) e as moléculas inibidoras de tirosina cinase (TKI), que apresentam mecanismos de ação e especificidade distintos para o mesmo alvo. Os mAbs se ligam à porção extracelular do receptor e competem com as moléculas ligantes, impedindo a ativação das cascatas de sinalização (Garrett *et al.*, 2002; Ogiso *et al.*, 2002; Yewale *et al.*, 2013); TKIs inibem a autofosforilação da porção citoplasmática de EGFR e competem com ATP endógeno pelo domínio catalítico da molécula (Yewale *et al.*, 2013).

1.6. Vias de sinalização alteradas em glioblastomas

As alterações genéticas em glioblastoma ocorrem com frequência em três vias de sinalização celular: (a) via RTK, RAS, e PI3K, (b) via da p53, e (c) via Rb (retinoblastoma-supressor tumoral), conforme ilustrado na Figura 5.

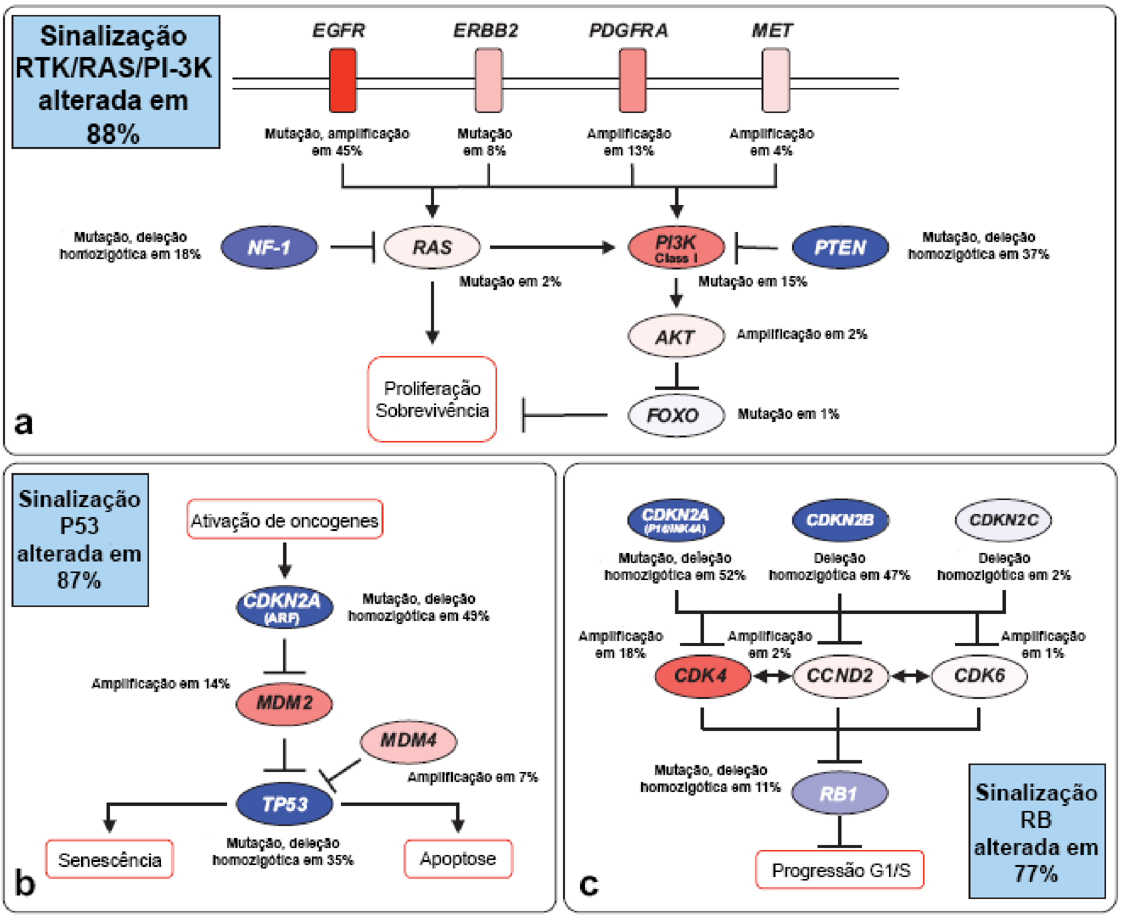
Sinalização RTK/RAS/PI-3K alterada em 88%
EGFR
ERBB2
PDGFRA
MET
Mutação, amplificação em 45%
Mutação em 8%
Amplificação em 13%
Amplificação em 4%
Mutação, deleção homozigótica em 18%
NF-1
RAS
PI3K Class I
PTEN
Mutação, deleção homozigótica em 37%
Mutação em 2%
Mutação em 15%
AKT
Amplificação em 2%
Proliferação Sobrevivência
FOXO
Mutação em 1%
a
Sinalização P53 alterada em 87%
Ativação de oncogenes
CDKN2A (ARF)
Mutação, deleção homozigótica em 49%
Amplificação em 14%
MDM2
MDM4
Amplificação em 7%
TP53
Senescência
Mutação, deleção homozigótica em 35%
Apoptose
b
CDKN2A (P16INK4A)
CDKN2B
CDKN2C
Mutação, deleção homozigótica em 52%
Deleção homozigótica em 47%
Deleção homozigótica em 2%
Amplificação em 18%
Amplificação em 2%
Amplificação em 1%
CDK4
CCND2
CDK6
Mutação, deleção homozigótica em 11%
RB1
Progressão G1/S
Sinalização RB alterada em 77%
c

Figura 5. As alterações no DNA e as mudanças no número de cópias nas seguintes vias de sinalização estão indicadas em (a) RTK, RAS, e PI3K, (b) supressor tumoral p53, e (c) Rb. As alterações genéticas são mostradas em vermelho (*upregulation*) e as que conduzem a uma perda de função são indicadas em azul. Podemos observar que os componentes alterados, o tipo de alteração e a percentagem de tumores que transportam cada alteração nessas vias. As caixas azuis contêm as percentagens totais de glioblastomas com alterações em pelo menos um gene conhecido da via designada. Adaptado de McLendon et al., 2008.

1.6.1. Via RTK/RAS e PI3K

EGFR torna-se ativado por meio da ligação de fatores de crescimento em seu domínio extracelular, através de homo ou heterodimerização com outros receptores levando a eventos de fosforilação. Sua ativação estimula principalmente duas vias de sinalização: via da Ras e via da PI3K/Akt (PKB) (Krakstad e Chekenya, 2010).

1.6.1.1. Via da RAS

A Ras é uma proteína G monomérica, pertencente à família das Proteínas Cinases ativadas por mitógenos (MAPK), cujas respostas desencadeadas pela via estão relacionadas com a progressão do ciclo celular, a transcrição de genes, a sobrevivência tumoral, a proliferação celular e a reorganização do citoesqueleto (Malumbres e Barbacid, 2003). A ativação via fosforilação da Ras inicia uma cascata de sinalização através de MAPKs e ERK-1 e 2, cinases que irão ativar alvos citoplasmáticos como p90RSK. Esta serina/treonina cinase transloca para o núcleo onde ativa fatores de transcrição, como o CREB, que regulam a sobrevivência e proliferação de células de glioma (Sturgill *et al.*, 1988; Sözeri *et al.*, 1992; Moodie *et al.*, 1993; Krakstad e Chekenya, 2010).

1.6.1.2. Via PI3K

A PI3K é translocada para a membrana plasmática por meio da ligação de fosfotirosina a resíduos dos RTKS. A PI3K fosforila o PIP2 (fosfatidilinositol-4,5-bifosfato) à PIP3 (fosfatidilinositol-3,4,5-trifosfato), este, por sua vez, funciona como um importante sinalizador intracelular coordenando processos de crescimento celular, migração, metabolismo e regulação do ciclo celular (Feldkamp *et al.*, 1999; Krakstad e Chekenya, 2010). O acúmulo de PIP3 recruta a PDK1 (*Phosphoinositide-Dependent Kinase 1*) e Akt/PKB à membrana plasmática. Akt é ativa quando fosforilada em dois resíduos, ao mesmo tempo: Thr308 (por PDK1) e Ser473 (por mTORC2-mTOR-Rictor Kinase Complex 2). PDK1 e o complexo mTORC2 são ambos ativados por PI3K (Guha *et al.*, 1997; Feldkamp *et al.*, 1999; Krakstad e Chekenya, 2010). A Akt é responsável pela fosforilação de vários substratos citosólicos e nucleares que regulam o metabolismo e o crescimento celular. A Akt está relacionada com a fosforilação de proteínas que regulam a apoptose (Bad, caspase-9, Double Minute murino 2 (MDM2), p21Waf1/Cip1, Fator de Transcrição "forkhead homeobox O1" (FOXO1) e GSK3β), proliferação e sobrevivência celular (Gesbert *et al.*, 2000). A GSK3β é um dos substratos da Akt, está envolvida na regulação de várias funções celulares, incluindo diferenciação, crescimento, motilidade, proliferação, progressão do ciclo celular, apoptose e resposta à insulina. A desregulação da expressão da GSK3β conduz a muitos estados patológicos: diabetes, doença de Alzeimer, Parkinson, distúrbios bipolares e câncer. A ativação da GSK3β (quando defosforilada – Ser-9) promove parada no ciclo celular e encaminhamento para apoptose (Gesbert *et al.*, 2000).

A sobrevida média de pacientes com GB que possuem mais ativa a via da PI3K (n = 42/56) e Akt (37/56) é de 11 meses em comparação com pacientes com níveis mais baixos de ativação, que foi de 40 meses. Este fato é significativamente mais frequente em pacientes com GB do que outros tipos de câncer (Chakravarti *et al.*, 2004; Krakstad e Chekenya, 2010).

1.6.1.3 Via da p53

O gene TP53 codifica uma proteína de 53kD, que desempenha um papel em vários processos celulares, incluindo regulação do ciclo celular, respostas à danos no DNA, morte celular, diferenciação celular e neovascularização. A proteína supressora tumoral, p53 apresenta-se mutada em 87% dos glioblastomas. A p53 induz parada no ciclo celular, podendo recrutar as proteínas de reparo do DNA ou encaminhar à morte celular após uma injúria (dano ao DNA). Esse mecanismo é responsável pelo *turnover* das células presentes nos tecidos e órgãos do nosso corpo, ao passo que animais que perdem p53 desenvolvem tumores ao longo da vida (Brenner e Mak, 2009; Guicciardi e Gores, 2009; Krakstad e Chekenya, 2010).

1.7. Apoptose

Apoptose é um processo essencial para a manutenção do desenvolvimento dos seres vivos, sendo importante para eliminar células em desuso ou defeituosas. Durante a apoptose, a célula sofre alterações morfológicas que incluem: a retração da célula, perda de aderência com a matriz extracelular e células vizinhas, condensação da cromatina, fragmentação internucleossômica do DNA e formação dos corpos apoptóticos. As alterações morfológicas observadas são consequência de uma cascata de eventos moleculares e bioquímicos específicos e geneticamente regulados (Koff *et al.*, 2015).

A apoptose pode ser iniciada de forma extrínseca e intrínseca (Koff *et al.*, 2015). A via extrínseca ocorre por ativação de receptores de morte celular chamados de fatores de necrose tumoral (TNFR) (Krakstad e Chekenya, 2010). As proteínas que formam o receptor estão organizadas em homotrímeros e são ativadas por ligação de diversos ligantes ao respectivo receptor. A ligação ao receptor pode resultar em várias respostas, incluindo a inflamação, proliferação e apoptose, dependendo das proteínas adaptadoras associadas com o tipo do receptor ativado. Os receptores que medeiam a apoptose são TNF-R1, Receptor 6 da Superfamília de TNF (FAS) e Receptor de Morte 4/5 (DR4/DR5), e os ligantes sinalizadores de morte são: TNFα (fator de necrose tumoral), FasL (ligante de Fas), TRAIL (ligante indutor de apoptose relacionado ao TNF), CD95 estão relacionados com a indução de apoptose (Chen *et al.*, 1997; Krakstad e Chekenya, 2010). A trimerização do receptor resulta no recrutamento de vários domínios de morte e eventualmente recrutamento e ativação de caspase-8 e caspase-10, que induzem a clivagem e ativação de caspases efetoras do processo apoptótico.

A via intrínseca é ativada por sinais intracelulares, tais como dano ao DNA, danos oxidativos, privação de oxigênio ou de fatores de crescimento. Essa via é modulada pela família de proteínas Bcl-2. A sinalização desencadeada por estas proteínas tem como finalidade modular a permeabilidade da membrana mitocondrial.

Após a ativação de sinais de morte, as proteínas pró-apoptóticas BAX e BAK principalmente, sofrem mudanças conformacionais e se inserem na membrana mitocondrial externa. Isto aumenta a permeabilidade da membrana através da formação e/ou regulação de canais da membrana que permitem a libertação de diversas moléculas do interior da mitocôndria para o citoplasma da célula, sendo o citocromo C o mais estudado (Brenner e Mak, 2009; Krakstad e Chekenya, 2010; Koff *et al.*, 2015). A liberação dos componentes mitocondriais leva a ativação da proteína citosólica Apaf-1, responsável pela formação do apoptossomo juntamente com ATP, facilitando o recrutamento e a clivagem da caspase-9, que ativa as caspases 3, 6 e 7 executoras do processo apoptótico.

1.8. Diagnóstico e Terapêutica

A avaliação inicial do paciente com tumor cerebral compreende exames clínico e neurológico detalhados além de exames de neuroimagem. O estadiamento tumoral é diagnosticado minimamente por tomografia axial computadorizada contrastada, seguida por ressonância magnética e espectroscopia (Eckley e Wargo, 2010).O diagnóstico definitivo é confirmado pelo estudo histopatológico de espécimes tumorais, obtido por biópsia estereotáxica ou a céu aberto, sendo essencial para o planejamento terapêutico (Eckley e Wargo, 2010).

Os sintomas clínicos podem incluir dores de cabeça progressivas, déficits neurológicos focais e convulsões (Tanwar *et al.*, 2002; Shai *et al.*, 2003; Davis, 2016). Os tratamentos utilizados na clínica para glioblastomas e tumores primários cerebrais incluem: ressecção cirúrgica, radiação ionizante e quimioterapia (Davis, 2016).

Os gliomas malignos são tumores heterogêneos, tanto na aparência como na expressão gênica. A necessidade de uso concomitante de medicamentos anticonvulsivantes muitas vezes limita a segurança da terapia antineoplásica.

Regimes terapêuticos contendo nitrosuréias (carmustina ou lomustina), alquilantes do DNA (procarbazina, dacarbazina ou temozolomida), derivados da platina (cisplatina ou carboplatina), vincristina, teniposídeo, hidroxiuréia, cloroquina, bevacizumabe (anti-VEGF) e irinotecano mostraram-se úteis no tratamento paliativo de gliomas cerebrais nos graus III ou IV, que, em geral, são administrados concomitantemente à radioterapia (Davis, 2016).

A TMZ pertence à classe dos quimioterápicos alquilantes do DNA, sendo um derivado da imidazotetrazina. Mesmo sendo um medicamento clássico para o tratamento de glioblastomas (TMZ, 75 mg/m^2), a sua ação terapêutica depende da habilidade de alquilar o DNA (Wick, A. *et al.*, 2011). Administrado por via oral, trata-se de um pró-fármaco, ou seja, apresenta atividade farmacológica quando hidrolisado *in vivo* para MTIC (5-(3-metiltriazeno-1-il)imidazol-4-carboxamida). O MTIC é quem possui a atividade citotóxica, agindo como agente alquilante.

Os pacientes, que utilizam o quimioterápico, apresentam uma sobrevida média de aproximadamente 15 meses. O fármaco apresenta uma meia vida muito baixa, cerca de 1,8 horas no plasma, o que aumenta a citotoxicidade do mesmo pois é administrado em doses altas (Zhang e Gao, 2007; Wen et al., 2011).

Devido à variedade de padrões moleculares dos GBs e a alta taxa de recorrência desses tumores malignos, os desafios terapêuticos atuais estão centrados na promessa do diagnóstico personalizado, bem como a própria terapia que podem conduzir a diferentes regimes de tratamento.

1.9. Doxazosina

A DOX [4 - (4-amino-6,7-dimetoxiquinazolina-2-il)-piperazina] 1-il - (2,3-diidro-1,4-benzodioxina-3-il) metanona, é um derivado quinazolínico que compreende a classe terapêutica dos alfa-bloqueadores adrenérgicos. São fármacos que bloqueiam seletivamente os receptores alfa-1 adrenérgicos (Figura 6).

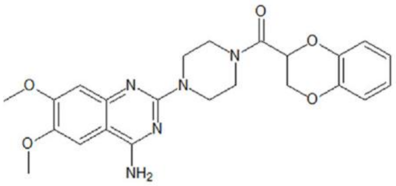

Figura 6: Estrutura química da doxazosina.

É utilizada na clínica como mesilato de doxazosina (Carduran®) para o tratamento de hipertensão, insuficiência cardíaca congestiva e hiperplasia benigna de próstata. Esses fármacos reduzem a resistência arteriolar e provocam aumento da capacitância venosa, o que resulta em reflexo simpático mediado pelo aumento da frequência cardíaca e da atividade do sistema renina-angiotensina plasmáticos. Durante a terapia crônica, a vasodilatação persiste, mas o débito cardíaco, a frequência cardíaca e a atividade da renina no plasma retornam à normalidade e o fluxo sanguíneo renal é inalterado (Wykretowicz *et al.*, 2008).

A principal via de eliminação da DOX, após a administração oral e intravenosa, é através das fezes para homens, ratos, camundongos e cães. Ademais, estudos mostraram que a DOX é completamente absorvida no homem, camundongo e rato, mas é moderadamente absorvida no cão (Kaye *et al.*, 1986).

Devido as suas características físico-químicas, a DOX consegue atingir o SNC, além de possuir uma meia vida longa, cerca de 12h. O fármaco é responsável por induzir a apoptose nas células prostáticas malignas através de um mecanismo alternativo ao relacionado com o adrenoceptor alfa-1 (Rasheed *et al.*, 1999; Holland, 2000). A DOX exerce efeitos pró-apoptóticos em células de câncer de mama e câncer de bexiga (Maher *et al.*, 2001; Wechsler-Reya e Scott, 2001). Sua ação anti-hipertensiva é devido à sua capacidade de se ligar a receptores alfa-1 adrenérgicos, mas os mecanismos de suas ações anti-proliferativas e pró-apoptóticas em células cancerosas ainda não são bem compreendidos.

Por apresentar em sua estrutura química o anel quinazolínico, a DOX pode ser útil como ponto de partida para a síntese de compostos que tenham atividade biológica como inibidores de RTKs. Quinazolinas possuem estrutura química semelhante aos derivados purínicos: ATP, AMP e ADP. Inclusive, a ação inibidora do receptor de tirosina cinase baseia-se na ocupação de sítios de acoplamento do ATP por esses compostos, provocando a inibição da RTKs (Goldstein *et al.*, 2008). Os derivados de quinazolinas têm efeitos pleiotrópicos com a capacidade de afetar as funções e atividades dos receptores alfa1-adrenérgicos, fosfodiesterases, tirosina cinases e a descoberta mais recente adenosina cinases. Nos últimos anos, estes compostos tiveram grande progresso no combate de doenças proliferativas como câncer, baseados principalmente na atividade inibidora de RTKs. São alvos de estudos do metabolismo da glicose e sinalização da insulina, porém ainda são pouco explorados.

Os RTKs desempenham um papel vital nos processos de controle da proliferação celular, diferenciação e evasão da apoptose. Até esta data, três ligantes reversíveis (anilinoquinazolinas) do EGFR (Gefitinib®, Erlotinib® e Lapatinib®) foram aprovadas pelo Administração de Alimentos e Medicamentos (FDA) para uso clínico no tratamento do câncer (Goldstein *et al.*, 2008; Chilin *et al.*, 2010). Devido as suas características químicas e farmacológicas, avaliamos o potencial efeito antitumoral da doxazosina em modelos de gliomas.

1.10. Fluorescência

O fenômeno da luminescência é dividido em duas categorias: a fluorescência e a fosforescência. A fluorescência é a emissão da luz a partir de um estado excitado singleto, no qual o elétron excitado não muda a orientação do spin, continuando desemparelhado (Valeur e Berberan-Santos, 2012). Consequentemente, o retorno ao estado fundamental é permitido e ocorre rapidamente via emissão de um fóton. A fluorescência é considerada uma emissão de luz que desaparece simultaneamente com o fim da excitação. Os fluoróforos emitem luz na faixa de comprimentos de onda do espectro visível, ou seja, entre infravermelho e ultravioleta. Em compostos orgânicos, o fenômeno da fluorescência ocorre tipicamente em estruturas aromáticas com ligações ressonantes (π) (Valeur e Berberan-Santos, 2012). Uma das vantagens dessa característica da molécula é a alta sensibilidade de detecção. Esse fenômeno permite estudar a dinâmica dos sistemas promovendo a informação espacial e temporal da amostra analisada. Alguns parâmetros físicos e químicos do microambiente podem influenciar na emissão da fluorescência de uma molécula, como por exemplo: pH, viscosidade, polaridade, pressão, temperatura, potencial elétrico e interações eletrostáticas com biomoléculas. Como consequencia dessa influência do meio na emissão da fluorescencia, algumas moléculas são geralmente usadas como *probes* para investigações fisico-químicas, bioquímicas e em sistemas biológicos (Valeur e Berberan-Santos, 2012; Chung e Eaton, 2013).

Na farmacologia essa característica é muito importante, principalmente quando se estuda tumores cerebrais infiltrativos. Desenvolver fármacos antitumorais que sejam fluorescentes significa ter a possibilidade de selecionar o alvo, quantificar, visualizar as células infiltrativas, facilitar a ressecção cirúrgica e monitorar a resposta terapêutica (Etrych *et al.*, 2016).

1.11. Nanotecnologia aplicada à farmacologia

Nanotecnologia significa, de maneira geral, a habilidade de manipulação dos átomos na escala de 0,1 e 100 nm, visando criar estruturas maiores diferindo das propriedas da matéria da que lhe deu origem, ou seja, criando fundamentalmente uma nova organização estrutural (Illia, 2015). Neste trabalho abordaremos a forma farmacêutica estruturada em nanocápsulas. Na figura 7 é apresentado um desenho esquemático de uma nanocápsula carregada com mesilato de doxazosina.

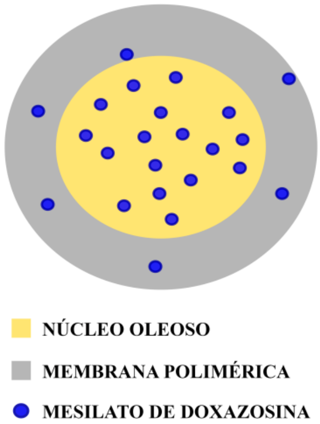

Figura 7. Desenho esquemático da composição de uma nanocápsula com mesilato de doxazosina.

Muitos fármacos atualmente utilizados na terapia antitumoral não diferenciam entre a célula sadia e a neoplásica, gerando grande toxicidade. Problemas farmacodinâmicos, como por exemplo, a rápida eliminação e ampla distribuição do fármaco, requerem administração de grandes quantidades dos agentes antitumorais. Isso resulta muitas vezes em aumento de toxicidade, posologia inadequada e diminuição da adesão ao tratamento. A ampla distribuição é um problema, pois geralmente aumentam os efeitos adversos. A utilização de nanofármacos na terapia antineoplásica, principalmente em se tratando de cancer de SNC, aumenta a vetorização do fármaco no local de ação. As nanocápsulas atravessam a BHE com mais facilidade que o fármaco livre. Essa tecnologia aplicada a famarmacologia muitas vezes é capaz de aumentar a eficiência e eficácia do fármaco (Heath e Davis, 2008; Kang *et al.*, 2016).

Uma das características do tecido canceroso é a alta taxa proliferativa e a presença de neovascularizações. A angiogênese tecidual das células cancerosas resulta muitas vezes em uma arquitetura tecidual defeituosa. Nessas situações, o nanofármaco consegue maior acessibilidade ao local do tumor. Os poros presentes na vasculatura tumoral acumulam nanofármacos de 10 a 100 vezes mais quando comparado com o fármaco livre (Heath e Davis, 2008). Além disso, a entrada das nanopartículas nas células é via endocitose, portanto são capazes de passar pelos múltiplos mecanismos de resistência presentes na superfície celular, como glicoproteína P e bombas protéicas. Visando diminuir a dose terapêutica e aumentar a eficiência e eficácia da DOX, este fármaco foi utilizado na sua forma livre e nanoencapsulada nessa tese (Heath e Davis, 2008; Kang *et al.*, 2016).

2. OBJETIVOS

Objetivo geral

Investigação do potencial terapêutico da DOX em modelos de gliomas *in vitro e in vivo*.

Objetivo Específico 1: Analisar o efeito da hipóxia em modelo *in vitro* de gliomas (Capítulo I)

1) Desenvolver um modelo *in vitro* que se aproxime ao microambiente hipóxico tumoral utilizando células C6;

2) Observar as adaptações celulares (morfologia, marcadores proteicos, atividade mitocondrial) nas células (C6) expostas a hipóxia na presença e ausência de soro;

3) Analisar as adaptações celulares após a reoxigenação;

4) Estudar o tipo de morte celular e caracterizar o microambiente hipóxico.

Objetivo Específico 2: Avaliar o potencial antitumoral da DOX em modelo *in vitro* de gliomas com foco em vias de sinalização celular alteradas pelo fármaco (Capítulo II, III, e V)

1) Analisar o efeito antitumoral da DOX em linhagens de glioma humano (U138-MG) e de rato (C6), por meio da análise da densidade celular, proliferação e morte celular após tratamento em ambas as linhagens;

2) Verificar o envolvimento de algumas proteínas da via de sinalização PI3K/Akt e p53 após o tratamento (24 e 48 h);

3) Avaliar a citotoxicidade da DOX frente a modelos não tumorais: em células (cultura primária de astrócitos) e de fatias de hipocampo de ratos (cultura organotípica).

4) Analisar algumas proteínas envolvidas na sinalização entre a mitocôndria e o núcleo após tratamento com DOX durante 48 h;

5) Avaliar a possível molulação da neuro-inflamação, pela quantificaçãoda secreção de citocinas pró-inflamatórias no meio de cultivo após tratamento com doxazosina (TNF-alfa, IL-1β e IL-6).

6) Induzir superexpressão de EGFR em linhagem de células C6 tratadas com o ligante endógeno (EGF);

7) Analisar o efeito da DOX nas células que receberam pré-tratamento com EGF;

8) Analisar o envolvimento da DOX com a fosforilação do receptor EGFR utilizando o AG1478 (inibidor de RTK);

9) Analisar o efeito do pré-tratamento com EGF, seguido de tratamento com AG1478 e DOX sobre a linhagem celular C6 e propor um possível mecanismo de ação para o fármaco em estudo.

Objetivo Específico 3: Caracterizar a autofluorescência da DOX (Capítulo IV)

1) Analisar a fluorescência da doxazosina no ambiente celular;

2) Investigar a distribuição do fármaco nas células e a captação celular do fármaco;

3) Relacionar (se possível) a distribuição do fármaco nas células com o efeito fisiopatológico.

Objetivo Específico 4: Avaliar o efeito da DOX na sua forma livre e nanoencapsulada nas células de glioma de rato (C6) *in vitro* e *in vivo* (Capítulo VI)

1) Caracterizar, em modelo *in vivo* de implante de glioma, por análise patológica e histológica os grupos tratados com DOX livre, nanoencapsulada e sem tratamento;

2) Estudar o envolvimento da DOX com proteínas-alvo como CD133 e EGFR, *in vitro* e *in vivo*;

3) Avaliar a citotoxicidade do fámaco nanoencapsulado *in vitro* (cultura organotípica de hipocampo de ratos) e *in vivo* através de análise patológica e histológica dos órgãos e parâmetros bioquímicos.

3. CAPÍTULO I

Artigo: *Hypoxic and Reoxygenated Microenvironment: Stemness and Differentiation State in Glioblastoma*

Status: *Publicado no periódico Molecular Neurobiology*

Author's personal copy

Mol Neurobiol
DOI 10.1007/s12035-016-0126-6

Hypoxic and Reoxygenated Microenvironment: Stemness and Differentiation State in Glioblastoma

Mariana Maier Gaelzer[1,2] · **Mariana Silva dos Santos**[1] · **Bárbara Paranhos Coelho**[1] · **Alice Hoffman de Quadros**[1] · **Fabrício Simão**[3] · **Vanina Usach**[4] · **Fátima Costa Rodrigues Guma**[1] · **Patrícia Setton-Avruj**[4] · **Guido Lenz**[5] · **Christianne G. Salbego**[1]

Received: 3 August 2016 / Accepted: 12 September 2016
© Springer Science+Business Media New York 2016

Abstract Glioblastoma (GBM) is the most common and aggressive primary malignant brain tumor in adults. Hypoxia is a distinct feature in GBM and plays a significant role in tumor progression, resistance to treatment, and poor outcome. However, there is lack of studies relating type of cell death, status of Akt phosphorylation on Ser473, mitochondrial membrane potential, and morphological changes of tumor cells after hypoxia and reoxygenation. The rat glioma C6 cell line was exposed to oxygen deprivation (OD) in 5 % fetal bovine serum (FBS) or serum-free media followed by reoxygenation (RO). OD induced apoptosis on both 5 % FBS and serum-free groups. Overall, cells on serum-free media showed more profound morphological changes than cells on 5 % FBS. Moreover, our results suggest that OD combined with absence of serum provided a favorable environment for glioblastoma dedifferentiation to cancer stem cells, since nestin, and CD133 levels increased. Reoxygenation is present in hypoxic tumors through microvessel formation and cell migration to oxygenated areas. However, few studies approach these phenomena when analyzing hypoxia. We show that RO caused morphological alterations characteristic of cells undergoing a differentiation process due to increased GFAP. In the present study, we characterized an in vitro hypoxic microenvironment associated with GBM tumors, therefore contributing with new insights for the development of therapeutics for resistant glioblastoma.

Keywords Cancer · Glioma · Hypoxia · Reoxygenation · C6 · Cancer stem cell

Introduction

Glioblastoma (GBM) is the most common and most lethal form of primary brain tumor. Despite different combinations of treatments, such as radiotherapy and chemotherapy, the average survival for GBM patients is 15 months [1, 2]. These are morphologic, genetic, and phenotypically heterogeneous tumors [3].

GBMs display an elevated proliferation rate with extensive areas of necrosis and hypoxia as a result of this rapid tumor cell growth. Low O_2 levels favor tumor progression through activation of vascular endothelial growth factor (VEGF). In tumor cells, VEGF induces cell proliferation [4] and stimulates cell invasion [5] and is also responsible for maintenance of tumor cells in an undifferentiated phenotype [6].

The tumor microenvironment contains a minor fraction of cancer stem cells (CSCs). CSCs are characterized by self-renewal and maintenance of tumor mass. When transplanted, they are responsible for new tumor growth [7, 8], increased

---

Mariana Maier Gaelzer and Mariana Silva dos Santos contributed equally to this work.

Electronic supplementary material The online version of this article (doi:10.1007/s12035-016-0126-6) contains supplementary material, which is available to authorized users.

✉ Mariana Maier Gaelzer
marianamaierg@gmail.com

[1] Biochemistry Department, Federal University of Rio Grande do Sul, Porto Alegre, RS, Brazil

[2] Biochemistry Department, Institute of Health Sciences, 2600 Ramiro Barcelos Street, Porto Alegre, RS 90035-003, Brazil

[3] Harvard Medical School Joslin Diabetes Center, Boston, MA, USA

[4] Biological Chemistry Department, University of Buenos Aires, Ciudad Autónoma de Buenos Aires, Argentina

[5] Biophysics Department, Federal University of Rio Grande do Sul, Porto Alegre, RS, Brazil

Published online: 06 October 2016

Author's personal copy

chemotherapy resistance, and initiation of tumor invasion by stimulating migration of differentiated cancer cells [8, 9].

The C6 cell line is widely used in the study of gliomas. C6 cells contain a pool of cancer stem cells expressing CD133 and nestin [10], which are the established markers for brain CSCs and can be used for isolating them. Moreover, some studies suggest the use of cell size, granularity, and mitochondrial membrane potential for characterization and isolation of CSCs and stem cells in general [11].

The hypoxic environment drives the selection of more aggressive tumor cells through cellular adaptations [12]. Developing an in vitro model of the hypoxic microenvironment allows for a more in-depth study of those adaptations, contributing to the enhancement of therapies against these aggressive tumor cells. In order to mimic a tumor hypoxic niche and to analyze the adaptations of glioma C6 cells to these conditions, we exposed cells to oxygen deprivation (OD) on serum-free medium or with 5 % fetal bovine serum (FBS). We analyzed cell death; morphological changes; and Akt, VEGF, nestin, CD133, and glial fibrillary acidic protein (GFAP) levels during OD. Additionally, we observed morphological changes indicating phenotypic alterations in the cells during reoxygenation (RO) following OD. Our results provide insight into the cellular alterations caused by a hypoxic microenvironment on GBM tumor cells.

Materials and Methods

Chemicals and Materials

Cell culture media and FBS were obtained from Gibco-Invitrogen (Grand Island, NY, USA). Propidium iodide (PI) was obtained from Sigma Chemical Co (St. Louis, MO, USA). All other reagents were purchased from Sigma Chemical Co or Merck (Darmstadt, Germany). All other chemicals and solvents used were of analytical or pharmaceutical grade.

Cell Culture

The C6 rat glioma cell line was obtained from the American Type Culture Collection (Rockville, MD, USA). Cells were grown and maintained in Dulbecco's modified Eagle's Medium (DMEM; Gibco-Invitrogen) supplemented with 5 % (*v*/*v*) FBS (Gibco-Invitrogen) containing 2.5 mg/mL Fungizone and 100 U/L gentamicin (Shering do Brasil, São Paulo, SP, Brazil). Cells were incubated at 37 °C in a minimum relative humidity of 5 % CO_2 atmosphere. Experiments throughout this study were conducted either in serum-free DMEM or in serum-supplemented DMEM.

Oxygen Deprivation

OD was achieved according to the method described by Strasser and Fischer [13] with some modifications [14]. C6 glioma cells were seeded at 4.5×10^3 cells/well in DMEM/5 % FBS in six-well plates and grown for 72 h. Following the 72 h growth, the group that received serum during OD had its medium replaced by conventional 5 % FBS media previously bubbled with N_2 for 30 min. The group that did not receive serum had its medium replaced with serum-free DMEM, also previously bubbled with N_2 for 30 min. Plates were immediately transferred to an anaerobic chamber at 37 °C in a N_2-enriched atmosphere for 15 min, 1 h, or 3 h. Controls were maintained in an incubator with 5 % CO_2 atmosphere at 37 °C.

Flow Cytometry Analysis

Flow cytometry was used to evaluate size and granularity of cells, cell death, proteins levels, and mitochondrial mass and membrane potential. After OD, culture medium and cells were harvested with trypsin. Cells were then evaluated for size and granularity using the forward-scatter (FSC) and side-scatter (SSC) light parameters and stained with dyes or incubated with the proper antibodies for flow cytometry analysis using a FACSCalibur flow cytometer (Becton Dickinson, Franklin Lakes, NJ, USA). Analysis was performed using the FCS Express 5 software (De Novo Software, Los Angeles, CA, USA).

Classification of Cell Death

Apoptotic and necrotic cell deaths were analyzed by flow cytometry by double staining with fluorescein isothiocyanate (FITC)-conjugated annexin V and PI for 20 min. Staining was performed according to the manufacturer's instructions (BD Pharmingen, San Diego, CA, USA). Flow cytometry analysis was performed as described in "Flow Cytometry Analysis" section.

Classification of Cell Size and Granularity

As the population of cells appeared to be morphologically heterogeneous, parameters of cell size and granularity were measured by flow cytometry and plotted against markers of cell death. Cells were divided into three subpopulations based on size: small (S), medium (M), and large (L). To assess the distribution of granularity between viable and dead cells, cells were divided into two subpopulations based on flow cytometry

Author's personal copy

analysis according to their granularity: regular (G1) and granular (G2).

Immunodetection

To investigate cellular adaptations to hypoxia, key proteins were studied. After OD and RO periods, cells were fixed with phosphate-buffered saline (PBS) and 4 % paraformaldehyde for 20 min, then cells were permeabilized with PBS and 0.01 % Triton X-100 and/or incubated with the primary antibodies anti-VEGF (1:100; Santa Cruz Biotech, Dallas, TX, USA), anti-Akt (1:50; Cell Signaling Technology™, Beverly, MA, USA), anti-p-Akt$_{Ser473}$ (1:50; Cell Signaling Technology™), anti-nestin (1:50; Cell Signaling Technology™), anti-GFAP (1:50; Cell Signaling Technology™), and anti-CD133 (1:50; Cell Signaling Technology™) for 30 min. The secondary antibody, Alexa Fluor 488 anti-mouse or Alexa Fluor 555 anti-mouse (1:100; Gibco-Invitrogen), was added, and after a 60 min incubation, cells were analyzed by flow cytometry.

MitoTracker Staining

Mitochondrial mass and membrane potential were evaluated using MitoTracker® Green and MitoTracker® Red (Invitrogen®, Molecular Probes, Eugene, OR, USA), respectively. Cells were incubated in a PBS/MitoTracker Green/Red solution (100 nM) at 37 °C, in the dark, for 45 min.

Microscopy

To identify cell death, 5 μM PI and 2.5 μM 4′,6-diamidino-2-phenylindole (DAPI) was added to C6 glioma cells after induction of OD. PI fluorescence was excited at 515–560 nm using an inverted microscope (Nikon Eclipse TE300; Nikon, Tokyo, Japan) fitted with a standard rhodamine filter. For nucleous stain 2.5 μM of DAPI was added. DAPI was excited by the violet 405 nm laser line, and images were captured using a digital camera connected to the microscope. Sulforhodamine B (SRB) assay was used for staining cell proteins. Cells were fixed with PBS/FORMOL 4 % for 15 min and stained with SRB. Unbound stain was washed, and cells were analyzed on an Olympus FV1000 laser scanning confocal microscope. All images were processed with ImageJ software (NIH, Bethesda, MD, USA).

Reoxygenation Assay

OD was performed in serum-free medium for 15 min, 1 h, or 3 h, followed by cells being maintained in an incubator with 5 % CO_2 atmosphere at 37 °C for 15 min, 1 h, 3 h, or 24 h (RO) in 5 % FBS medium. Controls were maintained in an incubator with 5 % CO_2 atmosphere at 37 °C. After RO periods, images were captured using a digital camera connected to the microscope (Nikon Eclipse TE300, Nikon). Morphological changes during RO periods were analyzed and compared to OD groups.

Statistical Analysis

Data are expressed as mean ± SD. All results are representative of at least three independent experiments. One-way analysis of variance or Student's *t* test was applied to the means to determine statistical differences between experimental groups. Post hoc comparisons were performed by Tukey's test. Differences between mean values were considered significant at $p < 0.05$.

Results

OD Treatment Induces Apoptosis

For cells in 5 % FBS, viability was significantly reduced following a 3 h OD, while apoptosis increased during 1 and 3 h OD (Fig. 1a). Cells exposed to serum-free media, however, showed diminished viability with significant increase in apoptosis at the 1 and 3 h time points (Fig. 1b). These findings were supported by photomicrographs showing DAPI and PI staining results (Figs. S1 and S2).

C6 Glioma Cells Display Media-Specific Size Fluctuations

The majority of viable cells were sized in the M range, contrasting with the dead cells, which were frequently larger (Figs. 2 and S3). In 5 % FBS media, the viable cells decreased in size (from L to M) after 1 and 3 h OD (Figs. 2a and S3a). For dead cells, OD caused an increase in the number of S cells at the 1 h time point (Figs. 2a and S3a).

In serum-free media, although cell viability decreased with OD treatment, the remaining viable cells increased in size after 1 and 3 h OD (Figs. 2b and S3b). Meanwhile, following OD treatment, apoptotic cells displayed significant increases in cell size relative to the control apoptotic cells at the 1 and 3 h time points (Figs. 2b and S3b).

Author's personal copy

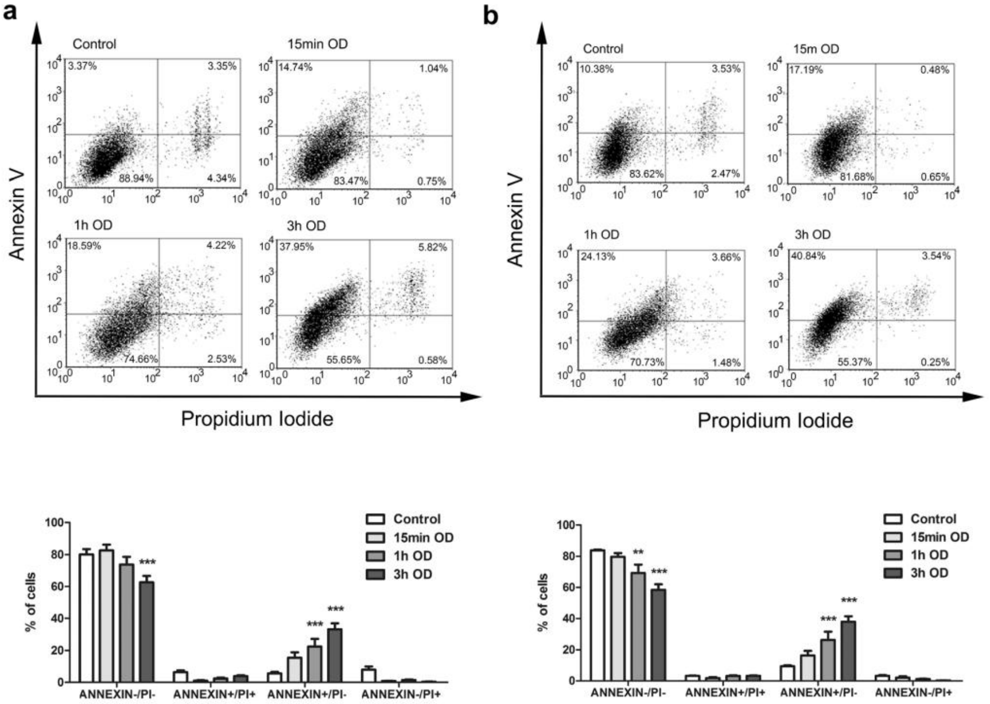

Fig. 1 OD treatment induces apoptotic cell death. *Dot-plot* analysis from flow cytometry of cells in **a** 5 % FBS medium or **b** serum-free medium. Percentage of cells according to viability and type of cell death: annexin V−/PI− (viable cells), annexin V+/PI+ (late apoptosis), annexin V+/PI− (apoptosis), and annexin V−/PI+ (necrosis). Data are represented as mean ± SEM ($n = 6$). $^{**}p < 0.01$, $^{***}p < 0.001$ vs. control

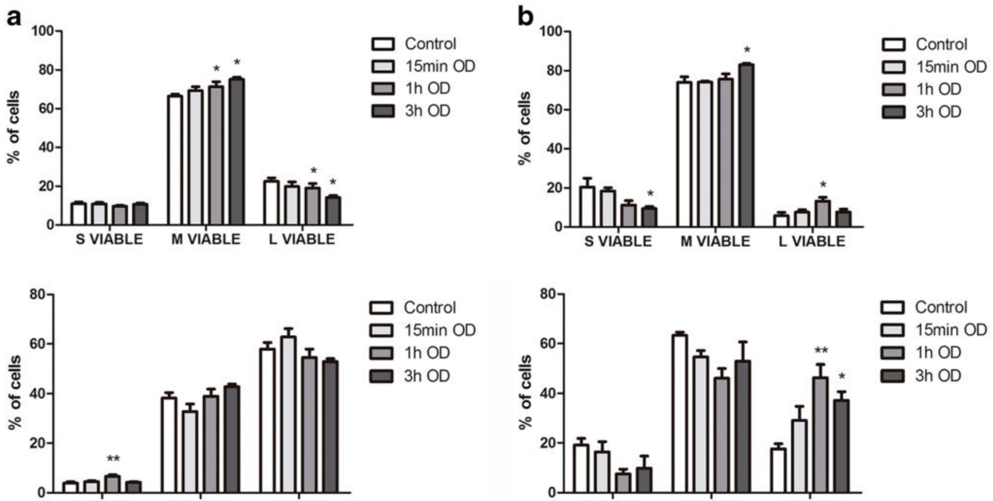

Fig. 2 Analysis of cell size. Cells were stained with annexin V and PI and categorized into three sizes: small [S], medium [M], and large [L]. Distribution of cell size in viable and dead cells in **a** 5 % FBS medium or **b** serum-free medium. Data are represented as mean ± SEM ($n = 6$). $^{*}p < 0.05$, $^{**}p < 0.01$ vs. control

Author's personal copy

Apoptotic Cell Granularity Increases in Serum-Free Media

The majority of viable cells in 5 % FBS media displayed regular granularity (G1) that remained unchanged after all OD time periods, while the majority of dead cells were observed in the G2 range (Figs. 3a and **S4**a).

In the control group of the serum-free media, the majority of viable cells displayed regular granularity (G1), with only a rare subpopulation of viable cells presenting as G2 (Figs. 3b and **S4**b). The number of viable cells presenting as G2 increased at the 15 min and 1 h OD time points, and this number appeared to decrease with OD duration (Figs. 3b and **S4**b). Regular granularity (G1) in the serum-free media group was also predominant in control dead cells; however, dead cells that had been exposed to OD exhibited increased granularity (Figs. 3b and **S4**b). These results suggested that cells exposed to serum-free media were more granular.

Mitochondrial Membrane Potential during OD

In the 5 % FBS group, a 3 h OD caused depolarization of the mitochondrial membrane in a subpopulation of cells, as reflected by the lower fluorescence intensity of MitoTracker Red on gate 2 (Fig. 4a). A small subpopulation of cells (gate 3) with hyperpolarized mitochondrial membrane increased after the 15 min OD (Fig. 4a).

In the serum-free group, depolarization occurred as early as 15 min OD and persisted during 1 and 3 h (Fig. 4b). The small subpopulation of cells with high hyperpolarized mitochondrial membrane (gate 3) increased during the 15 min and 1 h OD (Fig. 4b).

OD Alters Akt, VEGF, CD133, and Nestin Levels

Akt is involved in signaling pathways regulating differentiation/dedifferentiation and cell death control. During all OD times, p-$\mathrm{Akt}_{\mathrm{Ser473}}$ levels were decreased, on both 5 % FBS and serum-free groups (Fig. 5). Akt levels remained the same as the control group.

To analyze morphological changes and stemness, cells were analyzed for VEGF levels using flow cytometry (Fig. 6a). Our results indicated an increase in VEGF levels in cells exposed to 1 h OD compared with the control group, also on both 5 % FBS and serum-free groups (Fig. 6a). VEGFR levels remained unchanged (data not shown).

CD133 and nestin are cell markers of cancer stem cells. For cells in serum-free medium, nestin and CD133 were significantly increased in 1 h OD (Fig. 6b, c). In 5 % FBS, there was a tendency of an increase in CD133 levels (p = 0.0603). GFAP was unaltered (Fig. 6d).

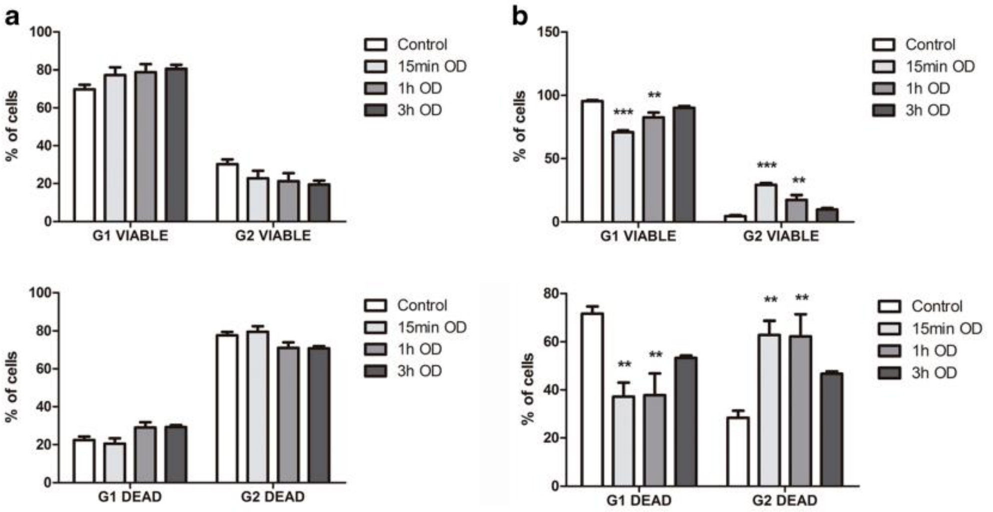

Fig. 3 Analysis of cell granularity. Cells were stained with annexin V and PI and categorized based on their granularity: regular [G1] and more granular [G2]. Distribution of granularity in viable and dead cells in **a** 5 % FBS medium or **b** serum-free medium. Data are represented as mean ± SEM (n = 6). $^{**}p < 0.01$, $^{***}p < 0.001$ vs. control

Author's personal copy

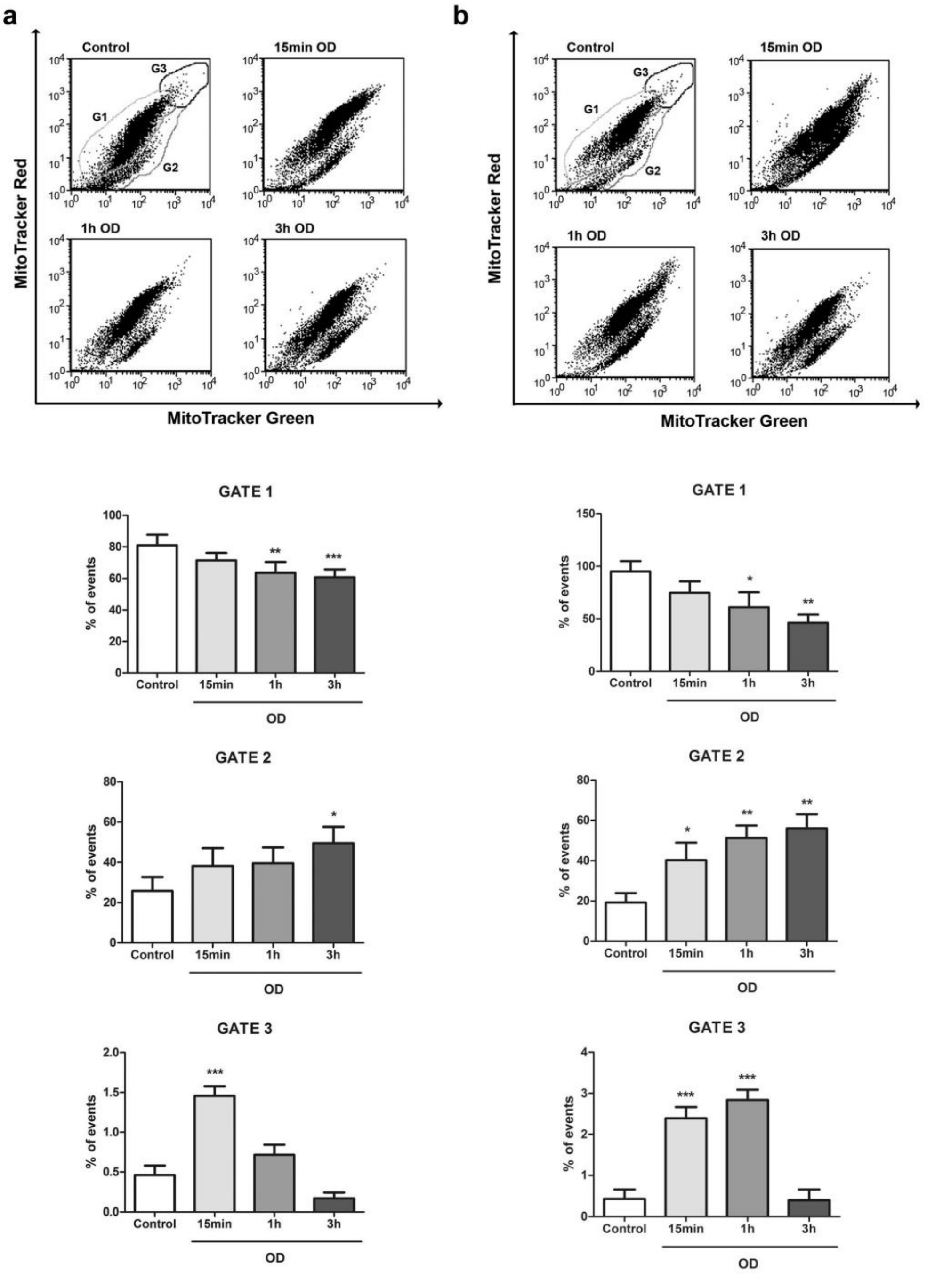

]

Author's personal copy

◀ **Fig. 4** *Dot-plot* analysis and distribution of gated events from flow cytometry of cells in **a** 5 % FBS medium or **b** serum-free medium stained with MitoTracker Green vs. MitoTracker Red. Cells were gated accordingly with different stained populations observed on control cells as shown on the *dot-plot* and as follows: *G1* gate 1; *G2* gate 2; *G3* gate 3. Data are represented as means ± SEM ($n = 6$). $^{*}p < 0.05$, $^{**}p < 0.01$, and $^{***}p < 0.001$ vs. control

Morphological and Protein Markers Changes Caused by Oxygen Deprivation and Reoxygenation

In C6 cells, 1 h OD in serum-free medium followed by 24 h RO increased CD133 and GFAP levels, while nestin remained unaltered (Fig. 7). Control cells displayed long spindles and evenly distributed processes (Figs. S1 and S2). After OD, cells became polygonal and processes decreased. As the time under OD conditions increased, the cells became oval-shaped and processes were absent (Figs. S1 and S2). As the duration of RO increased, cells became more long-spindled and displayed larger and thinner processes as well as decreased sizes (Figs. S3 and S4 and Table S1). These morphological changes were more pronounced during longer periods of hypoxia and RO.

Discussion

Tumor hypoxia is usually associated with poor patient prognosis and with resistance to therapy in GBMs [15]. In addition, this state contributes to glioblastoma cell proliferation, angiogenic drive, and metastasis/invasion [16, 17]. Hypoxic conditions also induce an immature phenotype on human neuroblastoma and breast cancer lines [18].

Hypoxia can lead to apoptotic or necrotic cell death with no consensus in the literature regarding the type of death [19–21]. Here, we exposed C6 cells to OD in the presence or absence of serum and observed that both groups presented mitochondrial membrane potential depolarization and cell death by apoptosis (Fig. 8).

Several studies demonstrated that hypoxia in vitro is a relatively strong inducer of apoptosis in colon carcinoma cell lines (HT29 and HCT116), oral cancer cells, glioma cell lines (U87, U251), and primary glioma cells [7, 12, 19]. One theory to explain the induction of apoptosis in cancer cells is that, due to tumor heterogeneity, some cells are more sensible to hypoxic DNA damage. Yao et al. [12] also hypothesized that mutational events are responsible for increased apoptosis susceptibility.

Previous studies have demonstrated that hypoxia activates Akt, which is in contrast with our findings. According to the literature, hypoxia induces phosphorylation of Akt at Ser473. In our study, however, $\text{pAkt}_{\text{Ser473}}$ levels were decreased during all OD times. Leszczynska et al. [22] demonstrated that activation of Akt occurred only in P53-null or mutant cells (HCT116 p53, H1299, OE21, and PSN1) but not in P53 wild-type (p53-wt) cells (RKO and HCT116). They suggest that p53 may be negatively regulating Akt activation on hypoxia and thus promoting apoptosis. C6 rat glioma cell line is p53-wt [23], and this could explain the decrease in Akt phosphorylation caused by hypoxia.

Zenali et al. [24] observed that increased granularity was related with an increase in CD133 expression. Cell size can be an important predictor of the metabolic state and metabolic reprogramming. CSCs are usually smaller than differentiated cancer cells, and the metabolic necessity is also lower [25]. Here, we show that hypoxia on the 5 % FBS group caused a decrease in viable cell size, but CSCs markers CD133 and nestin remained unaltered. This conditions were not sufficient to increase CD133 and nestin possibly because the environment was unsuitable, i.e., lacking autocrine factors that could induce cells to fully dedifferentiate.

On the other hand, hypoxia on the serum-free group caused an increase in viable cell size with increase in CD133 and nestin. Studies show a relationship between cell size and granularity on neural stem cells (NSCs): populations with increased size and granularity show enrichment of NSCs [26–28].

Increased mitochondrial membrane potential (Δψm) is proposed as a characteristic of CSCs [29]. Cells with intrinsically higher Δψm demonstrate higher resistance to hypoxia and increased CD133 expression and show greater potential to form tumors [30]. Moreover, glioblastoma CSCs expressing CD133 exhibited elevated Δψm [31]. These suggest that CSCs may have a different Δψm when compared with differentiated carcinoma cells [29, 32]. Here, a subpopulation of C6 cells with high Δψm was identified on normal culture conditions and on normoxia with serum-free medium. In the 5 % FBS group, 15 min OD increased this subpopulation of cells, and in the serum-free group, this increase was more pronounced and also appeared after 1 h OD. This result on the serum-free group corroborates with our hypothesis that the combination of hypoxia and the lack of serum promoted an increase in the CSCs population, since in the 1 h OD there was also an increase in CD133 and nestin expression.

Author's personal copy

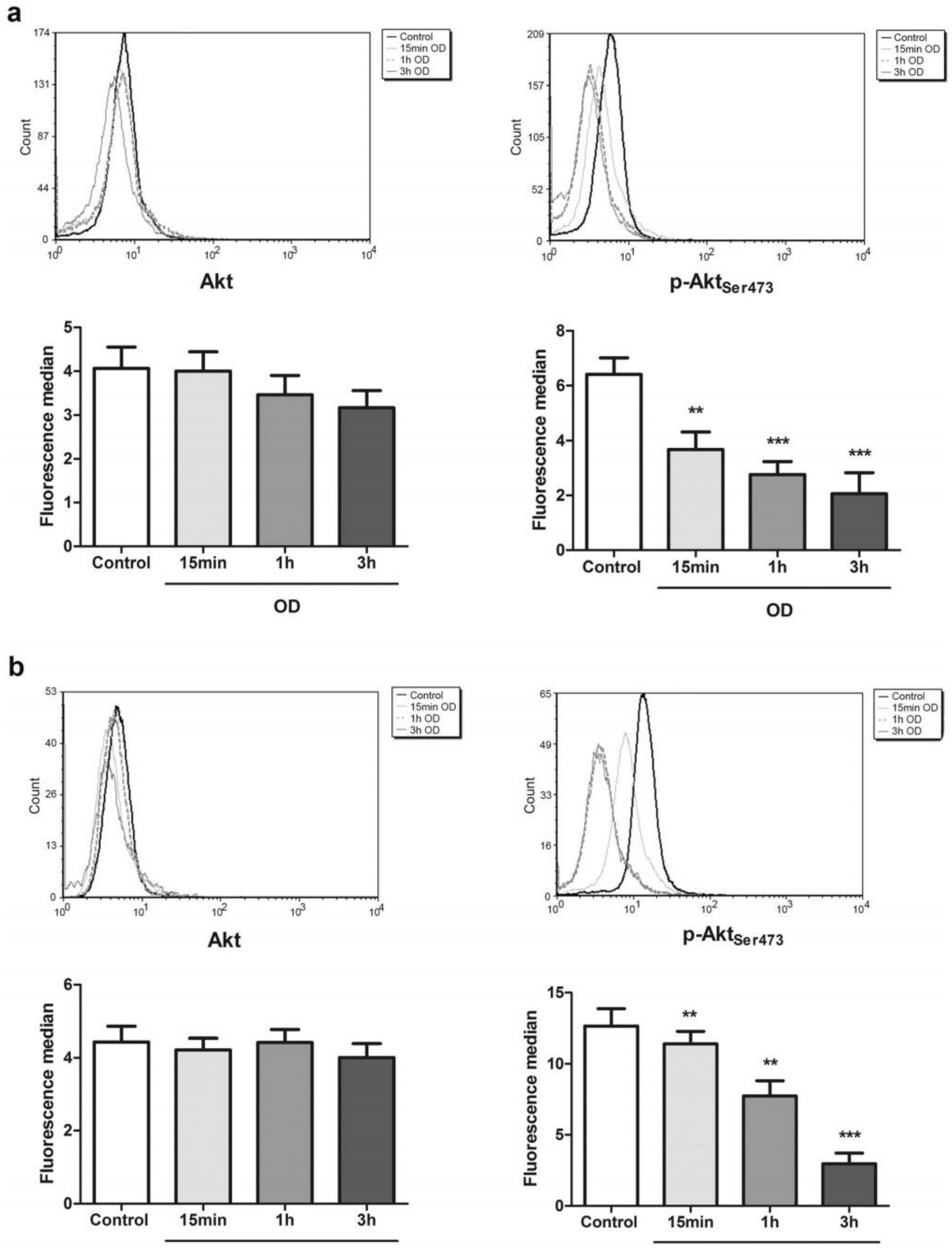

Fig. 5 Akt and p-Akt$_{Ser473}$ protein levels in C6 after OD, in **a** 5 % FBS and **b** serum-free media. Data are represented as means ± SEM ($n = 6$). **$p < 0.01$ and ***$p < 0.001$ vs. control

VEGF helps maintain tumor cells in a stemness phenotype [33, 6]. After 1 h OD, VEGF levels increased in 5 % FBS and serum-free groups. These results confirm the morphological changes that occurred during OD:

Author's personal copy

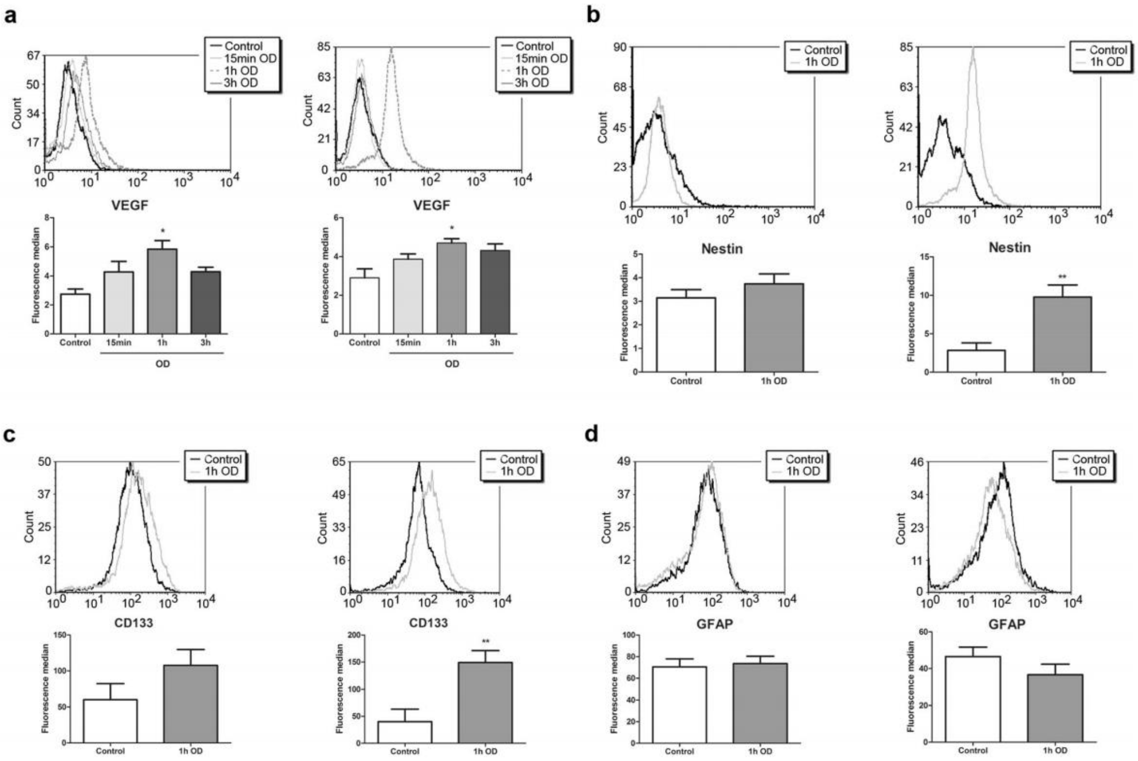

Fig. 6 Protein levels of **a** VEGF, **b** nestin, **c** CD133, and **d** GFAP in C6 cells after OD. On the *left side* of each protein level, the 5 % FBS group is represented, while the serum-free group is on the *right side*. Data are represented as mean ± SEM ($n = 6$). $^*p < 0.05$ and $^{**}p < 0.01$ vs. control

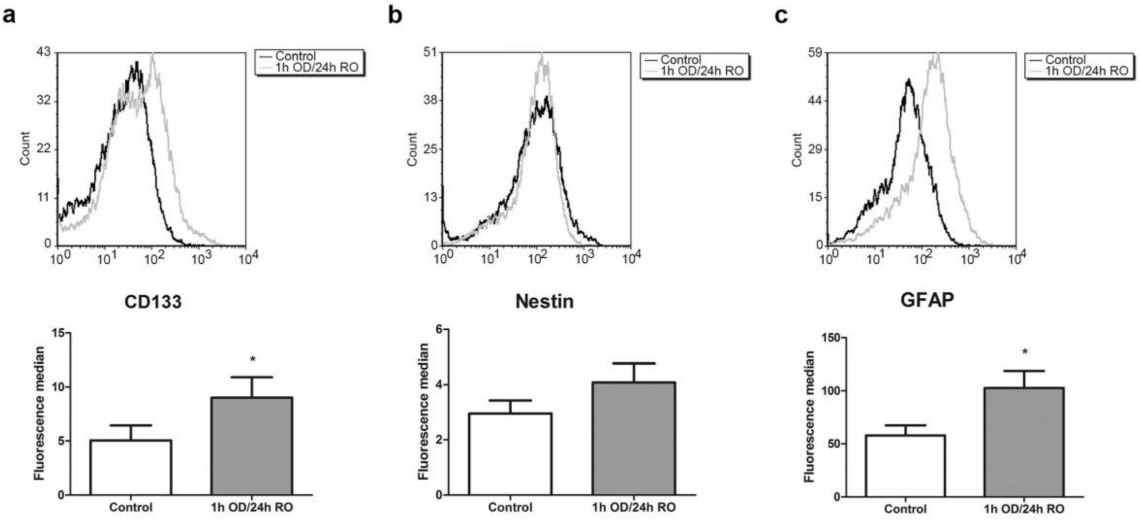

Fig. 7 Expression levels of **a** CD133, **b** nestin, and **c** GFAP after 1 h OD in serum free medium and 24 h RO in C6 cells. Data are represented as means ± SEM ($n = 6$). $^*p < 0.05$ vs. control

Author's personal copy

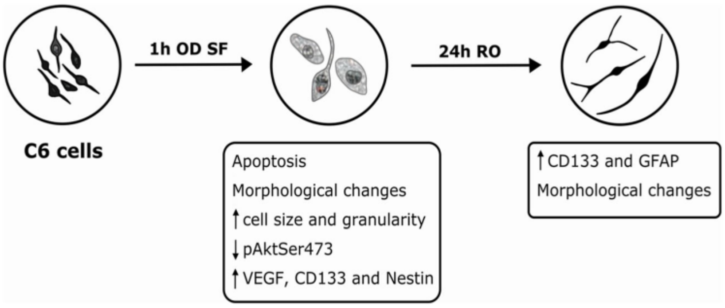

Fig. 8 Schematic illustration of the effects of in vitro oxygen deprivation in the absence of serum and of reoxygenation on C6 glioma cells

oval-shaped bodies and absence of cellular processes, a characteristic of stemness [7]. The serum-free group showed more profound changes in viable cell morphology than the 5 % FBS group. Moreover, nestin and CD133 levels increased after 1 h OD in the serum-free group, which is a characteristic of cancer stem cells. In the 5 % FBS group, however, nestin and CD133 levels remained unaltered after OD. Studies demonstrate that the absence of serum and the combination of basic fibroblast growth factor (bFGF) and platelet-derived growth factor (PDGF) seem to be able to maintain subpopulations of cancer stem cells [30, 34–37]. In addition, in vitro hypoxia can stimulate autocrine secretion of PDGF and bFGF [38]. The differences in our findings regarding the 5 % FBS and the serum-free groups highlight the importance of serum for cell dedifferentiation. In the presence of serum, hypoxia caused morphological changes characteristic of stem cells and increased VEGF levels, but did not induce dedifferentiation, since nestin and CD133 levels remained unaltered. The absence of serum in conjunction with hypoxia, however, seems to promote a favorable environment for cell dedifferentiation.

Segovia et al. [39] provide the evidence that C6 CSCs express proteins and mRNAs that are characteristic of both glia and neurons, and they can differentiate into both types of cells in vitro and in vivo. Li et al. [7] described that hypoxia induces dedifferentiation of differentiated glioma cells, causing them to acquire stemness. Moreover, neural precursors maintain undifferentiated phenotypes in low O_2 concentrations, while higher O_2 concentrations promote cellular differentiation.

Here, we showed that OD promoted C6 cell dedifferentiation, while reoxygenation appeared to cause differentiation of CSCs. The increase in GFAP levels and the cell morphology after 24 h RO supports this hypothesis. CD133 levels, however, also increased after 24 h RO, suggesting that some cells maintained stemness even in the presence of O_2, as occurs in the microenvironment of hypoxic tumors.

Therefore, models of GBM tumors in hypoxic conditions and the data presented in this study support the hypothesis that hypoxic niches contribute to GBM malignancy. Given that limited O_2 concentration is important for tumor progression and therapy resistance, studies of more efficient antitumoral strategies require increased understanding of the tumor microenvironment, which is characterized by lack of O_2.

Moreover, our study shows the importance of serum for in vitro analysis of the hypoxic tumoral microenvironment. Hypoxia in the absence of serum induced C6 cells to dedifferentiate to a CSCs phenotype, while the presence of serum caused subtle changes. Another important factor to be considered when studying in vitro hypoxia on cancer cells is p53 status. P53 mutations can confer apoptosis and chemotherapy resistance to cancer cells, and this can affect their response to hypoxia. We believe that the lack of consensus between different studies on hypoxia effects on tumor cells is due to varying approaches regarding these factors. Also, few studies analyze the reoxygenation period. In hypoxic tumors, reoxygenation can occur when cells receive oxygen from newly formed microvasculatures or when hypoxic-resistant cells migrate to more oxygenated areas. Therefore, analysis of reoxygenation in vitro is important to characterize those adaptive changes on cancer cells.

Regarding GBM, there needs to be greater understating of CSCs adaptations to the hypoxic microenvironment in order to develop effective treatments for this lethal tumor. Such knowledge can provide novel targets against therapy-resistant glioblastoma.

Author's personal copy

Compliance with Ethical Standards

Funding This study was funded by Conselho Nacional de Desenvolvimento Científico e Tecnológico (CNPq), Coordenação de Aperfeiçoamento de Pessoal de Nível Superior (Capes), and Fundação de Amparo à Pesquisa do Estado do Rio Grande do Sul (FAPERGS).

References

1. Oike T, Suzuki Y, K-i S, Shirai K, S-e N, Tamaki T, Nagaishi M, Yokoo H, Nakazato Y, Nakano T (2013) Radiotherapy plus concomitant adjuvant temozolomide for glioblastoma: Japanese mono-institutional results. PLoS One 8(11):e78943
2. Sengupta S, Marrinan J, Frishman C, Sampath P (2012) Impact of temozolomide on immune response during malignant glioma chemotherapy. Clin Dev Immunol 2012
3. Shen G, Shen F, Shi Z, Liu W, Hu W, Zheng X, Wen L, Yang X (2008) Identification of cancer stem-like cells in the C6 glioma cell line and the limitation of current identification methods. Vitro Cellular & Developmental Biology-Animal 44(7):280–289
4. Knizetova P, Ehrmann J, Hlobilkova A, Vancova I, Kalita O, Kolar Z, Bartek J (2008) Autocrine regulation of glioblastoma cell-cycle progression, viability and radioresistance through the VEGF-VEGFR2 (KDR) interplay. Cell Cycle 7(16):2553–2561
5. Bachelder RE, Wendt MA, Mercurio AM (2002) Vascular endothelial growth factor promotes breast carcinoma invasion in an autocrine manner by regulating the chemokine receptor CXCR4. Cancer Res 62(24):7203–7206
6. Hamerlik P, Lathia JD, Rasmussen R, Wu Q, Bartkova J, Lee M, Moudry P, Bartek J, Fischer W, Lukas J (2012) Autocrine VEGF–VEGFR2–Neuropilin-1 signaling promotes glioma stem-like cell viability and tumor growth. J Exp Med 209(3):507–520
7. Li P, Zhou C, Xu L, Xiao H (2013) Hypoxia enhances stemness of cancer stem cells in glioblastoma: an in vitro study. Int J Med Sci 10(4):399–407
8. Karamboulas C, Ailles L (2013) Developmental signaling pathways in cancer stem cells of solid tumors. Biochimica et Biophysica Acta (BBA)-General Subjects 1830(2):2481–2495
9. Swamydas M, Ricci K, Rego SL, Dréau D (2013) Mesenchymal stem cell-derived CCL-9 and CCL-5 promote mammary tumor cell invasion and the activation of matrix metalloproteinases. Cell Adhes Migr 7(3):315–324
10. Zhou X, Wang X, Qu F, Zhong Y, Lu X, Zhao P, Wang D, Huang Q, Zhang L, Li X (2009) Detection of cancer stem cells from the C6 glioma cell line. J Int Med Res 37(2):503–510
11. Ye X-Q, Wang G-H, Huang G-J, Bian X-W, Qian G-S, Yu S-C (2011) Heterogeneity of mitochondrial membrane potential: a novel tool to isolate and identify cancer stem cells from a tumor mass? Stem Cell Rev Rep 7(1):153–160
12. Yao K, Gietema J, Shida S, Selvakumaran M, Fonrose X, Haas N, Testa J, O'Dwyer P (2005) In vitro hypoxia-conditioned colon cancer cell lines derived from HCT116 and HT29 exhibit altered apoptosis susceptibility and a more angiogenic profile in vivo. Br J Cancer 93(12):1356–1363
13. Strasser U, Fischer G (1995) Quantitative measurement of neuronal degeneration in organotypic hippocampal cultures after combined oxygen/glucose deprivation. J Neurosci Methods 57(2):177–186
14. Cimarosti H, Rodnight R, Tavares A, Paiva R, Valentim L, Rocha E, Salbego C (2001) An investigation of the neuroprotective effect of lithium in organotypic slice cultures of rat hippocampus exposed to oxygen and glucose deprivation. Neurosci Lett 315(1):33–36
15. Keith B, Simon MC (2007) Hypoxia-inducible factors, stem cells, and cancer. Cell 129(3):465–472
16. Li Z, Bao S, Wu Q, Wang H, Eyler C, Sathornsumetee S, Shi Q, Cao Y, Lathia J, McLendon RE (2009) Hypoxia-inducible factors regulate tumorigenic capacity of glioma stem cells. Cancer Cell 15(6):501–513
17. Zagzag D, Lukyanov Y, Lan L, Ali MA, Esencay M, Mendez O, Yee H, Voura EB, Newcomb EW (2006) Hypoxia-inducible factor 1 and VEGF upregulate CXCR4 in glioblastoma: implications for angiogenesis and glioma cell invasion. Lab Investig 86(12):1221–1232
18. Axelson H, Fredlund E, Ovenberger M, Landberg G, Påhlman S (2005) Hypoxia-induced dedifferentiation of tumor cells—a mechanism behind heterogeneity and aggressiveness of solid tumors. In: Seminars in cell & developmental biology, vol 4. Elsevier, pp. 554–563
19. Nagaraj NS, Vigneswaran N, Zacharias W (2004) Hypoxia-mediated apoptosis in oral carcinoma cells occurs via two independent pathways. Mol Cancer 3(1):1
20. Harris AL (2002) Hypoxia—a key regulatory factor in tumour growth. Nat Rev Cancer 2(1):38–47
21. Weinmann M, Jendrossek V, Handrick R, Güner D, Goecke B, Belka C (2004) Molecular ordering of hypoxia-induced apoptosis: critical involvement of the mitochondrial death pathway in a FADD/caspase-8 independent manner. Oncogene 23(21):3757–3769
22. Leszczynska KB, Foskolou IP, Abraham AG, Anbalagan S, Tellier C, Haider S, Span PN, O'Neill EE, Buffa FM, Hammond EM (2015) Hypoxia-induced p53 modulates both apoptosis and radiosensitivity via AKT. J Clin Invest 125(6):2385–2398
23. Asai A, Miyagi Y, Sugiyama A, Gamanuma M, Hong SI, Takamoto S, Nomura K, Matsutani M, Takakura K, Kuchino Y (1994) Negative effects of wild-type p53 and s-Myc on cellular growth and tumorigenicity of glioma cells. J Neuro-Oncol 19(3):259–268
24. Zenali MJ, Tan D, Li W, Dhingra S, Brown RE (2010) Stemness characteristics of fibrolamellar hepatocellular carcinoma: immunohistochemical analysis with comparisons to conventional hepatocellular carcinoma. Annals of Clinical & Laboratory Science 40(2):126–134
25. Li Q, Rycaj K, Chen X, Tang DG (2015) Cancer stem cells and cell size: a causal link? In: Seminars in cancer biology. Elsevier, pp. 191–199
26. Murayama A, Matsuzaki Y, Kawaguchi A, Shimazaki T, Okano H (2002) Flow cytometric analysis of neural stem cells in the developing and adult mouse brain. J Neurosci Res 69(6):837–847
27. Rietze RL, Valcanis H, Brooker GF, Thomas T, Voss AK, Bartlett PF (2001) Purification of a pluripotent neural stem cell from the adult mouse brain. Nature 412(6848):736–739
28. Narayanan G, Poonepalli A, Chen J, Sankaran S, Hariharan S, Yu YH, Robson P, Yang H, Ahmed S (2012) Single-cell mRNA profiling identifies progenitor subclasses in neurospheres. Stem Cells Dev 21(18):3351–3362
29. J-j D, Qiu W, Xu S-l, Wang B, X-z Y, Y-f P, Zhang X, X-w B, Yu S-c (2013) Strategies for isolating and enriching cancer stem cells: well begun is half done. Stem Cells Dev 22(16):2221–2239
30. Zheng X, Shen G, Yang X, Liu W (2007) Most C6 cells are cancer stem cells: evidence from clonal and population analyses. Cancer Res 67(8):3691–3697

Author's personal copy

31. Michelakis E, Sutendra G, Dromparis P, Webster L, Haromy A, Niven E, Maguire C, Gammer T-L, Mackey J, Fulton D (2010) Metabolic modulation of glioblastoma with dichloroacetate. Sci Transl Med 2(31):31ra34
32. Schieke SM, Ma M, Cao L, McCoy JP, Liu C, Hensel NF, Barrett AJ, Boehm M, Finkel T (2008) Mitochondrial metabolism modulates differentiation and teratoma formation capacity in mouse embryonic stem cells. J Biol Chem 283(42):28506–28512
33. Seton-Rogers S (2011) Cancer stem cells: VEGF promotes stemness. Nat Rev Cancer 11(12):831–831
34. Yuan X, Curtin J, Xiong Y, Liu G, Waschsmann-Hogiu S, Farkas DL, Black KL, John SY (2004) Isolation of cancer stem cells from adult glioblastoma multiforme. Oncogene 23(58):9392–9400
35. Galli R, Binda E, Orfanelli U, Cipelletti B, Gritti A, De Vitis S, Fiocco R, Foroni C, Dimeco F, Vescovi A (2004) Isolation and characterization of tumorigenic, stem-like neural precursors from human glioblastoma. Cancer Res 64(19):7011–7021
36. Sakaki T, Yamada K, Otsuki H, Yuguchi T, Kohmura E, Hayakawa T (1995) Brief exposure to hypoxia induces bFGF mRNA and protein and protects rat cortical neurons from prolonged hypoxic stress. Neurosci Res 23(3):289–296
37. Kyurkchiev D (2014) Cancer stem cells from glioblastoma multiforme: culturing and phenotype. Stem Cells 2(1):3
38. Freyhaus H, Dagnell M, Leuchs M, Vantler M, Berghausen EM, Caglayan E, Weissmann N, Dahal BK, Schermuly RT, Östman A (2011) Hypoxia enhances platelet-derived growth factor signaling in the pulmonary vasculature by down-regulation of protein tyrosine phosphatases. Am J Respir Crit Care Med 183(8):1092–1102
39. Segovia J, Lawless GM, Tillakaratne NJ, Brenner M, Tobin AJ (1994) Cyclic AMP decreases the expression of a neuronal marker (GAD67) and increases the expression of an astroglial marker (GFAP) in C6 cells. J Neurochem 63(4):1218–1225

4. CAPÍTULO II

Artigo: *Phosphatidylinositol 3-Kinase/AKT Pathway Inhibition by Doxazosin Promotes Glioblastoma Cells Death, Upregulation of p53 and Triggers Low Neurotoxicity*

Status: *Publicado no periódico PLoS ONE*

PLOS | ONE

RESEARCH ARTICLE

Phosphatidylinositol 3-Kinase/AKT Pathway Inhibition by Doxazosin Promotes Glioblastoma Cells Death, Upregulation of p53 and Triggers Low Neurotoxicity

Mariana Maier Gaelzer[1]*, Bárbara Paranhos Coelho[1], Alice Hoffmann de Quadros[2], Juliana Bender Hoppe[1], Silvia Resende Terra[1], Maria Cristina Barea Guerra[1], Vanina Usach[3], Fátima Costa Rodrigues Guma[1,2], Carlos Alberto Saraiva Gonçalves[1,2], Patrícia Setton-Avruj[3], Ana Maria Oliveira Battastini[1,2], Christianne Gazzana Salbego[1,2]

1 Programa de Pós-Graduação em Ciências Biológicas: Bioquímica, Instituto de Ciências Básicas da Saúde, Universidade Federal do Rio Grande do Sul (UFRGS), Porto Alegre, RS, Brasil, **2** Departamento de Bioquímica, Instituto de Ciências Básicas da Saúde, Universidade Federal do Rio Grande do Sul (UFRGS), Porto Alegre, RS, Brasil, **3** Departamento de Química Biológica, Facultad de Farmácia y Bioquímica, Universidad de Buenos Aires (UBA), Ciudad Autónoma de Buenos Aires, Argentina

* marianamaierg@gmail.com

Abstract

Glioblastoma is the most frequent and malignant brain tumor. Treatment includes chemotherapy with temozolomide concomitant with surgical resection and/or irradiation. However, a number of cases are resistant to temozolomide, as well as the human glioblastoma cell line U138-MG. We investigated doxazosin's (an antihypertensive drug) activity against glioblastoma cells (C6 and U138-MG) and its neurotoxicity on primary astrocytes and organoptypic hippocampal cultures. For this study, the following methods were used: citotoxicity assays, flow cytometry, western-blotting and confocal microscopy. We showed that doxazosin induces cell death on C6 and U138-MG cells. We observed that doxazosin's effects on the PI3K/Akt pathway were similar as LY294002 (PI3K specific inhibitor). In glioblastoma cells treated with doxasozin, Akt levels were greatly reduced. Upon examination of activities of proteins downstream of Akt we observed upregulation of GSK-3β and p53. This led to cell proliferation inhibition, cell death induction via caspase-3 activation and cell cycle arrest at G0/G1 phase in glioblastoma cells. We used in this study Lapatinib, a tyrosine kinase inhibitor, as a comparison with doxazosin because they present similar chemical structure. We also tested the neurocitotoxicity of doxazosin in primary astrocytes and organotypic cultures and observed that doxazosin induced cell death on a small percentage of non-tumor cells. Aggressiveness of glioblastoma tumors and dismal prognosis require development of new treatment agents. This includes less toxic drugs, more selective towards tumor cells, causing less damage to the patient. Therefore, our results confirm the potential of doxazosin as an attractive therapeutic antiglioma agent.

OPEN ACCESS

Citation: Gaelzer MM, Coelho BP, de Quadros AH, Hoppe JB, Terra SR, Guerra MCB, et al. (2016) Phosphatidylinositol 3-Kinase/AKT Pathway Inhibition by Doxazosin Promotes Glioblastoma Cells Death, Upregulation of p53 and Triggers Low Neurotoxicity. PLoS ONE 11(4): e0154612. doi:10.1371/journal.pone.0154612

Editor: Ilya Ulasov, Swedish Neuroscience Institute, UNITED STATES

Received: January 12, 2016

Accepted: April 15, 2016

Published: April 28, 2016

Copyright: © 2016 Gaelzer et al. This is an open access article distributed under the terms of the Creative Commons Attribution License, which permits unrestricted use, distribution, and reproduction in any medium, provided the original author and source are credited.

Data Availability Statement: All relevant data are within the paper and its Supporting Information files.

Funding: The authors have no support or funding to report.

Competing Interests: The authors have declared that no competing interests exist.

Introduction

Gliomas are malignant primary brain tumors with no effective cure. Diffuse high grade gliomas (glioblastoma) patients have a short life expectancy despite aggressive therapeutic approaches based on surgical resection followed by adjuvant radiotherapy and concomitant chemotherapy [1].

Molecular mechanisms of glioblastoma multiform (GBM) resistance to therapy involve the PI3K/Akt pathway—which regulates cell proliferation, cell cycle, survival, apoptosis, chemotherapy resistance and tumorigenesis [2]. Transition from anaplasic astrocytoma to glioblastoma malignant evolution [3] and intrinsic radioresistance [4] are promoted by protein kinase B (Akt) activation, which is also a negative prognosis factor [5]. Glycogen synthase kinase-3β (GSK-3β) and p53, protein substrates downstream of the PI3K/Akt pathway, also regulate cellular sensitivity/resistance to cancer chemotherapy and are unregulated in glioblastoma multiform [6,7].

Doxazosin (2-{4-[(2,3-Dihydro-1,4-benzodioxin-2-yl)carbonyl]piperazin-1-yl}-6,7-dimethoxyquinazolin-4-amine) is a quinazoline compound and a selective α1-adrenoceptor antagonist widely used for treatment of high blood pressure and urinary retention related with benign prostatic hyperplasia [8]. Early studies showed doxazosin induced apoptosis in murine prostatic stromal and epithelial cells [9,10] and on urothelial cancer [11], pituitary adenoma [12], breast cancer [2] and human glioblastoma cells (U87-MG) [13]. Sakamoto et al. suggested that early administration of doxazosin may be useful in preventing clinical prostate tumor formation and supressing metastasis of human prostate cancer [14].

Many studies have focused on cytotoxic effects of doxazosin on cell death in tumor cells, but not in neural non-tumor cells. Moreover, chemotherapeutics used in glioma treatment have poor permeability through the blood brain barrier and short half-lives. Due to its physicochemical characteristics, doxazosin is able to permeate the blood-brain barrier [15] (BBB) and its relatively long half-life provides basis for once-daily dosing, which is a therapeutic advantage [16].

Here we show that doxazosin has low neurotoxicity and induces cell death and G0/G1 phase arrest on C6 and U138-MG glioblastoma cells. When compared with the tyrosine kianse inhibitor Lapatinib, doxazosin appears to be a more potent antiglioma agent. We demonstrated that doxazosin's antitumoral effects are due to downregulation of Akt and upregulation of GSK-3β and p53, in addition to activation of caspase 3. We also observed that doxazosin's effects on the Phosphatidylinositol 3-Kinase/AKT pathway were similar as LY294002 (PI3K specific inhibitor).

Materials and Methods

Chemicals and materials

Cell culture medium and fetal bovine serum (FBS) were obtained from Gibco-Invitrogen (Grand Island, NY, USA). Doxazosin was obtained from Sigma Chemical Co (St. Louis, MO, USA). All other reagents were purchased from Sigma Chemical Co. (St. Louis, MO, USA) or Merck (Darmstadt, Germany). All chemicals and solvents used were of analytical or pharmaceutical grade.

Cell culture

C6 rat (passage number 20–25) and U138-MG human glioma cell lines were obtained from American Type Culture Collection (Rockville, Mariland, Md., USA). C6 and U138-MG cells were grown and maintained in Dulbecco's Modified Eagle's Medium (DMEM, Gibco-

Invitrogen, Grand Island, NY, USA) supplemented with 5% and 10% (v/v) FBS (Gibco-Invitrogen, Grand Island, NY, USA), respectively, and containing 2.5 mg/mL of Fungizone® and 100 U/L of gentamicine (Shering do Brasil, São Paulo, SP, Brazil). Cells were kept at 37°C, in an atmosphere of 5% CO_2.

Ethics statement

All animal procedures were approved by the local animal ethics comission (Comissão de Ética no Uso de Animais/Universidade Federal do Rio Grande do Sul—CEUA/UFRGS, under project number 20.005) and follows national animal rights regulations (Law 11.794/2008), the National Institute of Health Guide for the Care and Use of Laboratory Animals (NIH publication No. 80–23, revised 1996) and Directive 2010/63/EU. We further attest that all efforts were made to minimize the number of animals used and their suffering.

Primary astrocyte culture

Primary astrocyte culture from Wistar rats was prepared as previously described [17]. Newborn Wistar rats (1–2 days-old) were maintained in a ventilated room at constant temperature, in breeding cages with their mother, on a 12h light/dark cycle. The newborn rats were decapitated, their cerebral cortices were removed and mechanically dissociated in Ca^2+ and Mg^2+ free balanced salt solution, pH 7.4, containing (in mM): 137 NaCl; 5.36 KCl; 0.27 Na_2HPO_4; 1.1 KH_2PO_4 and 6.1 glucose. Cortices were cleaned of meninges and mechanically dissociated by sequential passage through a Pasteur pipette. After centrifugation at 1400 rpm for 5 min, the pellet was resuspended in DMEM (pH 7.6) supplemented with 8.39 mM HEPES, 23.8 mM $NaHCO_3$, 0.1% amphotericin, 0.032% gentamicin and 10% Fetal Calf Serum (FCS). Cultures were maintained in DMEM containing 10% FCS in 5% CO_2/95% air at 37°C, allowed to grow to confluence, and used at 15 days *in vitro*.

Organotypic hippocampal slice culture

Organotypic hippocampal slice cultures were prepared according to the method of Stoppini [18] with modifications [19]. Wistar rats (6–8 days-old) were maintained in a ventilated room at constant temperature, in breeding cages with their mother, on a 12h light/dark cycle. The rats were decapitated, their hippocampi were removed and 400μM thick slices were prepared using a Mcllwain tissue chopper in ice-cold Hank's balanced salt solution (HBSS), pH 7.2. Slices were placed on MiIlicell® culture membranes and the inserts were transferred to a six-well culture plate. Each well contained 1mL of tissue culture medium consisting of Minimum Essential Media (MEM) with 25% of HBSS and 25% of horse serum supplemented with 36 mM glucose, 25 mM HEPES, 4 mM $NaHCO_3$, 1% Fungizone® and 0,1 mg/mL gentamicine, pH 7,3. The cultures were kept in an incubator 37°C and 5% of CO_2 for 14 days.

Culture treatments

C6 and U138-MG glioma cells were seeded in culture media and grown for 24 hours. Doxazosin was dissolved in 20% ethanol/milli-Q™ water (vehicle) and C6 cells were treated with concentrations ranging from 30 μM to 300 μM. U138-MG cells were treated with drug concentrations ranging from 5 μM to 75 μM. Primary astrocyte cultures and organotypic slice cultures were treated with doxazosin for 48 hours at 30–250 μM. Lapatinib was dissolved in DMSO and cells were treated with 500 nM.

MTT assay

C6 and U138-MG glioma cells were plated in 96-well plates at 10^3 cells/well and grown for 24 hours. Following treatment, cells were incubated with 0,5 mg/mL MTT (3-(4,5-methylthiazol-2-yl)-2,5-diphenyltetrazolium bromide) for 1 h. The solution was then removed from the precipitate and the formazan product in the cells was solubilized by adding DMSO. Absorbance was read by an ELISA plate reader (Biochrom Anthos Zenyth 200 Microplate Reader) at 490 nm.

LDH assay

Cell death was evaluated by measuring the activity of lactate dehydrogenase (LDH, E. C.1.1.1.27). After treatment, U138-MG and C6 cell culture medium was collected and LDH activity was determined by an enzymatic colorimetric reaction (Cytotoxity Detection Kit—LDH, Roche Applied Science). Absorbance was measured at 490 nm.

Sulforhodamine B assay

Sulforhodamine B (SRB) assay was used for cell density determination [20]. After treatment with doxazosin, cells were washed with Phosphate Buffered Saline (PBS) and fixed with PBS/FORMOL 4% for 15 minutes. Fixed cells were stained with SRB. Subsequently, wells were washed with deionized water to remove unbound stain. Culture plates were air dried and protein-bound SRB was solubilized in 1% SDS. Absorbance was measured by an ELISA plate reader (Biochrom Anthos Zenyth 200 Microplate Reader) at 515 nm.

Flow Cytometry

Cell death was analyzed by flow cytometry. For C6, U138-MG and primary astrocyte cultures, both floating and trypsinized adherent cells were collected. Organotypic hippocampal slices were dissociated in PBS containing 1% collagenase, 1% DNase, and 0.2% trypsine and filtered through a 40 μm membrane (Millipore). Annexin-V FITC/propidium iodide (PI) double stain kit was used, following the manufacturer's instructions (Invitrogen, Grand Island, NY, USA). Samples were incubated in binding buffer containing Annexin-V FITC and PI for 15 min in the dark at room temperature.

For cell cycle analysis, C6 and U138-MG cells were seeded in 6-well plates ($3x10^4$ cells/well). After treatments, cells were washed with PBS, trypsinized and counted. Cells were centrifuged at 400 x g for 5 min and resuspended (10^6 cells/mL) in PBS containing RNAse (100 μg/mL) and PI (5 μg/mL) for 15 min at room temperature.

For analysis of cleaved caspase 3, C6 and U138-MG cells were trypsinized and centrifuged at 400 x g for 5 min. Cells were resuspended in PBS containing 0,1% Triton X-100 and mouse anti-cleaved caspase 3 antibody (1:100; Cell Signaling), for 30 min at room temperature. Then, secondary antibody anti-mouse Alexa Fluor 488 (1:100, Invitrogen) was added and, after incubation for 30 min, fluorescence intensity was analyzed by flow cytometry.

Data acquisition was done by flow cytometry using a FACS Calibur cytometry system and Cell Quest software (BD Bioscience, Mountain View, CA, USA). Data obtained was analyzed with FCS Express 4 Software (De Novo Software, Los Angeles, CA, USA).

Western blotting

After treatments, cells were homogenized in lysis buffer (4% sodium dodecyl sulfate (SDS), 2 mM EDTA, 50 mM Tris). Protein concentration was determined by the Lowry method. Proteins were resolved (75 μg per lane) on 10 or 12% SDS-PAGE and transferred to nitrocellulose membranes (Hybond™ ECL™ nitrocellulose membrane, Amersham Biosciences™, Fryeburg, Germany) using a semi-dry transfer apparatus (Bio- Rad™, Trans-Blot SD, Hercules™, CA, USA). Membranes were incubated for 60 minutes at 4°C in blocking solution (Tris-buffered saline containing 5% powdered milk and 0.1% Tween-20, pH 7.4). and incubated overnight with specific antibodies. Primary antibodies (Cell Signaling Technology™, Beverly, MA, USA) against the following proteins were used: anti-p-AKT$_{Ser473}$ and anti-AKT (1:1000), anti-p-GSK-3β$_{Ser9}$ and anti-GSK-3β (1:1000), anti-p-p53$_{Ser15}$ (1:1000), anti-β-actin (1:1000). Membranes were then incubated with horseradish peroxidase conjugated anti-rabbit antibody (1:1000; Amersham Pharmacia Biotech, Piscataway, NJ, USA). Chemiluminescence (ECL, Amersham Pharmacia Biotech™) was detected using X-ray films (Kodak X-Omat™, Rochester, NY, USA).

Statistical analysis

Data are expressed as means±SEM. All results are representative of at least 4 independent experiments. Analysis of variance (ANOVA) was applied to the means to determine statistical differences between experimental groups. Post hoc comparisons were performed by Tukey test. Differences between mean values were considered significant when $p<0.05$.

Results

Evaluation of doxazosin toxicity on non tumoral tissue/cells

One of the problems of current cancer therapy is lack of specificity and selectivity of certain drugs used for tumor treatment [21]. In order to evaluate the drug toxicity on non-tumoral neural tissue, we exposed primary astrocyte cultures and organotypic hippocampal slice cultures to doxazosin for 48 hours.

Initially, we tested a concentration curve (30–250 μM) of doxazosin, with intermediate concentrations obtained from the literature [22]. In primary astrocyte culture (Fig 1 and S1 Table), 250 μM doxazosin increased total cell death (15.62%±2.674), while at concentrations of 75 and 180 μM was not observed significant cell death. Lapatinib (500 nM) caused total cell death of 27.61%±1.218, inducing necrosis in 20.07%±1.261. The toxicity on non-tumoral astrocytic cells by Lapatinib was higher than doxazosin 250 μM.

In organotypic cultures (Fig 1 and S1 Table), doxazosin caused cell death of 10.82%±1.232 at 180 μM and 18.27%±1.346 at 250 μM. Lapatinib (500 nM) caused cell death in 26.86% ±1.885 of cells, inducing necrosis in 17.28%±6.134 of cells. In non-tumoral neural tissue, Lapatinib cell death induction also was higher than doxazosin.

In relation to the distribution and type of cell death observed on organotypic cultures, doxazosin induced apoptosis and necrosis at 250 μM mostly on CA1 region (S1 Fig). Lapatinib induced apoptosis and necrosis on CA1 and mostly on the dentate gyrus (DG) regions.

Antiglioma activity of doxazosin

C6 and U138-MG cells were treated with a concentration curve of doxazosin for 48 hours, based on concentrations used for non-tumor cells. In C6 cells, we observed a significant reduction of cell viability with treatments from 150 μM to 300 μM of doxazosin for 48 h (Fig 2). Doxazosin increased LDH activity in the incubation medium of C6 cells when treated with 150 and 180 μM (Fig 2). In agreement with these results, cell density of C6 cells decreased to approximately 25% when treated with doxazosin 150 and 180 μM for 48 h (Fig 2).

For U138-MG cells, after 48 hours of treatment we observed a significant reduction on the percentage of viable cells in cultures treated with 75 μM of doxazosin (Fig 2). LDH activity

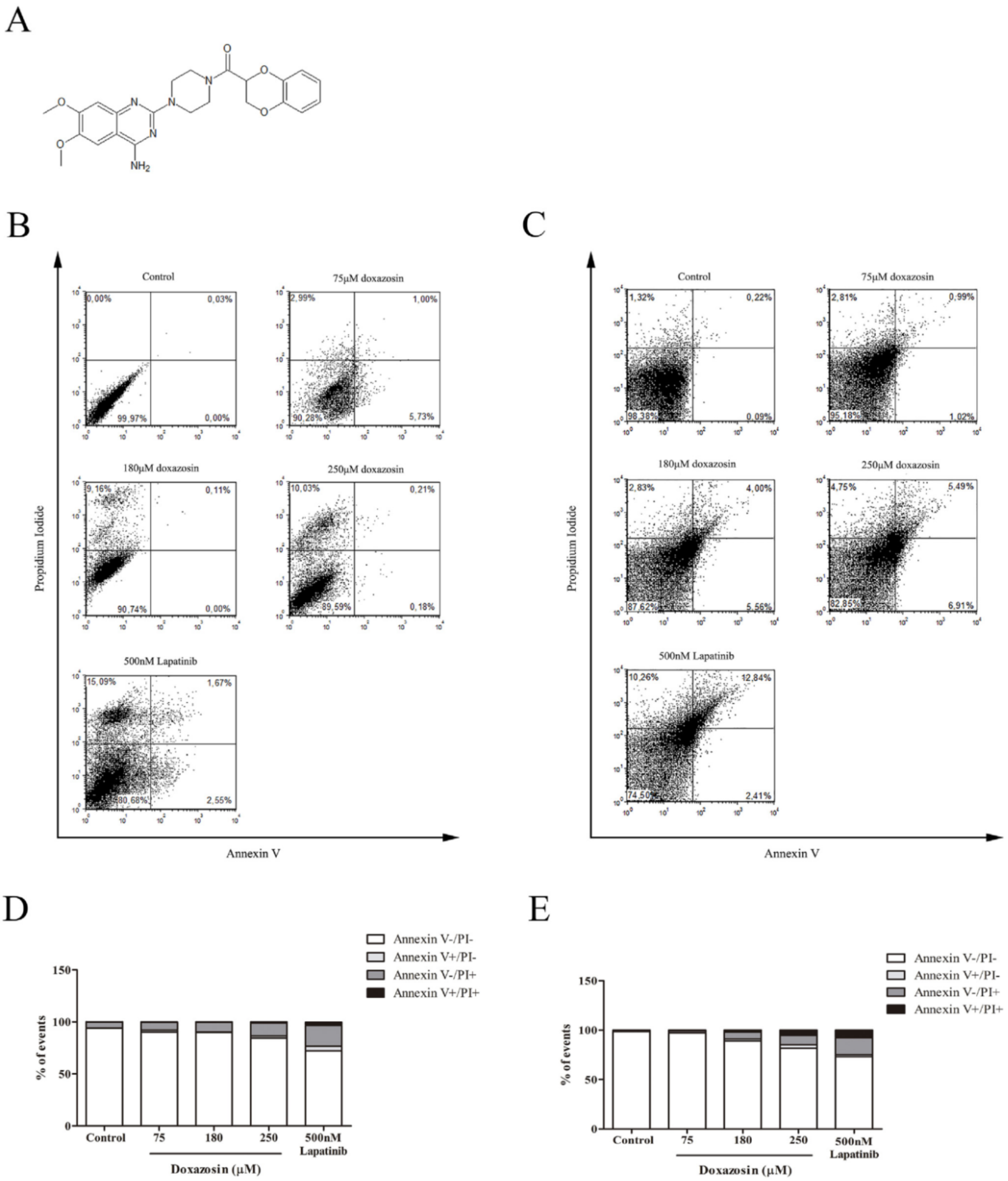

Fig 1. Effects of doxazosin and Lapatinib on non-tumor cells stained with Annexin V (AnV) and Propidium Iodide (PI). (A) Doxazosin's molecular structure. **(B)** Dot plot and graph **(D)** of primary astrocytes cultures after treatment with doxazosin and Lapatinib for 48h. **(C)** Dot plot and graph **(E)** of organotypic hippocampal cultures treated with doxazosin and Lapatinib for 48h. Data are represented as means (n = 4).

doi:10.1371/journal.pone.0154612.g001

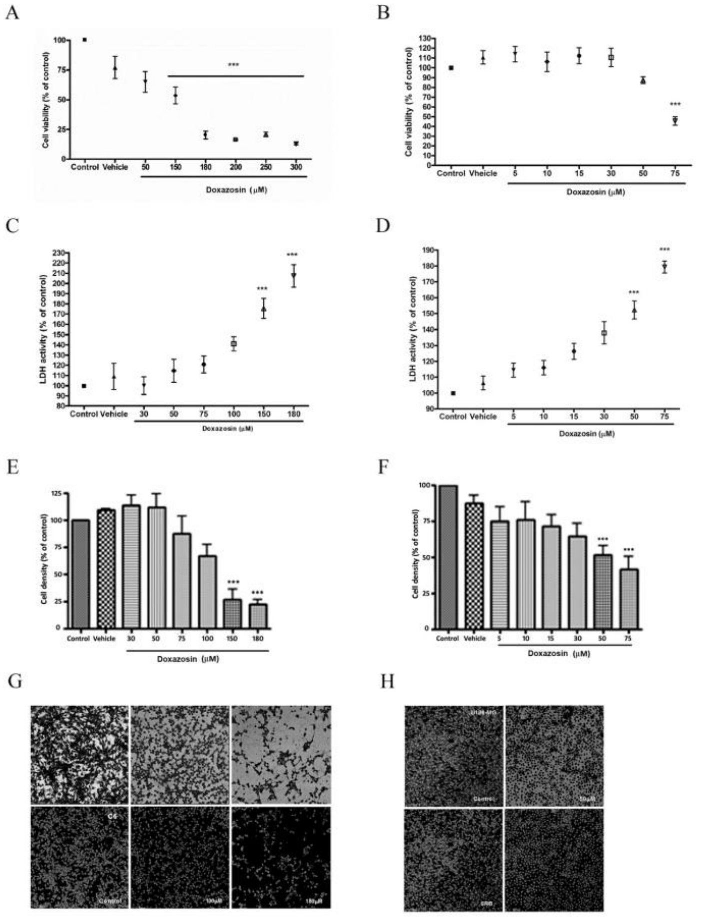

Fig 2. Citotoxicity of doxazosin on C6 (A,C,E,G) and U138-MG (B,D,F,H) cells after treatment for 48 h. MTT assay of C6 **(A)** and U138-MG **(B)**. LDH activity of C6 **(C)** and U138-MG **(D)**. SRB assay of C6 **(E)** and U138-MG **(F)**. Data are represented by means±SEM (n = 4). ***p<0.001 compared to respective control, ANOVA followed by Tukey's test. Confocal microscopy of C6 **(G)** and U138-MG **(H)**. Photomicrographs are on top and SRB staining in the bottom. Magnification: 10X + 2,5.

doi:10.1371/journal.pone.0154612.g002

increased in the incubation medium of U138-MG culture cells when treated with 50 and 75 μM doxazosin (Fig 2). Also at these concentrations, doxazosin decreased cell density to approximately 50% (Fig 2), supporting the results above. All together, these cytotoxicity assays suggest an antiglioma effect of doxazosin in C6 and U138-MG cell lines.

Doxazosin induced cell death by necrosis and caspase-dependent apoptosis in human and rat glioblastoma cell lines

Doxazosin induced necrosis and apoptosis in C6 cells after 48 h of treatment (Fig 3, S2 Table and S2 Fig). At concentration of 100 μM, the drug caused 36.68%±5.045 of cell death and this toxic effect increased with higher drug concentrations, reaching 69.71%±2.503 at 180 μM. At

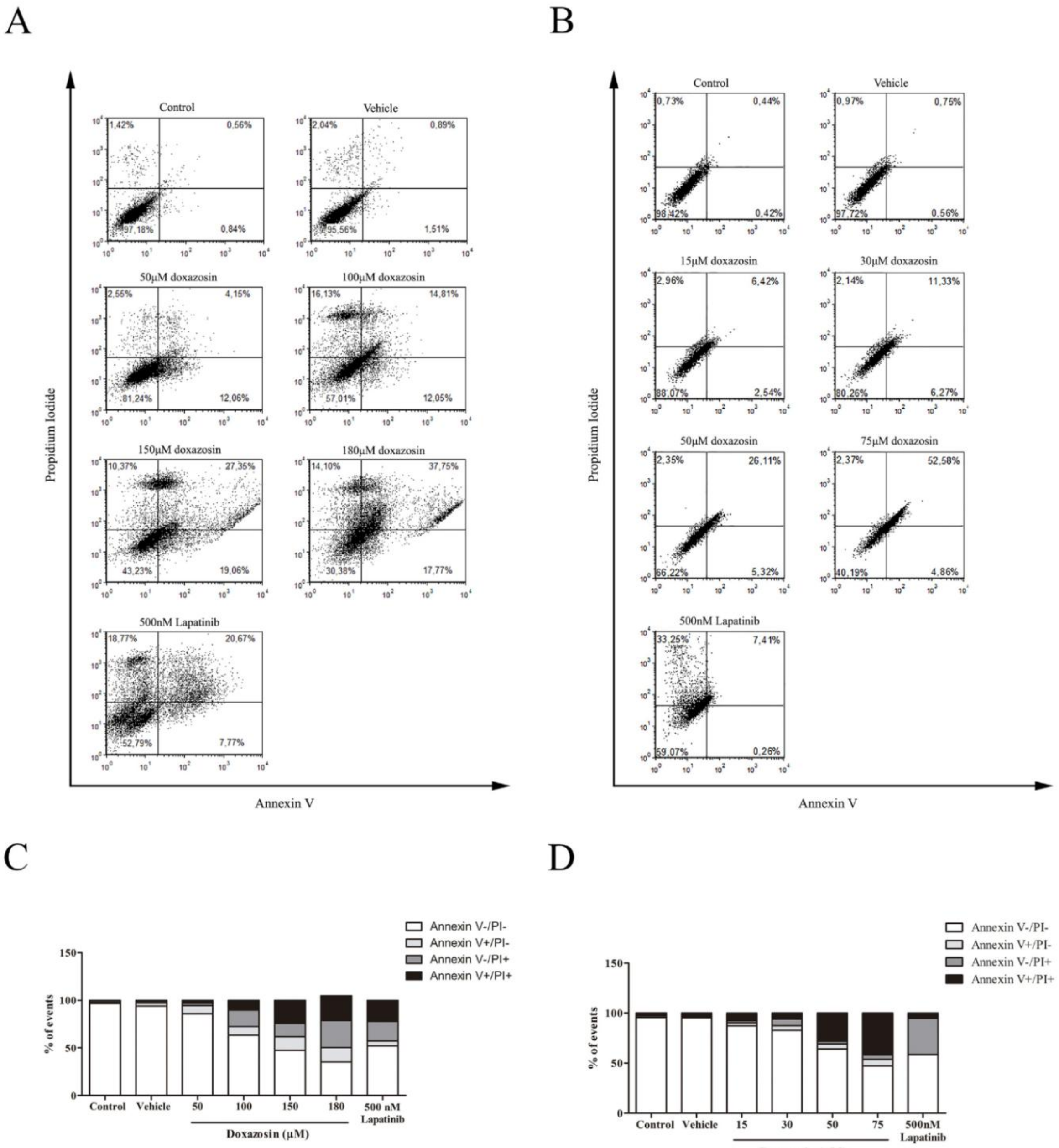

Fig 3. Effects of doxazosin and Lapatinib on glioma cells stained with Annexin V (AnV) and Propidium Iodide (PI). (A) Dot plot and graph **(C)** of C6 cells after treatment with doxazosin and Lapatinib for 48h. **(B)** Dot plot and graph **(D)** of U138-MG cells treated with doxazosin and Lapatinib for 48 h. Data are represented as means (n = 4).

doi:10.1371/journal.pone.0154612.g003

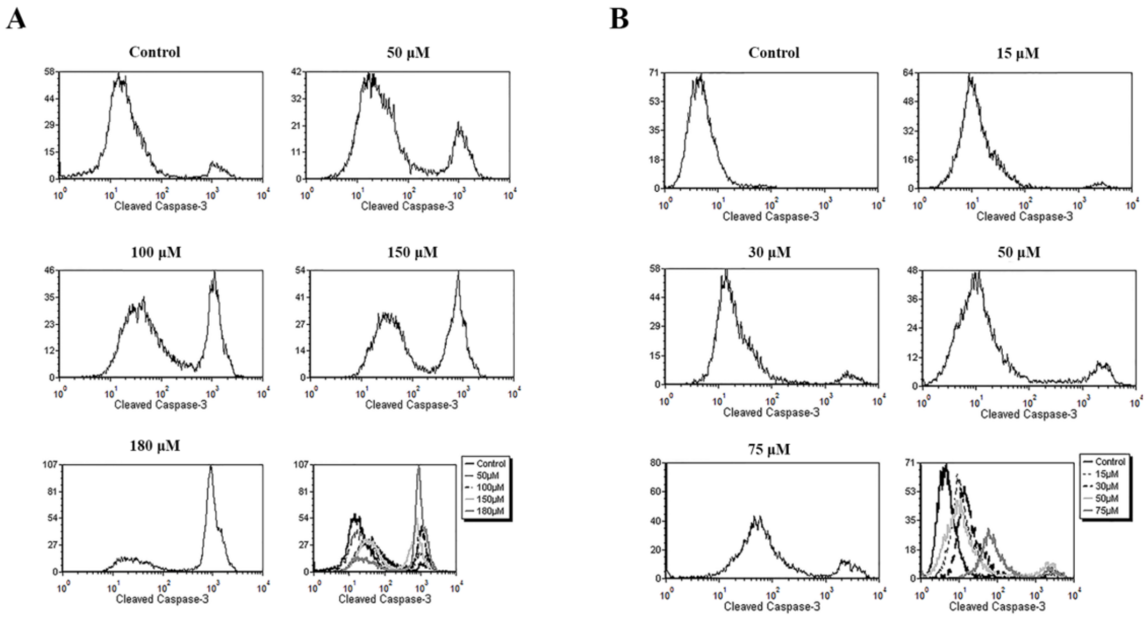

Fig 4. Flow cytometry of cleaved caspase-3 of C6 (A) and U138-MG (B) glioma cells.

doi:10.1371/journal.pone.0154612.g004

180 µM, doxazosin caused early apoptosis in approximately 14.89%±1.581 of cells and late apoptosis in approximately 26.20%±4.860. Necrosis occurred in 28.62%±6.373. While Lapatinib caused cell death in 47.96%±0.975 of C6 cells after 48 h, triggering necrosis in 20.56%±1.591 and late apoptosis in 22.01%±1.548 of cells. Lapatinib caused cell death on C6 cells to a less extent than doxazosin.

In U138-MG cells, doxazosin induced cell death in 35.9%±3.356 of cells at 50 µM and 52.69%±5.709 at 75 µM after 48 h (Fig 3 and S2 Table). Doxazosin 75 µM triggered mostly late apoptosis (41.86%±5.589) in U138-MG cells. Lapatinib caused cell death in 41.44%±0.466 of cells, and triggered mostly necrosis (36.13%±1.733) (Fig 3 and S2 Table).

After 48 h of treatment, doxazosin increased activation of caspase 3 in C6 and U138-MG (Fig 4) cell lines and this was proportional to increase in drug concentration. These results of cleaved caspase-3 levels confirm induction of apoptosis by doxazosin.

Doxazosin caused G0/G1 phase arrest on C6 and U138-MG glioblastomas

We next sought to analyze doxazosin's effect on cell cycle progression and mitotic index. As shown in Fig 5, after 48 h of treatment of C6 cells, doxazosin caused cell cycle arrest at the G0/G1 phase at concentrations of 100 and 180 µM compared to control. We analyzed the mitotic index of C6 cells in order to assess proliferation (Fig 5). Doxazosin decreased the mitotic index in the concentrations of 100, 150 and 180 µM after 48h of treatment, in agreement with cell cycle results.

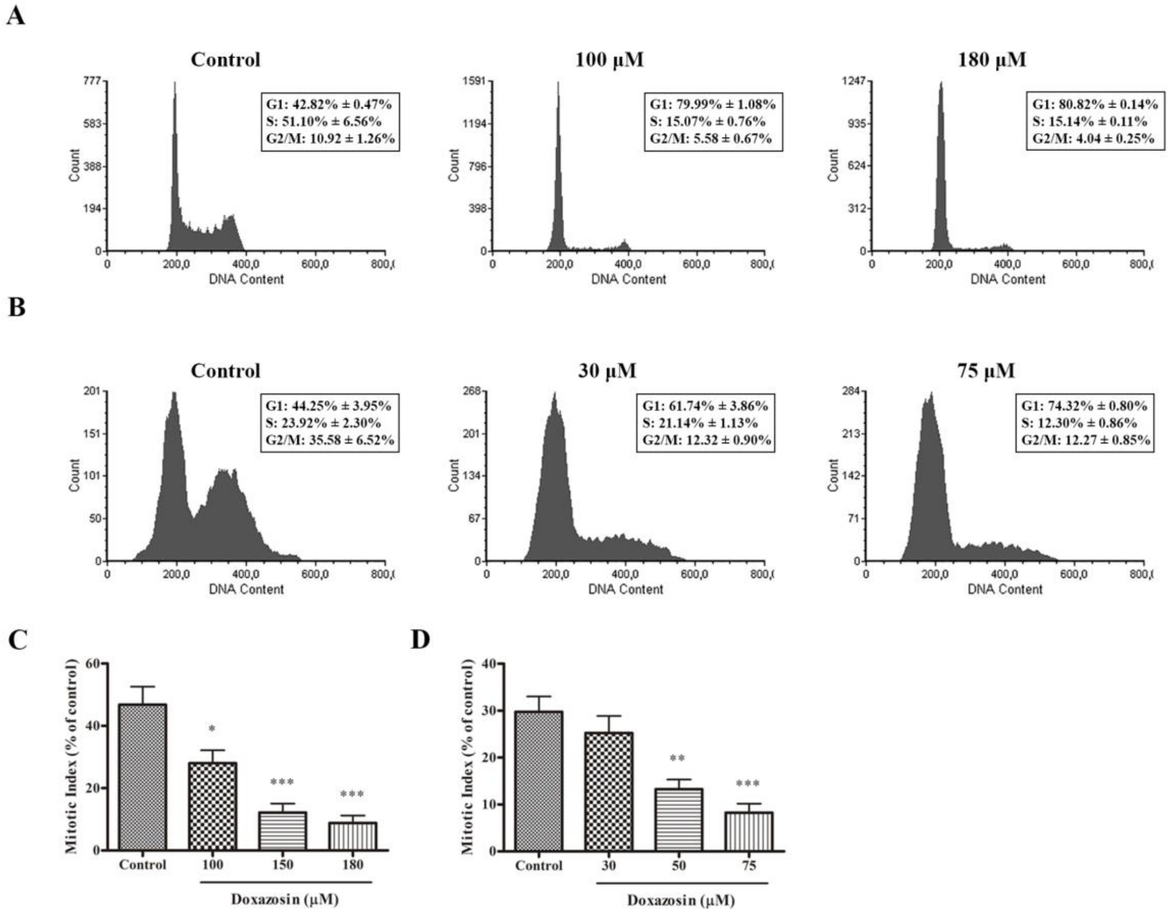

Fig 5. Cell cycle analysis (A,B) and mitotic index (C,D) of glioma cells treated with doxazosin for 48 h. (**A**) Cell cycle of C6 cells and (**B**) U138-MG cells. (**C**) Mitotic index of C6 cells and (**D**) U138-MG cells. Data are represented by means±SEM (n = 4). *p<0.05, **p<0.01, ***p<0.001 compared to respective control, ANOVA followed by Tukey's test.

doi:10.1371/journal.pone.0154612.g005

In U138-MG cells, doxazosin caused cell cycle arrest in G0/G1 phase at concentrations of 30 and 75 μM and decreased mitotic index in the concentrations of 50 and 75 μM after 48 h of treatment in U138-MG cells (Fig 5).

PI3K/Akt pathway: a possible doxazosin target

Next, we analyzed activation of proteins involved with apoptosis, cell cycle and glioma malignancy in rat and human glioblastoma cells. The phosphorylation levels of p-AKT$_{Ser473}$, p-GSK-3β$_{Ser9}$ and p-p53$_{Ser15}$ were analyzed for their role in cell survival, proliferation and apoptosis regulation. Doxazosin was added for 24 and 48 h. As shown in Fig 6, p-Akt$_{Ser473}$ levels decreased at 150 and 180 μM doxazosin in C6 cells after 48 h.

Additionally, we evaluated whether Akt downstream target GSK-3β was affected. As shown in Fig 6, the treatment of C6 cells with doxazosin, 150 and 180 μM, decreased p-GSK-3β$_{Ser9}$

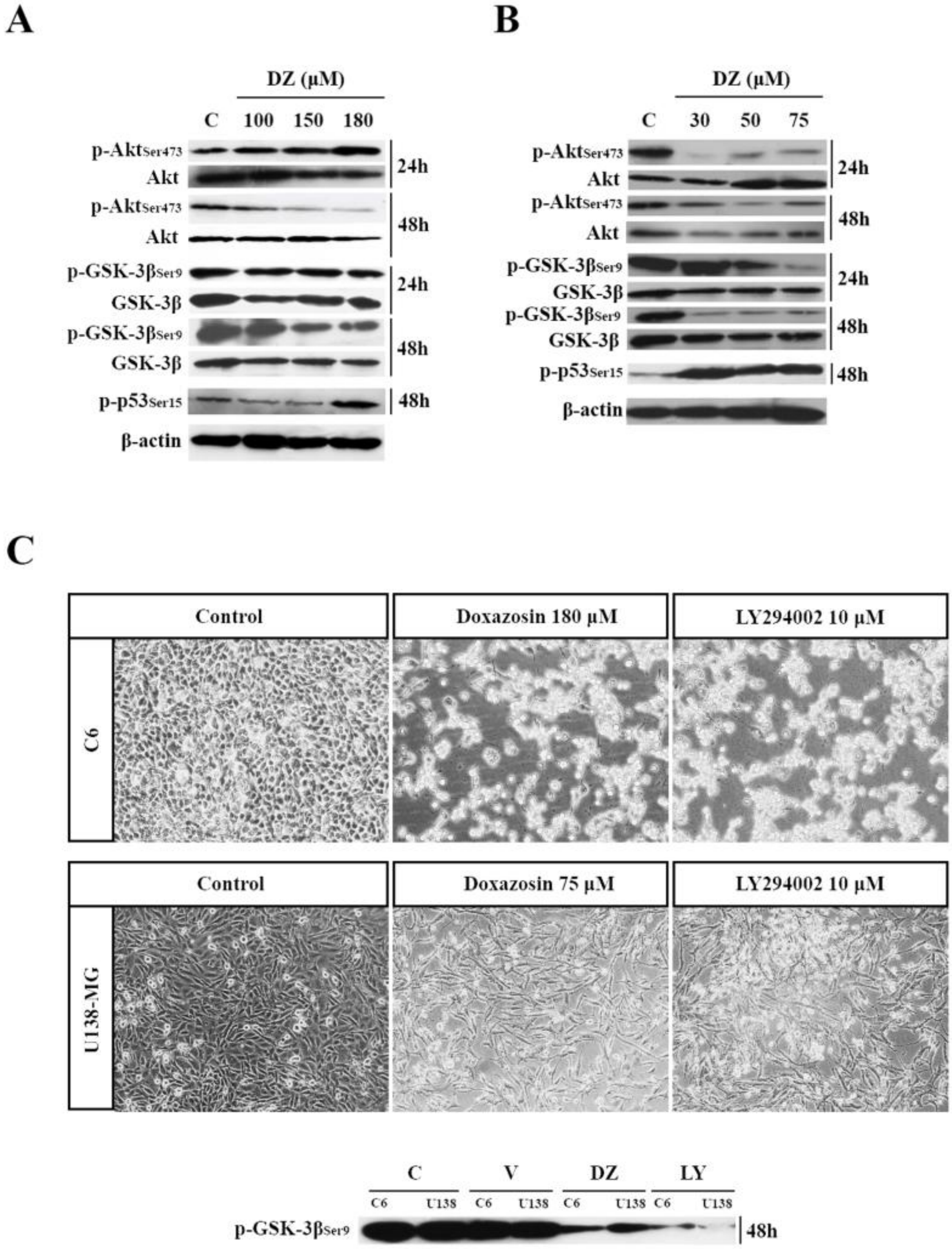
A
DZ (μM)
C 100 150 180
p-Akt Ser473
Akt
24h
p-Akt Ser473
Akt
48h
p-GSK-3β Ser9
GSK-3β
24h
p-GSK-3β Ser9
GSK-3β
48h
p-p53 Ser15
48h
β-actin
B
DZ (μM)
C 30 50 75
p-Akt Ser473
Akt
24h
p-Akt Ser473
Akt
48h
p-GSK-3β Ser9
GSK-3β
24h
p-GSK-3β Ser9
GSK-3β
48h
p-p53 Ser15
48h
β-actin
C
Control
Doxazosin 180 μM
LY294002 10 μM
C6
Control
Doxazosin 75 μM
LY294002 10 μM
U138-MG
C V DZ LY
C6 U138 C6 U138 C6 U138 C6 U138
p-GSK-3β Ser9
48h

Fig 6. Western blotting of C6 (A) and U138-MG (B) cells after treatment with doxazosin for 48h (n = 4). β-actin was used as a loading control. **(C)** Effect of doxazosin on cell death and GSK-3β Ser9 phosphorylation compared with LY294002 (**LY**) on glioma cells. Magnification: 40X. **C**–control; **V**–vehicle; **DZ**–doxazosin. Data are represented as means (n = 4).

doi:10.1371/journal.pone.0154612.g006

levels after 48 h. We also observed an increase of phosphorylation levels of p-p53$_{Ser15}$ after 48 h of treatment with doxazosin 180 μM in C6 cells (Fig 6).

In U138-MG cells, treatment with doxazosin during 24 h and 48 h at concentrations of 30, 50 and 75 μM, decreased p-Akt$_{Ser473}$ levels (Fig 6). By other hand, after 24 h only the treatments at concentrations of 50 and 75 μM of doxazosin were able to decrease the p-GSK-3β$_{Ser9}$ levels, while after 48 h this decrease was maintained and we also observed a decrease at 30 μM of doxazosin treatment (Fig 6). Regarding to the effect of doxazosin on the p53 protein in U138-MG cells, it was observed an increase in p-p53$_{Ser15}$ at the concentrations of 30, 50 and 75 μM (Fig 6). We analyzed immunocontent of these same phosphorylated proteins at earlier times and did not observe any differences (data not shown).

In order to analyze whether the PI3K signaling pathway by Akt activation and GSK-3β inactivation was involved in the effect of doxazosin, we carried out this experiment using LY294002, a specific inhibitor of PI3K [23]. Activated PI3K phosphorylates its downstream target Akt. Phosphorylated Akt directly affects GSK-3β by phosphorylating it at Ser9 and thus inhibiting its activity. LY294002 induced C6 and U138-MG cell death in 48 h and inhibited GSK-3β$_{Ser9}$ phosphorylation in the same manner as doxazosin (Fig 6). This result indicates a possible effect of doxazosin on the PI3K/Akt pathway on glioma cells.

Discussion

Current anticancer drugs have limitations by presenting cytotoxicity, low specificity and the prolonged use may result in lethal damage to healthy cells. Therefore, chemotherapeutic treatment of tumors in the central nervous system is associated with severe systemic side effects and therefore affecting patients quality of life [24]. Glioblastoma is a radio- and chemo-resistant cancer. This makes it necessary to increase chemotherapy dosage or add more drugs for treatment, which increases toxicity on non-tumor cells. Tumor surgical resection, in the case of glioblastomas, might compromise vital brain areas due to the cancer's aggressive and infiltrative characteristics [24].

Temozolomide (TMZ) is considered the standard therapy for treatment of glioblastoma multiforme. However TMZ must be administered at high doses systemically in order to achieve therapeutic levels in the brain, mainly due to its low half-life (about 1.8 h in plasma) [25]. It has been approved by the FDA in the USA for the treatment of GBM, showing a median survival of just 5.8 months [26]. Furthermore, prolonged systemic administration is associated with side effects such as nausea, vomiting, fatigue and headache.

Additionally, the central nervous system has another limitation regarding treatment: nerve tissue has a low rate of cell division and loss of non-tumor cells greatly affects the well-being of patients. For these reasons, the search for new therapeutic strategies and chemotherapeutics is necessary to improve effectiveness of glioma treatment, while preserving the quality of life of patients. Doxazosin is a FDA approved drug in the USA for treatment of hypertension and symptoms of benign prostatic hyperplasia, with mild side effects, like dizziness and hypotension [22,27]. However, doxazosin toxicity on nervous non-tumor tissue has never been evaluated so far.

In astrocytes, doxazosin increased total cell death only at the high concentration of 250 μM when compared to control. In organotypic cultures, doxazosin caused cell death at 180 and 250 μM concentrations when compared to control. Although there was no statistical difference between the types of cell death, doxazosin showed a tendency towards induction of necrosis and late apoptosis. These results show that doxazosin triggers different cell responses depending on its concentration and the best range of concentrations for further tests are below 250 μM.

We also tested Lapatinib citotoxicity on primary astrocytes and organotypic cultures, and compared its antitumoral effect with doxazosin on C6 and U138-MG glioma cells. Lapatinib is a tyrosine kinase inhibitor, which has a quinazolinic ring in its chemical structure. Compounds based on quinazoline scaffolds can target a range of kinases with varying degrees of selectivity [28]. Doxazosin also presents a quinazoline scaffold on its chemical structure. Lapatinib was used in this study as a comparison with doxazosin because they present similar chemical structure [29]. Reports show Lapatinib effective inhibition of human breast and prostate cancer cell lines, and in U87-MG and M059K glioblastoma cell lines [30]. Here we showed that Lapatinib 500 nM is more cytotoxic than doxazosin 250 μM on primary astrocytes and hippocampal organotypic cultures.

We observed that in hippocampal organotypic cultures doxazosin induced apoptosis on DG and CA1 cells, but necrosis was limited to CA1 area, possibly due to delayed cell death and DG's capability of apoptosis induction for tissue remodeling purposes [31]. Lapatinib also induced apoptosis and necrosis on both regions, but necrosis was more pronounced in the DG region. CA1 neurons react differently after lesions than DG cells, mainly because they present more dendritic remodeling and present high abundance of NMDA (*N*-methyl-D-aspartate) receptors, which could lead to glutamate excitotoxicity [32].

Several studies have demonstrated that doxazosin's concentrations responsible for cell death induction vary depending on the origin of the cells, the type of cancer and even between different cell lines of the same type of tumor [22,33]. On prostate cancer cells, for example, maximum concentration of doxazosin used is 100 μM [22,34]. On the other hand, colon cancer SW-480 cells and bladder cancer HTB1 cells were less sensitive to this concentration of doxazosin [22]. HeLa cells showed high sensitivity to doxazosin, while HepG-2 and MCF-7 cells showed an IC50 of around 200 μM [35].

We observed that C6 and U138-MG cell lines had different vulnerability against doxazosin. Results showed that doxazosin induced apoptosis and necrosis on C6 cells and only apoptosis on U138-MG cells. When compared with Lapatinib, doxazosin showed to be more effective in inducing apoptotic cell death in both C6 and in U138-MG cells. Although it has been observed that treatment with TMZ induces a decrease in cell viability in various glioma lines, it is well described that U138-MG lineage is resistant to this treatment [36]. Our results showed that doxazosin was able to induce apoptosis in both cell types, C6 and U138-MG. Differences observed between cell lines on cytotoxicity assays and types of cell death could be due to: different species, varying doubling times or characteristics and mutations between cell lineages. C6 cells have a doubling time of approximately 25–30 hours [37], while U138-MG cells' is 70 hours [38]. C6 cells proliferate faster, being more aggressive than U138-MG. Moreover, U138-MG cells have higher expression of the pro-apoptotic protein Bax, being more sensitive to apoptosis [33]. This could explain the different concentrations to which doxazosin was more effective (50 and 75 μM for U138-MG cells and 150 and 180 μM for C6 cells).

Doxazosin's effective concentrations used on this study on rat C6 cells (150 and 180 μM) exceeds the limits used for most cancer cells on the literature [22,34]. For the human cell line U138-MG, effective doxazosin concentrations are 50 and 75 μM, which is in accordance with what was used in the literature for other cancer cells. Future studies, however, are necessary to determine if this *in vitro* therapeutic concentrations of doxazosin are effective against glioblastoma *in vivo* models.

In addition to inducing cell death, doxazosin decreased proliferation, shown by cell cycle arrest in G0/G1 phase and decreased mitotic index. On human LNT-229 and U87-MG GB cells, doxazosin also induced G0/G1 cell cycle arrest and concentration-dependent apoptosis [13]. Several *in vitro* and *in vivo* studies show that the main mechanism underlying doxazosin-induced apoptosis is inhibition of receptor-mediated signaling [39,40,41]. Therefore, we suggest that those effects and the apoptosis induction may be related with the decrease of Akt phosphorylation/activation, which possibly affected the Akt downstream targets, GSK-3β and p53. In PC-3 cells, doxazosin induced apoptosis in part through downregulation of Akt cell signaling. Akt plays a pivotal role regulating cell growth and survival in cancer cells. This fact justifies the pharmacological use of doxazosin and derivatives, which possess quinazolinic rings, for the development of a new class of apoptosis-inducing agents, which blocks activation of Akt protein [42].

Moreover, doxazosin was shown to suppress PI3K and Akt phosphorylation on ovarian carcinoma cells [41]. The authors of this study suggest the hypothesis that doxazosin inhibits PI3K/Akt activity. GSK-3β is involved in the processes of apoptosis and cell cycle, as well as p53. One of the most important regulatory mechanism acting on GSK-3β is phosphorylation of Ser9, which inhibits the protein. Several kinases are able to phosphorylate this protein, including Akt [43]. Here we found that doxazosin, possibly through Akt inhibition, decreased GSK-3β Ser9 phosphorylation. Also we observed that doxazosin cell cycle arrest and the decrease on proliferation of C6 and U138-MG glioma cells appears to be mediated by GSK-3β dephosphorylation/activation.

In cancer, GSK-3β has been reported as a "tumor suppressor" by repressing neoplastic transformation and tumor development[44]. GSK-3β also appears to be involved in chemotherapy resistance. When treated with lithium, which is a GSK-3β inhibitor, hepatoma cells became resistant to etoposide and camptothecin. On the other hand, GSK-3β activation with LY294002 and with exogenous expression of Ser9 GSK-3β sensitizes hepatoma cells to apoptosis induced by those drugs [45]. LY294002 can also inhibit expression of p-Akt in cancer cells via PI3K suppression [46], which supports the induction of cell death on C6 and U138-MG cells shown here. Other reports show that GSK-3β activation enhances and sensitizes human breast cancer cells to paclitaxel, 5-fluorouracil, cisplatin, taxol and prodigiosin [43]. Also, other studies with GSK-3β inhibitors on GBM patients and two established cell lines (U251 and U87-MG) showed that inhibition of GSK-3β phosphorylation significantly reduced tumor invasiveness [6].

Another protein that we found altered by doxazosin treatment is p53. This is a tumor-suppressor protein that is activated upon various types of cellular stresses. The p53 protein is involved with apoptosis induction, with inhibition of cell cycle progression [47], as demonstrated here on C6 and U138-MG cells. In almost all types of cancer, p53 is frequently inactivated, being a central tumor-suppressor. The p53 protein can regulate and be regulated by Akt and also can interact with GSK-3β. It is well established that activation of Akt inhibits p53-mediated apoptosis [47].

The p53 gene is mutated in 30–50% of glioblastomas and this mutation confers increased malignancy and tumorigenicity to the cancer. Also it has been reported that p53 mutation decreases chemosensitivity of malignant gliomas to TMZ [7]. The U138-MG cell line has a TP53 mutation and is TMZ resistant [48]. Here we showed that doxazosin, unlike TMZ, decreased cell viability and induced apoptosis in U138-MG cells, and also increased p53 phosphorylation in these cells.

We also found that doxazosin activated caspase-3 on glioma cells. Caspase-3 can be activated through inhibition of Akt phosphorylation, and consequently leading to the inhibition of this kinase. When Akt is inactive, cells can undergo apoptosis through loss of mitochondrial membrane potential, leading to activation of caspase-9 and caspase-3, resulting in apoptosis [49].

In summary, our results suggest that doxazosin induces caspase-dependent apoptosis, decreased mitotic index and induced cell cycle arrest on C6 and U138-MG glioma cells, and this effect could be mediated by the inhibition of Akt and the activation of GSK-3β and p53

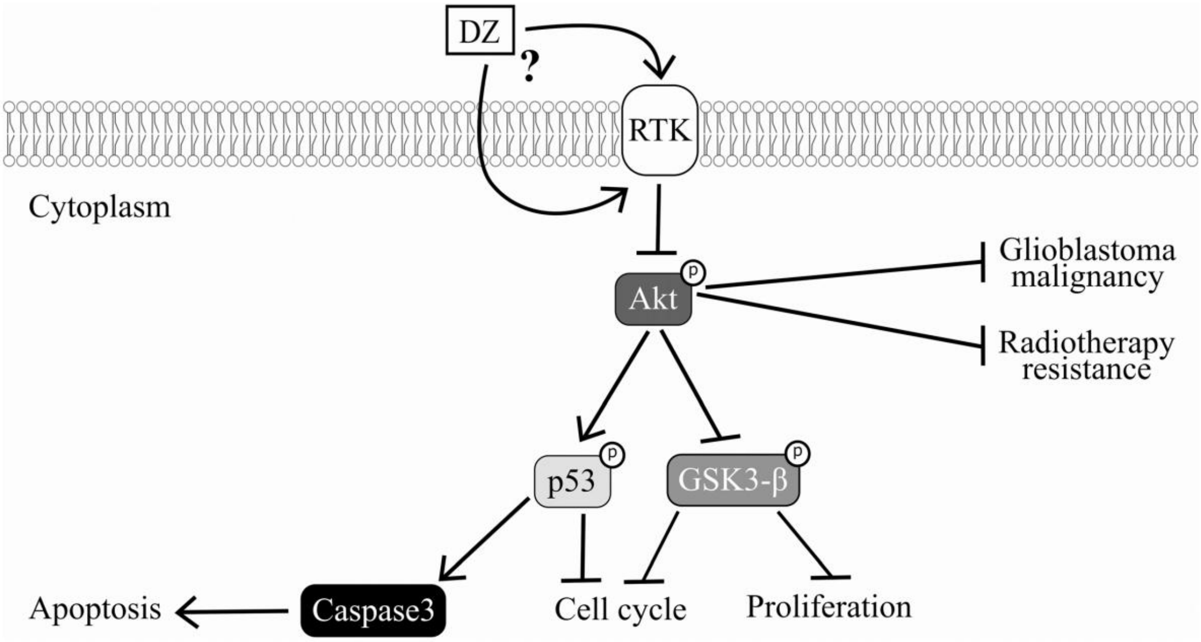

Fig 7. Suggested model of the effects of doxazosin on C6 and U138-MG glioma cells. Doxazosin promotes inhibition of PI3K/Akt pathway, which activates GSK-3β and p53. GSK-3β inhibits cell cycle progression and cell proliferation and p53 induce apoptosis via caspase-3 activation, and also inhibits cell cycle progression.

doi:10.1371/journal.pone.0154612.g007

proteins (Fig 7). Besides, we also show that doxazosin has low cytotoxicity on primary astrocytes and hippocampal organotypic cultures.

Conclusions

Development of new effective therapeutic strategies for the treatment of brain tumors is essential to reduce mortality and morbidity of the disease. Characterization of new drugs that may act as an adjuvant to other anti-tumor therapies could be a very useful strategy for treating gliomas. Doxazosin's pharmacology and safety profile is well-characterized in humans and its adverse-effect profile is acceptable [22], since the most frequent side-effects are dizziness and hypotension [50]. Moreover, Kyprianou and Benning [22] demonstrate that the therapeutic doses of doxazosin with antitumoral effect in mice (3 to 100 mg/Kg) are compared to intracellular doxazosin's concentrations effective on human prostate cancer cells *in vitro* (100 μM). They showed *in vivo* efficacy studies in which doxazosin treatment suppressed significantly the tumorigenic growth of prostate cancer xenographs in SCID mice. Chon et al. [9] and Vashist et al. [51] also demonstrated the in vivo functional significance of doxazosin's action in a mouse model of prostate hyperplasia and in the persistent reduction of intimal hyperplasia in a rabbit model, respectively.

Therefore, we and others [13,22,41,52] suggest that doxazosin can become a new pharmacotherapy alternative for the treatment of cancer, especially gliomas, although more experiments are needed to further elucidate the mechanism of action of this drug on tumor cells and animal models.

Supporting Information

S1 Fig. Distribution of cell death on hippocampal slices after treatment for 48h. (A) Photomicrographs of organotypic hippocampal slice cultures stained with Annexin V and Propidium Iodide after treatment with doxazosin or Lapatinib for 48 hours. Magnification: 40X. **(B)** Schematic representation of a hippocampal slice.
(TIF)

S2 Fig. Cell death on C6 culture after treatment for 48h. Photomicrographs of C6 glioma cells stained with Annexin V and Propidium Iodide after treatment with doxazosin or Lapatinib for 48 hours. Magnification: 200X.
(TIF)

S1 File. Methodology used for fluorescence microscopy analysis of cell death on organptypic hippocampal cultures, C6 and U138-MG cells. Describes the materials and methods used for fluorescence microscopy analysis of cell cultures.
(DOC)

S1 Table. Descriptive statistics of percentage of cell death on neural non-tumor cultures.
(DOC)

S2 Table. Descriptive statistics of percentage of cell death on glioma cell lines.
(DOC)

Author Contributions

Conceived and designed the experiments: MMG PS-A CGS. Performed the experiments: MMG BPC AHQ MCBG. Analyzed the data: MMG BPC JBH SRT VU. Contributed reagents/materials/analysis tools: FCRG CASG PS-A AMOB CGS. Wrote the paper: MMG BPC JBH CGS.

References

1. Van Meir EG, Hadjipanayis CG, Norden AD, Shu H-K, Wen PY, Olson JJ (2010) Exciting New Advances in Neuro-Oncology: The Avenue to a Cure for Malignant Glioma. CA: a cancer journal for clinicians 60: 166–193.
2. Hui H, Fernando MA, Heaney AP (2008) The α 1-adrenergic receptor antagonist doxazosin inhibits EGFR and NF-κB signalling to induce breast cancer cell apoptosis. European Journal of Cancer 44: 160–166. PMID: 18042375
3. Sonoda Y, Ozawa T, Aldape KD, Deen DF, Berger MS, Pieper RO (2001) Akt pathway activation converts anaplastic astrocytoma to glioblastoma multiforme in a human astrocyte model of glioma. Cancer research 61: 6674–6678. PMID: 11559533
4. Zhang Y, Zhang N, Dai B, Liu M, Sawaya R, Xie K, et al. (2008) FoxM1B transcriptionally regulates vascular endothelial growth factor expression and promotes the angiogenesis and growth of glioma cells. Cancer research 68: 8733–8742. doi: 10.1158/0008-5472.CAN-08-1968 PMID: 18974115
5. Jhanwar-Uniyal M, Labagnara M, Friedman M, Kwasnicki A, Murali R (2015) Glioblastoma: Molecular Pathways, Stem Cells and Therapeutic Targets. Cancers 7: 538. doi: 10.3390/cancers7020538 PMID: 25815458
6. Pyko IV, Nakada M, Sabit H, Teng L, Furuyama N, Hayashi Y, et al. (2013) Glycogen synthase kinase 3β inhibition sensitizes human glioblastoma cells to temozolomide by affecting O6-methylguanine DNA methyltransferase promoter methylation via c-Myc signaling. Carcinogenesis 34: 2206–2217. doi: 10.1093/carcin/bgt182 PMID: 23715499
7. Wang X, Chen J-x, Liu Y-h, You C, Mao Q (2013) Mutant TP53 enhances the resistance of glioblastoma cells to temozolomide by up-regulating O6-methylguanine DNA-methyltransferase. Neurological Sciences 34: 1421–1428. doi: 10.1007/s10072-012-1257-9 PMID: 23224642

8. Antonello A, Hrelia P, Leonardi A, Marucci G, Rosini M, Tarozzi A, et al. (2005) Design, synthesis, and biological evaluation of prazosin-related derivatives as multipotent compounds. Journal of medicinal chemistry 48: 28–31. PMID: 15633998
9. Chon JK, Borkowski A, PARTIN AW, ISAACS JT, JACOBS SC, KYPRIANOU N (1999) Alpha 1-adrenoceptor antagonists terazosin and doxazosin induce prostate apoptosis without affecting cell proliferation in patients with benign prostatic hyperplasia. The Journal of urology 161: 2002–2008. PMID: 10332490
10. Yang G, Timme TL, Park SH, Wu X, Wyllie MG, Thompson TC (1997) Transforming growth factor β1 transduced mouse prostate reconstitutions: II. Induction of apoptosis by doxazosin. The Prostate 33: 157–163. PMID: 9365542
11. Siddiqui EJ, Shabbir M, Thompson CS, Mumtaz FH, Mikhailidis DP (2005) Growth inhibitory effect of doxazosin on prostate and bladder cancer cells. Is the serotonin receptor pathway involved? Anticancer research 25: 4281–4286. PMID: 16309229
12. Fernando MA, Heaney AP (2005) α1-Adrenergic receptor antagonists: novel therapy for pituitary adenomas. Molecular Endocrinology 19: 3085–3096. PMID: 16020484
13. Staudacher I, Jehle J, Staudacher K, Pledl H-W, Lemke D, Schweizer PA, et al. (2014) HERG K+ channel-dependent apoptosis and cell cycle arrest in human glioblastoma cells. PloS one 9: e88164. doi: 10.1371/journal.pone.0088164 PMID: 24516604
14. Sakamoto S, Kyprianou N (2010) Targeting Anoikis Resistance in Prostate Cancer Metastasis. Molecular aspects of medicine 31: 205–214. doi: 10.1016/j.mam.2010.02.001 PMID: 20153362
15. Nikolic K, Filipic S, Smoliński A, Kaliszan R, Agbaba D (2013) Partial least square and hierarchical clustering in ADMET modeling: Prediction of blood–brain barrier permeation of α-adrenergic and imidazoline receptor ligands. Journal of Pharmacy & Pharmaceutical Sciences 16: 622–647.
16. Kaye B, Cussans N, Faulkner J, Stopher D, Reid J (1986) The metabolism and kinetics of doxazosin in man, mouse, rat and dog. British journal of clinical pharmacology 21: 19S–25S. PMID: 2939865
17. Gottfried C, Valentim L, Salbego C, Karl J, Wofchuk ST, Rodnight R (1999) Regulation of protein phosphorylation in astrocyte cultures by external calcium ions: specific effects on the phosphorylation of glial fibrillary acidic protein (GFAP), vimentin and heat shock protein 27 (HSP27). Brain research 833: 142–149. PMID: 10375689
18. Stoppini L, Buchs P-A, Muller D (1991) A simple method for organotypic cultures of nervous tissue. Journal of neuroscience methods 37: 173–182. PMID: 1715499
19. Horn AP, Gerhardt D, Geyer AB, Valentim L, Cimarosti H, Tavares A, et al. (2005) Cellular death in hippocampus in response to PI3K pathway inhibition and oxygen and glucose deprivation. Neurochemical research 30: 355–361. PMID: 16018579
20. Vichai V, Kirtikara K (2006) Sulforhodamine B colorimetric assay for cytotoxicity screening. Nature protocols 1: 1112–1116. PMID: 17406391
21. Parhi P, Mohanty C, Sahoo SK (2012) Nanotechnology-based combinational drug delivery: an emerging approach for cancer therapy. Drug Discovery Today 17: 1044–1052. doi: 10.1016/j.drudis.2012.05.010 PMID: 22652342
22. Kyprianou N, Benning CM (2000) Suppression of human prostate cancer cell growth by α1-adrenoceptor antagonists doxazosin and terazosin via induction of apoptosis. Cancer research 60: 4550–4555. PMID: 10969806
23. Vlahos CJ, Matter WF, Hui KY, Brown RF (1994) A specific inhibitor of phosphatidylinositol 3-kinase, 2-(4-morpholinyl)-8-phenyl-4H-1-benzopyran-4-one (LY294002). Journal of Biological Chemistry 269: 5241–5248. PMID: 8106507
24. Wen PY, Schiff D, Lee EQ (2011) Neurologic complications of cancer therapy: Demos Medical Publishing.
25. Zhang H, Gao S (2007) Temozolomide/PLGA microparticles and antitumor activity against Glioma C6 cancer cells in vitro. International Journal of Pharmaceutics 329: 122–128. PMID: 17000068
26. Dehdashti AR, Hegi ME, Regli L, Pica A, Stupp R (2006) New trends in the medical management of glioblastoma multiforme: the role of temozolomide chemotherapy. Neurosurg Focus 20: E6.
27. Lepor H (2007) Alpha Blockers for the Treatment of Benign Prostatic Hyperplasia. Reviews in Urology 9: 181–190. PMID: 18231614
28. Li D-D, Fang F, Li J-R, Du Q-R, Sun J, Gong H-B, et al. (2012) Discovery of 6-substituted 4-anilinoquinazolines with dioxygenated rings as novel EGFR tyrosine kinase inhibitors. Bioorganic & medicinal chemistry letters 22: 5870–5875.
29. Zhang J, Yang PL, Gray NS (2009) Targeting cancer with small molecule kinase inhibitors. Nature Reviews Cancer 9: 28–39. doi: 10.1038/nrc2559 PMID: 19104514

30. Giannopoulou E, Dimitropoulos K, Argyriou A, Koutras A, Dimitrakopoulos F, Kalofonos H (2010) An in vitro study, evaluating the effect of sunitinib and/or lapatinib on two glioma cell lines. Investigational New Drugs 28: 554–560. doi: 10.1007/s10637-009-9290-0 PMID: 19603143

31. Harry GJ, Lefebvre d'Hellencourt C (2003) Dentate Gyrus: Alterations that Occur with Hippocampal Injury. NeuroToxicology 24: 343–356. PMID: 12782100

32. Kaku DA, Giffard RG, Choi DW (1993) Neuroprotective effects of glutamate antagonists and extracellular acidity. Science 260: 1516–1518. PMID: 8389056

33. Vogelbaum MA, Tong JX, Perugu R, Gutmann DH, Rich KM (1999) Overexpression of bax in human glioma cell lines. Journal of neurosurgery 91: 483–489. PMID: 10470825

34. Petty A, Myshkin E, Qin H, Guo H, Miao H, Tochtrop GP, et al. (2012) A small molecule agonist of EphA2 receptor tyrosine kinase inhibits tumor cell migration in vitro and prostate cancer metastasis in vivo. PloS one 7: e42120. doi: 10.1371/journal.pone.0042120 PMID: 22916121

35. El Sharkawi FZ, El Shemy HA, Khaled HM (2013) Possible anticancer activity of rosuvastatine, doxazosin, repaglinide and oxcarbazepin. Asian Pacific journal of cancer prevention: APJCP 15: 199–203.

36. Ryu CH, Yoon WS, Park KY, Kim SM, Lim JY, Woo JS, et al. (2012) Valproic acid downregulates the expression of MGMT and sensitizes temozolomide-resistant glioma cells. BioMed Research International 2012.

37. (2016) Dsmz.de—C6.

38. (2016) Dsmz.de—U-138-MG.

39. Partin J, Anglin I, Kyprianou N (2003) Quinazoline-based α1-adrenoceptor antagonists induce prostate cancer cell apoptosis via TGF-β signalling and IκBα induction. British journal of cancer 88: 1615–1621. PMID: 12771931

40. Garrison JB, Kyprianou N (2006) Doxazosin Induces Apoptosis of Benign and Malignant Prostate Cells via a Death Receptor–Mediated Pathway. Cancer research 66: 464–472. PMID: 16397262

41. Park MS, Kim B-R, Dong SM, Lee S-H, Kim D-Y, Rho SB (2014) The antihypertension drug doxazosin inhibits tumor growth and angiogenesis by decreasing VEGFR-2/Akt/mTOR signaling and VEGF and HIF-1α expression. Oncotarget 5: 4935. PMID: 24952732

42. Salagierski M, Sosnowski M (2009) Therapeutic implications of quinazoline-derived α-1 adrenoreceptor inhibitors in BPH and Prostate Cancer. Central European Journal of Urology 62.

43. Luo J (2009) Glycogen synthase kinase 3β (GSK3β) in tumorigenesis and cancer chemotherapy. Cancer Letters 273: 194–200. doi: 10.1016/j.canlet.2008.05.045 PMID: 18606491

44. Medina M, Wandosell F (2011) Deconstructing GSK-3: The Fine Regulation of Its Activity. International Journal of Alzheimer's Disease 2011: 12.

45. Rocha C, Garcia C, Vieira D, Quinet A, de Andrade-Lima L, Munford V, et al. (2014) Glutathione depletion sensitizes cisplatin-and temozolomide-resistant glioma cells in vitro and in vivo. Cell death & disease 5: e1505.

46. Chen L, Han L, Shi Z, Zhang K, Liu Y, Zheng Y, et al. (2012) LY294002 enhances cytotoxicity of temozolomide in glioma by down-regulation of the PI3K/Akt pathway. Molecular medicine reports 5: 575–579. doi: 10.3892/mmr.2011.674 PMID: 22086271

47. Oren M (0000) Decision making by p53: life, death and cancer. Cell Death Differ 10: 431–442. PMID: 12719720

48. Rocha CRR, Garcia CCM, Vieira DB, Quinet A, de Andrade-Lima LC, Munford V, et al. (2014) Glutathione depletion sensitizes cisplatin- and temozolomide-resistant glioma cells in vitro and in vivo. Cell Death Dis 5: e1505. doi: 10.1038/cddis.2014.465 PMID: 25356874

49. Nikoletopoulou V, Markaki M, Palikaras K, Tavernarakis N (2013) Crosstalk between apoptosis, necrosis and autophagy. Biochimica et Biophysica Acta (BBA)-Molecular Cell Research 1833: 3448–3459.

50. Carruthers SG (1994) Adverse effects of α1-adrenergic blocking drugs. Drug Safety 11: 12–20. PMID: 7917078

51. Vashisht R, Sian M, Franks P, O'Malley M (1992) Long-term reduction of intimal hyperplasia by the selective alpha-1 adrenergic antagonist doxazosin. British journal of surgery 79: 1285–1288. PMID: 1486418

52. Rundle-Thiele D, Head R, Cosgrove L, Martin JH (2015) Repurposing some older drugs that cross the blood–brain barrier and have potential anticancer activity to provide new treatment options for glioblastoma. British journal of clinical pharmacology.

5. CAPÍTULO III

Artigo: *Mitochondrial biogenesis and apoptosis: doxazosin's targets in glioma*

Status: *em preparação*

Mitochondrial biogenesis and apoptosis: doxazosin's targets in glioma

Mariana Maier Gaelzer[1], Bárbara Paranhos Coelho[1], Alice Hoffman de Quadros[1], Vanina Usach[2], Elisa Nicoloso Simões Pires[3], Fátima Costa Rodrigues Guma[1], Patrícia Setton-Avruj[2], Cristiane Matté[1],Christianne G. Salbego[1].

[1]Programa de Pós-Graduação em Ciências Biológicas-Bioquímica Instituto de Ciências Básicas da Saúde, Universidade Federal do Rio Grande do Sul, Porto Alegre, RS, Brasil-

[2]Universidad de Buenos Aires Departamento de Química Biologica, Ciudad Autónoma de Buenos Aires, Argentina.

[3]Departamento de Ciências Biológicas, Universidade Federal do Rio de Janeiro , Rio de Janeiro, RJ, Brasil.

[4]Departamento de Biofísica, Universidade Federal do Rio Grande do Sul, Porto Alegre, RS, Brasil.

Corresponding author:

Mariana Maier Gaelzer

Departamento de Bioquímica, Instituto de Ciências Básicas da Saúde, UFRGS

Rua Ramiro Barcelos, 2600 – anexo, CEP 90035-003, Porto Alegre, RS, Brasil

Telephone: +55 (51) 3308.5547

Fax: +55 (51) 3308.5535

E-mail: marianamaierg@gmail.com

Funding: Conselho Nacional de Desenvolvimento Científico e Tecnológico (CNPq); Coordenação de Aperfeiçoamento de Pessoal de Nível Superior (Capes); Fundação de Amparo à Pesquisa do Estado do Rio Grande do Sul (FAPERGS).

Abstract

Malignant tumors, including gliomas, are the most common primary intracranial brain tumor in adults. This cancer display abnormal energy production and inherent resistance to apoptosis, suggesting an underlying involvement of dysfunctional mitochondria in glioma pathophysiology. The PI3K/Akt pathway is involved with glioma tumorigenesis and resistance to therapy. GSK-3β, a substrate of Akt, is reported as a tumor suppressor and is involved with induction of intrinsic apoptosis. Nucleomitochondrial interactions depend on the interplay between transcription factors (TFAM) and regulated coactivators (PGC-1α). CREB is a transcription factor and a Akt substrate that enhances tumor proliferation, chemotherapy resistance, PGC-1α transcription and impairs apoptosis induction. Moreover, the cytokines TNF-α, IL-1β and IL-6 are negative regulators of PGC-1α and increase tumor growth, malignancy and therapy resistance. Here, we analyzed how doxazosin (an antihipertensive agent) treatment affected signaling between mitochondria and cytoplasm/nucleus. In addition, we analyzed secretion of TNF-α, IL-1β and IL-6 by C6 cells after doxazosin exposure. Our results provide insight into doxazosin's effect on mitochondrial dynamics and cytoplasmatic interaction in glioma. Understanding aberrant mitochondrial function in gliomas is essential to provide new directions in the development of novel research approaches that translate into therapies.

Keywords: Glioma, mitochondrial biogenesis, doxazosin, TFAM, PGC-1α, apoptosis

Introduction

Glioblastoma (GB), is the most common primary intracranial brain tumor in adults. GBs are aggressive, resistant and invasive tumors. This leads to a high recurrence rate of about 90% [1]. They constitute the second most common malignant neoplasia, representing 16% of all primary brain tumors [2]. Diagnosis and management of this type of cancer results in extensive individual, social, healthcare and economic burden [3]. Therefore, it is important to investigate new therapeutic strategies, due to GBs high recurrence rate (90%) and mortality rate close to 100% [4].

The α1-adrenoceptor antagonist doxazosin is a quinazoline-based drug and is the most frequently prescribed drug, being approved by the FDA (Food and Drugs Administration) for benign prostatic hyperplasia (BPH) and elevated blood pressure [5]. BPH or hypertension patients who were treated long-term with α1-adrenoceptor antagonists showed a significantly lower incidence of prostate cancer (a drop of 31.7%) [6]. In other studies doxazosin induced apoptosis of normal and malignant prostate cells through an alternative mechanism unrelated to the α1-adrenoceptor [7]. The drug also exerted pro-apoptotic effects in breast cancer [8], urothelial cancer [9], human prostatic stromal and in prostate cancer LNCaP cells [10-11].

Advantages of repurposing drugs are the well-defined pharmacokinetics and side effects, and the drug has passed the required toxicity and safety tests with settled protocols and dosing [12]. Regarding doxazosin, it is established the drug's antitumoral effects are not related with its α1-adrenoceptor antagonism [7]. Due to its physicochemical characteristics, doxazosin is able to permeate the BBB [13], and we found the drug presented low neurotoxicity on non-tumor cells [14].

Cancer cells can adapt and resist to various environmental changes, e.g. decrease in oxygen concentrations and nutrients, as well as drug exposure. GB metabolism is dynamical in order to maintain growth, survival and high proliferative rate even within a hostile enviroment [15], which can provide resistance to many anticancer drugs [3]. Targeted therapies can also induce deep metabolic changes that regulate treatment response due to cancer cells metabolic plasticicity [3, 16].

Mitochondria have a fundamental role regulating apoptosis, cell proliferation, energy metabolism and reactive oxygen species balance [3]. Those processes are deregulated in gliomas, with few studies investigating mitochondrial function and dynamics in cancer cells [3].

Several studies demonstrate that mitochondrial metabolism greatly influences cancer cell survival, proliferation, invasion, apoptosis and indicate a role for this organelle in development of resistance to many anticancer drugs [3, 17-18]. Considering the importance of mitochondria for cancer cells plasticity and GB's innate treatment resistance, we analyzed doxazosin's effects on mitochondrial biogenesis and the signaling pathways involved with this process on C6 glioma cells. Previously we showed doxazosin induces apoptosis in glioma cells via PI3K/Akt pathway inhibition and G0/G1 arrest via p53 activation [14].

Mitochondrial biogenesis and function is regulated by nuclear and mitochondrial transcriptional factors and coativators, e.g. mitochondrial transcription factor A (TFAM) and peroxisome proliferator-activated receptor-γ coactivator-1α (PGC-1α), respectively [19-22]. It is believed PGC-1α serves as a link between nuclear regulatory events and mitochondrial transcription machinery, neuroprotection and therapy resistance [21-24].

In addition, gliomas are characterized by a deregulated network of cytokines [25]. Cytokines are known for their role in immune response, however they have a vital participation in other cellular processes, including cell differentiation and proliferation [26].

Here, we analyzed how doxazosin's treatment affected signaling between mitochondria and cytoplasm/nucleus. Moreover, we analyzed secretion of the cytokines tumor necrosis factor α (TNF-α), interleukin-1β (IL-1β) and interleukin-6 (IL-6) by C6 cells after doxazosin exposure, since these cytokines are negative regulators of PGC-1α [27-29]. Our results provide insight into doxazosin's effect on mitochondrial dynamics and cytoplasmatic interaction in glioma.

Materials and methods

Chemicals and materials

Cell culture media and fetal bovine serum (FBS) were obtained from Gibco-Invitrogen (Grand Island, NY, USA). Doxasozin and Propidium iodide (PI) were obtained from Sigma Chemical Co (St. Louis, MO, USA). All other reagents were purchased from Sigma Chemical Co. (St. Louis, MO, USA) or Merck (Darmstadt, Germany). All other chemicals and solvents used were of analytical or pharmaceutical grade.

Cell culture

C6 rat glioma cell line was obtained from American Type Culture Collection (Rockville, Mariland, Md., USA). C6 cells were grown and maintained in Dulbecco’s Modified Eagle’s Medium (DMEM, Gibco-Invitrogen, Grand Island, NY, USA) supplemented with 5% (v/v) FBS (Gibco-Invitrogen, Grand Island, NY, USA), and containing 2.5 mg/mL of Fungizone® and 100 U/L of gentamicine (Shering do Brasil, São Paulo, SP, Brazil). Cells were kept at 37ºC, in an atmosphere of 5% CO_2 and were used until the 30th passage.

Doxazosin treatment

C6 glioma cells were seeded in DMEM/5% FBS in 24 well plates and grown for 24 hours. Doxazosin was dissolved in 20% ethanol/ milli-Q™ water (vehicle). Cells were treated with the drug for 48 hours with concentrations ranging from 50 µM to 180 µM [14]. Control groups were processed in parallel without receiving treatment with doxazosin. The results of vehicle groups were similar to control groups.

Caspase-3 activity

Caspase-3 activity was determined by fluorometric measurement of the kinetics of 7-amino-4-trifluoromethyl coumarin (AFC) release from the fluorogenic substrate Ac-DEVDAFC (Sigma–Aldrich) in the presence of cell lysates. Cells were washed in PBS and lysed on ice-cold PBS and 0.2% Triton X-100 solution. Extracts were clarified by centrifugation at 10,000g for 5 min.For assays, 30 µg proteins were mixed with assay buffer (g/mL) (Sucrose 0.1, CHAPS 0.001, BSA 0.0001 and HEPES-NaOH 0.024 , pH 7.4) plus 10 µL of substrate solution (0.2 mg/ml). Caspase-3-mediated substrate cleavage was monitored during 40 min (37°C) in a SpectraMax M5 Microplate Reader (excitation 390 nm/emission 520 nm).

Enzyme-linked immunosorbent assay (ELISA)

ELISA was used to determine cytokine levels in the culture medium of C6 cells after doxazosin treatment. After 48h of doxazosin exposure (150 and 180 μM), the culture medium was collected, rapidly frozen, and stored at -20 ºC for later measurement of IL-1β, IL-6 and TNF-α levels using specific ELISA kits (R&D Systems, Minneapolis, MN, USA) in accordance with the manufacturer's recommendations. Standard curves were obtained using recombinant rat IL-1β, IL-6 and TNF-α.

Flow Cytometry

Mitochondrial superoxide was measured using the MitoSOX® Red (Invitrogen®, Molecular Probes, Eugene, OR – USA), while mitochondrial mass and membrane potential were evaluated using Mito Tracker® Green and Mito Tracker® Red (Invitrogen®, Molecular probes Eugene, OR – USA), respectively (FACS Calibur, BD Bioscience, Mountain View, CA, USA). Cells were harvested by tripsinization and incubated in a solution of phosphate-buffered saline (PBS) pH 7,4 with 1 μM MitoSOX for 10 min or 100 nM Mitotracker Green/Red for 45 min at 37°C, in the dark.

For analysis of TFAM and PGC-1α, C6 cells were trypsinized and centrifuged at 400 x *g* for 5 min. Cells were resuspended in PBS containing 0,1% Triton X-100 and incubated with the following antibodies: mouse anti-cleaved caspase 3 (1:100; Cell Signaling), for 30 min at room temperature. Then, secondary antibody anti-mouse Alexa Fluor 488 (1:100, Invitrogen) was added and, after incubation for 30 min, fluorescence intensity was analyzed by flow cytometry.

Data acquisition was done by flow cytometry using a FACS Calibur cytometry system and Cell Quest software (BD Bioscience, Mountain View, CA, USA). Data obtained was analyzed with FlowJo software (FlowJo, LLC, Ashland, Oregon, USA).

Confocal microscopy

Cells were seeded on coverlips and, 24h later, were treated with 180 µM doxazosin. After 48h of treatment, cells were fixed with 4% (w/v) paraformaldehyde and stained with 10µg/ml Hoechst 33342 (Sigma) in the presence of 0.1% Triton X-100 and processed for immunocytochemistry. Cells were incubated with blocking solution (5% albumin in PBS) for 2h. Then cells were incubated with primary antibodies p-Akt$_{Ser473}$ (1:500; Cell Signaling), p-GSK-3β$_{Ser9}$(1:500; Cell Signaling) and p-CREB$_{Ser133}$ (1:500; Cell Signaling) for 1h followed by incubation with secondary antibodies Alexa Fluor 488 (1:1000, Invitrogen) or Alexa Fluor 555 (1:1000, Invitrogen) for 1h. Confocal images were taken in an Olympus FV-1000 confocal microscope.

Statistical analysis

Data are expressed as means±SE. All results are representative of at least 4 independent experiments. Analysis of variance (ANOVA) was applied to the means to determine statistical differences between experimental groups. Post hoc comparisons were performed by Newman-Keuls Multiple Comparison test. Differences between mean values were considered significant when $p<0.05$.

Results

Doxazosin increased mitochondrial biogenesis and superoxide production

Initially, we analyzed superoxide (SO) production in C6 cells after doxazosin treatment. At concentrations of 150 and 180 µM, doxazosin increased SO production (Fig. 1a).

In order to evaluate mitochondrial biogenesis in C6 treated with doxazosin, we used MitoTracker Green (MTG) and MitoTracker Red (MTR). We used the fluorescence intensity emitted by MTG as an estimate of the overall mitochondrial mass, since it accumulates in the mitochondria in a membrane potential independent manner. We used MTR to analyze mitochondrial membrane potential (Δψm). MTR stains mitochondria in live cells and accumulates in proportion to the membrane potential. At concentrations of 150 and 180 µM, doxazosin increased MTG (Fig. 1b) and MTR (Fig. 1c) staining. In summary, doxazosin treatment increased SO generation and induced mitochondrial biogenesis in C6 cells.

C6 cells decrease secretion of TNF-α after doxazosin exposure

Gliomas are characterized by a deregulated network of cytokines [25]. These are a large group of secreted peptide molecules that act as paracrine messengers [25]. Secreted cytokine levels were assessed in C6 cells after doxazosin treatment. After 48h of treatment, doxazosin decreased the release of TNF-α by C6 cells, while levels of IL-1β and IL-6 remained the same (Fig. 2).

Caspase-3 activation by doxazosin induces apoptosis

Doxazosin increased caspases 3 activity after 48h treatment at 150 and 180 µM (Fig. 3a). In Fig. 3b, it is shown, by Hoechst staining, the presence of picnotic nuclei - for the concentration of 180 µM doxazosin.

Doxazosin treatment affects signaling between mitochondria and cytoplasm/nucleus

Peroxisome proliferator-activated receptor-γ coactivator-1α (PGC-1α) is a potent inducer of mitochondrial biogenesis and also of a diverse range of mitochondrial processes [22-23]. Mitochondrial transcription factor A (TFAM) is involved with the control of mitochondrial DNA (mtDNA) maintenance and transcriptional expression [19]. Doxazosin treatment for 48 h at 180 µM increased both, TFAM and PGC-α protein levels, in C6 (Fig. 4a).

Next, we analyzed activation of proteins involved with glioma cell survival and proliferation. As shown in figure 4 (Fig. 4b, c and d), p-Akt$_{Ser473}$, p-GSK-3β$_{Ser9}$ and p-CREB$_{Ser133}$ immunostaining decreased with 180 µM doxazosin treatment.

Discussion

Malignant tumors, including gliomas, display abnormal energy production and inherent resistance to apoptosis, suggesting an underlying involvement of dysfunctional mitochondria in glioma pathophysiology [3, 30-32]. In this study, we found doxazosin increased MitoSox and MitoTracker staining as well as PGC-1α and TFAM protein levels in C6 cells. Therefore, treatment increased mitochondrial superoxide production and induced mitochondrial biogenesis. In addition, we showed doxazosin induced apoptosis in

C6 cells through increase of caspase-3 activity and picnotic nuclei detection and the drug decreased p-Akt$_{Ser473}$, p-GSK3β$_{Ser9}$ and p-CREB$_{Ser133}$ immunostaining.

Akt regulates cell proliferation and survival and, when active (phosphorylated), Akt phosphorylates and inhibits GSK-3β at Ser9 [8, 14]. In hepatocellular carcinoma cells and in glioma cells, when GSK-3β is phosphorylated by Akt, association of Hexokinase II (HKII) to the outer mitochondrial membrane (OMM) is enhanced. This association contributes with the Warburg effect and cell proliferation in cancer cells and maintain the mitochondrial permeability transition pore (PTP) locked, which contributes to the anti-apoptotic phenotype in cancer cells. Moreover, activation of GSK-3β by Akt inhibition favour mitochondrial detachment of HKII, allows for the opening of the PTP and leads to apoptosis activation [33-36].

In addition, Akt phosphorylates CREB at Ser133 enhancing CREB's transcriptional activity [37]. In tumors, studies show phosphorylated CREB enhances tumor proliferation, chemotherapy resistance and impair apoptosis induction [38]. Therefore, here and previously [14] we found doxazosin inhibits a central survival signaling in gliomas: the PI3K/Akt pathway. We showed several downstream targets of Akt are influenced by doxazosin, ultimately leading to cell cycle arrest and apoptosis induction.

In regards to mitochondrial function in gliomas, there is lack of study on this topic. In this study we showed doxazosin increased mitochondrial SO production and mitochondrial biogenesis. Benhar et al. [39] demonstrated anticancer agents can induce prolonged increase in ROS levels resulting in potentiation of apoptosis. Thus, ROS modulates the ability of stress kinases to stimulate cell growth or death. In accordance with this observations, Skildum et. al [40] showed troglitazone (a PPARγ ligand) increased mitochondrial superoxide generation and inhibition of cellular proliferation in breast cancer cell lines and co-treatment with troglitazone potentiated the antitumoral effects of doxorubicin. This was acomplished by increase in PGC1-α mRNA levels. In our study, doxazosin alone was able to induce glioma cell death, while increased mitochondrial SO generation, PGC-1a and TFAM protein levels and mitochondrial mass and membrane potential (which lead to mitochondrial biogenesis).

Nonetheless, it may seem contradictory that a drug induces both apoptosis and mitochondrial biogenesis, but this was observed in some types of cancer. Yadav et al. [16] demonstrated that chemotherapy induce mitochondrial biogenesis independently of caspase-activated apoptosis in several cancer cell lines. In addition, Wang and Moraes [41] treated three human cancer cell lines (HeLa – cervical carcinoma; 143B – osteosarcoma; MDA-MB-231 – breast cancer) with bezafibrate - a PPARs panagonist that also enhances PGC-1α expression and induces mitochondrial biogenesis - and found cells had decreased glycolytic and growth rates. Furthermore, Wu et al. [42] showed in SH-SY5Y neuroblastoma cells that methanphetamine increased mitochondrial mass after 24h treatment and, after 48 h, induced apoptosis, decreased mtDNA copy number and decreased mitochondrial protein contents per mitochondrion.

On the other hand, some studies associate mitochondrial biogenesis as a drug resistance mechanism by cancer cells. Zhang et al. [43] found BRAF^{V600}-mutated melanoma cell lines (this mutation results in constitutively activated MAPK signaling) increased mitochondrial biogenesis and oxidative phosphorylation (OXPHOS) to survive MAPK inhibitors treatment. In adittion, Vellinga et al. [24] showed on liver metastases of colon cancer that mitochondrial biogenesis genes had higher expression levels in chemotherapy-treated tumors in comparison with nontreated tumors. Furthermore, the authors treated patient-derived colonosphere cultures with chemotherapy and found increased mitochondria mass and shifted glycolysis to OXPHOS via sirtuin1/PGC-1α.

Here, p-CREB$_{Ser133}$ levels decreased with doxazosin treatment. Studies show p-CREB-mediated increase of PGC-1α transcription relates to changes in the cell metabolism in response to alterations in the environment [19]. We found doxazosin increased PGC-1α independently from CREB regulation. The increase in mitochondrial biogenesis could be a mechanism of doxazosin's antitumoral effects, instead of a mechanism of C6 cells resistance to the treatment.

Furthermore, we previously found doxazosin induces cell death on glioma cells (C6 and U138-MG) and at 250μM presents low neurotoxicity on non-tumor cells (primary astrocyte and hippocampal organotypic cultures), having a selectivity towards the cancer cells [14]. Doxazosin's increase in PGC-1α levels found here could provide an explanation to the drug's low toxicity in non-tumor cells. Dabrowska et al. [44] demonstrated PGC-1α exerts neuroprotective effects by promoting mitochondrial biogenesis and functioning in dopaminergic neurons exposed to lead insult. However, the precise regulatory role of PGC-1α in the control of mitochondrial dynamics and neurotoxicity is still largely unknown.

We found doxazosin treatment decreased secretion of TNF-α. This cytokine is involved in survival, differentiation and death in non-tumoral cells. Balkwill [45] showed TNF-α can act as tumor promotor when produced and secreted by the cancer cells via stimulation of growth, proliferation, invasion, metastasis and angiogenesis. The balance between cell survival and death in TNF-α signaling is determinant for cellular response. Several studies have demosntrated TNF-α plasma levels increase in patients with cancer

[46-48]. In addition, the cytokines TNF-α, IL-1β and IL-6 are negative regulators of PGC-1α [27-29]. Therefore, the increase we found in PGC-1α levels in cells treated with doxazosin could be related to the decrease of TNF-α secretion.

Our findings demonstrate doxazosin alters mitochondrial dynamics in glioma cells. Mitochondrial function is aberrant in gliomas and these organelles can influence cancer cells therapy resistance. Therefore, understanding the effects of new therapeutic agents on tumor cells mitochondria can improve the development of novel antiglioma therapies.

References

1. Jackson, R.J., et al., *Limitations of stereotactic biopsy in the initial management of gliomas.* Neuro-oncology, 2001. 3(3): p. 193-200.
2. Dolecek, T.A., et al., *CBTRUS statistical report: primary brain and central nervous system tumors diagnosed in the United States in 2005–2009.* Neuro-oncology, 2012. 14(suppl 5): p. v1-v49.
3. Ordys, B.B., et al., *The role of mitochondria in glioma pathophysiology.* Molecular neurobiology, 2010. 42(1): p. 64-75.
4. Scott, J., et al., *Long-term glioblastoma multiforme survivors: a population-based study*. Canadian Journal of Neurological Sciences/Journal Canadien des Sciences Neurologiques, 1998. 25(03): p. 197-201.
5. Antonello, A., et al., *Design, synthesis, and biological evaluation of prazosin-related derivatives as multipotent compounds.* Journal of medicinal chemistry, 2005. 48(1): p. 28-31.

6. Sakamoto, S. and N. Kyprianou, *Targeting anoikis resistance in prostate cancer metastasis.* Molecular aspects of medicine, 2010. 31(2): p. 205-214.

7. González-Juanatey, J.R., et al., *Doxazosin induces apoptosis in cardiomyocytes cultured in vitro by a mechanism that is independent of α1-adrenergic blockade.* Circulation, 2003. 107(1): p. 127-131.

8. Hui, H., M.A. Fernando, and A.P. Heaney, *The α 1-adrenergic receptor antagonist doxazosin inhibits EGFR and NF-κB signalling to induce breast cancer cell apoptosis.* European Journal of Cancer, 2008. 44(1): p. 160-166.

9. SIDDIQUI, E.J., et al., *Growth inhibitory effect of doxazosin on prostate and bladder cancer cells. Is the serotonin receptor pathway involved?* Anticancer research, 2005. 25(6B): p. 4281-4286.

10. Chon, J.K., et al., *Alpha 1-adrenoceptor antagonists terazosin and doxazosin induce prostate apoptosis without affecting cell proliferation in patients with benign prostatic hyperplasia.* The Journal of urology, 1999. 161(6): p. 2002-2008.

11. Yang, G., et al., *Transforming growth factor β1 transduced mouse prostate reconstitutions: II. Induction of apoptosis by doxazosin.* The Prostate, 1997. 33(3): p. 157-163.

12. Pantziarka, P., et al., *The repurposing drugs in oncology (ReDO) project.* 2014.

13. Nikolic, K., et al., *Partial least square and hierarchical clustering in ADMET modeling: Prediction of blood–brain barrier permeation of α-adrenergic and imidazoline receptor ligands.* Journal of Pharmacy & Pharmaceutical Sciences, 2013. 16(4): p. 622-647.

14. Gaelzer, M.M., et al., *Phosphatidylinositol 3-Kinase/AKT pathway inhibition by doxazosin promotes glioblastoma cells death, upregulation of p53 and triggers low neurotoxicity*. PloS one, 2016. 11(4): p. e0154612.

15. Gaelzer, M.M., et al., *Hypoxic and Reoxygenated Microenvironment: Stemness and Differentiation State in Glioblastoma.* Molecular neurobiology, 2016: p. 1-12.

16. Yadava PhD, N., *Oxidative phosphorylation-dependent regulation of cancer cell apoptosis in response to anticancer agents.* 2015.

17. Rasola, A. and F. Chiara, *GSK-3 and mitochondria in cancer cells.* Frontiers in oncology, 2013. 3: p. 16.

18. Farrand, L., et al., *Piceatannol enhances cisplatin sensitivity in ovarian cancer via modulation of p53, X-linked inhibitor of apoptosis protein (XIAP), and mitochondrial fission.* Journal of Biological Chemistry, 2013. 288(33): p. 23740-23750.

19. Scarpulla, R.C., *Transcriptional paradigms in mammalian mitochondrial biogenesis and function.* Physiological reviews, 2008. 88(2): p. 611-638.

20. Hock, M.B. and A. Kralli, *Transcriptional control of mitochondrial biogenesis and function.* Annual review of physiology, 2009. 71: p. 177-203.

21. Ventura-Clapier, R., A. Garnier, and V. Veksler, *Transcriptional control of mitochondrial biogenesis: the central role of PGC-1α.* Cardiovascular research, 2008. 79(2): p. 208-217.

22. Fernandez-Marcos, P.J. and J. Auwerx, *Regulation of PGC-1α, a nodal regulator of mitochondrial biogenesis*. The American journal of clinical nutrition, 2011. 93(4): p. 884S-890S.

23. O'Donnell, K.C., et al., *Axon degeneration and PGC-1α-mediated protection in a zebrafish model of α-synuclein toxicity.* Disease models & mechanisms, 2014. 7(5): p. 571-582.

24. Vellinga, T.T., et al., *SIRT1/PGC1α-dependent increase in oxidative phosphorylation supports chemotherapy resistance of colon cancer.* Clinical cancer research, 2015. 21(12): p. 2870-2879.

25. Christofides, A., M. Kosmopoulos, and C. Piperi, *Pathophysiological mechanisms regulated by cytokines in gliomas.* Cytokine, 2015. 71(2): p. 377-384.

26. Rivest, S., *Molecular insights on the cerebral innate immune system.* Brain, behavior, and immunity, 2003. 17(1): p. 13-19.

27. Palomer, X., et al., *TNF-α reduces PGC-1α expression through NF-κB and p38 MAPK leading to increased glucose oxidation in a human cardiac cell model.* Cardiovascular research, 2009. 81(4): p. 703-712.

28. Tang, K., P.D. Wagner, and E.C. Breen, *TNF-α-mediated reduction in PGC-1α may impair skeletal muscle function after cigarette smoke exposure.* Journal of cellular physiology, 2010. 222(2): p. 320-327.

29. Kim, M.S., et al., *Tumor necrosis factor and interleukin 1 decrease RXRα, PPARα, PPARγ, LXRα, and the coactivators SRC-1, PGC-1α, and PGC-1β in liver cells.* Metabolism, 2007. 56(2): p. 267-279.

30. Furnari, F.B., et al., *Malignant astrocytic glioma: genetics, biology, and paths to treatment.* Genes & development, 2007. 21(21): p. 2683-2710.

31. Ziegler, D.S., A.L. Kung, and M.W. Kieran, *Anti-apoptosis mechanisms in malignant gliomas.* Journal of Clinical Oncology, 2008. 26(3): p. 493-500.

32. Seyfried, T.N. and P. Mukherjee, *Targeting energy metabolism in brain cancer: review and hypothesis.* Nutrition & metabolism, 2005. 2(1): p. 30.

33. Kim, W., et al., *Apoptosis-inducing antitumor efficacy of hexokinase II inhibitor in hepatocellular carcinoma.* Molecular cancer therapeutics, 2007. 6(9): p. 2554-2562.

34. Machida, K., Y. Ohta, and H. Osada, *Suppression of apoptosis by cyclophilin D via stabilization of hexokinase II mitochondrial binding in cancer cells.* Journal of Biological Chemistry, 2006. 281(20): p. 14314-14320.

35. Mathupala, S., Y.a. Ko, and P. Pedersen, *Hexokinase II: cancer's double-edged sword acting as both facilitator and gatekeeper of malignancy when bound to mitochondria.* Oncogene, 2006. 25(34): p. 4777-4786.

36. Robey, R.a. and N. Hay, *Mitochondrial hexokinases, novel mediators of the antiapoptotic effects of growth factors and Akt.* Oncogene, 2006. 25(34): p. 4683-4696.

37. Du, K. and M. Montminy, *CREB is a regulatory target for the protein kinase Akt/PKB.* Journal of Biological Chemistry, 1998. 273(49): p. 32377-32379.

38. Steven, A. and B. Seliger, *Control of CREB expression in tumors: from molecular mechanisms and signal transduction pathways to therapeutic target.* Oncotarget, 2016. 7(23): p. 35454.

39. Benhar, M., D. Engelberg, and A. Levitzki, *ROS, stress-activated kinases and stress signaling in cancer.* EMBO reports, 2002. 3(5): p. 420-425.

40. Skildum, A., K. Dornfeld, and K. Wallace, *Mitochondrial amplification selectively increases doxorubicin sensitivity in breast cancer cells with acquired antiestrogen resistance.* Breast cancer research and treatment, 2011. 129(3): p. 785-797.

41. Wang, X. and C.T. Moraes, *Increases in mitochondrial biogenesis impair carcinogenesis at multiple levels.* Molecular oncology, 2011. 5(5): p. 399-409.

42. Wu, C.-W., et al., *Enhanced oxidative stress and aberrant mitochondrial biogenesis in human neuroblastoma SH-SY5Y cells during methamphetamine induced apoptosis.* Toxicology and applied pharmacology, 2007. 220(3): p. 243-251.

43. Zhang, G., et al., *Targeting mitochondrial biogenesis to overcome drug resistance to MAPK inhibitors.* The Journal of clinical investigation, 2016. 126(5): p. 1834.

44. Dabrowska, A., *PGC1α controls mitochondrial biogenesis and dynamics in lead-induced neurotoxicity*. 2015, Imperial College London.

45. Balkwill, F., *Tumor necrosis factor or tumor promoting factor?* Cytokine and Growth Factor Reviews, 2002. 13(2): p. 135-141.

46. Yoshida, N., et al., *Interleukin-6, tumour necrosis factor α and interleukin-1β in patients with renal cell carcinoma.* British journal of cancer, 2002. 86(9): p. 1396-1400.

47. Pfitzenmaier, J., et al., *Elevation of cytokine levels in cachectic patients with prostate carcinoma.* Cancer, 2003. 97(5): p. 1211-1216.

48. Michalaki, V., et al., *Serum levels of IL-6 and TNF-α correlate with clinicopathological features and patient survival in patients with prostate cancer.* British journal of cancer, 2004. 90(12): p. 2312-2316.

Figure Legends:

Figure 1. Analysis of mitochondrial parameters after 48 h treatment with doxazosin in C6 cells. Cells were stained in **a** with MitoSox, in **b** with MitoTracker Green and in **c** with

MitoTracker Red. Data are represented as means ± SEM ($n = 6$). *$p < 0.05$, **$p < 0.01$ and ***$p < 0.001$ vs. control.

Figure 2. Levels of secreted cytokines by C6 cells after 48 h treatment with doxazosin. In **a** are the IL-1β levels, in **b** is IL-6 and TNF-α in **c**. Data are represented as means ± SEM ($n = 6$). *$p < 0.05$ vs. control.

Figure 3. Analysis of caspase activity and cell death (tem o Hoechst) in C6 cells after doxazosin treatment for 48 h. Caspase 3 activity in **a**. In **b**, Hoechst staining with arrows pointing to picnotic nuclei.Data are represented as means ± SEM ($n = 8$). ***$p < 0.001$ vs. control.

Figure 4. Analysis of proteins involved in signaling between mitochondria and cytoplasm/nucleus after doxazosin treatment in C6 cells. Histogram of TFAM and PGC-1α protein levels in **a**. Immunostaining of p-Akt$_{\mathrm{Ser473}}$ in **b**, p-GKS-3β$_{\mathrm{Ser9}}$ in **c** and p-CREB$_{\mathrm{Ser133}}$ in **d**.

Figure 5. Suggested model of the effects of doxazosin on mitochondrial dynamics on C6 glioma cells. Doxazosin inhibits the PI3K/Akt pathway, which activates GSK-3β. In turn, GSK-3β influences induction of mitochondrial apoptosis through mitochondrial permeability transition pore (mPTP) opening and caspase 3 activation. Doxazosin also decreases TNF-α secretion, which could lead to PGC-1α activation. PGC-1α enhances TFAM transcription, which induces mitochondrial biogenesis. **HKII:** hexokinase II.

Figure 1

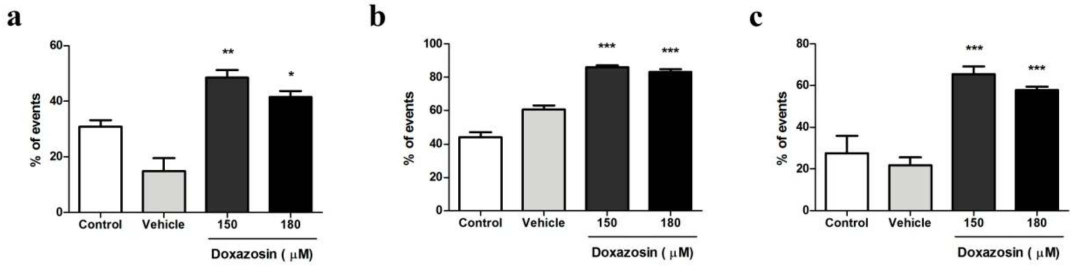
a
60
40
20
0
% of events
**
*
Control
Vehicle
150
180
Doxazosin (μM)
b
100
80
60
40
20
0
% of events
***
***
Control
Vehicle
150
180
Doxazosin (μM)
c
80
60
40
20
0
% of events
***
***
Control
Vehicle
150
180
Doxazosin (μM)

Figure 2

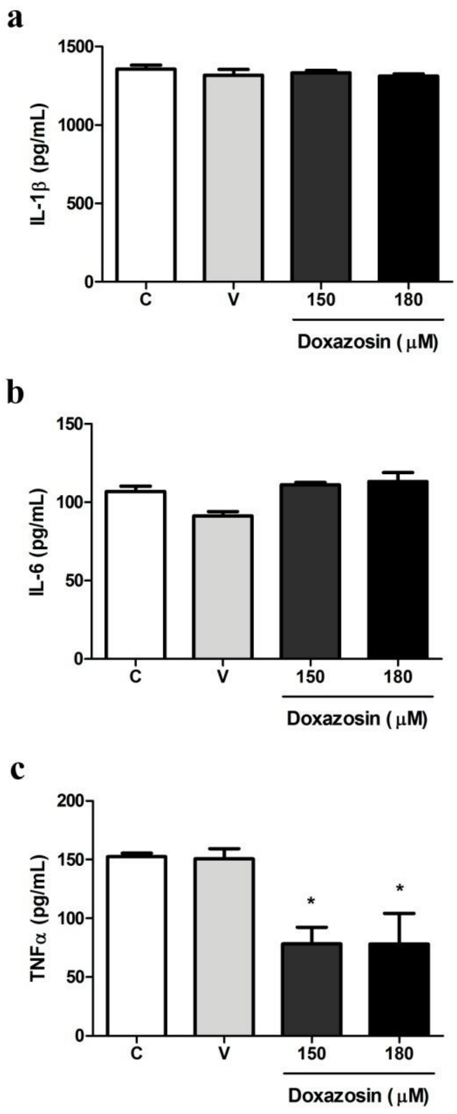
a
1500
1000
500
0
IL-1β (pg/mL)
C
V
150
180
Doxazosin (μM)
b
150
100
50
0
IL-6 (pg/mL)
C
V
150
180
Doxazosin (μM)
c
200
150
100
50
0
TNFα (pg/mL)
*
*
C
V
150
180
Doxazosin (μM)

Figure 3

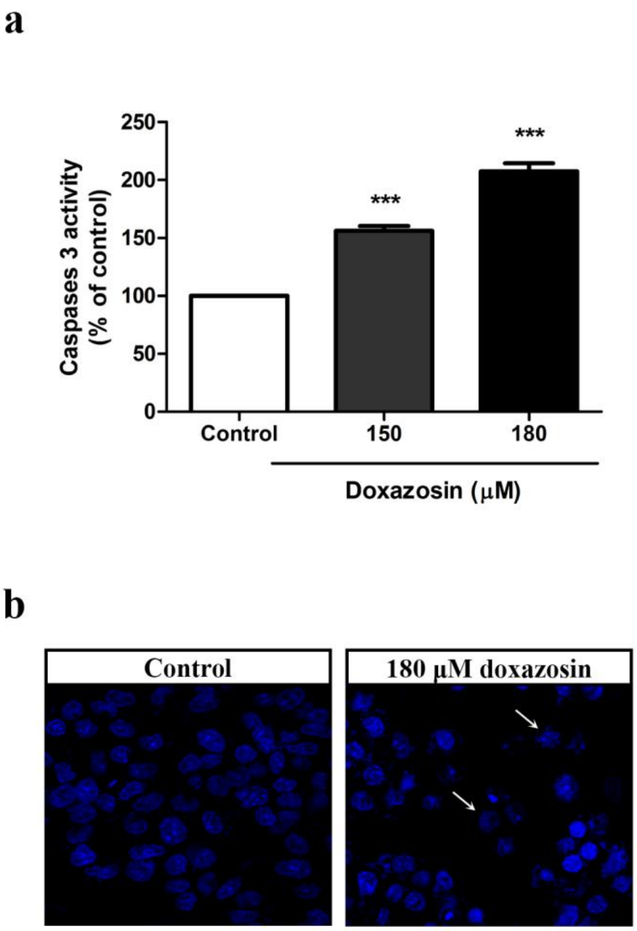
a
Caspases 3 activity
(% of control)
250
200
150
100
50
0
***
***
Control
150
180
Doxazosin (μM)
b
Control
180 μM doxazosin

Figure 4

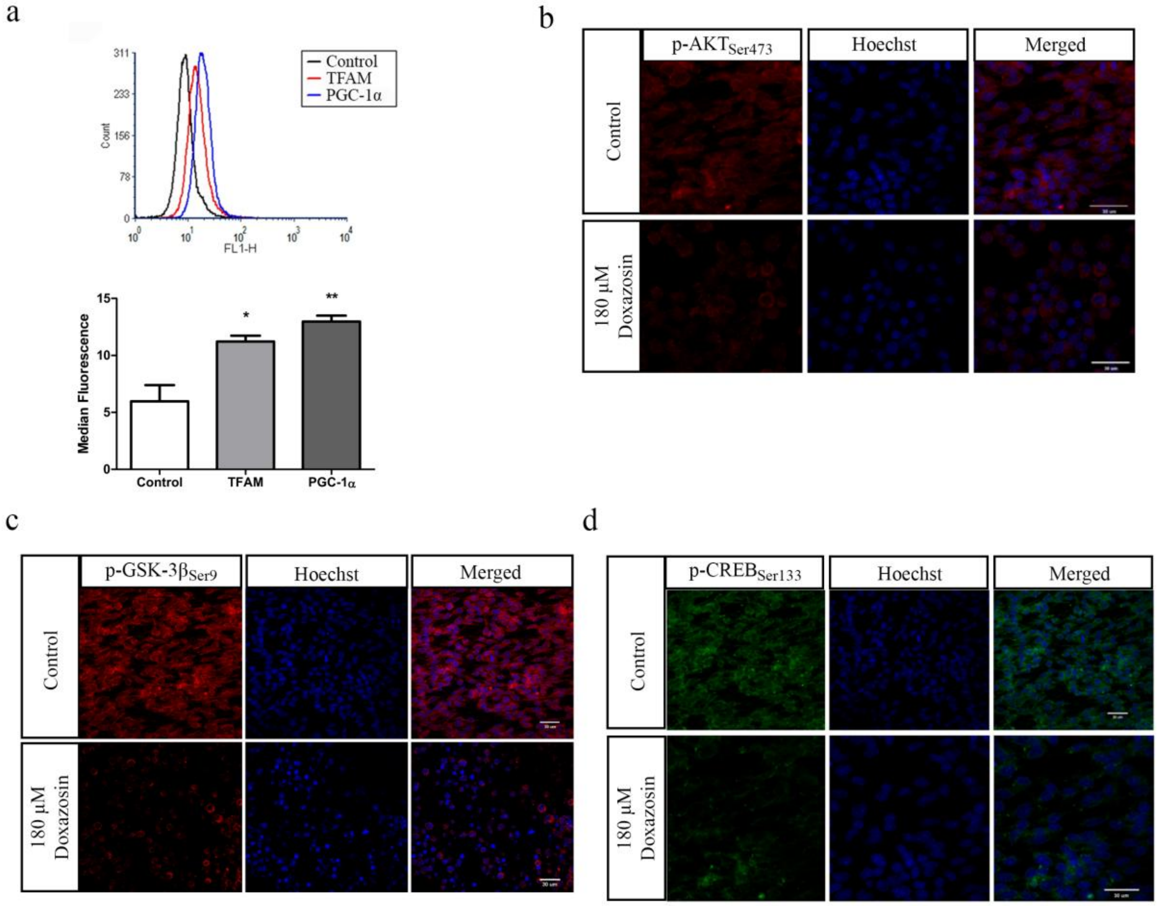
a
311
233
156
78
0
Count
10^0
10^1
10^2
10^3
10^4
FL1-H
Control
TFAM
PGC-1α
Median Fluorescence
15
10
5
0
*
**
Control
TFAM
PGC-1α
b
p-AKT$_{Ser473}$
Hoechst
Merged
Control
180 μM Doxazosin
c
p-GSK-3β$_{Ser9}$
Hoechst
Merged
Control
180 μM Doxazosin
d
p-CREB$_{Ser133}$
Hoechst
Merged
Control
180 μM Doxazosin

Figure 5

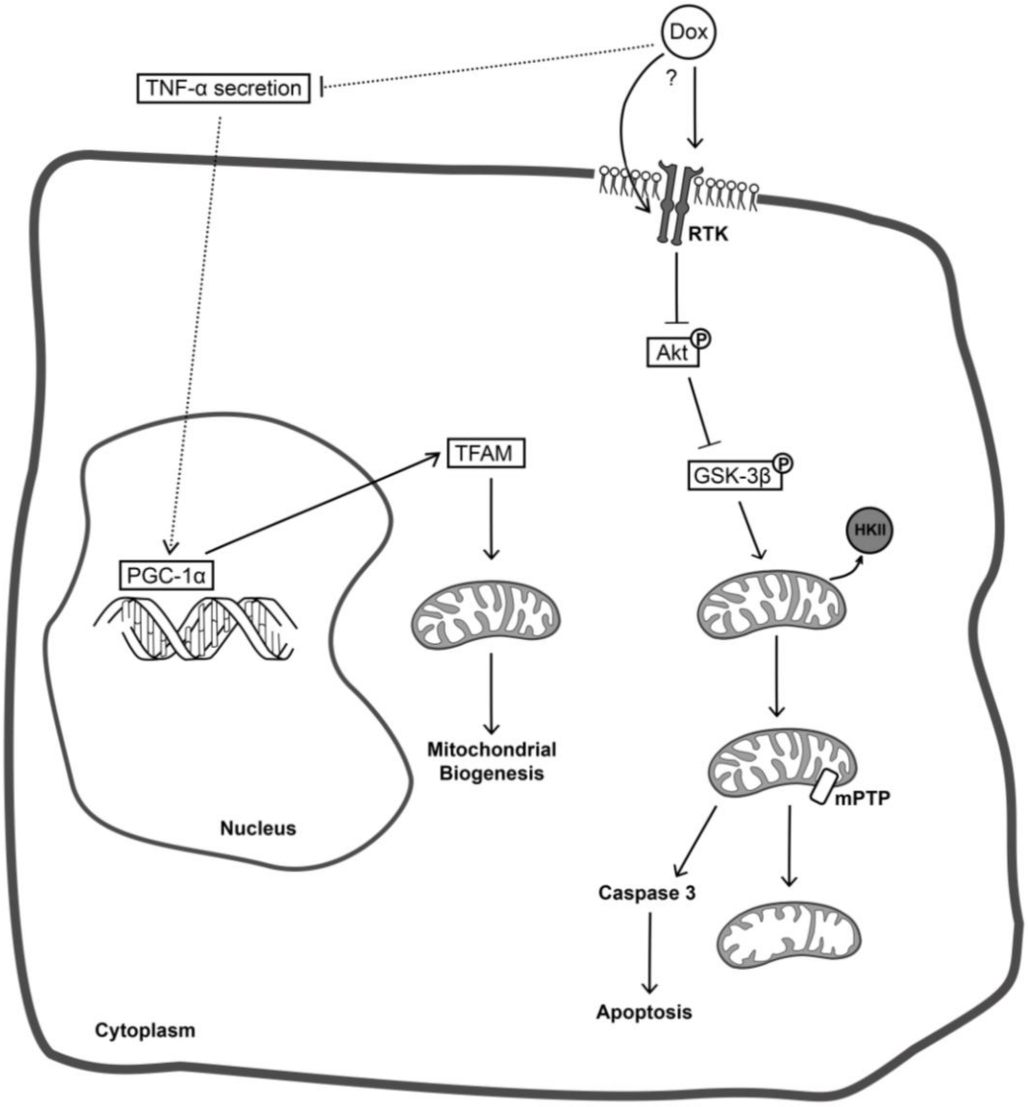
Dox
TNF-α secretion
?
RTK
Akt P
GSK-3β P
HKII
TFAM
PGC-1α
Mitochondrial Biogenesis
mPTP
Nucleus
Caspase 3
Apoptosis
Cytoplasm

6. CAPÍTULO IV

Artigo: *Doxazosin's real-time autofluorescence on glioma cells: uptake, distribution and pathophysiological response*

Status: *submetido ao periódico Oncotarget*

Doxazosin's real-time autofluoresce on glioma cells: uptake, distribution and pathophysiologycal response

Mariana Maier Gaelzer[1], Bárbara Paranhos Coelho[1], Alice Hoffmann de Quadros[1] Fátima Costa Rodrigues Guma[1], Ana Carolina Zeri[2], Leandra Franciscato Campo[3], Christianne G. Salbego[1]

[1]Programa de Pós-Graduação em Ciências Biológicas-Bioquímica_ Instituto de Ciências Básicas da Saúde, Universidade Federal do Rio Grande do Sul, Porto Alegre, RS, Brasil
[2]Laboratório Nacional de Biociências (LNBio), CNPEM, Campinas, SP, Brasil
[3]Departamento de Química, Instituto de Química, , Universidade Federal do Rio Grande do Sul, Porto Alegre, RS, Brasil.

Corresponding author:
Mariana Maier Gaelzer
Departamento de Bioquímica, Instituto de Ciências Básicas da Saúde, UFRGS
Rua Ramiro Barcelos, 2600 – anexo, CEP 90035-003, Porto Alegre, RS, Brasil
Telephone: +55 (51) 3308.5547
Fax: +55 (51) 3308.5535
E-mail: marianamaierg@gmail.com

Keywords: glioblastoma, doxazosin autofluorescence, heterogeneity, doxazosin uptake, doxazosin distribution

Abstract

Glioblastoma (GB), a malignant primary brain tumor, is a devastating disease with no effective cure. Doxazosin is an α-adrenergic blocker that has become a promising antiglioma agent. The drug's chemical structure has several characteristics that indicate the molecule is autofluorescent. We characterized doxazosin's intrinsic fluorescence in different solvents and in the presence of biomolecules. Doxazosin's fluorescence in hydro-alcoholic solution is blue and it changes in intensity and color (green and red) in different solvents. The drug also interacts with biomolecules in solution. Due to the drug's fluorescence, it was possible to analyze its uptake, distribution and real-time monitoring on C6 glioma cells. Doxazosin's uptake and distribution were heterogeneous; the drug localization was perinuclear and appeared to be vesiculated. With Proton Nuclear Magnetic Resonance analysis, we show that doxazosin is not present in C6 conditioned medium, meaning the drug is arrested intracellularly. The greatest challenge of the current pharmacotherapy, especially against GB, is the cells heterogeneity, since the cells may respond differently to therapy. Therefore, studies should focus on the heterogeneity of this tumor. The fluorescence allows the visualization and tracking of molecules and events in living cells and it is a valuable tool for the study of cancer biology.

Keywords: doxazosin, glioma, fluorescence, uptake, cellular distribution

Introduction

Glioblastoma (GB) is a central nervous system tumor [1]. GB is often characterized by rapid growth and invasiveness into surrounding normal brain tissue [2]. This diffusely infiltrative nature of GBs is one of the major obstacles to successful local resection, which in turn causes failure of curative treatment, with most recurrences occurring at the site of the original tumor [3].

There are many reasons for the therapy resistance of glioblastomas:

(1) The tumor can be located on and often invades inaccessible functional brain areas, making it impossible to surgically remove the GB (infiltrative tumors) without motor and/or cognitive impairment [4-5];

(2) The blood-brain barrier (BBB) protects the central nervous system from systemically administered drugs, which prevents many chemotherapeutics from reaching the tumor site. For this reason, many drug treatments that have been proven effective against other malignancies may not be applicable in the treatment of primary brain tumors [6];

(3) Glioblastomas are characterized by having a variety of genetic abnormalities. This heterogeneity may be a therapeutic challenge because the cells may respond differently to therapy [7].

This difficult clinical situation has stimulated interest in additional approaches to the treatment of glioblastomas. A more specific local therapy is required to eradicate unresectable tumor cells invading adjacent normal brain tissue. Fluorescent drugs can be used for fluorescence imaging at cellular and systemic levels for monitoring of drug delivery, therapeutic response and even diagnostics [8].

Doxazosin is an alpha-adrenergic blocker used in the treatment of hypertension and urinary retention [9]. Studies demonstrate its effects as an antitumoral agent in glioblastoma [10-11], urothelial cancer [12], pituitary adenoma [13], breast cancer [14] and HeLa cells [15]. Sakamoto et al. showed that early administration of doxazosin may prevent prostate tumor formation and supress metastasis of human prostate cancer [16].

Due to its physicochemical characteristics, doxazosin is able to permeate the BBB [17] and its relatively long half-life provides basis for once-daily dosing, which is a therapeutic advantage [18]. Our research group [10] showed that 75-180µM doxazosin induces cell death on glioblastoma cells (C6 and U138-MG) and at 250µM presents low toxicity on neural non-tumor cells (primary astrocyte and hippocampal slice organotypic cultures).

Fluorescence detection in analytical and biomedical techniques has been employed to monitor drug release kinetics. It has been considered as a convenient and fundamental tool to quantify the amount of drug released in less accessible intracellular environments [8].

In addition, recent advances in imaging and quantitative analysis of image data have led to earlier diagnosis of tumors and tumor response to therapy, providing oncologists with a greater time window for therapy management [8].

In this study, we report the characterization of doxazosin's autofluorescence and uptake in C6 tumor cells. Fluorescence microscopy, flow cytometry and nuclear magnetic resonance were used to investigate drug's uptake and distribution in glioblastoma cells.

Monitoring fluorescence spectral changes permits analysis of three-dimensional imaging, cellular uptake, real-time drug release in tumor cells, cellular distribution and accumulation of the drug [8]. This could provide more accurate treatment approaches in the future.

Results

Doxazosin's autofluorescence

The presence of certain chemical groups in the chemical structure of molecules favors the process of fluorescence. These are referred to as chromophoric groups [19-21]. These groups are present on the chemical structure of doxazosin, as we can observe on figure 1a.

We first analyzed doxazosin's autofluorescence in different solutions and in the presence of biomolecules. In hydro-alcoholic solution, doxazosin has an absorption peak at 340 nm, approximately. Based on the results from the absorption spectrum, doxazosin was excited at 340 nm in different solvents in order to analyze the autofluorescence. The drug emits blue fluorescence with higher intensity in ethanol as compared to the drug in cell medium and in H_2O. Phenol red from the culture medium does not interfere with the drug's fluorescence (figure 1b).

Next, we sought to analyze doxazosin's fluorescence in solvents with different polarities, pH and presence of proteins, lipids and DNA isolated from C6 cells (figure 1c). In the apolar solvent Dimethylsulfoxide (DMSO), doxazosin's blue fluorescence increased and the drug has green and red fluorescence. In acetonitrile, doxazosin's blue fluorescence decreases, while the green and red fluorescence also appear, but less intense than in DMSO.

In the polar solvent ethanol, doxazosin's fluorescence was similar as in DMSO solution. In acid and basic pH, the blue fluorescence increased, while the green and red fluorescence appeared only in basic pH (figure 1c).

In the presence of proteins, doxazosin's blue fluorescence increases and is also intensely red. When incubated with apolar lipids, doxazosin's blue fluorescence increased; and with polar lipids, the blue fluorescence remained unchanged, while the green and red increased. In the presence of DNA, the blue fluorescence increased (figure 1c). These results show that doxazosin's fluorescence present blue, green and red colors, that the fluorescence can change depending on the solvent and that the drug interacts with biomolecules.

Doxazosin's uptake is heterogeneous

In order to determine if doxazosin's uptake occurs, we analyzed the intracellular drug fluorescence, using C6 cells. We used flow cytometry and confocal microscopy to determine if fluorescent changes occurred after 6h, 24h and 48h of treatment with varying drug concentrations. The excitation optics of the flow cytometer used was a 488 nm argon-ion laser. Therefore, we were able to analyze doxazosin's green and red fluorescence with this system and the blue fluorescence was detected with a fluorescent microscope. At 6h, there is a small population of cells with increased green and red doxazosin fluorescence at 180 µM (figure 2a). At this concentration, doxazosin blue fluorescence was not detected (figure 2b). Also, there is an increase in cell granularity (figure 2c).

At 24h, the majority of cells show both green and red fluorescence (figure 3a). Green fluorescence alone appeared in a small percentage of cells (less than 1%). Blue fluorescence also appears at 24h, at the concentration of 180 µM (figure 3b). From the photomicrographs, it is possible to observe that doxazosin is distributed around the nucleus. There were three populations of cells with different granularities and the fluorescent cells showed higher granularity (figure 3c).

At 48h, there were few cells with both fluorescences (figure 4a). A large percentage of cells showed green doxazosin fluorescence alone and the percentage of green cells did not increase with the drug concentration. Virtually no cells showed red fluorescence alone. This occurred with all concentrations used. Blue florescence was present and was detected in cells presenting green fluorescence (figure 4b). Again it is possible to observe a perinuclear distribution of doxazosin. At this time, only two populations with different granularities were observed (figure 4c).

We carried out a Proton Nuclear Magnetic Resonance (1H-NMR) analysis of the conditioned medium in order to verify if drug remains in the C6 medium, if it enters the cell and/or if it is biotransformed. In figure 5a, we show doxazosin's 1H-NMR spectrum with the positions of the characteristic peaks of the molecule (in red). In figure 5b, the dotted red lines represent the characteristic positions of doxazosin in the spectrum (the same points shown in figure 5a); the full lines represent the samples of C6 conditioned medium. As shown in figure 5b, doxazosin is not detectable in the conditioned medium at 6, 24 and 48h, meaning the drug is internalized by the cell. As shown in figure 5c, doxazosin's uptake is heterogenous: 24h after treatment, some cells show no doxazosin fluorescence, while others show varying degrees of blue fluorescence intensity. Moreover, doxazosin appears to be vesiculated and is distributed around the nucleus. At 48h, the majority of cells are dead, as we demonstrated previously. In figure 5c doxazosin appears vesiculated and perinuclear.

Therefore, the increase in granularity observed with the flow cytometry could be due to increase in vesicles and accumulation of doxazosin in the cell.

Intracellular distribution of doxazosin

In C6 cells, doxazosin presents blue, green and red fluorescence in the cytoplasm, nucleus and cellular processes. Upon analysis of the shots after 1h treatment, we chose 3 cells from the same field for further analysis based on their different morphology and response to the drug. Cells numbers 1 and 2 showed little to none morphological changes, while cell number 3 showed formation of blebs on the cytoplasm and nucleus. First we analyzed the average fluorescence in each cell compartment (cytoplasm, nucleus and cellular processes) in order to compare doxazosin’s distribution and fluorescence between the cells and through the entire 60 min.

In the cytoplasm of all the observed cells, the peak in fluorescence average occurs until 20 min after treatment for all colors and starts to decrease at this time-point (figures 6a, 7a and 8a). In the nucleus, doxazosin fluorescence is different between the cells and regarding the fluorescence color. Cell #1 showed similar doxazosin distribution for all fluorescence colors: a peak in fluorescence average until 20 min and decrease after this time-point. Cell #2 blue nuclear fluorescence peaked later, around 35 min and remained slightly higher than that of the cytoplasm and constant until the end of the 60 min. The green fluorescence was similar to that of the cytoplasm, being slightly higher at the end. Cell #2 red fluorescence was constant during the period analyzed and was lower than the cytoplasmic red fluorescence. Nuclear fluorescence of cell #3 was similar to the cytoplasmic fluorescence for colors green and red; the nuclear blue color remained constant during the time-points.

In the cellular processes, doxazosin's fluorescence in cells #1 and #2 were similar to that of the cytoplasm for all colors, but less intense.

Observing these results of fluorescence average, it is clear that doxazosin's distribution and fluorescence color differs between the cells. In order to analyze specifically these differences in doxazosin's distribution, we generated heatmaps using the separation of the cells in grids of squares with 3 µm and showed the fluorescence mean of each square distributed throughout the cells cytoplasm, nucleus and processes. Based on the results above, we chose the time-points of 0, 5, 10, 15, 20, 30, 40, 50 and 60 min for the heatmap analysis.

With this, is possible to observe in cell #1 that the red fluorescence is higher (more intense) than the green, which is higher than the blue throughout the cell and the time-points. The green fluorescence distribution is homogenous through the cell, while the blue and red fluorescence accumulate in one side of the cytoplasm, being perinuclear. This accumulation occurs between 15 to 30 min for the blue color, and between 10 to 50 min for the red. Also, red and green doxazosin appear in both cellular processes, while blue doxazosin is evident in only one of them. Interestingly, doxazosin's fluorescence is weak in the nucleus of these cell and the higher intensities observed for the blue color are at 10-30 min while for the red color they occur earlier and last longer (5-50 min).

In cell #2, doxazosin's fluorescence is similar in some aspects to cell #1. However, while the blue doxazosin accumulates at one side of the cytoplasm, the red color is accumulated in the cytoplasm around the whole nucleus. Moreover, the blue doxazosin starts increasing in fluorescence intensity at 5 min, as well as the red fluorescence. Another difference between both cells is that cell #2 red fluorescence in the cellular processes is more intense in one of them, while the blue fluorescence is weak in this region of the cell. The blue fluorescence is weaker in the nucleus than in the cytoplasm, but the red fluorescence is slightly more intense in the nucleus at 20 min.

As stated above, cell #3 showed morphological changes that included the formation of blebs, in contrast to cells #1 and #2. The blebs started forming at 30 min. Cell #3 showed weak perinuclear blue fluorescence intensity, with higher intensity on the cytoplasm starting at 5 min, until 20 min of treatment. Also, a weak blue fluorescence is present in the nucleus. The green fluorescence was homogenous, with slight increases in intensity in parts of the cytoplasm and nucleus. The red fluorescence was overall more intense than the others, being strong on one side of the cytoplasm, on a small perinuclear portion and inside the nucleus. The fluorescence intensities started decreasing earlier than in cells #1 and #2, from 30 to 60 min. However, a strong red fluorescence signal was still detected in the nucleus and cytoplasm during this period. Therefore, in addition to doxazosin's uptake being heterogeneous, the drug fluorescence distribution varies between the C6 cells.

Discussion

Doxazosin is clinically used for hypertension and benign prostatic hyperplasia. Several studies, however, have been repurposing the drug as an antitumoral agent. This effect was demonstrated in glioblastoma [10-11], prostate cancer [22-23], breast cancer [14]and bladder cancer [12]. The advantages of drug repurposing is availability of data on pharmokinetics, bioavailability, toxicities, established protocols and dosing [24].

As shown in our previous study, doxazosin induces cell cycle arrest and cell death in approximately 70% of C6 cells in 48hs, and has low neurotoxicity in organotypic hippocampal cultures and primary astrocytes cultures [10]. Here, we describe doxazosin's autofluorescence, the changes in fluorescence caused by different solvents and the drug's interaction with biomolecules, and we also demonstrate the drug's uptake and distribution in glioma C6 cells.

The presence of certain groups in the chemical structure of molecules, for example, the grouping $-NH_2$ present in doxazosin (shown in figure 1a) favors the process of radioactive fluorescence. Molecules with rigid aromatic rings and the presence of imines groups (N=C), as is the case for doxazosin, also can exhibit fluorescence [19-21]. When a fluorescent molecule interacts with other molecules, it can temporarily lose fluorescence or shift to another color [25].

Doxazosin's autofluorescence in hydro-alcoholic solution is blue and intracellularly presents green and red colors and the blue fluorescence intensity varies. The different pH values inside cellular compartments can protonate/deprotonate fluorescent molecules and influence its fluorescence (in intensity and color shift) [19]. Here we show that changes in pH solutions alter the intensity of doxazosin's blue fluorescence and basic pH causes a red shift. The different polarities of cellular components, e.g. proteins, lipids and DNA, and the drug interactions with these biomolecules can also influence fluorescence intensity and color. This occurred with doxazosin's fluorescence: in the presence of proteins and lipids the drug's fluorescence can change and in the presence of DNA the intensity varies. This suggests that the drug's fluorescence is dependent on the environment and on interactions with biomolecules.

Doxazosin’s uptake in C6 cells was heterogenous, especially at 24h, as shown by flow cytometry and microscopy. At 24h, doxazosin showed both green and red fluorescence in the majority of cells; in 48h, however, the green fluorescence alone is in the majority of cells. This does not mean that doxazosin’s fluorescence shifted from red to green. This could be due to a temporarily loss of fluorescence caused by interaction with different cellular components. It is important to note, however, that the photomicrographs (Figures 3b and 4b) show the occurrence of three or two fluorescence colors at the same position in one cell and also cells presenting only the green color.

The 1H-NMR analysis showed the drug was not detected in the extracellular medium. Previously we described that at 48h of treatment (180 µM) doxazosin induces apoptosis and necrosis in approximately 55% and 15% of cells, respectively [10]. Interestingly, even with cellular death, doxazosin and its biotransformation products are not detected in the conditioned medium. This could mean that the drug is arrested inside of the cell, possibly interacting with anchored proteins or inside vesicles.

We showed that doxazosin is internalized by the cells and accumulates around the nucleus as early as 1h of treatment; however, doxazosin induces a statistical significant physiological response only after 48h of being arrested inside the cell [10]. This raises the question of why does it takes so much time for the drug to induce cell death. Due to an intrinsic property of doxazosin we were able to demonstrate the heterogeneity in the drug uptake, in its distribution and in the different physiological responses of the glioma cells, without changes in the cells microenvironment. In a previous study we showed that C6 cells dedifferentiate to cancer stem cells in a hypoxic environment [26]. Here, we maintained the same culture conditions during all times studied and still found great differences between the cells responses to the same molecule.

Studying mechanisms of cell death induction of antitumoral drugs and analyzing total cell death is important. However, the greatest challenge of the current pharmacotherapy, especially against glioblastomas, is the cells heterogeneity, since the cells may respond differently to therapy.

In a large retrospective study with patients with glioblastoma, Scott et al. [27-28] showed that the final mortality rate was close to 100%. This is an alarming statistic, especially due to the advances in cancer therapy accomplished nowadays. Future studieson glioblastoma pharmacotherapy should focus on the heterogeneity of this tumor and on the understanding of the mechanisms of drug resistance. Moreover, the use of fluorescent drugs like doxazosin for the study of this heterogeneity could greatly contribute for this purpose.

Materials and Methods

Chemicals and materials

Cell culture medium and fetal bovine serum (FBS) were obtained from Gibco-Invitrogen (Grand Island, NY, USA). Doxazosin was obtained from Sigma Chemical Co (St. Louis, MO, USA). All other reagents were purchased from Sigma Chemical Co. (St. Louis, MO, USA) or Merck (Darmstadt, Germany). All chemicals and solvents used were of analytical or pharmaceutical grade.

Fluorescence analysis

Doxazosin’s absorption and fluorescence spectra were determined with a UV-2450 UV-Vis Spectrophotometer (Shimadzu Corporation, Kyoto, Japan) and a RF-5301PC Spectrofluorphotometer (Shimadzu Corporation, Kyoto, Japan). Doxazosin in the concentration of 180 µM was diluted in ethanol, ethanol and water solution, culture medium and PBS for determination of the spectra. Spectral shifts were analyzed in solvents with different polarities, pH and cellular components.

Cell culture

C6 rat glioma cell line was obtained from American Type Culture Collection (Rockville, Mariland, Md., USA). C6 cells were grown and maintained in Dulbecco’s Modified Eagle’s Medium (DMEM, Gibco-Invitrogen, Grand Island, NY, USA) supplemented with 5% (v/v) FBS (Gibco-Invitrogen, Grand Island, NY, USA), and containing 2.5 mg/mL of Fungizone® and 100 U/L of gentamicine (Shering do Brasil, São Paulo, SP, Brazil). Cells were kept at 37ºC, in an atmosphere of 5% CO_2.

Treatment

Doxazosin was dissolved in 20% ethanol/ milli-Q^{TM} water (vehicle) and cells were treated with concentrations ranging from 50 µM to 180 µM and at 1, 6, 24 and 48h.

Flow Cytometry

For uptake assay, C6 cells were seeded in 6-well plates ($3x10^4$ cells/well) and grown for 24 h. After treatments, cells were washed with PBS, trypsinized and fluorescence intensity was analyzed by flow cytometry at different time points. Data was acquired with a

FACS Calibur cytometry system (FACS Calibur, BD Bioscience, Mountain View, CA, USA) and Cell Quest software (BD Bioscience, Mountain View, CA, USA). Data obtained was analyzed with FCS Express 4 Software (De Novo Software, Los Angeles, CA, USA).

Nuclear Magnetic Resonance (1H-NMR)

C6 conditioned medium after treatment for 48 hours with doxazosin was filtered through Amicon Ultra-15 membranes (3 kDa). Fractions with metabolites smaller than 3kDa were mixed with phosphate buffer, D_2O, and 1 mM DSS (4,4-dimethyl-sulfonic acid 4-silapentano-1-acid) to a final volume of 600 uL. Samples were processed at a 600 MHz, Varian Inova, (with triple resonance cryogenic probe system and room temperature probe) NMR spectrometer and analyzed with Chenomx NMR Suite 7.0 program.

Confocal Microscopy

To quantify doxasozin and verify its distribution on C6 cells, confocal microscopy analysis was carried out. Cells were seeded in 4-well glass bottom dishes with 10^4 cells in each well and grown for 24 hours. For live cell imaging, cells were kept on a proprietary CO_2 incubator, maintained with 90% humidity and 5% CO_2. Cells were treated with doxazosin at the time of shooting and shots were made for 1 h. Photomicrographs were also taken after treatment for 6, 24 and 48 hours. A Confocal Laser Scanning Biological Microscope FV1000 (Olympus Corporation, Tokyo, Japan) was used for live cell shooting and for image acquisition. Doxazosin fluorescence was measured after excitation with laser beams of 405, 473 and 559 nm. After live cell shooting, 3 cells were chosen for image analysis based on their different morphology alterations during the 1h treatment with doxazosin.

The image field of each cell was divided by a grid of 3 µm squares and mean fluorescence was measured in each square using ImageJ 1.50i software. The average of the fluorescence in each time-point was plotted using GraphPad Prism 5.01 software (GraphPad Software, La Jolla, CA, USA). The time-points of 0, 5, 10, 15, 20, 30, 40, 50 and 60 min were chosen based on the previous graph of time versus average fluorescence. For the selected time-points, a heatmap plot was generated using the R language for analysis of the fluorescence distribution on the cells.

Abbreviations

1H-NMR: Proton Nuclear Magnetic Resonance

BBB: Blood-brain barrier

DMSO: Dimethylsulfoxide

FBS: Fetal bovine serum

GB: Glioblastoma

Author Contributions

Study conception and design: M.M. Gaelzer; Acquisition of data: M.M. Gaelzer, B.P. Coelho, A.H. Quadros, F.C.R. Guma, A.C. Zeri, L.F. Campos; Analysis and interpretation of data: M.M. Gaelzer, B.P. Coelho, A.C. Zeri, L.F. Campos; Drafting of manuscript: M.M. Gaelzer, B.P. Coelho, L.F. Campos, C.G. Salbego; Final approval of the version to be published: M.M. Gaelzer, B.P. Coelho, A.H. Quadros, F.C.R. Guma, A.C. Zeri, L.F. Campos, C.G. Salbego.

Acknowledgments

We acknowledge the Nuclear Magnetic Resonance (NMR) Facility at Brazilian Biosciences National Laboratory (LNBio), CNPEM, Campinas, Brazil for their support with the use of 600 MHz Varian Inova NMR spectrometer.

Conflicts of Interest

The authors declare that there are no conflicts of interest.

Funding

Conselho Nacional de Desenvolvimento Científico e Tecnológico (CNPq); Coordenação de Aperfeiçoamento de Pessoal de Nível Superior (Capes); Fundação de Amparo à Pesquisa do Estado do Rio Grande do Sul (FAPERGS).

References

1. Kilian A. Glioblastoma Tumours: Complex Challenges and Deadly Outcomes. The Meducator. 2016; 1.

2. Wirsching H-G, Weller M. The Role of Molecular Diagnostics in the Management of Patients with Gliomas. Current treatment options in oncology. 2016; 17: 51.

3. de Robles P, Fiest KM, Frolkis AD, Pringsheim T, Atta C, Germaine-Smith CS, Day L, Lam D, Jette N. The worldwide incidence and prevalence of primary brain tumors: a systematic review and meta-analysis. Neuro-oncology. 2015; 17: 776-83.

4. Sanai N, Berger MS. Glioma extent of resection and its impact on patient outcome. Neurosurgery. 2008; 62: 753-66.

5. Sanai N, Mirzadeh Z, Berger MS. Functional outcome after language mapping for glioma resection. New England Journal of Medicine. 2008; 358: 18-27.

6. Westphal M, Lamszus K. The neurobiology of gliomas: from cell biology to the development of therapeutic approaches. Nature Reviews Neuroscience. 2011; 12: 495-508.

7. Agnihotri S, Burrell KE, Wolf A, Jalali S, Hawkins C, Rutka JT, Zadeh G. Glioblastoma, a brief review of history, molecular genetics, animal models and novel therapeutic strategies. Archivum immunologiae et therapiae experimentalis. 2013; 61: 25-41.

8. Etrych T, Lucas H, Janoušková O, Chytil P, Mueller T, Mäder K. Fluorescence optical imaging in anticancer drug delivery. Journal of Controlled Release. 2016; 226: 168-81.

9. Antonello A, Hrelia P, Leonardi A, Marucci G, Rosini M, Tarozzi A, Tumiatti V, Melchiorre C. Design, synthesis, and biological evaluation of prazosin-related derivatives as multipotent compounds. Journal of medicinal chemistry. 2005; 48: 28-31.

10. Gaelzer MM, Coelho BP, de Quadros AH, Hoppe JB, Terra SR, Guerra MCB, Usach V, Guma FCR, Gonçalves CAS, Setton-Avruj P. Phosphatidylinositol 3-Kinase/AKT Pathway Inhibition by Doxazosin Promotes Glioblastoma Cells Death, Upregulation of p53 and Triggers Low Neurotoxicity. PloS one. 2016; 11: e0154612.

11. Staudacher I, Jehle J, Staudacher K, Pledl H-W, Lemke D, Schweizer PA, Becker R, Katus HA, Thomas D. HERG K+ channel-dependent apoptosis and cell cycle arrest in human glioblastoma cells. PloS one. 2014; 9: e88164.

12. Siddiqui EJ, Shabbir M, Thompson CS, Mumtaz FH, Mikhailidis DP. Growth inhibitory effect of doxazosin on prostate and bladder cancer cells. Is the serotonin receptor pathway involved? Anticancer research. 2005; 25: 4281-6.

13. Fernando MA, Heaney AP. α1-Adrenergic receptor antagonists: novel therapy for pituitary adenomas. Molecular Endocrinology. 2005; 19: 3085-96.

14. Hui H, Fernando MA, Heaney AP. The α 1-adrenergic receptor antagonist doxazosin inhibits EGFR and NF-κB signalling to induce breast cancer cell apoptosis. European Journal of Cancer. 2008; 44: 160-6.

15. Gan L, Yan F, Zhang J. Involvement of transcription factor activator protein-2α in doxazosin-induced HeLa cell apoptosis1. Acta pharmacologica Sinica. 2008; 29: 465-72.

16. Sakamoto S, Kyprianou N. Targeting anoikis resistance in prostate cancer metastasis. Molecular aspects of medicine. 2010; 31: 205-14.

17. Nikolic K, Filipic S, Smoliński A, Kaliszan R, Agbaba D. Partial least square and hierarchical clustering in ADMET modeling: Prediction of blood–brain barrier permeation of α-adrenergic and imidazoline receptor ligands. Journal of Pharmacy & Pharmaceutical Sciences. 2013; 16: 622-47.

18. Kaye B, Cussans N, Faulkner J, Stopher D, Reid J. The metabolism and kinetics of doxazosin in man, mouse, rat and dog. British journal of clinical pharmacology. 1986; 21: 19S-25S.

19. Mason WT. (1999). Fluorescent and luminescent probes for biological activity: a practical guide to technology for quantitative real-time analysis: Academic Press).

20. Ingle Jr JD, Crouch SR. Spectrochemical analysis. 1988.

21. Lakowicz JR. (2013). Principles of fluorescence spectroscopy: Springer Science & Business Media).

22. Chon JK, Borkowski A, Partin AW, Isaacs JT, Jacobs SC, Kyprianou N. Alpha 1-adrenoceptor antagonists terazosin and doxazosin induce prostate apoptosis without

affecting cell proliferation in patients with benign prostatic hyperplasia. The Journal of urology. 1999; 161: 2002-8.

23. Yang G, Timme TL, Park SH, Wu X, Wyllie MG, Thompson TC. Transforming growth factor β1 transduced mouse prostate reconstitutions: II. Induction of apoptosis by doxazosin. The Prostate. 1997; 33: 157-63.

24. Pantziarka P, Bouche G, Meheus L, Sukhatme V, Sukhatme VP, Vikas P. The repurposing drugs in oncology (ReDO) project. 2014.

25. March J. (1992). Advanced organic chemistry: reactions, mechanisms, and structure: John Wiley & Sons).

26. Gaelzer MM, dos Santos MS, Coelho BP, de Quadros AH, Simão F, Usach V, Guma FCR, Setton-Avruj P, Lenz G, Salbego CG. Hypoxic and Reoxygenated Microenvironment: Stemness and Differentiation State in Glioblastoma. Molecular Neurobiology. 2016: 1-12.

27. Scott J, Rewcastle N, Brasher P, Fulton D, Hagen N, MacKinnon J, Sutherland G, Cairncross J, Forsyth P. Long-term glioblastoma multiforme survivors: a population-based study. Canadian Journal of Neurological Sciences/Journal Canadien des Sciences Neurologiques. 1998; 25: 197-201.

28. Roy S, Lahiri D, Maji T, Biswas J. Recurrent Glioblastoma: Where we stand. South Asian journal of cancer. 2015; 4: 163.

Figure Legends

Figure 1. Doxazosin’s autofluorescence in diferrent solutions. **(a)** Chemical structure of doxazosin[4-4-amino-6 ,7-dimethoxyquinazoline-2-yl)-piperazine]yl-1 (2,3-dihydro-1,4-

benzodioxine-3-yl). In **a**, **1** and **2** indicate the presence of chromophore groups that could contribute for the process of radioactive fluorescence of doxazosin. **(b)** Doxazosin's fluorescence spectrum in: hydro-alcoholic solution (**EtOH**), Water (**H_2O**), cell culture medium, and we analyzed the culture medium without the drug. The solutions were excited at 340 nm. **(c)** Doxazosin's (**DZ**) fluorescence analyzed in solvents with different polarities,pHs, and in the presence of proteins, lipids and DNA.

Figure 2. Analysis of doxazosin's uptake by C6 glioma cells after 6h of treatment. **(a)** Dot plot demonstrating doxazosin's green (x-axis) and red (y-axis) fluorescence in C6 cells. **(b)** Photomicrographs of doxazosin's fluorescence blue, green and red fluorescence in C6 cells.Magnification: 600x. **(c)** Dot plot analysis of C6 cells granularity after doxazosin's treatment.

Figure 3. Analysis of doxazosin's uptake by C6 glioma cells after 24h of treatment. **(a)** Dot plot demonstrating doxazosin's green (x-axis) and red (y-axis) fluorescence in C6 cells. **(b)** Photomicrographs of doxazosin's fluorescence blue, green and red fluorescence in C6 cells.Magnification: 1000x. **(c)** Dot plot analysis of C6 cells granularity after doxazosin's treatment.

Figure 4. Analysis of doxazosin's uptake by C6 glioma cells after 48h of treatment. **(a)** Dot plot demonstrating doxazosin's red (x-axis) and green (y-axis) fluorescence in C6 cells. **(b)** Photomicrographs of doxazosin's fluorescence blue, green and red fluorescence in C6 cells.Magnification: 600x. **(c)** Dot plot analysis of C6 cells granularity after doxazosin's treatment.

Figure 5. Doxazosin's NMR spectrum in **(a)** hydro-alcoholic solution and in **(b)** conditioned medium from C6 cells after treatment for 48h. **(a)** Characteristic peaks of the molecule (in red). Number **1** in **a** indicates the characteristic peak of water and number **2** indicates the characteristic peak of ethanol. **(b)** NMR spectrum of the conditioned medium from C6 cells. Red dotted lines indicated by the number **3** represent the positions where doxazosin should be found in the spectrum; continue colored lines represent the samples of

conditioned medium after treatment with different doxazosin concentrations (as shown in the legend). **(c)** Doxazosin's uptake after 24h (**left**) and 48h (**right**) of treatment is heterogenous. Some cells show no doxazosin fluorescence, while others show varying degrees of blue, green and red fluorescence intensity. Doxazosin appears to be vesiculated and is distributed around the nucleus.

Figure 6. Intracellular distribution of doxazosin. Analysis of the shots for 1h of treatment for cell number**#1**. **(a)** Doxazosin average fluorescence in each cell compartment (cytoplasm, nucleus and cellular processes), during al time-points. **(b)** Heatmaps using the separation of the cells in grids of squares with 3 µm show the fluorescence mean of each square distributed throughout the cells cytoplasm, nucleus and processes.

Figure 7. Intracellular distribution of doxazosin. Analysis of the shots for 1h of treatment for cell number**#2**. **(a)** Doxazosin average fluorescence in each cell compartment (cytoplasm, nucleus and cellular processes), during al time-points. **(b)** Heatmaps using the separation of the cells in grids of squares with 3 µm show the fluorescence mean of each square distributed throughout the cells cytoplasm, nucleus and processes.

Figure 8. Intracellular distribution of doxazosin. Analysis of the shots for 1h of treatment for cell number**#3**. **(a)** Doxazosin average fluorescence in each cell compartment (cytoplasm and nucleus), during al time-points. **(b)** Heatmaps using the separation of the cells in grids of squares with 3 µm show the fluorescence mean of each square distributed throughout the cells cytoplasm and nucleus.

Figure 9. Schematic representation of doxazosin's autofluorescence in solution and in C6 glioma cells. **(a)** In hydro-alcoholic solution, doxazosin shows blue fluorescence (blue circles), while in contact with lipids, proteins and DNA, it shows blue/green/red, blue/red and blue fluorescence, respectively. **(b)** In C6 cells, doxazosin's uptake, distribution and cell death induction is heterogeneous.

Figure 1

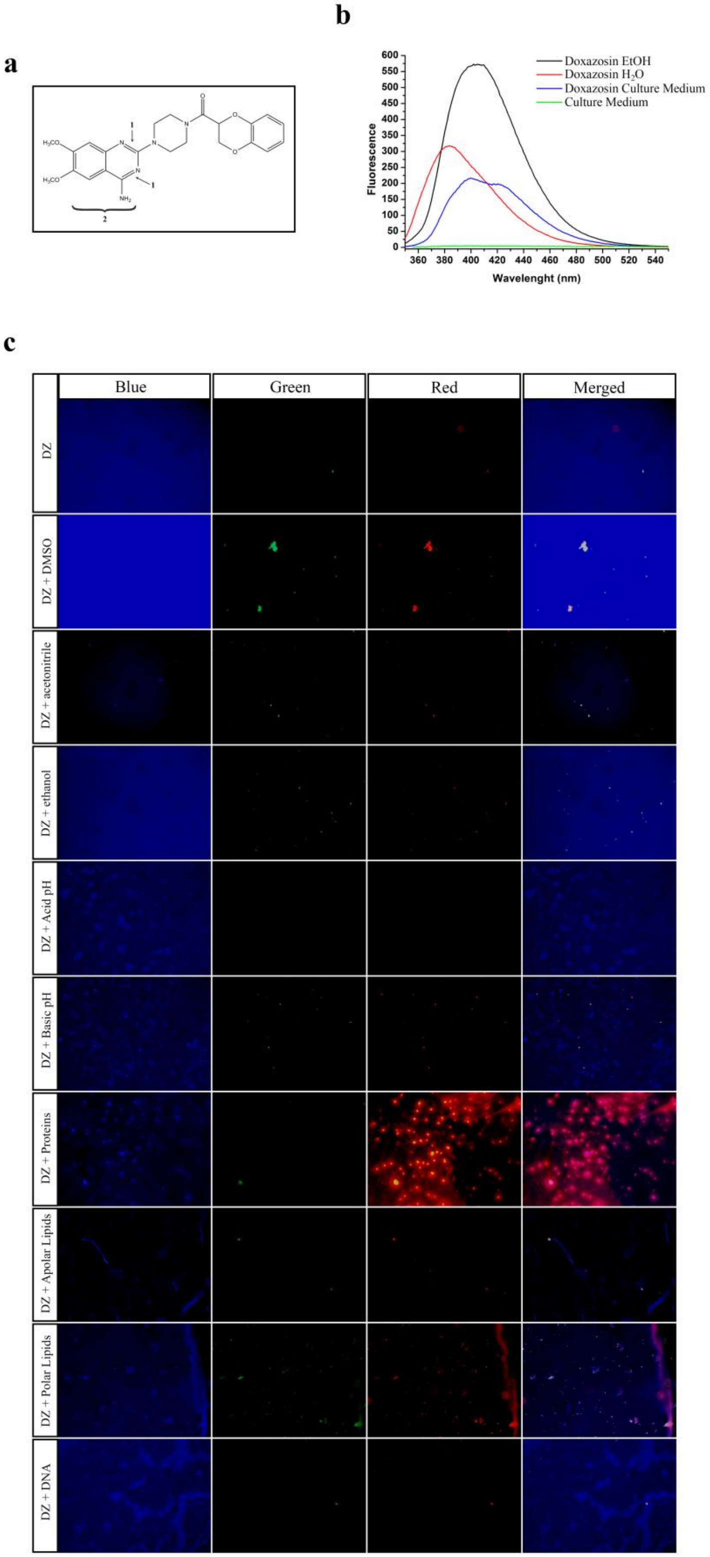
a
b
c
H$_3$CO
H$_3$CO
NH$_2$
N
N
N
N
O
O
O
1
1
2
Fluorescence
Wavelenght (nm)
Doxazosin EtOH
Doxazosin H$_2$O
Doxazosin Culture Medium
Culture Medium
0
50
100
150
200
250
300
350
400
450
500
550
600
360
380
400
420
440
460
480
500
520
540
Blue
Green
Red
Merged
DZ
DZ + DMSO
DZ + acetonitrile
DZ + ethanol
DZ + Acid pH
DZ + Basic pH
DZ + Proteins
DZ + Apolar Lipids
DZ + Polar Lipids
DZ + DNA

Figure 2

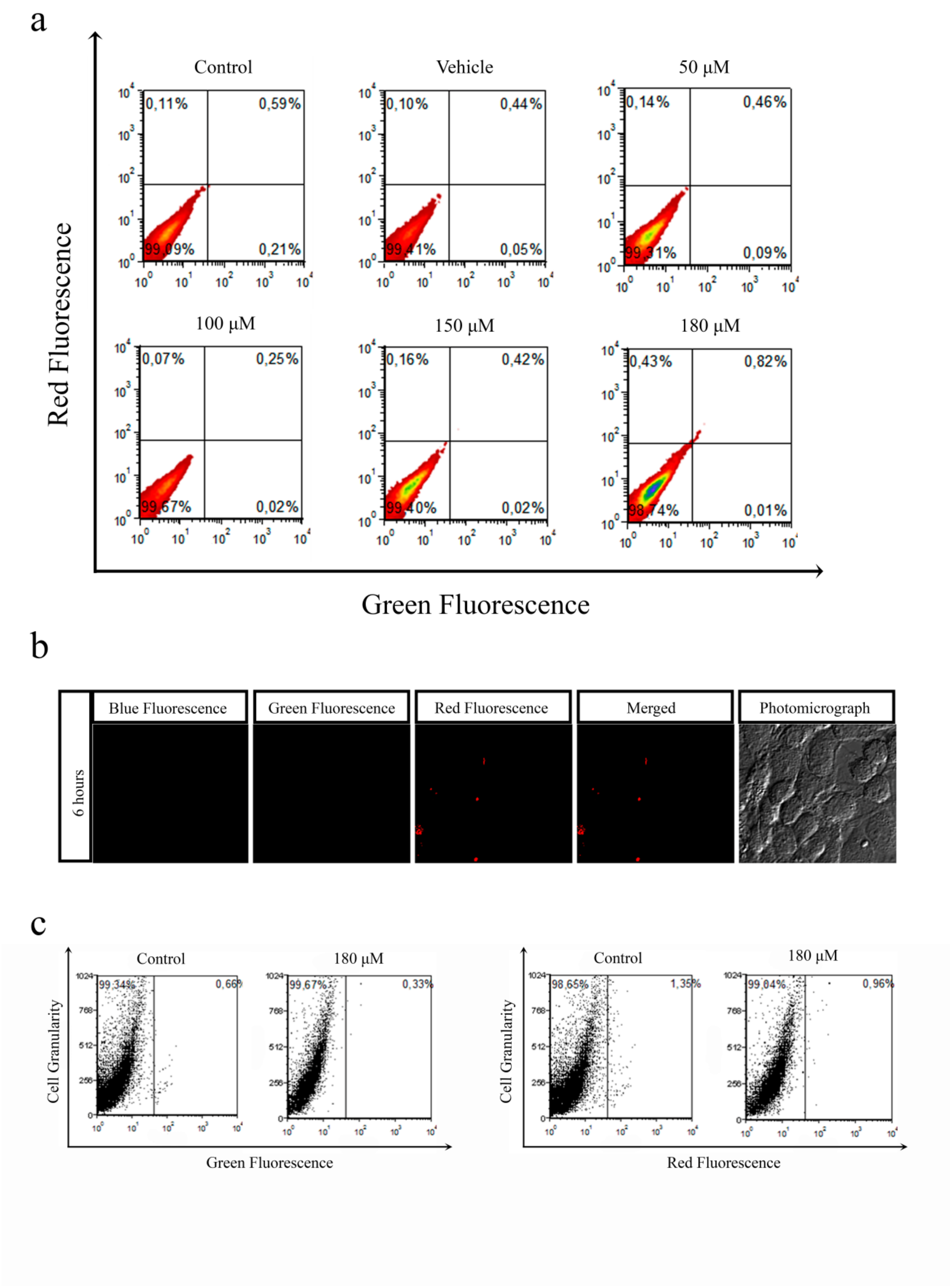
a
Red Fluorescence
Green Fluorescence
Control
0,11%
0,59%
99,09%
0,21%
Vehicle
0,10%
0,44%
99,41%
0,05%
50 µM
0,14%
0,46%
99,31%
0,09%
100 µM
0,07%
0,25%
99,67%
0,02%
150 µM
0,16%
0,42%
99,40%
0,02%
180 µM
0,43%
0,82%
98,74%
0,01%
b
6 hours
Blue Fluorescence
Green Fluorescence
Red Fluorescence
Merged
Photomicrograph
c
Cell Granularity
Control
99,34%
0,66%
180 µM
99,67%
0,33%
Green Fluorescence
Cell Granularity
Control
98,65%
1,35%
180 µM
99,04%
0,96%
Red Fluorescence

Figure 3

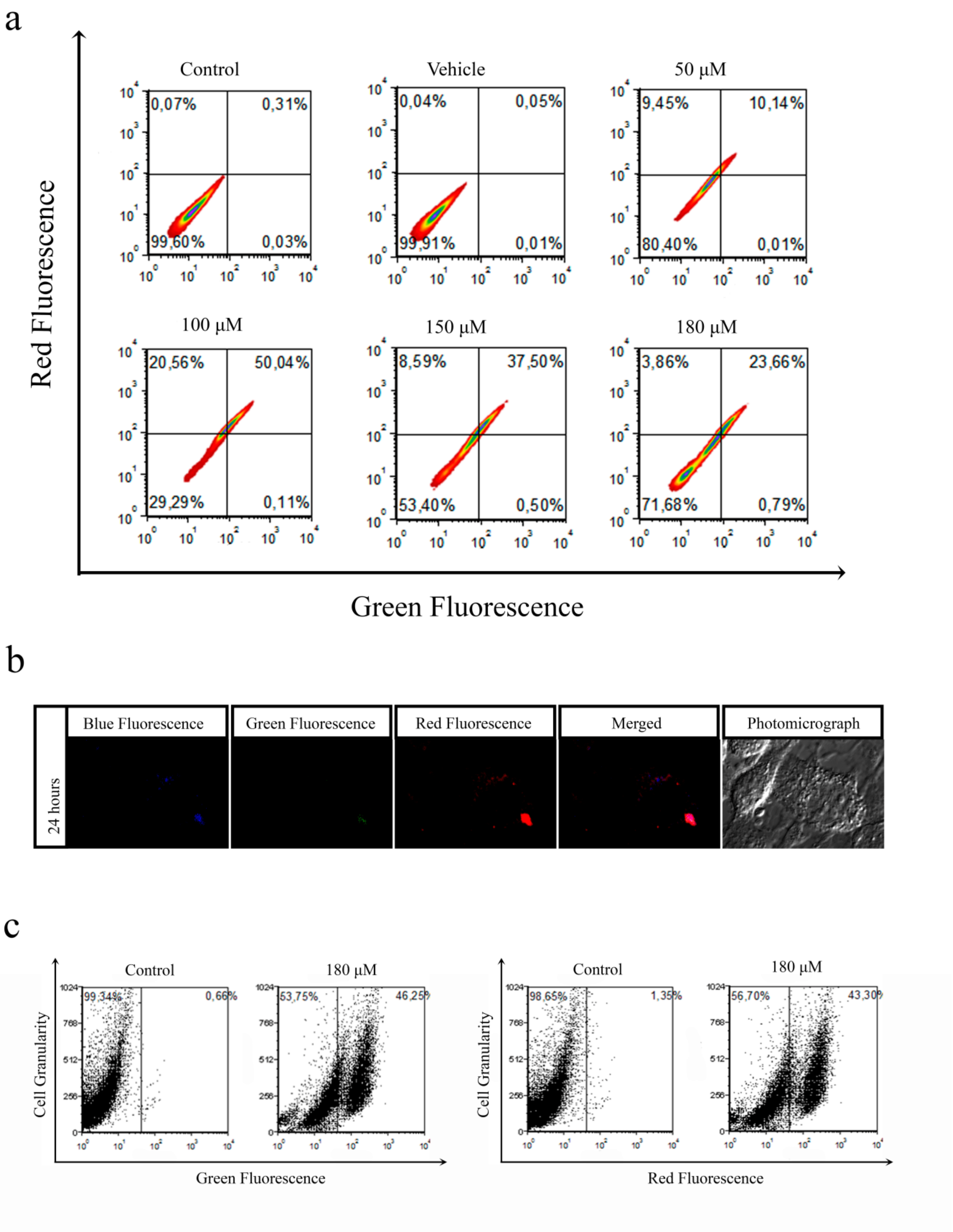
a
Red Fluorescence
Green Fluorescence
Control
0,07%
0,31%
99,60%
0,03%
Vehicle
0,04%
0,05%
99,91%
0,01%
50 µM
9,45%
10,14%
80,40%
0,01%
100 µM
20,56%
50,04%
29,29%
0,11%
150 µM
8,59%
37,50%
53,40%
0,50%
180 µM
3,86%
23,66%
71,68%
0,79%
10^0
10^1
10^2
10^3
10^4
b
24 hours
Blue Fluorescence
Green Fluorescence
Red Fluorescence
Merged
Photomicrograph
c
Cell Granularity
Control
99,34%
0,66%
180 µM
53,75%
46,25%
Green Fluorescence
Control
98,65%
1,35%
180 µM
56,70%
43,30%
Red Fluorescence
1024
768
512
256
0

Figure 4

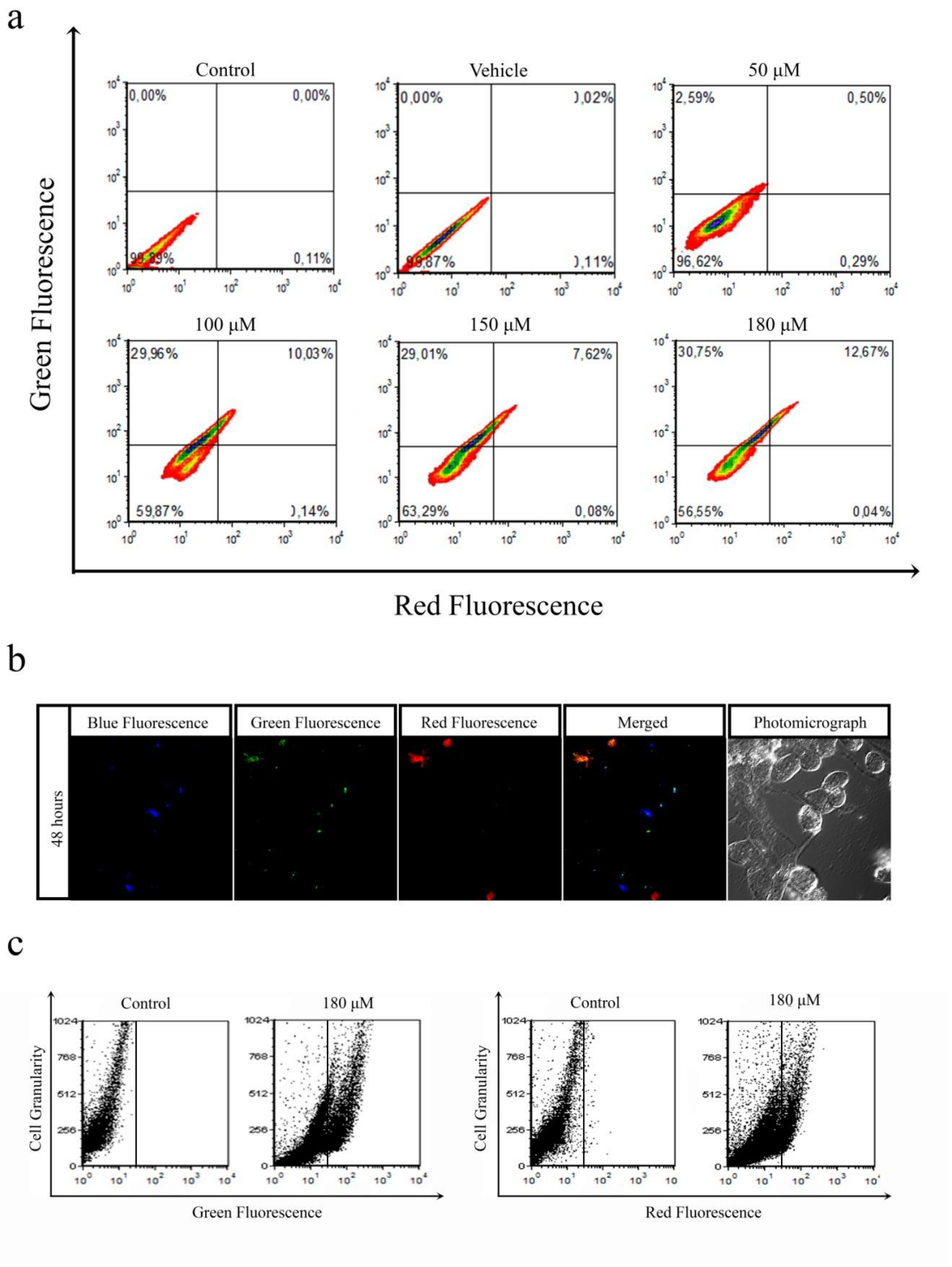
a
Green Fluorescence
Red Fluorescence
Control
0,00%
0,00%
99,89%
0,11%
Vehicle
0,00%
),02%
99,87%
),11%
50 μM
2,59%
0,50%
96,62%
0,29%
100 μM
29,96%
10,03%
59,87%
),14%
150 μM
29,01%
7,62%
63,29%
0,08%
180 μM
30,75%
12,67%
56,55%
0,04%
b
Blue Fluorescence
Green Fluorescence
Red Fluorescence
Merged
Photomicrograph
48 hours
c
Control
180 μM
Cell Granularity
Green Fluorescence
Red Fluorescence
1024
768
512
256
0

Figure 5

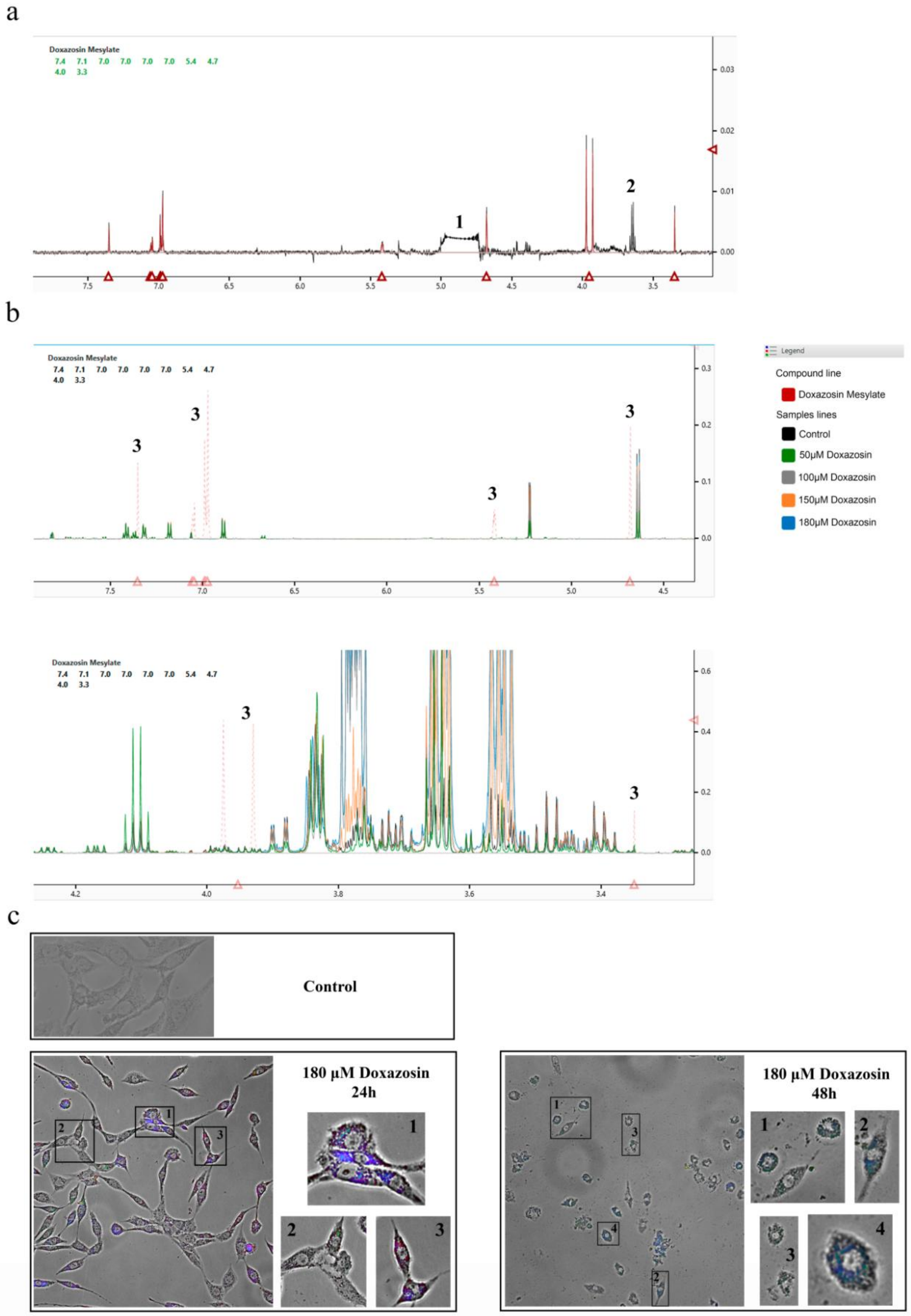
a
Doxazosin Mesylate
7.4 7.1 7.0 7.0 7.0 7.0 5.4 4.7
4.0 3.3
1
2
0.03
0.02
0.01
0.00
7.5
7.0
6.5
6.0
5.5
5.0
4.5
4.0
3.5
b
Doxazosin Mesylate
7.4 7.1 7.0 7.0 7.0 7.0 5.4 4.7
4.0 3.3
3
3
3
3
0.3
0.2
0.1
0.0
7.5
7.0
6.5
6.0
5.5
5.0
4.5
Legend
Compound line
Doxazosin Mesylate
Samples lines
Control
50µM Doxazosin
100µM Doxazosin
150µM Doxazosin
180µM Doxazosin
Doxazosin Mesylate
7.4 7.1 7.0 7.0 7.0 7.0 5.4 4.7
4.0 3.3
3
3
0.6
0.4
0.2
0.0
4.2
4.0
3.8
3.6
3.4
c
Control
180 µM Doxazosin
24h
1
2
3
180 µM Doxazosin
48h
1
2
3
4

Figure 6

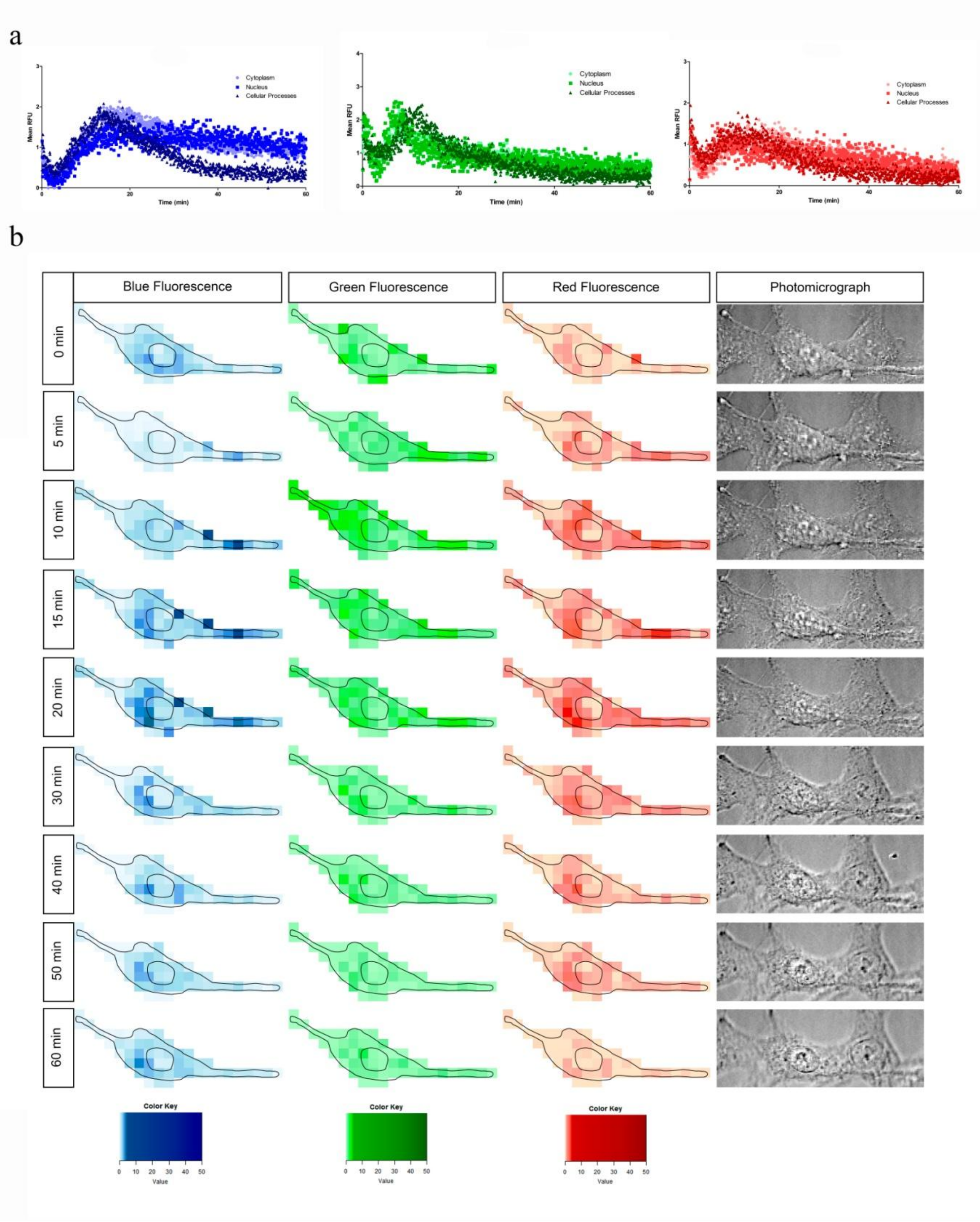
a
Mean RFU
Time (min)
0
20
40
60
Cytoplasm
Nucleus
Cellular Processes
b
Blue Fluorescence
Green Fluorescence
Red Fluorescence
Photomicrograph
0 min
5 min
10 min
15 min
20 min
30 min
40 min
50 min
60 min
Color Key
0 10 20 30 40 50
Value

Figure 7

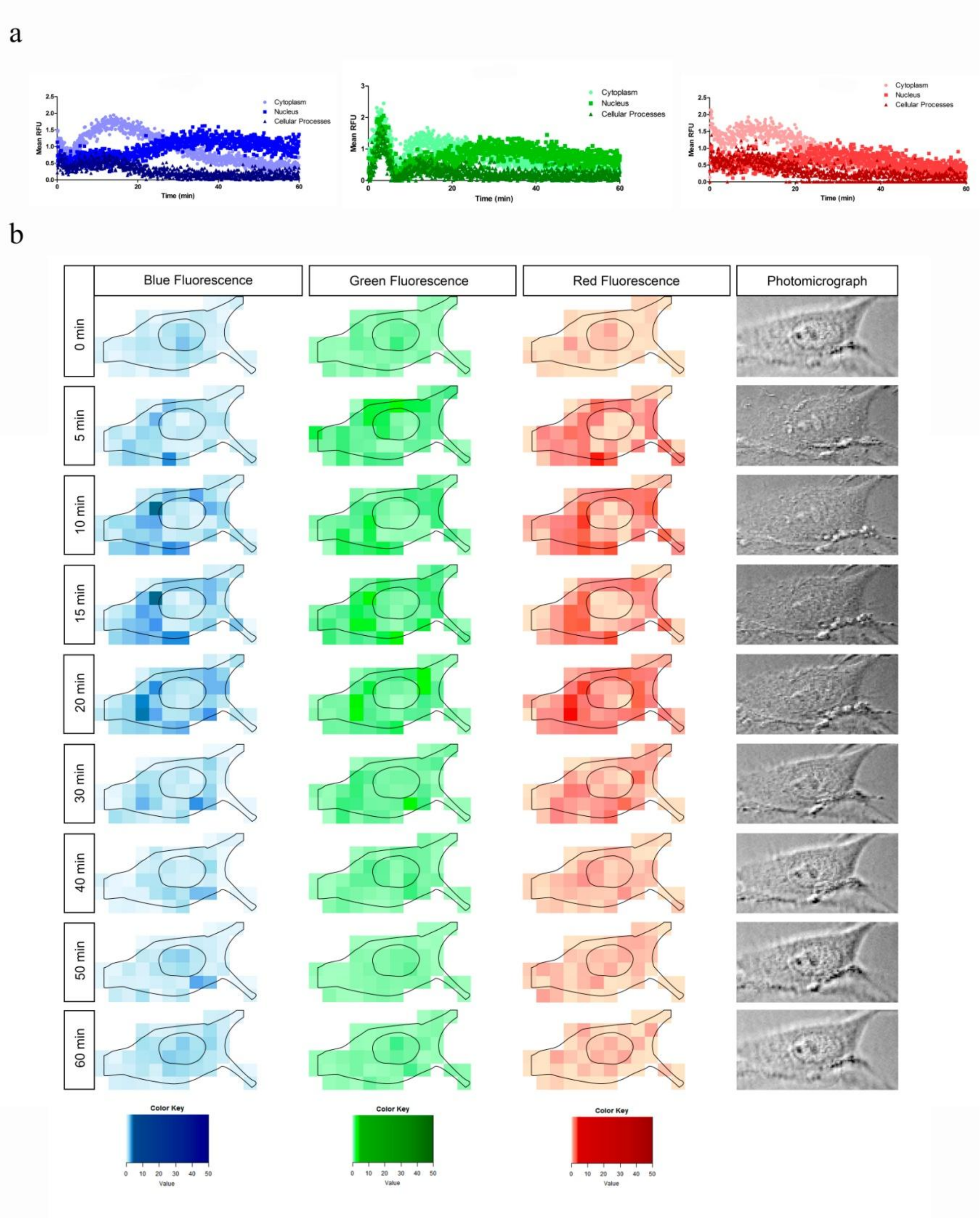
a
Mean RFU
Time (min)
0
20
40
60
Cytoplasm
Nucleus
Cellular Processes
0.0
0.5
1.0
1.5
2.0
2.5
0
1
2
3
b
Blue Fluorescence
Green Fluorescence
Red Fluorescence
Photomicrograph
0 min
5 min
10 min
15 min
20 min
30 min
40 min
50 min
60 min
Color Key
Value
0 10 20 30 40 50

Figure 8

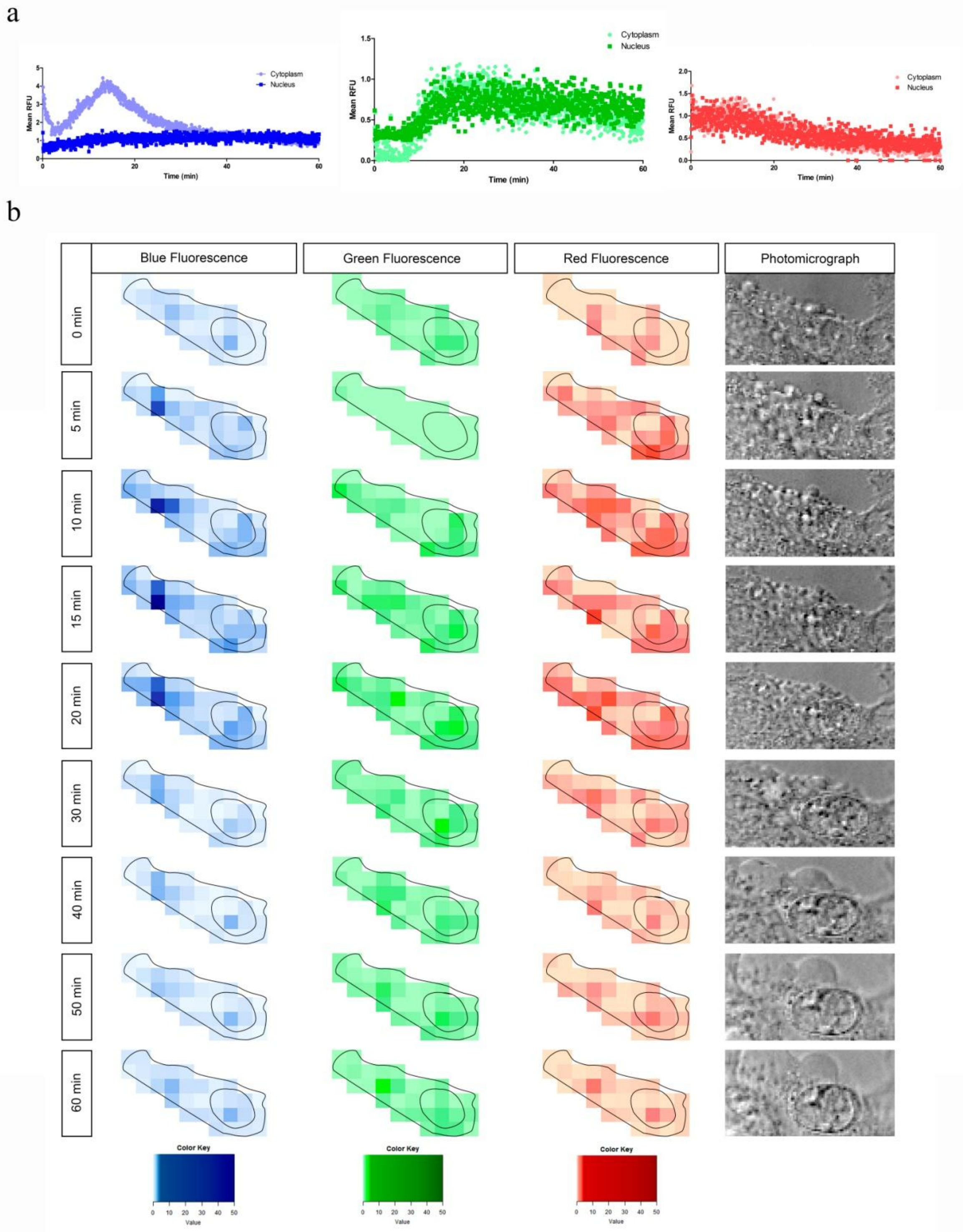
a
Mean RFU
Time (min)
Cytoplasm
Nucleus
0
20
40
60
1
2
3
4
5
0.0
0.5
1.0
1.5
2.0
b
Blue Fluorescence
Green Fluorescence
Red Fluorescence
Photomicrograph
0 min
5 min
10 min
15 min
20 min
30 min
40 min
50 min
60 min
Color Key
0 10 20 30 40 50
Value

Figure 9

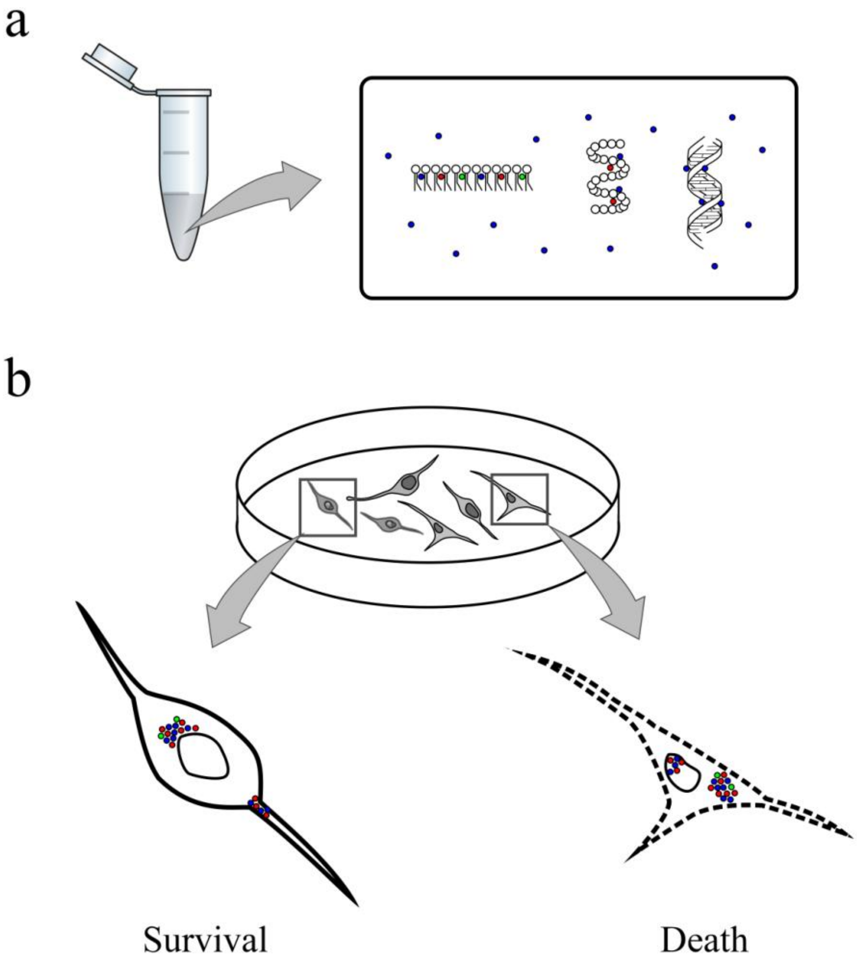
a
b
Survival
Death

7. CAPÍTULO V

Artigo: *Doxazosin targets EGFR and EGF pretreatment potentiates the drug's antiglioma effects*

Status: *em preparação*

Doxazosin targets EGFR and EGF pretreatment potentiates the drug's antiglioma effects

Mariana Maier Gaelzer[1], Bárbara Paranhos Coelho[1], Helena Flores Mello[2], Alice Hoffman de Quadros[1], Fátima Costa Rodrigues Guma[1], Christianne G. Salbego[1].

[1]Programa de Pós-Graduação em Ciências Biológicas-Bioquímica Instituto de Ciências Básicas da Saúde, Universidade Federal do Rio Grande do Sul, Porto Alegre, RS, Brasil
[2]Rutgers University, Rutgers, The State University of New Jersey-Newark, Newark, NJ

Corresponding author:
Mariana Maier Gaelzer
Departamento de Bioquímica, Instituto de Ciências Básicas da Saúde, UFRGS
Rua Ramiro Barcelos, 2600 – anexo, CEP 90035-003, Porto Alegre, RS, Brasil
Telephone: +55 (51) 3308.5547
Fax: +55 (51) 3308.5535
E-mail: marianamaierg@gmail.com

Funding: Conselho Nacional de Desenvolvimento Científico e Tecnológico (CNPq); Coordenação de Aperfeiçoamento de Pessoal de Nível Superior (Capes); Fundação de Amparo à Pesquisa do Estado do Rio Grande do Sul (FAPERGS).

Abstract

Receptor tyrosine kinases (RTKs) are regulators of the growth factor signaling that controls cellular proliferation, metabolism and survival in response to environmental cues. Glioblastomas are highly resistance to treatment with radiation and chemotherapy and aberrant Epidermal Growth Factor Receptor (EGFR) signaling contributes to this resistance. Amplifications and/or mutations of RTKs were detected in 66% of primary GBs. This deregulated signaling system plays an important role in cancer pathogenesis and therefore is an attractive target for therapeutic intervention. Doxazosin is a quinazoline with antitumoral effects on glioma and several types of cancer. The quinazolinic ring that is present in doxazosin's molecular structure has been studied as a ligand of the ATP binding site of EGFR. Here, we analyzed if the antiglioma action of doxazosin is involved with EGFR and we co-treated glioma cells with doxazosin and AG1478, an EGFR inhibitor. First, we pretreated glioma cells with Epidermal Growth Factor (EGF) and found it increased cell proliferation and EGFR expression and phosphorylation. Moreover, doxazosin treatment decreased p-EGFR levels and AG1478 treatment decreased EGFR phosphorylation and induced necrosis on glioma cells. Co-treatment of doxazosin and AG1478 decreased EGFR phosphorylation and caused necrosis. Upon increase in doxazosin concentration in the presence of AG1478, however, cell death by apoptosis occurred. In addition, pretreatment of EGF sensitized glioma cells to doxazosin and AG1478, leading to cell death by apoptosis. Previously we showed doxazosin's antiglioma action was due to inhibition of the PI3K/Akt pathway. Our findings suggest doxazosin's mechanism of action involves EGFR signaling and we propose doxazosin as a potential antiglioma agent.

Keywords: glioma, doxazosin, EGFR, EGF, AG1478

Introduction

Glioblastoma (GB) is the most common primary brain tumor in adults. GBs are aggressive, resistant and invasive, presenting a high recurrence rate [1]. They are the second most common malignant neoplasia, representing 16% of all primary brain tumors [2].

Genetic alterations on receptor tyrosine kinase (RTKs), including the epidermal growth factor receptor (EGFR), have an important role on development, progression and treatment resistance of GBs. One of the most common mutations associated with malignant glioma is amplification of EGFR (also known as ERBB1 or HER1) with a frequency of approximately 50% [3]. EGFR is a member of the superfamily HER of RTKs, in addition to ERBB2, ERBB3 and ERBB4. Ligands that activate EGFR include epidermal growth factor (EGF), transforming growth factor alfa (TGF-α), amphiregulin, betacellulin, among others [4].

While inactive, EGFR appears on the plasma membrane as a monomer. Interaction with EGF or other ligand (TGF-α, anfiregulina, betacelulina) induces conformational changes that allow for the interaction between two monomers. This results in autophosphorylation of the cytoplasmic domain and activation of downstream signaling pathways, e.g. Ras-ERK (MAPK) and PI3K/Akt [5]. Moreover, upon ligand binding, EGFR translocates to the nucleus, where it can modulate gene transcription and promote radio and chemoresistance. It is interesting to mention that EGFR can also translocate to the mitochondria [6].

In approximately 50% of tumors with EGFR amplification, a mutant form of the receptor is detected: EGFRvIII, also known as type III EGFR. Most GBs (54%) overexpress EGFR wild-type (wtEGFR) and 31% overexpress wtEGFR and EGFRvIII.

EGFRvIII has a deletion of exons 2-7, resulting in deletion of 267 aminoacids from the extracellular domain of the receptor [7]. Therefore, EGFRvIII is absent of the extracellular domain on which the ligand interacts and this mutation maintains the receptor constantly active.

In non-tumor cells, there are $4x10^4$ to $1x10^5$ EGFR molecules on the plasma membrane, while tumor cells express more than $2x10^6$ receptors per cell [4, 8]. For these reasons, several therapeutic strategies against cancer are targeting EGFR.

RTK inhibitors (TKI) are promising agents for glioma treatment. They compete with endogenous ATP for the catalitic domain of EGFR, therefore inhibiting autophosphorylation of the cytoplasmic domain [4]. Tyrphostin 4-(3-chloroanilino)-6,7-dimethoxyquinazoline (AG1478) is one of those competitive inhibitors of EGFR. AG1478 has anti-proliferative effects both on in vitro and in vivo glioblastoma models [9].

Doxazosin is an alfa-adrenergic blocker used for hypertension and urinary retention treatment and the drug is being tested against several types of cancer [10-15]. The quinazolinic ring that is present in doxazosin's molecular structure has been studied as a ligand of the ATP binding site of EGFR [16]. Staudacher et al. [14] showed doxazosin had pro-apoptotic effects on breast cancer through EGFR inhibition and NFκB signaling activation. Liao et al. [16] propose a possible interaction of doxazosin with EGFR on breast cancer cells. Moreover, doxazosin's molecular structure is similar to AG1478 and to the small molecule EGFR inhibitors Erlotinib and Gefitinib.

Previously we showed doxazosin induces glioma cell death through inhibition of the PI3K/Akt pathway [15]. Here we investigated doxazosin's effect on EGFR activation. We also analyzed the effects of EGF pretreatment on EGFR expression and on the response of glioma cells to doxazosin and AG1478 treatments after EGF pretreatment.

Materials and Methods

Chemicals and materials

Cell culture medium and fetal bovine serum (FBS) were obtained from Gibco-Invitrogen (Grand Island, NY, USA). Doxazosin, 5-Bromodeoxiuridin (5-BrdU) and human recombinant epidermal growth factor (EGF) were obtained from Sigma Chemical Co (St. Louis, MO, USA). All other reagents were purchased from Sigma Chemical Co. (St. Louis, MO, USA) or Merck (Darmstadt, Germany). All chemicals and solvents used were of analytical or pharmaceutical grade.

Cell culture

C6 rat glioma cell line was obtained from American Type Culture Collection (Rockville, Mariland, Md., USA). C6 cells were grown and maintained in Dulbecco's Modified Eagle's Medium (DMEM, Gibco-Invitrogen, Grand Island, NY, USA) supplemented with 5% (v/v) FBS (Gibco-Invitrogen, Grand Island, NY, USA), and containing 2.5 mg/mL of Fungizone® and 100 U/L of gentamicine (Shering do Brasil, São Paulo, SP, Brazil). Cells were kept at 37ºC, in an atmosphere of 5% CO_2.

Treatment

For EGF concentration curve, C6 cells were seeded on 6-well plates ($2x10^4$ cells/well) and grown for 24h. EGF was used at 2,5 ng/mL, 5 ng/mL and 10 ng/mL, during 24h and 48h. The concentrations used were obtained from the literature [17].

Doxazosin was dissolved in 20% ethanol/milli-Q^{TM} water (vehicle) and cells were treated with 100, 150 and 180 µM of doxazosin alone for 48h or after treatment with EGF 10 ng/mL for 48h.

Flow Cytometry

C6 cells were seeded in 6-well plates ($2x10^4$ cells/well) and grown for 24 h. After treatments, cells were washed with PBS, trypsinized and cell counting was performed by measuring the volume flow rate.

For cell cycle analysis, C6 cells were centrifuged at 400 x g for 5 min and resuspended (10^6 cells/mL) in PBS containing 0,1% Nonidet, RNAse (100 µg/mL) and PI (5 µg/mL) for 15 min at room temperature.

Cell death was analyzed by flow cytometry. Both floating and trypsinized adherent cells were collected. Annexin-V FITC/propidium iodide (PI) double stain kit was used, following the manufacturer’s instructions (Invitrogen, Grand Island, NY, USA). Samples were incubated in binding buffer containing Annexin-V FITC and PI for 15 min in the dark at room temperature.

For pEGFR immunoquantification, cells were fixed with phosphate-buffered saline (PBS) and 4% paraformaldehyde for 20 min, then were permeabilized with PBS and 0.01% Triton X-100 and incubated with the primary antibody anti-pEGFR (1:50; Cell Signaling Technology™) for 30 min. The secondary antibody, Alexa Fluor 488 anti-mouse (1:100; Gibco-Invitrogen), was added, and after a 60 min incubation, cells were analyzed by a flow cytometer.

Data was acquired with a FACS Calibur cytometry system (FACS Calibur, BD Bioscience, Mountain View, CA, USA) and Cell Quest software (BD Bioscience, Mountain View, CA, USA). Data obtained was analyzed with FCS Express 4 Software (De Novo Software, Los Angeles, CA, USA).

Quantitative PCR

RNA was isolated using TRIzol Reagent (Invitrogen). RNA was quantified using BioPhotometer Plus (Eppendorf, Hamburg, Germany) to measure the absorbance at 260 nm relative to that at 280 nm. It was added 300 ng of total RNA to each cDNA synthesis reaction, using SuperScript®-III RT First-Strand Synthesis SuperMix (Invitrogen). Specific primers for each gene were designed using IDT Design Software (Integrated DNA Technologies Inc., USA). Primers used for EGFR were the following: 5’-CCTGGAAGAGACCTGCATTATC-3’ (forward) and 5’-CAGAGCTGTCAAACCCACTAC-3’ (reverse). Beta-2 microglobulin gene was used as the internal control gene for all relative expression calculations. Primers for β2M were: 5’-TCCTGGCTCACACTGAATTC-3’ (forward) and 5’-CTTTGTGGATAAATTGTATAGCA-3’ (reverse). q-PCR reactions were carried out in a Step One Plus real-time cycler (Applied-Biosystem, New York, NY, USA), performed in triplicates and containing 0.2 μM of forward and reverse primers, 0.5 ng/μl cDNA and Platinum® SYBR® Green qPCR SuperMix-UDG with ROX (Invitrogen Corp., USA) in the thermal cycling conditions: 2 min at 50º C, 2 min at 95ºC, followed by 40 cycles of 95ºC for 15 s, 60ºC for 30 s. Mean Ct values from triplicate measurements were used to calculate expression of the target gene using the ΔΔCt formula [18].

Statistical analysis

Data are expressed as means±SEM. All results are representative of at least 3 independent experiments. Student’s *t* test or analysis of variance (ANOVA) were applied to the means to determine statistical differences between experimental groups. Post hoc comparisons were performed by Tukey test. Differences between mean values were considered significant when $p<0.05$.

Results

EGF increases glioma cells proliferation and induces EGFR expression

EGF treatment at 5 and 10 ng/mL for 48h increased the number of C6 cells in G2/M cycle phase (Fig. 1). EGF treatment also induced EGFR expression (Fig. 1d).

EGFR phosphorylation is decreased by doxazosin and AG1478 treatment

In agreement with what was demonstrated for other glioma cell lines [19], AG1478 decreased p-EGFR protein levels on C6 glioma cells (Fig. 2). Doxazosin decreased EGFR phosphorylation at 100, 150 and 180 µM. Inhibition of EGFR phosphorylation was enhanced with co-treatment of AG1478 and 180 µM doxazosin (Fig. 2).

EGF pretreatment and doxazosin on EGFR phosphorylation

Next we pretreated C6 cells with EGF for 48h and either exposed cells to doxazosin (EGF pretreatment + doxazosin groups) or maintained cells without any treatment for another 48h (EGF pretreatment group) (Fig. 3). In the EGF pretreatment group, p-EGFR protein levels were increased compared with the control (Fig. 3). Doxazosin treatment after EGF pretreatment was able to decrease EGFR phosphorylation, but only at 150 and 180 µM (Fig. 3).

Co-treatment of doxazosin and AG1478 induces glioma cells death

Co-treatment of doxazosin and AG1478 induced necrosis on approximately 60% of cells at doxazosin’s concentrations of 150 and 180 µM (Fig. 4). Doxazosin’s concentration of 180 µM in the presence of AG1478 also increased late apoptosis. AG1478 alone caused cell death by necrosis. Previously we showed 100 µM doxazosin induces ~40% of glioma cell death, while here co-treatment of inhibitor and 100 µM doxazosin did not caused C6 cell death (Fig. 4).

EGF pre-treatment sensitizes glioma cells do doxazosin

Previously we showed 180 µM doxazosin treatment for 48h induces glioma cell death at approximately 70% of cells. Here, pre-treatment of EGF for 48h followed by 180 µM doxazosin treatment induced early and late apoptosis on approximately 13% and 86%, respectively (Fig. 5). AG1478 induced early and late apoptosis in approximately 29% and 67% of cells, respectively (Fig. 5).

Discussion

Glioblastoma is the most common primary brain tumor in adults. These tumors are characterized as highly infiltrative, lethal and resistant to radio and chemotherapy [1]. EGFR gene amplification is one of the most common genetic alterations in glioblastoma [20]. Thus, therapeutic strategies targeting EGFR are being investigated as potential treatments for GBs [4].

Response of glioma cells to EGF treatment is influenced by the microenvironment, the ligand concentration and the type of cell line [21-22]. Our present findings demonstrate EGF treatment induced proliferation and increased EGFR expression on C6 glioma cells. In accordance with our findings, Lund-Johansen et al. [23] found that treatment with EGF increased glioma cell growth, migration and invasion on D247-MG and D37-MG cells and this was dependent on the expression levels of EGFR. Furthermore, Pedersen et al. [24] found EGF-induced cell proliferation occurred on invasive glioma cells that contained the highest levels of EGFR mRNA (D-37MG, D-57MG and GaMG), but not on non-invasive cells with low EGFR expression (U-1251MG and D-263MG) (1994). In addition, Korc et al. [25] found EGF and EGFR are expressed at higher levels in human pancreatic cancer when compared with normal human pancreas.

In contrast, Högnason et al. [26] demonstrated that expression of a dominant negative Ras mutant in EGFR overexpressing cells potentiates EGF-induced apoptosis. However, in this study we demonstrated EGF treatment induced C6 glioma proliferation instead of cell death with the cells overexpressing EGFR. These results we found could be because C6 do not express dominant negative Ras. Supporting our findings, Sibenaller et al. [27] showed EGFR and Ras expression are increased in C6 cells compared with expression in normal astrocytes.

Previously we demonstrated doxazosin inhibits PI3K/Akt pathway on glioma cells [15]. In order to evaluate if this action could be through EGFR inhibition, in this study we analyzed doxazosin's connection with EGFR phosphorylation. We found that doxazosin was able to decrease p-EGFR levels at 100, 150 and 180 µM and, beyond that, this effect seems to be similar to AG1478 (an EGFR inhibitor). Furthermore, co-treatment of C6 cells with 180 µM doxazosin and AG1478 potentiates the decrease of EGFR phosphorylation.

Next we analyzed EGFR phosphorylation status on C6 cells after EGF pretreatment. In the EGF pretreatment group, p-EGFR levels increased even in the absence of the ligand, while 150 and 180 µM doxazosin treatment was able to decreased EGFR phosphorylation.

Glioma cells express a truncated form of EGFR that has a deletion of exons 2-7 (EGFRvIII) and therefore, lacks the extracellular domain and is constitutively active [7]. Ligand interaction with wtEGFR results in fast receptor internalization, followed by dephosphorylation and receptor degradation or recycling [28]. EGFRvIII expression results in constitutive tyrosine phosphorylation of the receptor. Since EGF binding to EGFRvIII is hindered, the receptor internalization is delayed, promoting a continued state of basal signaling from the mutated receptor on the plasma membrane [28]. However, the increase in expression we found in this study could be of both forms of the EGFR, since the primers we used do not discriminate between wild type EGFR (wtEGFR) and EGFRvIII. Several studies that correlate the increase in EGFR expression with increased EGF expression do not discriminate between both forms of the receptor [23-25]. Since our objective was to analyze the pharmacodynamics between doxazosin and EGFR, we first tested whether the endogenous ligand was able to increase the receptor expression, based on evidences from the literature [29].

Therefore, the increase in p-EGFR we found in EGF pretreated cells could be due to increase of wtEGFR and EGFRvIII on the cell membrane. Furthermore, Luwor et al. [30] showed that EGFRvIII can form dimmers with and activate wtEGFR. Wiley et al. [31] demonstrated that cells overexpressing EGFR increase ligand-independent receptor activation. Moreover, since the recycling of EGFRvIII is delayed and this mutated receptor is intrinsically active [28], the pretreatment with EGF could have caused increase in the EGFRvIII expression. In this context, higher concentrations of doxazosin were necessary to decrease p-EGFR levels after EGF pretreatment.

In order to evaluate the mechanism of action of doxazosin on glioma cells, we treated C6 cells with AG1478 alone and with doxazosin. Previously we showed doxazosin induces apoptosis and necrosis on C6 cells, and that 100 µM doxazosin caused ~40% of cell death [15]. In this study, however, co-treatment of 100 µM doxazosin with AG1478 did not induced C6 cell death. The EGFR inhibitor AG1478 could be interfering with doxazosin's action. Thus, these quinazoline drugs could be competing for the same ligand site on the receptor.

Here we demonstrated AG1478's mechanism of C6 cell death is via necrosis. Previously we showed 150 µM doxazosin induces necrosis on approximately 10% and apoptosis on ~45% of cells [15]. In this study, however, we found co-treatment of 150 µM doxazosin with AG1478 induced ~60% of necrosis on C6 cells. Moreover, the co-treatment of 180 µM doxazosin and AG1478 caused a more pronounced necrotic death, but also induces ~12% of apoptosis. These results could mean doxazosin in higher concentrations is able to displace AG1478 and to exert its actions on the cells.

Furthermore, we showed in the present study that pretreatment of C6 cells with EGF increased EGFR expression and sensitized the cells to doxazosin and AG1478. Wiley et al. [31] demonstrated EGFRvIII increases the signaling pathways affected by EGFR activation in the absence of ligands. The pretreatment with EGF appear to have sensitized the resistance cells to doxazosin and AG1478 treatment, since the percentage of total cell death increased in this experiment. Moreover, studies show AG1478 presents higher specificity to EGFRvIII than wtEGFR [32]. EGF pretreatment could be increasing EGFRvIII expression and sensitizing the resistant cells to both doxazosin and AG1478.

EGF is present in the blood stream and, therefore, can reach tumoral cells in vivo. Here we showed pretreatment with EGF increases EGFR expression and sensitizes C6 cells to treatment. However, more studies are needed to evaluate the mechanisms of EFGR expression induction by EGF.

In glioblastomas, approximately 50% of patients have amplification of EGFR and can express EGFRvIII [7]. Moreover, McLendon et al. [20] showed RTK/Ras/PI3K signaling is altered in 88% of these tumors. Liao et al. [16] previously showed doxazosin inhibits EGFR on breast cancer cells. Petty et al. [33] demonstrated doxazosin is an agonist of the RTK EphA2. Eph receptors, unlike other RTKs, use Ras and PI3K/Akt signaling to inhibit cell growth [34]. Here we found doxazosin decreases EGFR phosphorylation and previously we showed this drug inhibits the PI3K/Akt pathway.

Doxazosin is a quinazoline drug with similar molecular structure as Lapatinib (a RTK inhibitor), Erlotinib (an EGFR inhibitor) and AG1478 (an EGFR inhibitor). Lapatinib is currently in clinical trials for breast cancer [35] and Erlotinib is approved by the FDA for non-small cell lung cancer and pancreatic cancer, and is in clinical trial for several types of cancer [36-37]. Here and previously we demonstrated doxazosin’s mechanism of action involves EGFR and PI3K/Akt inhibition. Moreover, since doxazosin is used in the clinic for treatment of hypertension and benign prostatic hyperplasia, the drug’s side effects and safety profiles are well known. Therefore, we propose doxazosin is a potential candidate for repourposing as an antitumoral agent.

References

1. Jackson, R.J., et al., *Limitations of stereotactic biopsy in the initial management of gliomas.* Neuro-oncology, 2001. **3**(3): p. 193-200.

2. Dolecek, T.A., et al., *CBTRUS statistical report: primary brain and central nervous system tumors diagnosed in the United States in 2005–2009.* Neuro-oncology, 2012. **14**(suppl 5): p. v1-v49.
3. Furnari, F.B., et al., *Heterogeneity of epidermal growth factor receptor signalling networks in glioblastoma.* Nature reviews. Cancer, 2015. **15**(5): p. 302.
4. Yewale, C., et al., *Epidermal growth factor receptor targeting in cancer: a review of trends and strategies.* Biomaterials, 2013. **34**(34): p. 8690-8707.
5. Tebbutt, N., M.W. Pedersen, and T.G. Johns, *Targeting the ERBB family in cancer: couples therapy.* Nature Reviews Cancer, 2013. **13**(9): p. 663-673.
6. Han, W. and H.-W. Lo, *Landscape of EGFR signaling network in human cancers: biology and therapeutic response in relation to receptor subcellular locations.* Cancer letters, 2012. **318**(2): p. 124-134.
7. Hatanpaa, K.J., et al., *Epidermal growth factor receptor in glioma: signal transduction, neuropathology, imaging, and radioresistance.* Neoplasia, 2010. **12**(9): p. 675-684.
8. Herbst, R.S. and D.M. Shin, *Monoclonal antibodies to target epidermal growth factor receptor–positive tumors.* Cancer, 2002. **94**(5): p. 1593-1611.
9. Ellis, A., et al., *Preclinical analysis of the analinoquinazoline AG1478, a specific small molecule inhibitor of EGF receptor tyrosine kinase.* Biochemical pharmacology, 2006. **71**(10): p. 1422-1434.
10. Hui, H., M.A. Fernando, and A.P. Heaney, *The α 1-adrenergic receptor antagonist doxazosin inhibits EGFR and NF-κB signalling to induce breast cancer cell apoptosis.* European Journal of Cancer, 2008. **44**(1): p. 160-166.

11. Yang, G., et al., *Transforming growth factor β1 transduced mouse prostate reconstitutions: II. Induction of apoptosis by doxazosin.* The Prostate, 1997. **33**(3): p. 157-163.

12. SIDDIQUI, E.J., et al., *Growth inhibitory effect of doxazosin on prostate and bladder cancer cells. Is the serotonin receptor pathway involved?* Anticancer research, 2005. **25**(6B): p. 4281-4286.

13. Fernando, M.A. and A.P. Heaney, *α1-Adrenergic receptor antagonists: novel therapy for pituitary adenomas.* Molecular Endocrinology, 2005. **19**(12): p. 3085-3096.

14. Staudacher, I., et al., *HERG K+ channel-dependent apoptosis and cell cycle arrest in human glioblastoma cells.* PloS one, 2014. **9**(2): p. e88164.

15. Gaelzer, M.M., et al., *Phosphatidylinositol 3-Kinase/AKT pathway inhibition by doxazosin promotes glioblastoma cells death, upregulation of p53 and triggers low neurotoxicity.* PloS one, 2016. **11**(4): p. e0154612.

16. Liao, C.H., et al., *Anti-angiogenic effects and mechanism of prazosin.* The Prostate, 2011. **71**(9): p. 976-984.

17. zu Schwabedissen, H.E.M., et al., *Epidermal growth factor-mediated activation of the map kinase cascade results in altered expression and function of ABCG2 (BCRP).* Drug metabolism and disposition, 2006. **34**(4): p. 524-533.

18. Livak, K.J. and T.D. Schmittgen, *Analysis of relative gene expression data using real-time quantitative PCR and the 2− ΔΔCT method.* methods, 2001. **25**(4): p. 402-408.

19. Huang, P.H., et al., *Quantitative analysis of EGFRvIII cellular signaling networks reveals a combinatorial therapeutic strategy for glioblastoma.*

Proceedings of the National Academy of Sciences, 2007. **104**(31): p. 12867-12872.

20. McLendon, R., et al., *Comprehensive genomic characterization defines human glioblastoma genes and core pathways.* Nature, 2008. **455**(7216): p. 1061-1068.

21. Roth, P. and M. Weller, *Challenges to targeting epidermal growth factor receptor in glioblastoma: escape mechanisms and combinatorial treatment strategies.* Neuro-oncology, 2014. **16**(suppl 8): p. viii14-viii19.

22. E Taylor, T., F. B Furnari, and W. K Cavenee, *Targeting EGFR for treatment of glioblastoma: molecular basis to overcome resistance.* Current cancer drug targets, 2012. **12**(3): p. 197-209.

23. Lund-Johansen, M., et al., *Effect of epidermal growth factor on glioma cell growth, migration, and invasion in vitro.* Cancer research, 1990. **50**(18): p. 6039-6044.

24. Pedersen, P.H., et al., *Heterogeneous response to the growth factors [EGF, PDGF (bb), TGF-α, BFGF, il-2] on glioma spheroid growth, migration and invasion.* International journal of cancer, 1994. **56**(2): p. 255-261.

25. Korc, M.a., et al., *Overexpression of the epidermal growth factor receptor in human pancreatic cancer is associated with concomitant increases in the levels of epidermal growth factor and transforming growth factor alpha.* Journal of Clinical Investigation, 1992. **90**(4): p. 1352.

26. Högnason, T., et al., *Epidermal growth factor receptor induced apoptosis: potentiation by inhibition of Ras signaling.* FEBS letters, 2001. **491**(1-2): p. 9-15.

27. Sibenaller, Z.A., et al., *Genetic characterization of commonly used glioma cell lines in the rat animal model system.* Neurosurgical focus, 2005. **19**(4): p. 1-9.

28. Tomas, A., C.E. Futter, and E.R. Eden, *EGF receptor trafficking: consequences for signaling and cancer.* Trends in cell biology, 2014. **24**(1): p. 26-34.

29. Hayat, M.A., *Handbook of Immunohistochemistry and in Situ Hybridization of Human Carcinomas: Molecular Pathology, Colorectal Carcinoma, and Prostate Carcinoma*. Vol. 2. 2005: Academic Press.

30. Luwor, R.B., et al., *The tumor-specific de2–7 epidermal growth factor receptor (EGFR) promotes cells survival and heterodimerizes with the wild-type EGFR.* Oncogene, 2004. **23**(36): p. 6095-6104.

31. Wiley, H.S., *Anomalous binding of epidermal growth factor to A431 cells is due to the effect of high receptor densities and a saturable endocytic system.* J Cell Biol, 1988. **107**(2): p. 801-810.

32. Han, Y., et al., *Tyrphostin AG 1478 preferentially inhibits human glioma cells expressing truncated rather than wild-type epidermal growth factor receptors.* Cancer research, 1996. **56**(17): p. 3859-3861.

33. Petty, A., et al., *A small molecule agonist of EphA2 receptor tyrosine kinase inhibits tumor cell migration in vitro and prostate cancer metastasis in vivo.* PloS one, 2012. **7**(8): p. e42120.

34. Lisabeth, E.M., G. Falivelli, and E.B. Pasquale, *Eph receptor signaling and ephrins.* Cold Spring Harbor perspectives in biology, 2013. **5**(9): p. a009159.

35. Baselga, J., et al., *Lapatinib with trastuzumab for HER2-positive early breast cancer (NeoALTTO): a randomised, open-label, multicentre, phase 3 trial.* The Lancet, 2012. **379**(9816): p. 633-640.

36. Zhu, C.-Q., et al., *Role of KRAS and EGFR as biomarkers of response to erlotinib in National Cancer Institute of Canada Clinical Trials Group Study BR. 21.* Journal of clinical oncology, 2008. **26**(26): p. 4268-4275.

37. Siu, L.L., et al., *Phase I/II trial of erlotinib and cisplatin in patients with recurrent or metastatic squamous cell carcinoma of the head and neck: a Princess Margaret Hospital phase II consortium and National Cancer Institute of Canada Clinical Trials Group Study*. Journal of clinical oncology, 2007. **25**(16): p. 2178-2183.

Figure Legends

Figure 1. Effects of pretreatment of EGF on C6 glioma cells. In **a**, cell cycle quantification of cells treated with EGF for 24h and in **b** for 48h. **(c)** Histograms of DNA content in C6 cells treated with EGF for 48h. **(d)** mRNA expression of EGFR on C6 cells after EGF exposure for 48h. Data are represented as means ± SEM (n = 4). *p< 0.05 and ***p<0.001 vs. control.

Figure 2. Histogram and graph of p-EGFR protein levels of C6 cells after treatment with AG1478 alone or in co-treatment with doxazosin for 48h. Data are represented as means ± SEM (n = 4). ***p<0.001 vs. control.

Figure 3. Histogram and graph of p-EGFR protein levels of C6 cells pretreated with EGF for 48h followed by treatment with doxazosin 48h. Data are represented as means ± SEM (n = 4). *p< 0.05 and **p<0.01 vs. control.

Figure 4. Analysis of cell death on C6 cells after treatment with AG1478 alone or co-treatment of both quinazoline molecules for 48h. Dot plot and graph of cells stained

with Annexin V and Propidium Iodide. Data are represented as means ± SEM (*n* = 4). *$p<0.05$ and ***$p<0.001$ vs. control.

Figure 5. Analysis of cell death on C6 cells after pretreatment with EGF for 48h followed by treatment with AG1478 or doxazosin for 48h. Dot plot and graph of cells stained with Annexin V and Propidium Iodide. Data are represented as means ± SEM (*n* = 4). *$p<0.05$ and ***$p<0.001$ vs. control.

Figure 6. Suggested model of doxazosin's mechanism of action on glioma C6 cells. EGF treatment for 48h induces C6 cell proliferation, EGFR phosphorylation and increases EGFR messenger RNA. AG1478 alone decreases p-EGFRTyr1048 on C6 cells and induces necrosis. Doxazosin alone decreases p-EGFRTyr1048 and induces cell death, mostly by apoptosis. Co-treatment of doxazosin and AG1478 decreases EGFR phosphorylation and causes cell death mostly by necrosis. After EGF pretreatment, C6 cells maintain elevated levels of p-EGFRTyr1048, while treatment with AG1478 or doxazosin decreases EGFR phosphorylation and dramatically increases apoptosis.

Figure 1

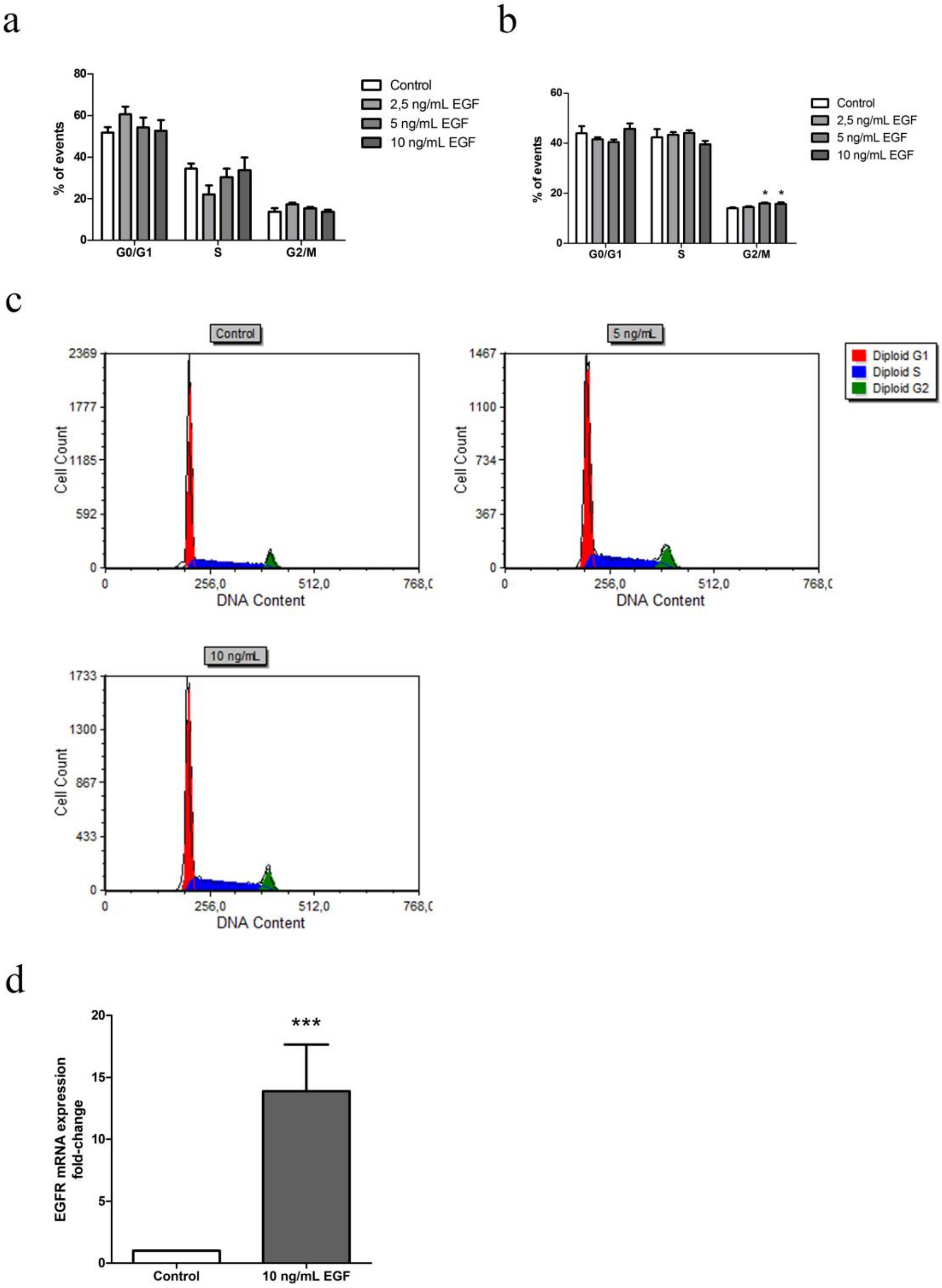

a
b
c
d
% of events
80
60
40
20
0
G0/G1
S
G2/M
Control
2,5 ng/mL EGF
5 ng/mL EGF
10 ng/mL EGF
*
*
Control
5 ng/mL
10 ng/mL
Cell Count
2369
1777
1185
592
1467
1100
734
367
1733
1300
867
433
DNA Content
0
256,0
512,0
768,0
Diploid G1
Diploid S
Diploid G2
EGFR mRNA expression fold-change
***
15
10
5
Control
10 ng/mL EGF

Figure 2

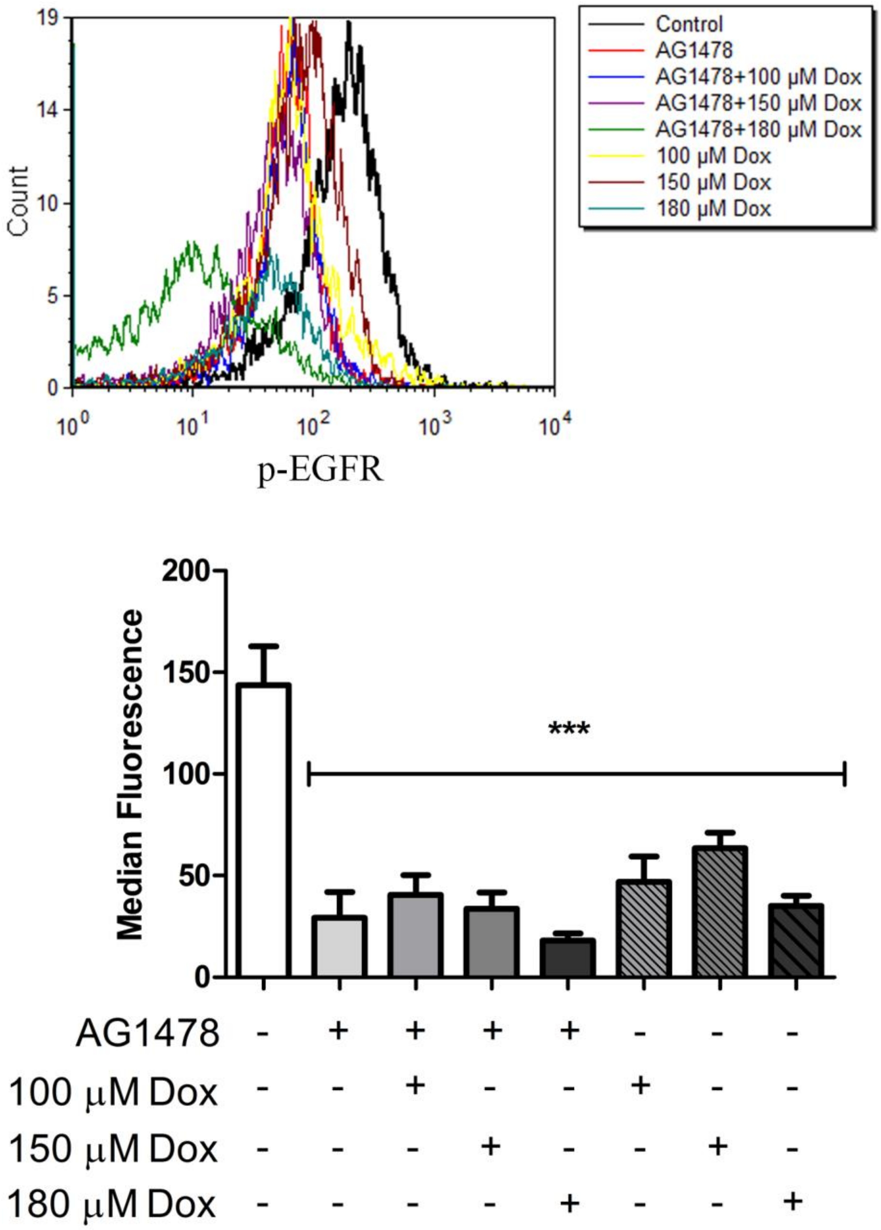
Count
19
14
10
5
0
10^0
10^1
10^2
10^3
10^4
p-EGFR
Control
AG1478
AG1478+100 µM Dox
AG1478+150 µM Dox
AG1478+180 µM Dox
100 µM Dox
150 µM Dox
180 µM Dox
Median Fluorescence
200
150
100
50
0
***
AG1478 - + + + + - - -
100 µM Dox - - + - - + - -
150 µM Dox - - - + - - + -
180 µM Dox - - - - + - - +

Figure 3

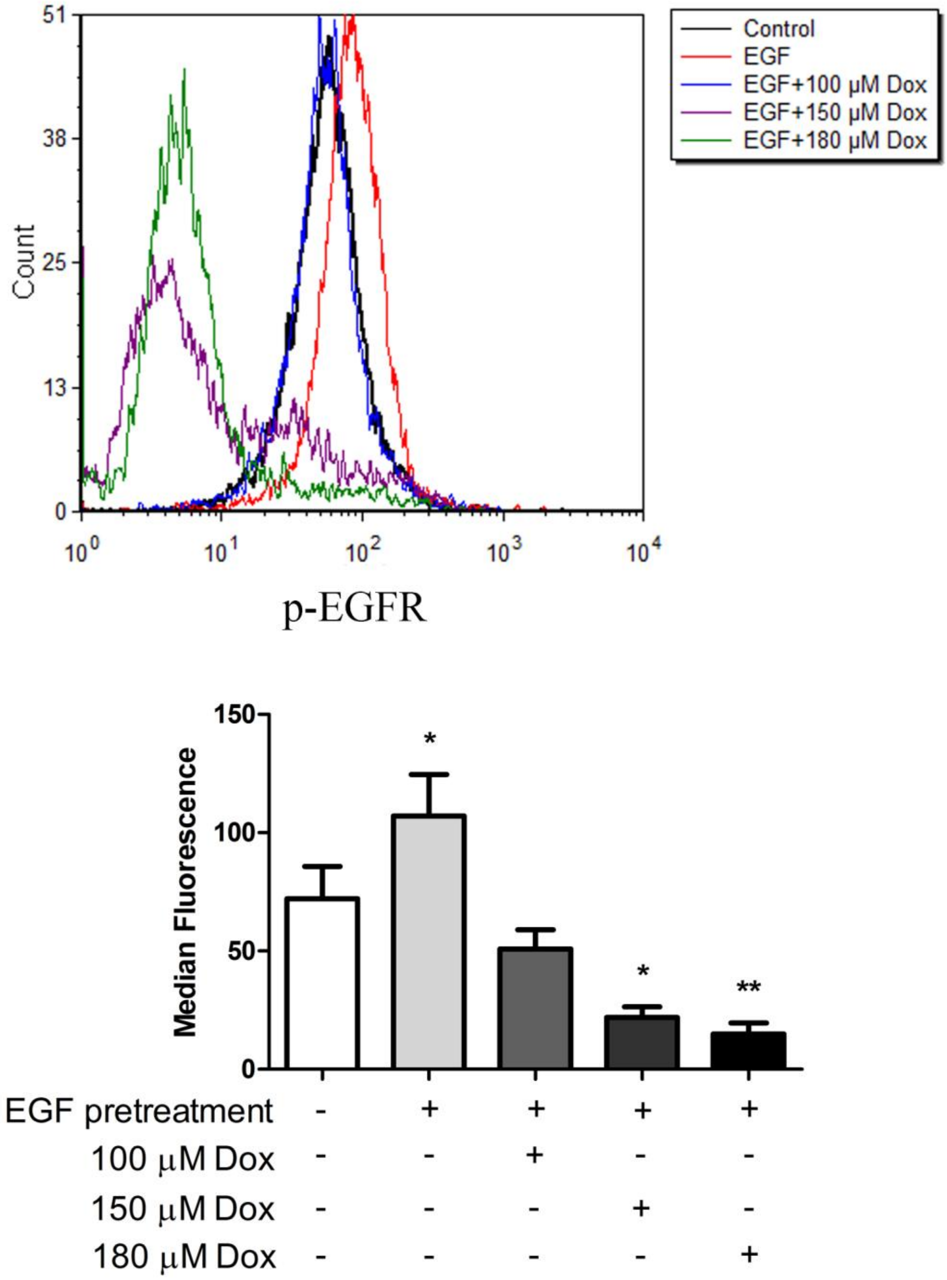
51
38
25
13
0
Count
10^0
10^1
10^2
10^3
10^4
p-EGFR
Control
EGF
EGF+100 μM Dox
EGF+150 μM Dox
EGF+180 μM Dox
150
100
50
0
Median Fluorescence
*
*
**
EGF pretreatment - + + + +
100 μM Dox - - + - -
150 μM Dox - - - + -
180 μM Dox - - - - +

Figure 4

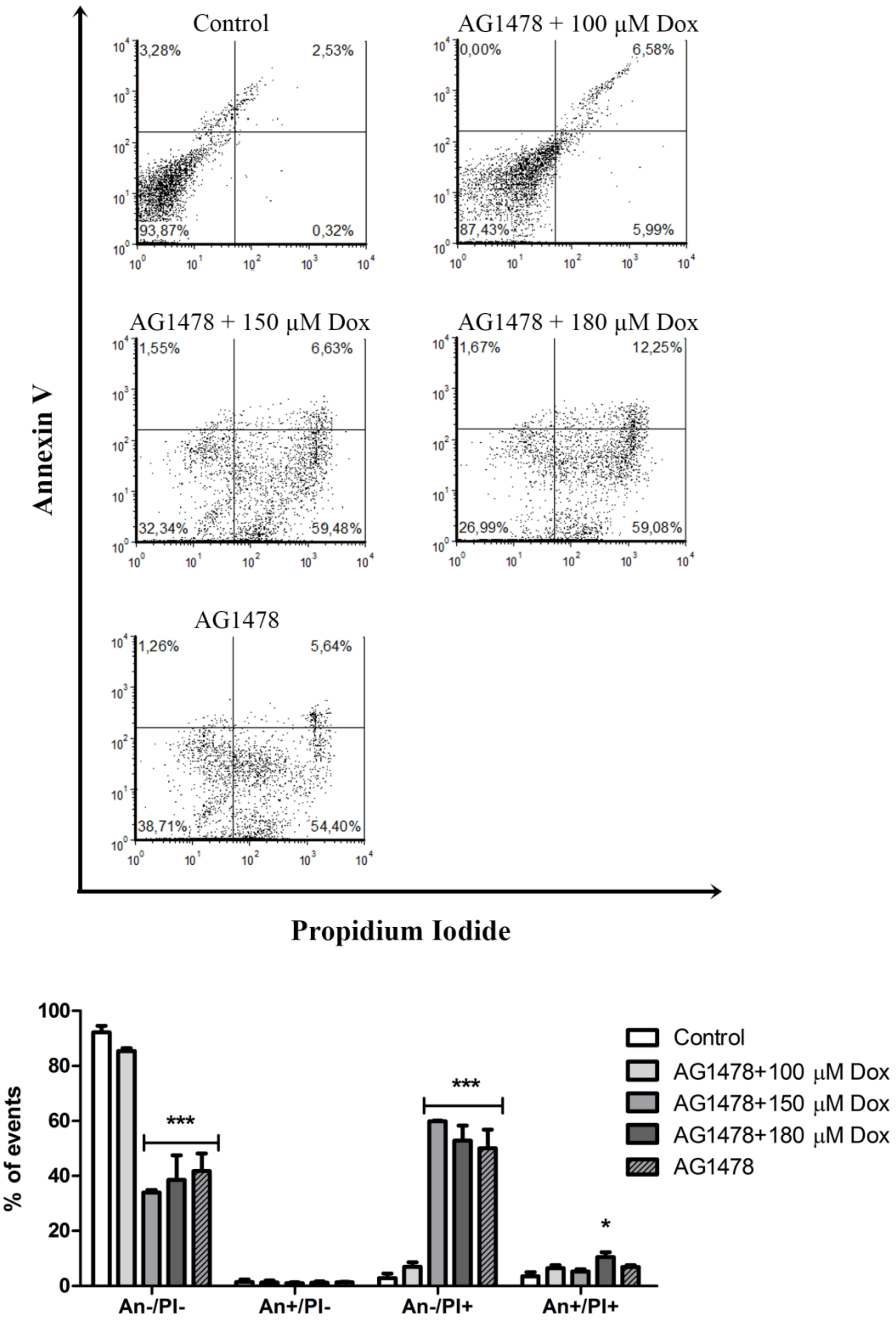
Control
3,28%
2,53%
93,87%
0,32%
AG1478 + 100 µM Dox
0,00%
6,58%
87,43%
5,99%
AG1478 + 150 µM Dox
1,55%
6,63%
32,34%
59,48%
AG1478 + 180 µM Dox
1,67%
12,25%
26,99%
59,08%
AG1478
1,26%
5,64%
38,71%
54,40%
Annexin V
Propidium Iodide
% of events
100
80
60
40
20
0
***
***
*
An-/PI-
An+/PI-
An-/PI+
An+/PI+
Control
AG1478+100 µM Dox
AG1478+150 µM Dox
AG1478+180 µM Dox
AG1478

Figure 5

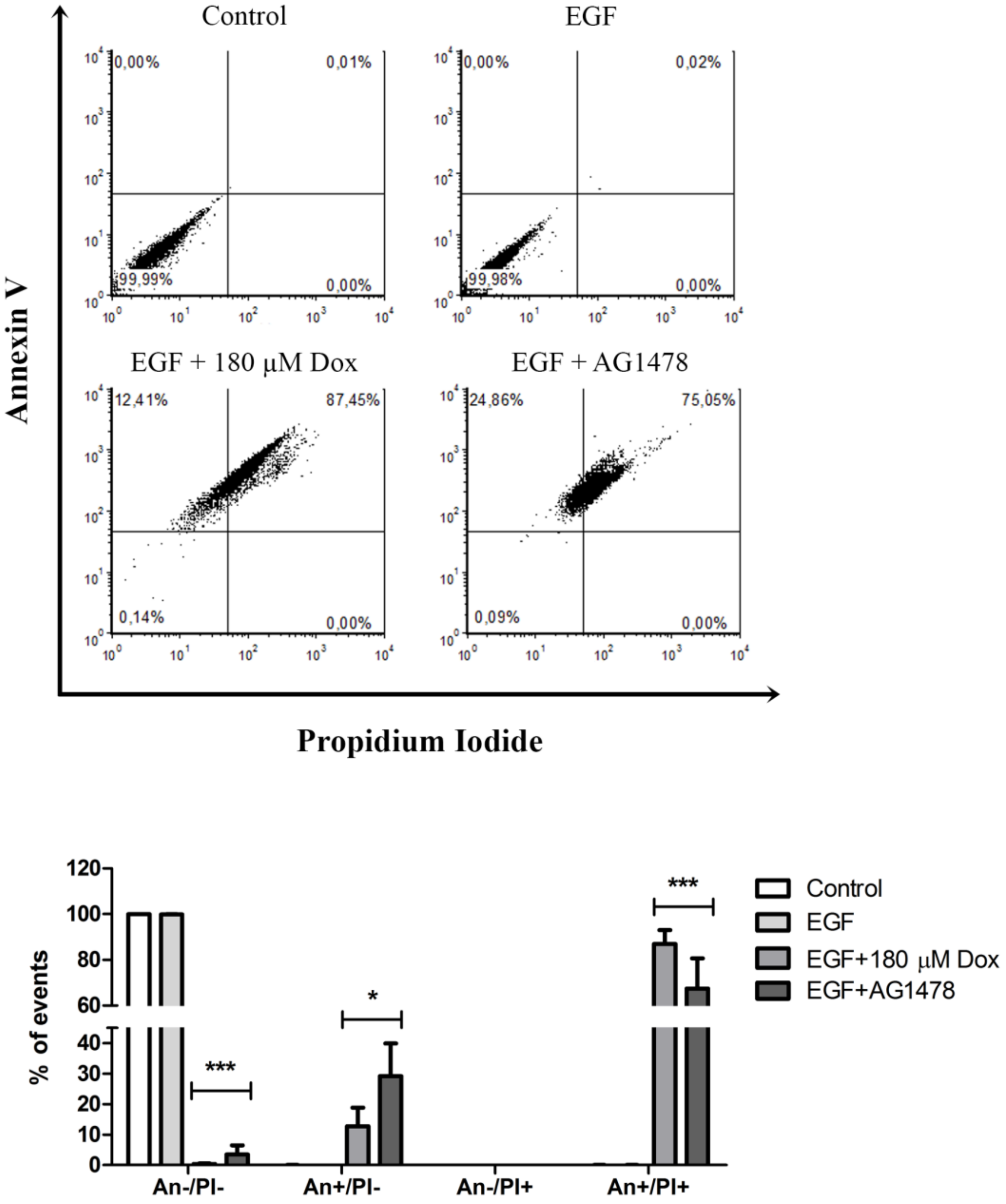
Control
EGF
EGF + 180 μM Dox
EGF + AG1478
0,00%
0,01%
99,99%
0,00%
0,00%
0,02%
99,98%
0,00%
12,41%
87,45%
0,14%
0,00%
24,86%
75,05%
0,09%
0,00%
Annexin V
Propidium Iodide
% of events
120
100
80
60
40
30
20
10
0
***
*
***
An-/PI-
An+/PI-
An-/PI+
An+/PI+
Control
EGF
EGF+180 μM Dox
EGF+AG1478

Figure 6

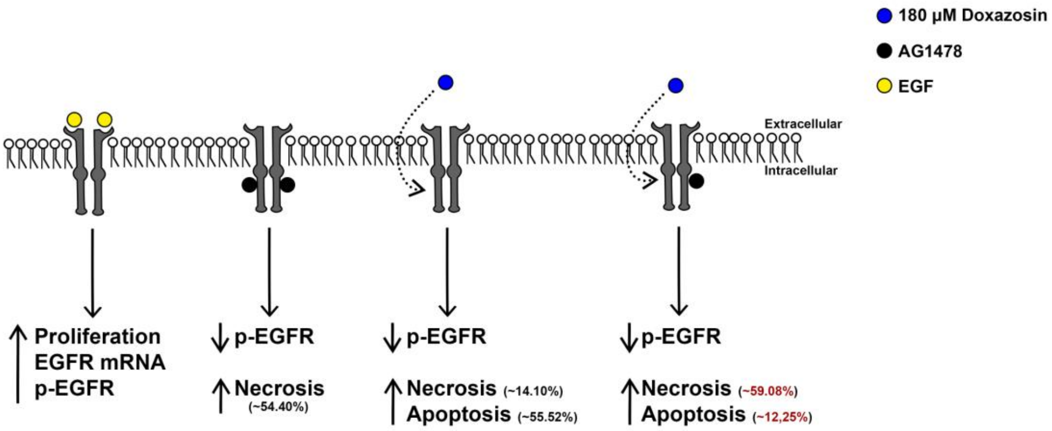

● 180 µM Doxazosin
● AG1478
○ EGF
Extracellular
Intracellular
↑ Proliferation
EGFR mRNA
p-EGFR
↓ p-EGFR
↑ Necrosis (~54.40%)
↓ p-EGFR
↑ Necrosis (~14.10%)
Apoptosis (~55.52%)
↓ p-EGFR
↑ Necrosis (~59.08%)
Apoptosis (~12,25%)

After EGF pretreatment:

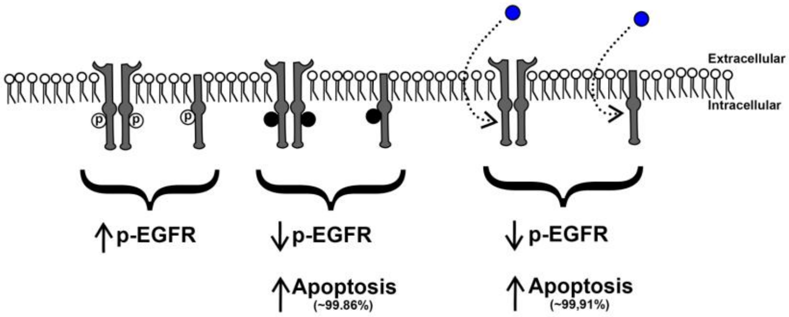

Extracellular
Intracellular
P
P
P
↑ p-EGFR
↓ p-EGFR
↑ Apoptosis (~99.86%)
↓ p-EGFR
↑ Apoptosis (~99,91%)

8. CAPÍTULO VI

Artigo: *Doxazosin-loaded nanocapsules: possible* in vivo *and* in vitro *antiglioma agent*

Status: *em preparação*

Doxazosin-loaded nanocapsules: possible *in vivo* and *in vitro* antiglioma agent

Mariana Maier Gaelzer[1], Bárbara Paranhos Coelho[1], Alice Hoffman de Quadros[1]; Guilherme Konradt[2], Jessica Saldanha Krai[3], Juliana B. Hoppe[1], Denise Zancan[4], Fátima Costa Rodrigues Guma[1], Ana M. O. Battastini[1], Ruy Carlos Ruver Beck[3], David Driemeier[2], Christianne G. Salbego[1].

[1]Programa de Pós-Graduação em Ciências Biológicas-Bioquímica, Instituto de Ciências Básicas da Saúde, Universidade Federal do Rio Grande do Sul, Porto Alegre, RS, Brasil.

[2]Departamento de Patologia Veterinária, Universidade Federal do Rio Grande do Sul, Porto Alegre, RS, Brasil.

[3]Programa de Pós-Graduação em Ciências Farmacêuticas, Faculdade de Farmácia, Universidade Federal do Rio Grande do Sul, Porto Alegre, RS, Brasil.

[4]Departamento de Fisiologia, Universidade Federal do Rio Grande do Sul, Porto Alegre, RS, Brasil

Corresponding author:
Mariana Maier Gaelzer
Departamento de Bioquímica, Instituto de Ciências Básicas da Saúde, UFRGS
Rua Ramiro Barcelos, 2600 – anexo, CEP 90035-003, Porto Alegre, RS, Brasil
Telephone: +55 (51) 3308.5547
Fax: +55 (51) 3308.5535
E-mail: marianamaierg@gmail.com

Funding: Conselho Nacional de Desenvolvimento Científico e Tecnológico (CNPq); Coordenação de Aperfeiçoamento de Pessoal de Nível Superior (Capes); Fundação de Amparo à Pesquisa do Estado do Rio Grande do Sul (FAPERGS).

Abstract

Glioblastoma, a subtype of glioma (GB-grade IV), is a malignant Central Nervous System tumor. This neuropathology is associated with uncontrolled tumor proliferation and resistance to apoptosis. GB is often characterized by rapid growth and invasiveness into surrounding normal brain tissue. Doxazosin is clinically used for the treatment of hypertension and urinary retention, and has become a promising drug in glioblastoma treatment. In this study, we evaluated nanoencapsuled doxazosin's (DOX-NC) citotoxicity on *in vitro* and *in vivo* models and its neurotoxicity on organotipic hippocampal cultures and the drug's systemic toxicity. We previously described doxazosin's antitumoral effects on glioma cells and here we found DOX-NC caused apoptotic and necrotic cell death in concentrations 100x smaller than free doxazosin (DOX). Furthermore, DOX-NC and DOX decreased tumor area in a model of glioma implantation on rat brains. Previously we showed DOX has low *in vitro* neurotoxicity and in the present study we found this also occurred for DOX-NC. Both treatments showed no signs of systemic toxicity on rats. Therefore, doxazosin is more selective towards tumor cells *in vitro* and *in vivo.* Additionally, we found DOX-NC decreased CD133 protein levels *in vitro* and both DOX-NC and DOX decreased CD133 *in vivo*. We also demonstrate DOX-NC and DOX decreased pEGFR protein levels *in vitro* and pEGFR immunoreactivity in *vivo*. Both CD133 and EGFR are involved with glioma tumorigenesis, proliferation and therapy resistance. Nanotechnology applied to antitumoral therapy, especially in the case of CNS cancer can increase drug vetorization, evade mechanisms of resistence to drug uptake, and permeate the bood-brain barrier more easily than free drug. Those characteristics are important requirements for the development of novel therapeutic strategies against brain tumours. Therefore, our results confirm the potential of doxazosin as an attractive antiglioma agent.

Keywords: glioma; *in vivo*; C6; doxazosin; glioma implantation; nanocapsules

INTRODUCTION

Gliomas are the most common cancer of the Central Nervous System (CNS). They represent more than 30% of all primary tumors and 80% of malignant tumors of the CNS. Incidence of primary tumors of the CNS is estimated in 18,71 for 100,000 individuals per year [1].

Glioblastoma (GB) is a subtype of glioma, with characteristics of level IV gliomas, presenting high rate of mitosis, presence of vascular proliferation and elevated density of atypical cells [2]. GBs are characterized as invasive tumors with no clear margins, not being possible to perform complete surgical resection [3]. Recurrence occurs in 90% of patients with this tumor [4].

The ineffectiveness of drugs against GBs highlights the importance of appropriate rodent models in the study of new therapies for the treatment of these tumors. When implanted in Wistar rats, C6 glioma cells originate tumors with regions of focal invasion into brain tissue, similar to the infiltrating pattern found in GBs [5-6]. C6 glioma cells show several general histopathological and specific tumor markers similar with human GBs [6-7] and C6 tumors display areas of necrosis, nuclear polymorphism and high mitotic rates [6].

Due to the variety of molecular patterns and high recurrence rates of GBs, present therapeutic studies are focusing in vetorized therapy, which presents less adverse effects. Many of the drugs being used in antitumoral therapy are toxic to both tumoral and non-tumoral cells [8]. Pharmacodynamic issues as fast drug elimination and ample drug distribution require administration of elevated doses of the antitumoral drugs. This can lead to increase in toxicity, inappropiate dosage and decrease in treatment compliance. Moreover, ample drug distribution usually increase adverse effects [8].

Nanodrugs applied to antitumoral therapy, especially in the case of CNS cancer, increases drug vetorization to the tumor site [9]. Nanocapsules permeate the blood-brain barrier more easily than the free drug. This technology applied to pharmacology is able to increase drug efficiency and efficacy.

The α1-adrenoceptor antagonist doxazosin is the most frequently prescribed drug, being approved by the FDA (Food and Drugs Administration) for benign prostatic hyperplasia (BPH) and elevated blood pressure [10]. We previously showed doxazosin’s antitumoral effects on glioma cells [11]. Other studies have shown the drug’s antitumoral potential on urothelial cancer [12], pituitary adenoma [13] and breast cancer [14]. Sakamoto et al. [15] suggested early administration of doxazosin may prevent clinical prostate tumor formation and suppress metastasis of human prostate cancer.

Here we evaluated nanoencapsulated and free doxazosin’s citotoxicity *in vitro* and on an *in vivo* model of glioma implantation. We analyzed nanoencapsulated doxazosin’s neuro- and sytemic toxicity on organotypic hippocampal cultures and histopathologic exam *in vivo*, respectively. Moreover, we evaluated protein levels of PARP on organotypic cultures, and CD133 and EGFR *in vivo* and *in vitro*, after treatments with the drug.

MATERIALS AND METHODS

Cell culture

C6 rat glioma cell line was obtained from American Type Culture Collection (Rockville, Mariland, Md., USA). C6 cells were grown and maintained in Dulbecco's Modified Eagle's Medium (DMEM, Gibco-Invitrogen, Grand Island, NY, USA) supplemented with 5% (v/v) FBS (Gibco-Invitrogen, Grand Island, NY, USA), and containing 2.5 mg/mL of Fungizone® and 100 U/L of gentamicine (Shering do Brasil, São Paulo, SP, Brazil). Cells were kept at 37ºC, in an atmosphere of 5% CO_2.

Ethics statement

All animal procedures were approved by the local animal ethics comission (Comissão de Ética no uso de Animais/Universidade Federal do Rio Grande do Sul – CEUA/UFRGS, under project number 26122) and follows national animal rights regulations (Law 11.794/2008), the National Institute of Health Guide for the Care and Use of Laboratory Animals (NIH publication No. 80-23, revised 1996) and Directive 2010/63/EU. We further attest all efforts were made to minimize the number of animals used and their suffering.

Organotypic hippocampal slice culture

Organotypic hippocampal slice cultures were prepared according to the method of Stoppini [17] with modifications [18] and as described previously [11]. Briefly, Wistar rats (6-8 days-old) were decapitated, their hippocampi were removed and cut as 400 µm thick slices in ice-cold Hank's balanced salt solution (HBSS), pH 7.2. Slices were placed on Millicell culture membranes and the inserts were transferred to a six-well culture plate. Each well contained 1mL of tissue culture medium consisting of Minimum Essential Media (MEM) with 25% of HBSS and 25% of horse serum supplemented with 36 mM glucose, 25 mM HEPES, 4 mM $NaHCO_3$, 1% Fungizone and 0,1 mg/mL gentamicine, pH 7,3. The cultures were kept in an incubator 37°C and 5% of CO_2 for 14 days.

Cultures treatment

Doxazosin-loaded nanocapsules (DOX-NC) were prepared as previously described [19]. Nanocapsules without drug (unloaded nanocapsules – NC) were also prepared using the same method. Nanocapsule suspensions were kept at room temperature and protected from light until use. Cells and organotypic hippocampal cultures were treated with DOX-NC with concentrations ranging from 0,05 µM to 0,18 µM for 48h. This values were previously tested in a concentration curve.

Fluorescence Microscopy

To identify cellular death, Annexin-V fluorescein isothiocyanate (FITC)/propidium iodide (PI) double stain kit was used (Invitrogen, Grand Island, NY, USA). For organotypic cultures, 2 µL of Annexin-V FITC and 1 µL of PI were added to 6 well plates containing 2 mL per well, and incubated for 15 min in the dark at 37°C. Annexin-V FITC and PI fluorescence were analyzed in an inverted microscope (Nikon Eclipse TE300). Images were captured using a digital camera connected to the microscope and analyzed using MacBiophotonics ImageJ software.

Flow Cytometry

Cell death was analyzed by flow cytometry. For C6, both floating and trypsinized adherent cells were collected. Organotypic hippocampal slices were dissociated as previously described [11]. Annexin-V FITC/propidium iodide (PI) double stain kit was used, following the manufacturer's instructions (Invitrogen, Grand Island, NY, USA). Samples were incubated in binding buffer containing Annexin-V FITC and PI for 15 min in the dark at room temperature.

For cleaved PARP, CD133 and pEGFR immunoquantification, cells were fixed with phosphate-buffered saline (PBS) and 4%paraformaldehyde for 20 min, then were permeabilized with PBS and 0.01% Triton X-100 and incubated with the primary antibodies anti-cleaved PARP (1:50; Cell Signaling Technology™), anti-CD133 (1:50; Cell SignalingTechnology™) and anti-pEGFR (1:50; Cell Signaling Technology™) for 30 min. The secondary antibody, Alexa Fluor 488 anti-mouse or Alexa Fluor 555 anti-mouse (1:100; Gibco-Invitrogen), was added, and aftera 60 min incubation, cells were analyzed by a flow cytometer.

Data acquisition was done by flow cytometry using a FACS Calibur cytometry system and Cell Quest software (BD Bioscience, Mountain View, CA, USA). Data obtained was analyzed with FCS Express 4 Software (De Novo Software, Los Angeles, CA, USA).

Glioma implantation

Glioma implantation was performed as previously described [16]. Briefly, C6 rat glioma cells at around 80% confluency were trypsinized, washed once in DMEM/5% FBS, pelleted and ressuspended in the same medium. A total of one million cells in a volume of 3 µL were injected at a depth of 0.6 mm in the right striata (coordinates with regard to bregma: 0.5 mm posterior and 3.0 mm lateral) of anesthesized male Wistar rats (9 weeks-old, 250-270 g). After 20 days, rats were weighted, followed by decapitation. Blood was collected for hematocrit and plasma proteins analysis in a certified animal laboratory (Bluts, Porto Alegre, RS, Brazil). The entire brain and organs were removed and weighted. After, organs were fixed with 10% formaldehyde for pathological analysis.

Animal treatment

After 10 days of glioma implantation, animals were randomly separated in the following groups: non-treated (tumor); treatment with 20% ethanol in 0,9% NaCl solution (vehicle); treatment with 25 mg/Kg doxazosin in solution (DOX); treatment with unloaded nanocapsules (NC); treatment with 2.5 mg/Kg doxazosin nanoencapsulated (DOX-NC). The sham group was submitted to stereotaxic surgery, but the animals did not receive C6 cells injection. Animals were treated by oral gavage during 10 days, once a day.

Pathological analysis

Hematoxylin and eosin (H&E) sections (3 µm thick, paraffin embedded) from at least three animals of each experimental group were analyzed by the Veterinary Pathology Department of Universidade Federal do Rio Grande do Sul. The veterinary pathologists also examined other organs of the treated animals, such as lungs, spleen, liver, kidneys, intestine, stomach and heart. For tumor area determination, images were captured by a CCD camera attached to a Nikon Eclipse E600 microscope. Images of the tumors at 40x magnification were used to determine tumor area with Image J software.

Imunohistochemical staining

Paraffin embedded, 3-µm formalin fixed tissue sections were mounted on microscope slides. Tissue sections were heated at 60°C for 40 min, dewaxed in xylene and rehydrated with alcohol-destilled water baths. Sections were washed twice with 1%

Triton X-100 in phosphate buffered saline (PBS), followed by incubation in blocking solution containing 5% Fetal Calf Serum (FCS) in PBS for 2h at room temperature. Incubation with the following antibodies was performed overnight at 4°C in a humid chamber: anti-CD133 (1:50; Cell Signaling) or anti-phospho-EGFR (1:50; Cell Signaling). Following this, sections were washed twice with PBS and incubated with secondary antibody Alexa Fluor 594 (Invitrogen) for 2h at room temperature. Slides were then washed with PBS, stained with Hoechst 33342 and mounted with mineral oil. Slides were maintained at 4°C in the dark until microscopic analysis. Images were captured using a Nikon Eclipse E600 Fluorescence Microscope and were analyzed with Image J software.

Statistical analysis

Data are expressed as means±SEM. All results are representative of at least 4 independent experiments or from at least 10 animals per group. Analysis of variance (ANOVA) was applied to the means to determine statistical differences between experimental groups. Post hoc comparisons were performed by Tukey test. Differences between mean values were considered significant when $p<0.05$.

RESULTS

Evaluation of nanoencapsulated doxazosin toxicity on organotypic hippocampal culture

In organotypic culture (Fig. 1), nanoencapsuled doxazosin caused necrosis in a small percentage of cells at 0,18 µM. Cell death was more pronounced at CA1 region, as demonstrated by photomicrographs with Annexin V and PI staining (Fig. 1b).

Furthermore, cleaved PARP levels of organotypic hippocampal cultures remained unaltered after DOX-NC treatment (Fig. 2).

Nanoencapsuled doxazosin is 100 times more potent than free drug

Previously we have shown doxazosin induces apoptosis in C6 cells at 180 µM [11]. Here, cells were treated with a concentration curve of DOX-NC for 48 (Fig. 3). DOX-NC induced necrosis on C6 cells at 0.05, 0.15 and 0.18 µM and late apoptosis at 0.05-0.15 µM.

Next we compared the effects of DOX-NC treatment and the free drug (DOX) on CD133 and pEGFR protein levels (Fig. 4). DOX-NC decreased CD133 at 0.15 and 0.18 µM (Fig. 4a), while DOX treatment did not alter CD133 protein levels (Fig. 4b). In addition, DOX-NC decreased pEGFR levels at all concentrations tested (Fig. 4c), while DOX decreased EGFR phosphorylation at 50, 100 and 180µM (unpublished data).

Nanoencapsuled doxazosin showed no systemic toxicity

Cytopathological reports of major drug absorption, biotransformation and excretion organs showed both DOX and DOX-NC did not cause systemic toxicity (Figs. 5 and 6). In small intestine, the tumor group showed increase in organ percentage of body weight, while both DOX-NC and DOX treatments returned this measure to the sham group levels (Fig. 5). In the liver, DOX, NC and DOX-NC decreased percentage of body weight (Fig. 5), as compared with the sham group, although no alteration on liver histology was detected (Fig. 6). In addition, hematocrit and plasma protein levels remained unaltered with the tumor implantation and treatments (Fig. 5).

Nanoencapsulated and free doxazosin decrease tumor area on a glioma implantation model

Glioma implantation resulted in tumor formation with intense tumor cell proliferation from the corpus callosum to striatum, arranged in a solid form, nonencapsulated and infiltrating the adjacent neuropil (Figs. 7b and 8). Tumor cells were elongated to oval-shaped, with eosinophilic cytoplasm. Nuclei are oval, with granular chromatin and inconspicuous nucleoli. There is moderate anisocytosis and anisokaryosis and a mean of three atypical mitose figures per higher magnification field (400x). In addition, there is marked inflammatory infiltration composed of macrophages and lymphocytes as well as formation of perivascular cuffs adjacent to the neoplasic lesion (Fig. 7b).

Treatment with DOX decreased the tumor area in about half (Fig. 7c). In the majority of animals treated with DOX-NC, tumoral cells were not detected, although there were signs of inflammatory infiltration. In the DOX-NC-treated animals that showed detectable tumors, tumor area decreased to approximately 80% when compared with untreated animals (Fig. 7c).

Evaluation of *in vivo* CD133 and pEGFr levels

Both treatments decreased the number of CD133-positive cells in the tumor tissue (Fig. 9a). With DOX treatment, some CD133-positive cells with high immunoreactivity were detected, while with DOX-NC CD133-immunoreactivity was faint. pEGFR-immunoreactivity decreased with both treatments, while the number of pEGFR-positive cells remained unaltered (Fig. 9b).

DISCUSSION

Gliomas are common central nervous system tumors, and glioblastoma (GB-grade IV), which is a subtype of glioma, has poor prognosis and is the most lethal of all brain tumors [20-21].

In vitro culture models allow the evaluation of cell signaling, biochemistry and molecular mechanisms, as well as study of new pharmacological targets and of the microenvironment with high reproductivity. The microenvironment formed favors signal integration that shape the phenotypic behavior of cells [22]. However, cultured cells do not represent all interactions between organs and systems, as occurs *in vivo*. The model of C6 glioma cells implantation on rat brains was proposed by Takano et al. [5] and is suited for investigation of tumor biology as well as studies on new therapeutic approaches for glioma treatment.

Our results demonstrate nanoencapsulated doxazosin (DOX-NC) caused cell death on C6 glioma cells at all concentrations tested (0.05-0.18 µM). We previously showed doxazosin (DOX) induced cell death on glioma cells at concentrations ranging from 50 to 180 µM [11]. In the present study, DOX-NC induced glioma cell death at concentrations 100 times smaller than the free drug.

DOX treatment decreased tumor area at about half, while DOX-NC caused approximately 80% of tumor regression. Furthermore, both treatments decreased tumor malignity, as observed by the decrease in angiogenesis and perivascular scuffs as well as mitotic figures.

One of the characteristics of solid tumors is high proliferativerate and the presence of neovascularizations. Tumor angiogenesis often results in defective tissue architecture [23]. In this context, nanodrugs have more accessibility to the tumor site than free drug. Heath and Davis [9] found the pores present in tumoral vasculature accumulate 10 to 100 times more nanodrugs than free drugs.

Current anticancer drugs have limitations by presenting cytotoxicity, low specificity and prolonged use may be lethal to healthy cells [24]. Glioblastoma is a radio- and chemio-resistant cancer. This makes it necessary to increase chemotherapy dosage or add more drugs for treatment, which increases toxicity on non-tumour cells [24].

Additionaly, Béduneau et al. found [25] nanoparticles enter cells via endocytosis. Therefore, nanodrugs can evade mechanisms of resistance to drug uptake as glicoprotein P and other protein pumps.

Here we found DOX-NC has low toxicity on organotypic hippocampal cultures and both DOX-NC and DOX showed no systemic cytotoxicity on rats. We previously showed DOX was also more selective towards tumor cells [11], demonstrating the drug shows certain specificity to cancer cells. This selectivity could be due to doxazosin's acting on signaling pathways that are altered in tumor cells but not in non-tumoral cells. However, at this time it is not clear why this drug specificity occurs. Nevertheless, it is a positive characteristic of doxazosin because the drug could be targeting infiltrative tumor cells separated from the tumor bulk.

In addition, we found DOX-NC did not induced poly(ADP-ribose) polymerase (PARP) cleavage on organotypic cultures. PARP is a nuclear protein involved with DNA repair and is one of the earliest proteins targeted for cleavage during apoptosis [26]. Studies have demonstrated in various cell death models that PARP cleavage of the 89-kDa signature fragment implies activation of caspase 3-like activity [27-28]. PARP cleavage is a very sensitive assay of apoptosis, detecting cell death very early in different models and it detects apoptosis even in minor populations of cells [26, 29].

GBs are characterized by their infiltrating nature, high proliferation rate and resistance to chemotherapy and radiation [2]. This cancer results from accumulation of genetic and epigenetic alterations that drive the transformation of normal cells to malignant cells [29-30]. Therefore, chemotherapeutic treatment of tumors in the CNS is associated with severe systemic side effects and affects patient's quality of life.

In gliomas, CD133 is used to enrich a highly tumorigenic cancer cells subpopulation [32]. In addtition, CD133-positive cells influence long-term tumor growth [33], and Zeppernick et al. [34] showed CD133 expression correlates with patient survival in gliomas. We found treatment with DOX-NC decreased CD133 protein levels on C6 cells. In agreement with those results, both treatments decreased CD133-positive cells in the tissue, with a more pronounced decrease in the DOX-NC group.

The epidermal growth factor receptor (EGFR) pathway is frequently upregulated in glioblastomas through gene amplification and by mutations that constitutively activates the receptor [35-36]. Preclinical and clinical studies suggest EGFR signaling plays an important role in radiation resistance [37-39] in human gliomas and Chakravarti [40] demonstrated expression of EGFR increases tumor cell malignancy, decreasing patient survival. Furthermore, EGFR and its ligands are associated with molecular abnormalities that affect signal transduction, transcription factors, apoptosis, angiogenesis and the extracellular matrix [41-42]. Under normal conditions, these factors conduct central nervous system growth and development and are expressed from embryogenesis, throughout brain development and adulthood. These factors are involved in the proliferation, migration, differentiation, and survival of all CNS cell types and their precursors [43].

Previously we showed doxazosin decreased activation of key kinases in the EGFR signaling pathway cascade [11]. Here we found EGFR phosphorylation decreased in C6 cells treated with both DOX-NC and DOX, and pEGFR-immunoreactivity was also decreased *in vivo* by the treatments. The EGFR-family of tyrosine-kinase receptors are being studied as a target for possible glioma therapeutic interventions [44]. Hui et al. [14] showed doxazosin inhibits EGFR signaling and induces breast cancer cell apoptosis. However, Petty et al. [45] found doxazosin induced EphA2 tyrosine kinase receptor internalization and decreased migration of prostate cancer, breast cancer and glioma cells. The authors also showed doxazosin reduced distal metastasis and prolonged survival in an *in vivo* model of prostate cancer.

The major therapeutic challenges of CNS tumors are accessibility to the brain through the blood-brain barrier (BBB) and, in the case of glioblastomas, the highly infiltrative nature of the disease. It is important for novel antitumoral agents to display tumor selectivity and low toxicity. Doxazosin is able to permeate the BBB [46], has long half-life [47] and we showed here and previously [11] the drug is selective to tumor cells. Since the drug is already used clinically and is FDA-approved as an antihypertensive, its pharmacology and safety profile are well-characterized in humans and its adverse-effects are mild and acceptable [48].

In this study we showed nanoencapsulated doxazosin induced glioma cell death and decreased CD133 and pEGFR protein levels *in vitro* and demonstrated DOX and DOX-NC decreased tumor area and malignancy *in vivo*, with DOX-NC being more potent than DOX in glioma regression. Nanoencapsulation of doxazosin allowed for decrease of drug concentrations of 100 times *in vitro* and 10 times *in vivo*, with the same or better results. Additionally, we found both free doxazosin and nanoencapsulated doxazosin are more selective towards tumor cells.

Application of polymeric nanoparticles for use as carriers for anticancer drugs enhance drug vetorization, efficient drug protection, cell internalization, as well as drug transport, release and retention at the tumor site [9].

Nanotechnology applied to pharmacology can enhance antitumoral drug efficiency and efficacy. Those characteristics are important requirements for the development of novel therapeutic strategies against gliomas.

REFERENCES

1. States, C.B.T.R.o.t.U., *CBTRUS statistical report: primary brain and central nervous system tumors diagnosed in the United States in 2004-2006.* Hinsdale, IL: Central Brain Tumor Registry of the United States, 2010.
2. Eckley, M. and K.A. Wargo, *A review of glioblastoma multiforme.* US Pharm, 2010. **35**(5): p. 3-10.
3. Jackson, R.J., et al., *Limitations of stereotactic biopsy in the initial management of gliomas.* Neuro-oncology, 2001. **3**(3): p. 193-200.
4. Roy, S., et al., *Recurrent glioblastoma: where we stand.* South Asian journal of cancer, 2015. **4**(4): p. 163.
5. Takano, T., et al., *Glutamate release promotes growth of malignant gliomas.* Nature medicine, 2001. **7**(9): p. 1010-1015.
6. Jacobs, V.L., et al., *Current review of in vivo GB rodent models: emphasis on the CNS-1 tumour model.* ASN neuro, 2011. **3**(3): p. AN20110014.
7. Zhou, X., et al., *Detection of cancer stem cells from the C6 glioma cell line.* Journal of International Medical Research, 2009. **37**(2): p. 503-510.
8. Plotkin, S.R. and P.Y. Wen, *Neurologic complications of cancer therapy.* Neurologic clinics, 2003. **21**(1): p. 279-318.
9. Heath, J.R. and M.E. Davis, *Nanotechnology and cancer.* Annu. Rev. Med., 2008. **59**: p. 251-265.

10. Antonello, A., et al., *Design, synthesis, and biological evaluation of prazosin-related derivatives as multipotent compounds.* Journal of medicinal chemistry, 2005. **48**(1): p. 28-31.

11. Gaelzer, M.M., et al., *Phosphatidylinositol 3-Kinase/AKT pathway inhibition by doxazosin promotes glioblastoma cells death, upregulation of p53 and triggers low neurotoxicity.* PloS one, 2016. **11**(4): p. e0154612.

12. SIDDIQUI, E.J., et al., *Growth inhibitory effect of doxazosin on prostate and bladder cancer cells. Is the serotonin receptor pathway involved?* Anticancer research, 2005. **25**(6B): p. 4281-4286.

13. Fernando, M.A. and A.P. Heaney, *α1-Adrenergic receptor antagonists: novel therapy for pituitary adenomas.* Molecular Endocrinology, 2005. **19**(12): p. 3085-3096.

14. Hui, H., M.A. Fernando, and A.P. Heaney, *The α 1-adrenergic receptor antagonist doxazosin inhibits EGFR and NF-κB signalling to induce breast cancer cell apoptosis.* European Journal of Cancer, 2008. **44**(1): p. 160-166.

15. Sakamoto, S. and N. Kyprianou, *Targeting anoikis resistance in prostate cancer metastasis.* Molecular aspects of medicine, 2010. **31**(2): p. 205-214.

16. Bernardi, A., et al., Indomethacin-loaded nanocapsules treatment reduces in vivo glioblastoma growth in a rat glioma model. Cancer Lett, 2009. **281**(1): p. 53-63.

17. Stoppini, L., P.-A. Buchs, and D. Muller, *A simple method for organotypic cultures of nervous tissue.* Journal of neuroscience methods, 1991. **37**(2): p. 173-182.

18. Horn, A.P., et al., *Cellular death in hippocampus in response to PI3K pathway inhibition and oxygen and glucose deprivation.* Neurochemical research, 2005. **30**(3): p. 355-361.

19. Saldanha Krai, J., *Development and Validation of a Simple LC-UV Method to Assay Doxazosin in Polymeric Nanocapsules and Tablets.* Current Pharmaceutical Analysis. **12**.

20. Oike, T., et al., *Radiotherapy plus concomitant adjuvant temozolomide for glioblastoma: Japanese mono-institutional results.* PloS one, 2013. **8**(11): p. e78943.

21. Sengupta, S., et al., *Impact of temozolomide on immune response during malignant glioma chemotherapy.* Clinical and Developmental Immunology, 2012. **2012**.

22. Freshney, R.I., *Animal cell culture: a practical approach*. Vol. 8. 1986: IRL press Oxford:.

23. Persano, L., et al., *Glioblastoma cancer stem cells: role of the microenvironment and therapeutic targeting.* Biochemical pharmacology, 2013. **85**(5): p. 612-622.

24. Lee, E.Q., D. Schiff, and P.Y. Wen, *Neurologic complications of cancer therapy*. 2011: Demos Medical Publishing.

25. Béduneau, A., P. Saulnier, and J.-P. Benoit, *Active targeting of brain tumors using nanocarriers.* Biomaterials, 2007. **28**(33): p. 4947-4967.

26. Duriez, P. and G.M. Shah, *Cleavage of poly (ADP-ribose) polymerase: a sensitive parameter to study cell death.* Biochemistry and Cell Biology, 1997. **75**(4): p. 337-349.

27. Kaufmann, S.H., *Proteolytic cleavage during chemotherapy-induced apoptosis.* Molecular medicine today, 1996. **2**(7): p. 298-303.

28. Shah, G.M., S.H. Kaufmann, and G.G. Poirier, *Detection of poly (ADP-ribose) polymerase and its apoptosis-specific fragment by a nonisotopic activity–Western blot technique.* Analytical biochemistry, 1995. **232**(2): p. 251-254.

29. Patel, T., G.J. Gores, and S.H. Kaufmann, *The role of proteases during apoptosis.* The FASEB Journal, 1996. **10**(5): p. 587-597.

30. Huse, J.T., E. Holland, and L.M. DeAngelis, *Glioblastoma: molecular analysis and clinical implications.* Annual review of medicine, 2013. **64**: p. 59-70.

31. Wirsching, H.-G. and M. Weller, *The Role of Molecular Diagnostics in the Management of Patients with Gliomas.* Current treatment options in oncology, 2016. **17**(10): p. 51.

32. Singh, S.K., et al., *Identification of a cancer stem cell in human brain tumors.* Cancer research, 2003. **63**(18): p. 5821-5828.

33. Vescovi, A.L., R. Galli, and B.A. Reynolds, *Brain tumour stem cells.* Nature Reviews Cancer, 2006. **6**(6): p. 425-436.

34. Zeppernick, F., et al., *Stem cell marker CD133 affects clinical outcome in glioma patients.* Clinical Cancer Research, 2008. **14**(1): p. 123-129.

35. Wong, A.J., et al., *Increased expression of the epidermal growth factor receptor gene in malignant gliomas is invariably associated with gene amplification.* Proceedings of the National Academy of Sciences, 1987. **84**(19): p. 6899-6903.

36. Wong, A.J., et al., *Structural alterations of the epidermal growth factor receptor gene in human gliomas.* Proceedings of the National Academy of Sciences, 1992. **89**(7): p. 2965-2969.

37. Chakravarti, A., et al., *The epidermal growth factor receptor pathway mediates resistance to sequential administration of radiation and chemotherapy in primary human glioblastoma cells in a RAS-dependent manner.* Cancer research, 2002. **62**(15): p. 4307-4315.

38. Lammering, G., et al., *Epidermal growth factor receptor as a genetic therapy target for carcinoma cell radiosensitization.* Journal of the National Cancer Institute, 2001. **93**(12): p. 921-929.

39. O'Rourke, D.M., et al., *Conversion of a radioresistant phenotype to a more sensitive one by disabling erbB receptor signaling in human cancer cells.* Proceedings of the National Academy of Sciences, 1998. **95**(18): p. 10842-10847.

40. Chakravarti, A., et al., *Prognostic and pathologic significance of quantitative protein expression profiling in human gliomas.* Clinical Cancer Research, 2001. **7**(8): p. 2387-2395.

41. Feldkamp, M.M., et al., *Expression of activated epidermal growth factor receptors, Ras-guanosine triphosphate, and mitogen-activated protein kinase in human glioblastoma multiforme specimens.* Neurosurgery, 1999. **45**(6): p. 1442.

42. Ding, H., et al., *Astrocyte-specific expression of activated p21-ras results in malignant astrocytoma formation in a transgenic mouse model of human gliomas.* Cancer research, 2001. **61**(9): p. 3826-3836.

43. Nicholas, M.K., et al., *Epidermal growth factor receptor–mediated signal transduction in the development and therapy of gliomas.* Clinical Cancer Research, 2006. **12**(24): p. 7261-7270.

44. Chakravarti, A., A. Dicker, and M. Mehta, *The contribution of epidermal growth factor receptor (EGFR) signaling pathway to radioresistance in human gliomas: a review of preclinical and correlative clinical data.* International Journal of Radiation Oncology* Biology* Physics, 2004. **58**(3): p. 927-931.

45. Petty, A., et al., *A small molecule agonist of EphA2 receptor tyrosine kinase inhibits tumor cell migration in vitro and prostate cancer metastasis in vivo.* PloS one, 2012. **7**(8): p. e42120.

46. Nikolic, K., et al., *Partial least square and hierarchical clustering in ADMET modeling: Prediction of blood–brain barrier permeation of α-adrenergic and imidazoline receptor ligands.* Journal of Pharmacy & Pharmaceutical Sciences, 2013. **16**(4): p. 622-647.

47. Kaye, B., et al., *The metabolism and kinetics of doxazosin in man, mouse, rat and dog.* British journal of clinical pharmacology, 1986. **21**(S1): p. 19S-25S.

48. Lepor, H., *Alpha blockers for the treatment of benign prostatic hyperplasia.* Reviews in urology, 2007. **9**(4): p. 181.

FIGURE LEGENDS

Figure 1. Analysis of cell death in organotypic hippocampal cultures after nanoencapsulated doxazosin treatment for 48h. **(a)** Dot plot and graph of cultures stained with Annexin V and Propidium Iodide. **(b)** Photomicrographs of organotypic hippocampal slice cultures stained with Annexin V and Propidium Iodide after treatment with nanoencapsulated doxazosin. Magification: 40X. **(c)** Schematic representation of a hippocampal slice. Data are represented as means ± SEM (n = 6). **p<0.01 vs control.

Figure 2. Histogram and graph of cleaved PARP protein levels of organotypic hippocampal cultures after treatment with nanoencapsulated doxazosin. Data are

represented as means ± SEM (*n* = 6). **DOX-NC:** nanoencapsulated doxazosin; **NC:** unloaded nanocapsule.

Figure 3. Analysis of cell death on C6 cells after nanoencapsulated doxazosin treatment for 48h. Dot plot and graph of cells stained with Annexin V and Propidium Iodide. Data are represented as means ± SEM (*n* = 4). *$p<0.05$, **$p<0.01$, ***$p<0.001$ vs. control. **DOX-NC:** nanoencapsulated doxazosin; **NC:** unloaded nanocapsule.

Figure 4. CD133 and pEGFR protein levels on C6 cells after treatment with nanoencapsulated and free doxazosin for 48h. Histogram and graph of CD133 levels after treatment with **(a)** nanoencapsulated and **(b)** free drug. **(c)** Histogram and graph of pEGFR levels after treatment with nanoencapsulated doxazosin. Data are represented as means ± SEM (*n* = 4). *$p<0.05$, **$p<0.01$, ***$p<0.001$ vs. control.**DOX-NC:** nanoencapsulated doxazosin; **NC:** unloaded nanocapsule. **DOX:** free doxazosin.

Figure 5. **(a)** Systemic toxicity analysis of nanoencapsulated and free doxazosin on Wistar rats. Graphs show the percentage of body weight of each organ analyzed and photographs demonstrate the result of the necropsies from each organ. **(b)** Graphs of hematocrit and plasma protein levels of animals exposed to treatment. Data are represented as means ± SEM (*n* = 10). *$p<0.05$, **$p<0.01$ vs. control.**S**: sham; **T**: tumor; **V**: vehicle; **DOX:** free doxazosin. **DOX-NC:** nanoencapsulated doxazosin; **NC:** unloaded nanocapsule.

Figure 6. Histopathological analysis (HE staining) of rat organs after tumor implantation and/or nanoencapsulated and free doxazosin treatment (n = 10). **DOX:** free

doxazosin. **DOX-NC:** nanoencapsulated doxazosin; **NC:** unloaded nanocapsule. Magnification: 200X.

Figure 7. Effect of nanoencapsulated and free doxazosin on tumor regression and morphology on an *in vivo* model of C6 glioma cells implantation. **(a)** Graph of percentage of body weight of the brain. **(b)** Photographs demonstrate the result of the brain necropsies. **(c)** Histopathological analysis (HE staining) of rat brains from experimental animals showing tumor location and morphology. **(d)** Graph of tumor area quantification. Data are represented as means ± SEM ($n = 10$). $^{***}p<0.001$ vs. control.**S**: sham; **T**: tumor group; **V**: vehicle; **DOX:** free doxazosin. **DOX-NC:** nanoencapsulated doxazosin; **NC:** unloaded nanocapsule; **t**: indicates tumor location. Magification: 2.5X, 40X and 200X.

Figure 8. Histopathological analysis (HE staining) of rat brains from experimental animals showing tumor tissue morphology after tumor implantation and/or nanoencapsulated and free doxazosin treatment. **V:** indicates neovascularization; **dashed lines** separate tumor tissue from healthy tissue; **arrows** indicate mitotic figures. Magification: 200X and 400X.

Figure 9. Immunofluorescence of CD133 and pEGFR of rat brains after tumor implantation and/or nanoencapsulated and free doxazosin treatment (n = 4). **DOX:** free doxazosin. **DOX-NC:** nanoencapsulated doxazosin.

Figure 10. Schematic representation of free (DOX) or nanoencapsulated (DOX-NC) doxazosin effects on *in vitro* and *in vivo* glioma/non-tumoral models. On organotypic

hippocampal cultures, DOX-NC showed low neurotoxicity, while on C6 glioma cells it induced necrotic and apoptotic death with decrease in pEGFR and CD133 levels. On an *in vivo* model of glioma implantation, both DOX and DOX-NC showed no apparent toxicity and decreased tumor area, mitotic figures, vascularization and CD133 levels. Moreover, DOX-NC decreased pEGFR immunoreactivity *in vivo*.

Figure 1

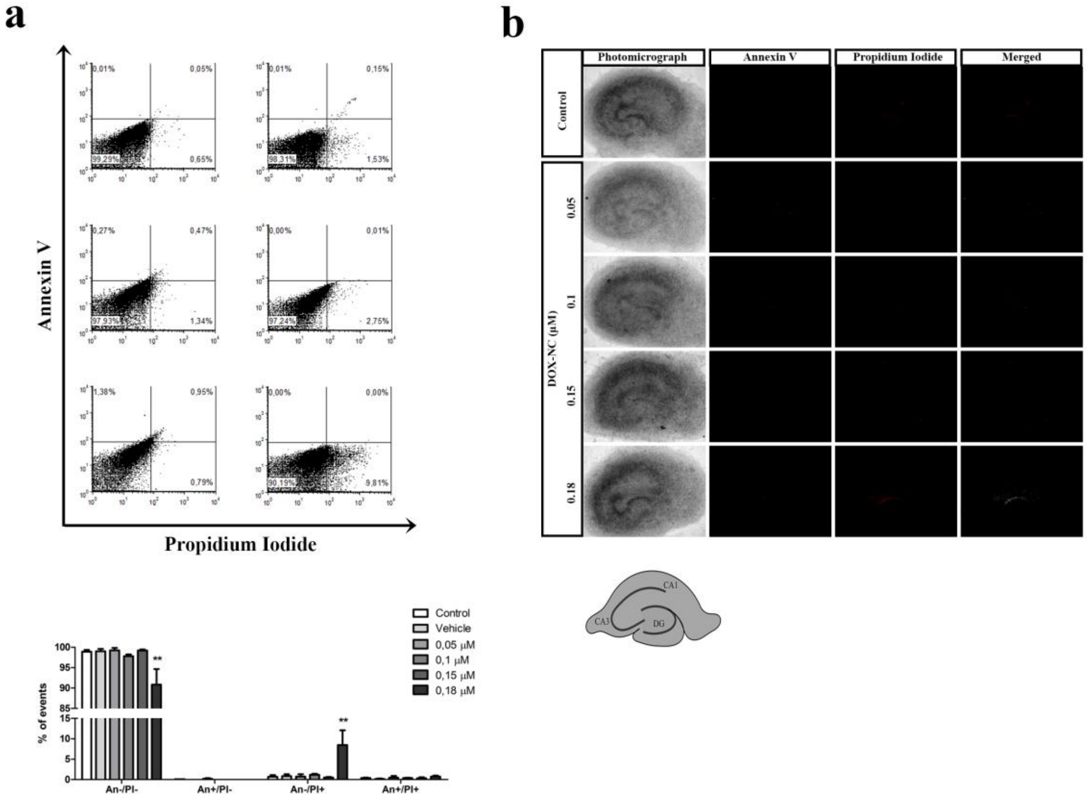

a
Annexin V
Propidium Iodide
0,01%
0,05%
99,29%
0,65%
0,01%
0,15%
98,31%
1,53%
0,27%
0,47%
97,93%
1,34%
0,00%
0,01%
97,24%
2,75%
1,38%
0,95%
0,79%
0,00%
0,00%
90,19%
9,81%
Control
Vehicle
0,05 μM
0,1 μM
0,15 μM
0,18 μM
% of events
**
An-/PI-
An+/PI-
An-/PI+
An+/PI+
b
Photomicrograph
Annexin V
Propidium Iodide
Merged
Control
DOX-NC (μM)
0,05
0.1
0.15
0.18
CA1
CA3
DG

Figure 2

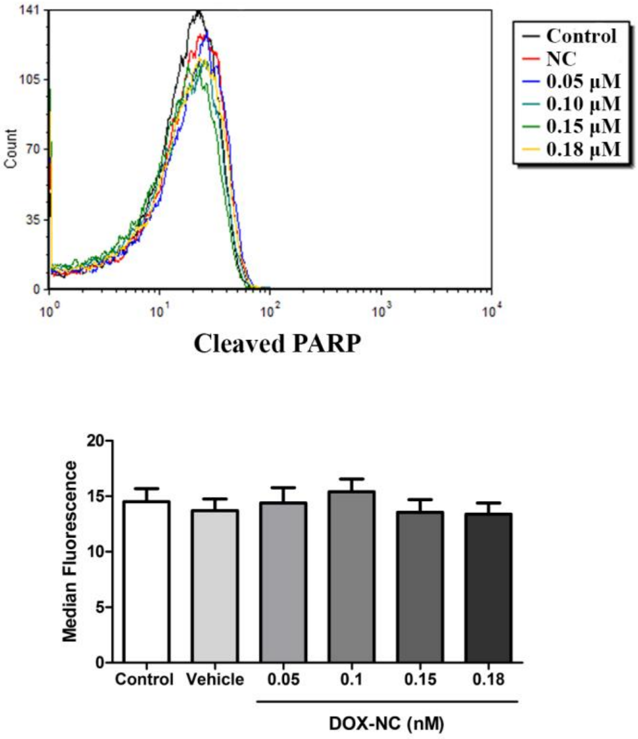
141
105
70
35
0
Count
10^0
10^1
10^2
10^3
10^4
Cleaved PARP
Control
NC
0.05 µM
0.10 µM
0.15 µM
0.18 µM
20
15
10
5
0
Median Fluorescence
Control
Vehicle
0.05
0.1
0.15
0.18
DOX-NC (nM)

Figure 3

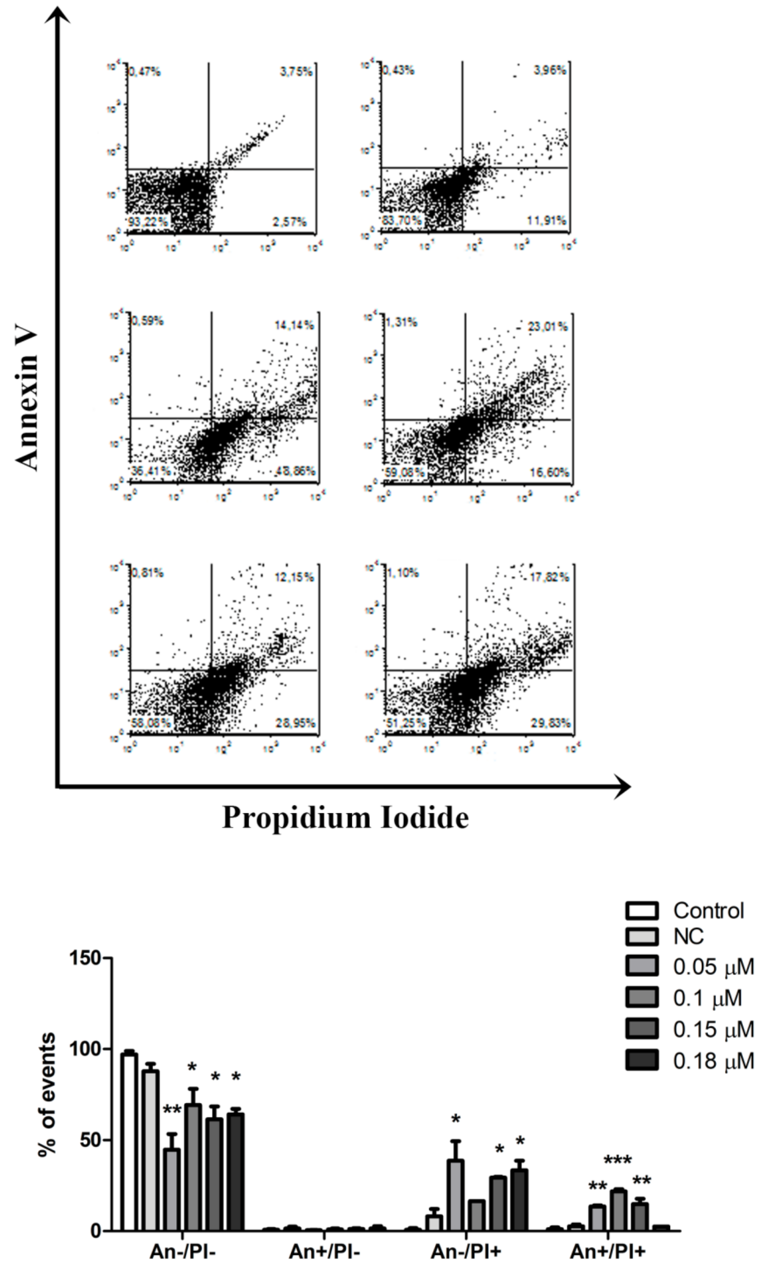
Annexin V
Propidium Iodide
0,47%
3,75%
93,22%
2,57%
0,43%
3,96%
83,70%
11,91%
0,59%
14,14%
36,41%
48,86%
1,31%
23,01%
59,08%
16,60%
0,81%
12,15%
58,08%
28,95%
1,10%
17,82%
51,25%
29,83%
10^0
10^1
10^2
10^3
10^4
% of events
150
100
50
0
An-/PI-
An+/PI-
An-/PI+
An+/PI+
*
**
***
Control
NC
0.05 μM
0.1 μM
0.15 μM
0.18 μM

Figure 4

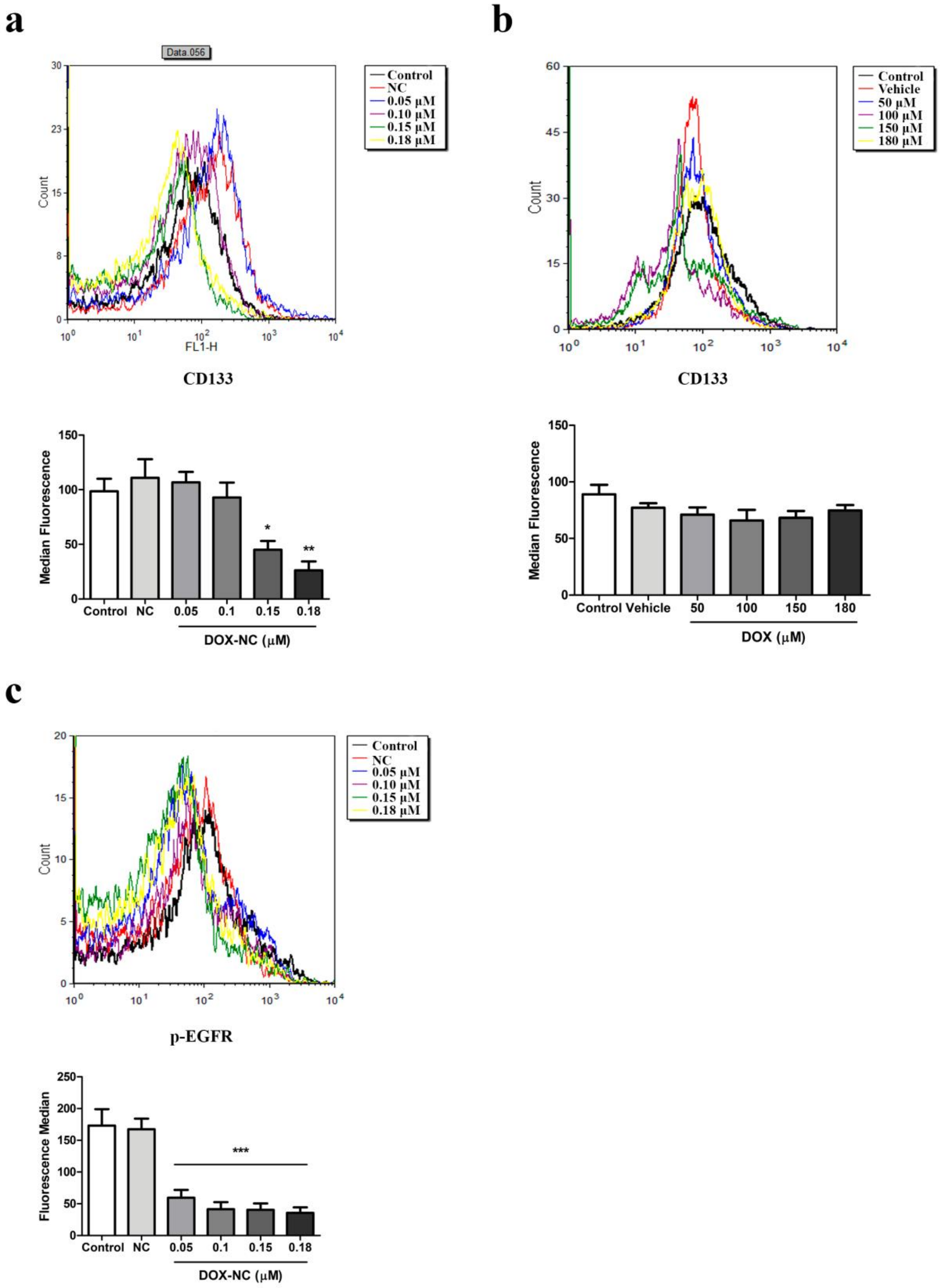
a
Data.056
Control
NC
0.05 μM
0.10 μM
0.15 μM
0.18 μM
Count
FL1-H
CD133
Median Fluorescence
Control
NC
0.05
0.1
0.15
0.18
DOX-NC (μM)
*
**
b
Control
Vehicle
50 μM
100 μM
150 μM
180 μM
Count
CD133
Median Fluorescence
Control
Vehicle
50
100
150
180
DOX (μM)
c
Control
NC
0.05 μM
0.10 μM
0.15 μM
0.18 μM
Count
p-EGFR
Fluorescence Median
Control
NC
0.05
0.1
0.15
0.18
DOX-NC (μM)
***

Figure 5

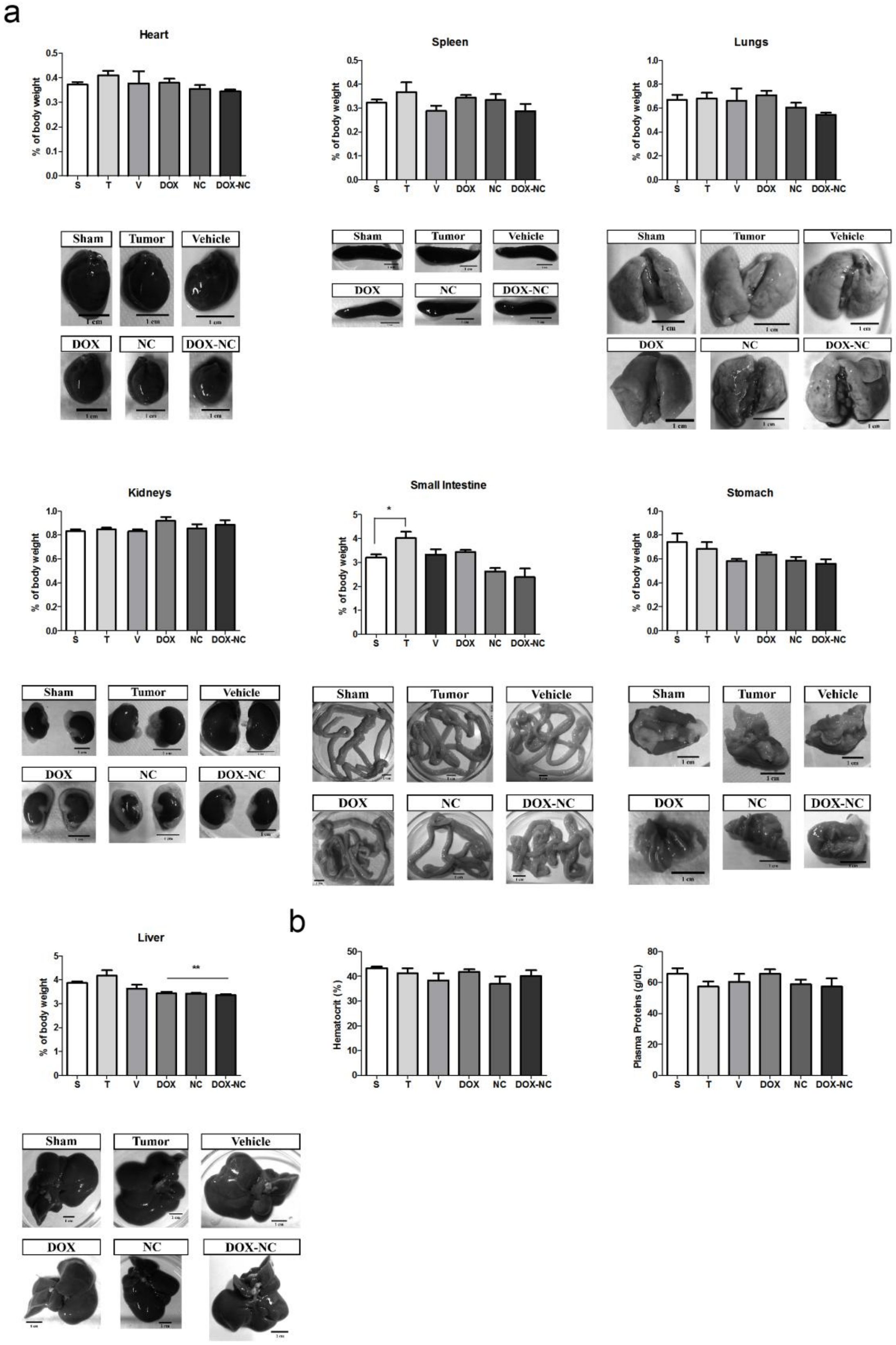
a
Heart
Spleen
Lungs
% of body weight
S
T
V
DOX
NC
DOX-NC
Sham
Tumor
Vehicle
1 cm
Kidneys
Small Intestine
Stomach
*
Liver
**
b
Hematocrit (%)
Plasma Proteins (g/dL)

Figure 6

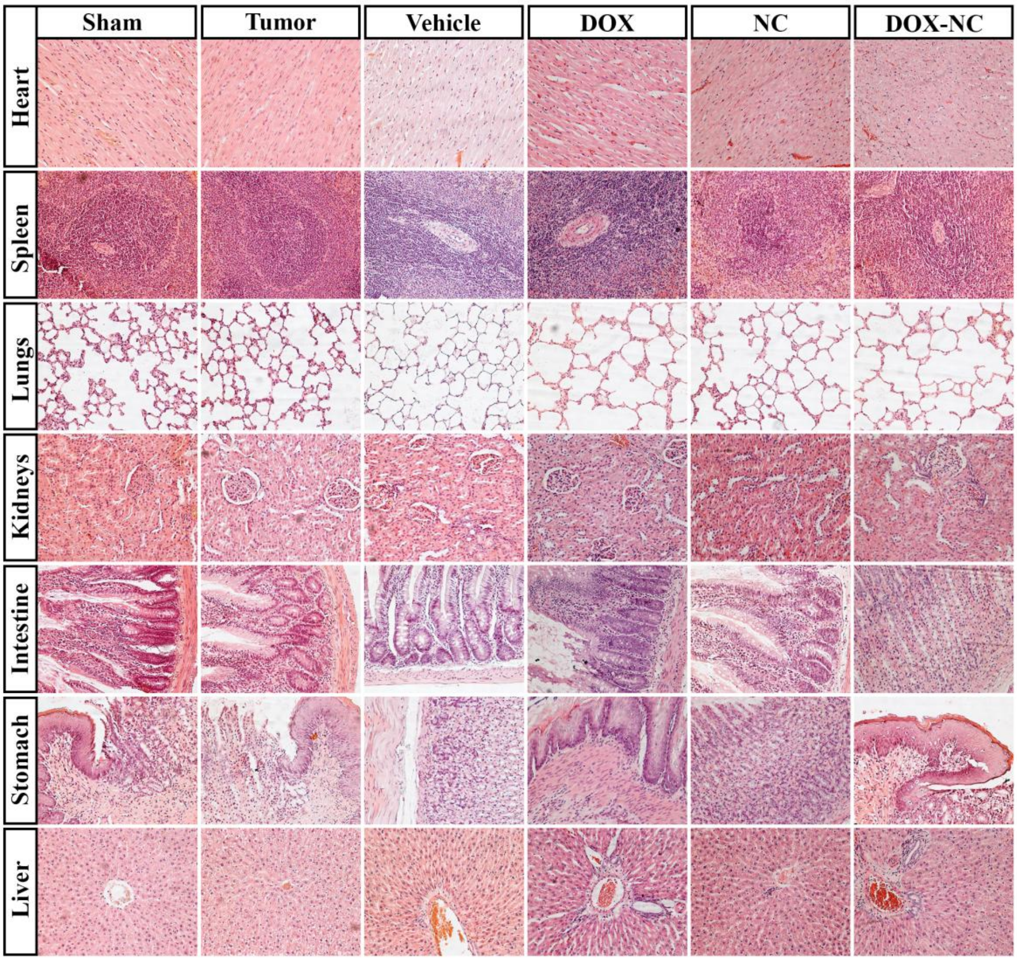
Sham
Tumor
Vehicle
DOX
NC
DOX-NC
Heart
Spleen
Lungs
Kidneys
Intestine
Stomach
Liver

Figure 7

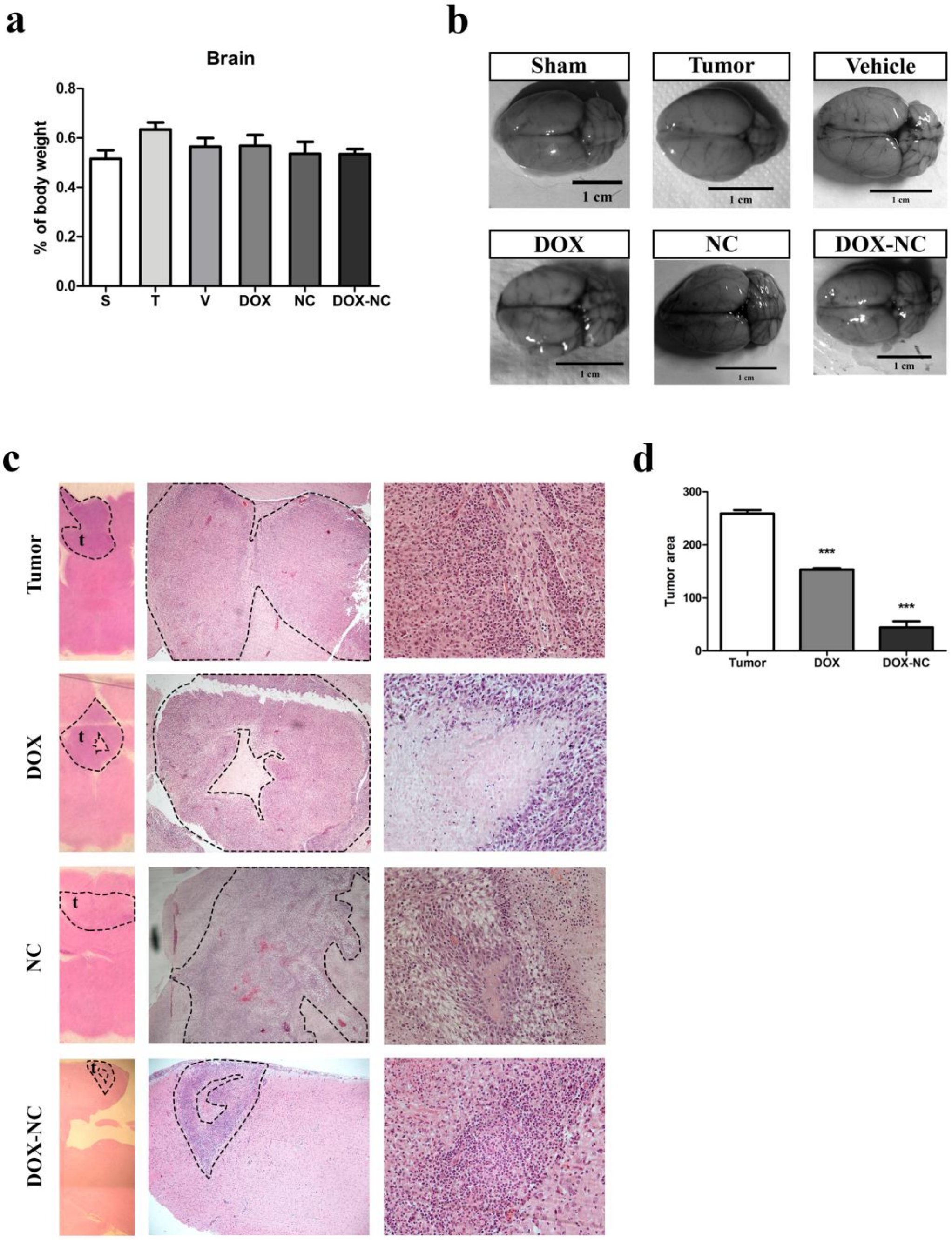
a
Brain
% of body weight
0.0
0.2
0.4
0.6
0.8
S
T
V
DOX
NC
DOX-NC
b
Sham
Tumor
Vehicle
DOX
NC
DOX-NC
1 cm
c
Tumor
DOX
NC
DOX-NC
t
d
Tumor area
0
100
200
300
***
***
Tumor
DOX
DOX-NC

Figure 8

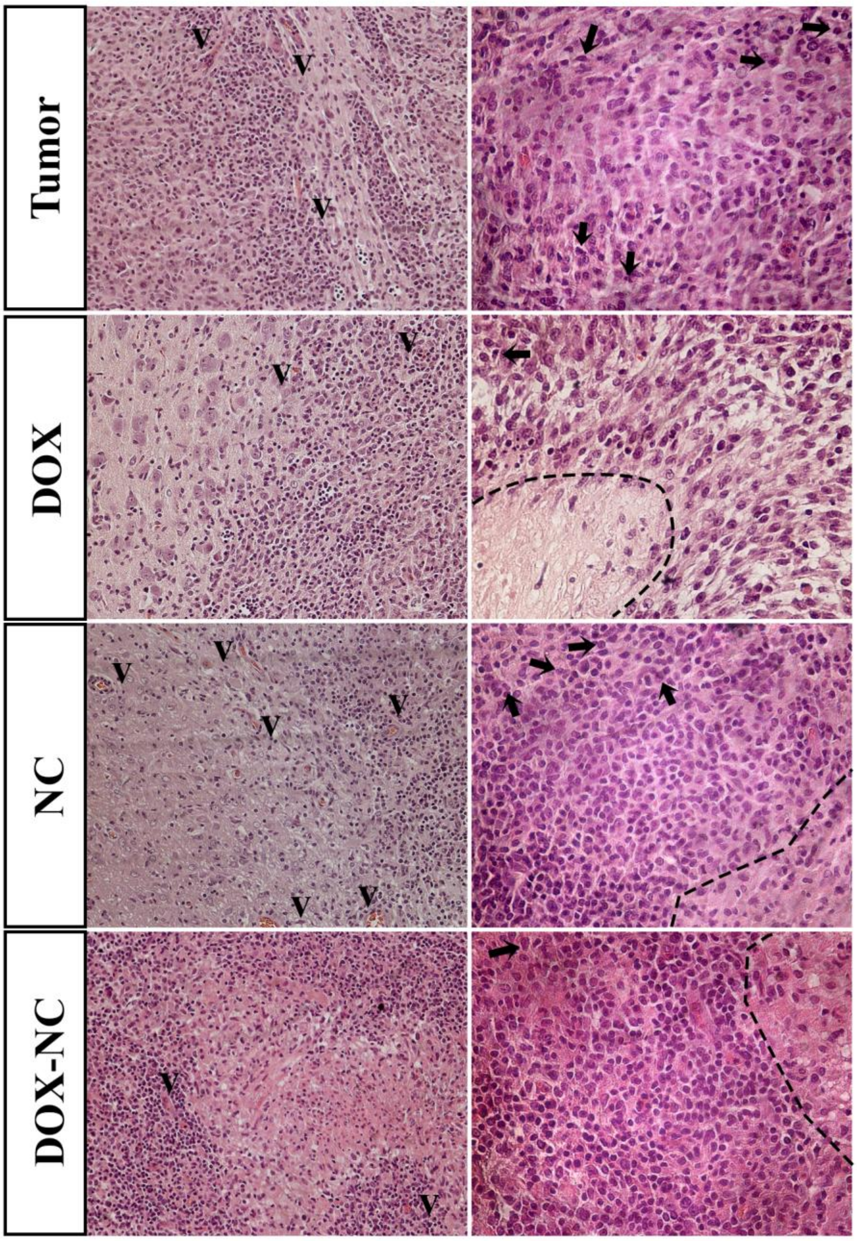
Tumor
DOX
NC
DOX-NC
V

Figure 9

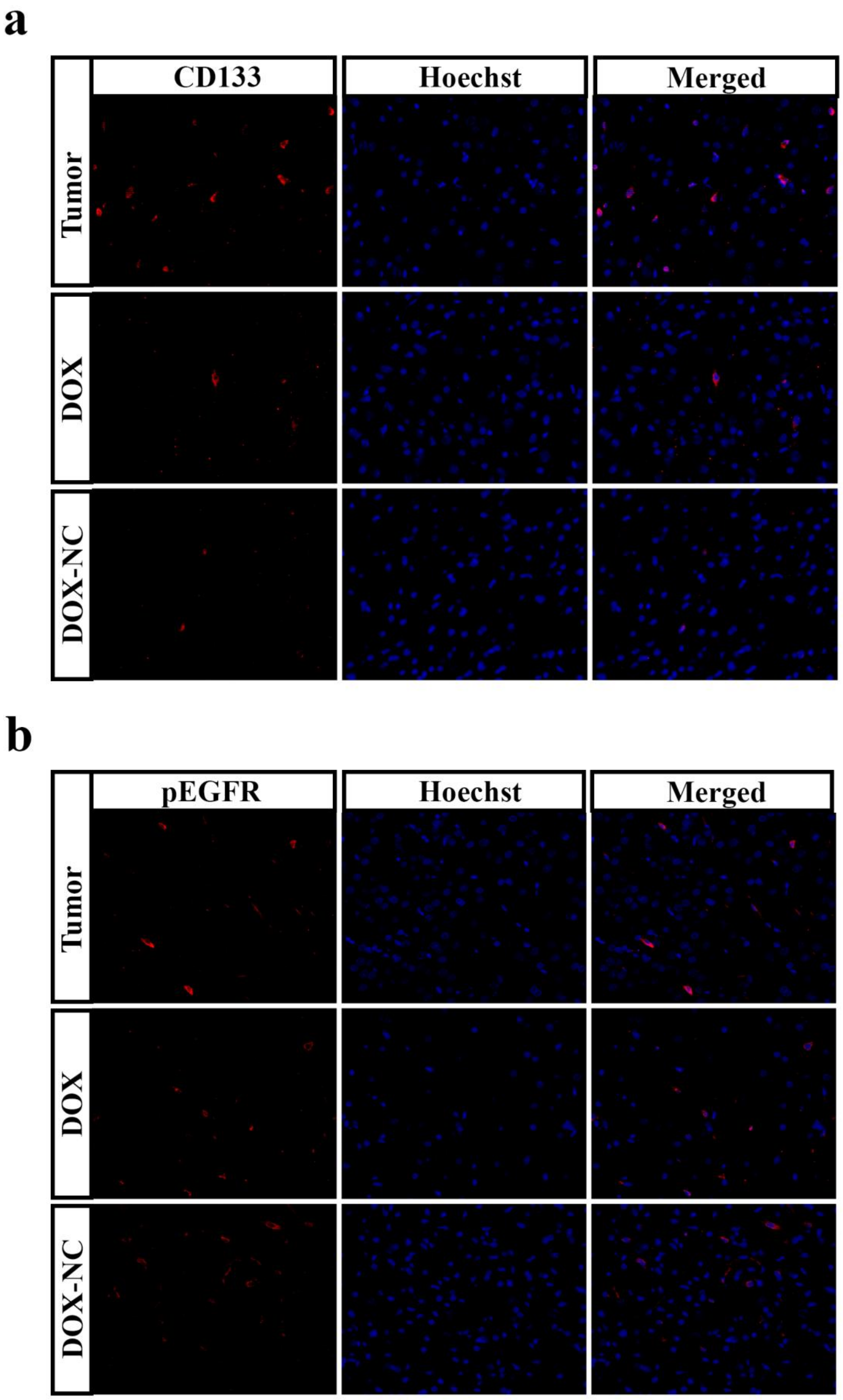
a
CD133
Hoechst
Merged
Tumor
DOX
DOX-NC
b
pEGFR
Hoechst
Merged
Tumor
DOX
DOX-NC

Figure 10

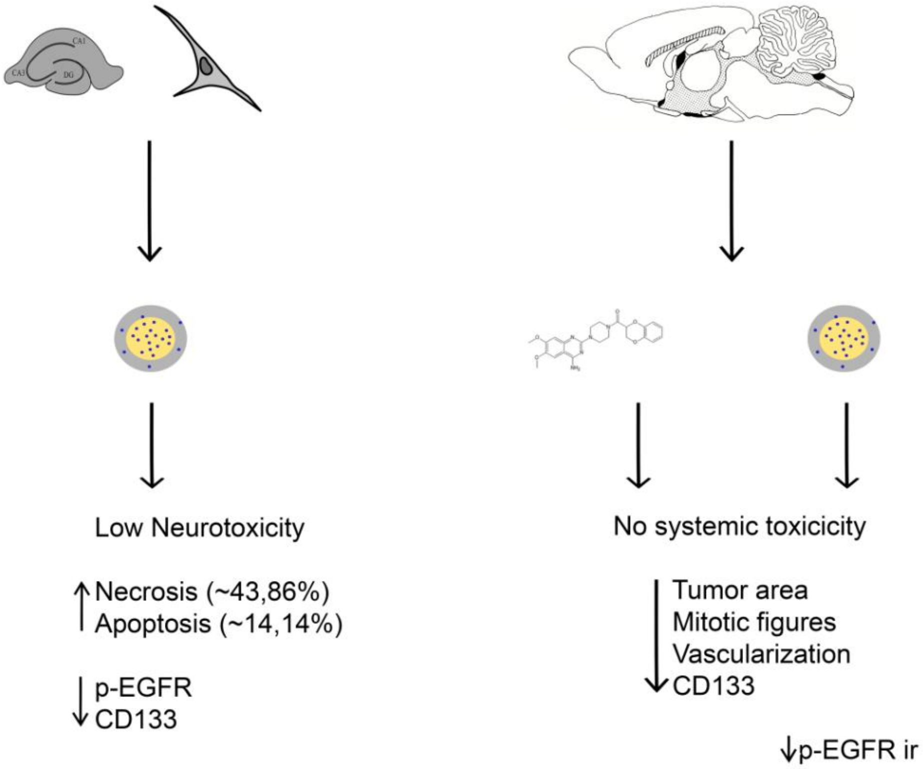
CA1
CA3
DG
Low Neurotoxicity
↑ Necrosis (~43,86%)
Apoptosis (~14,14%)
↓ p-EGFR
CD133
No systemic toxicicity
↓ Tumor area
Mitotic figures
Vascularization
CD133
↓p-EGFR ir

9. DISCUSSÃO

O glioblastoma representa o mais comum e maligno tumor primário cerebral. Possui alta taxa proliferativa e é muito invasivo, sendo resistente aos tratamentos utilizados na clínica (Dolecek *et al.*, 2012; Huse *et al.*, 2013). Pacientes com esse tipo de câncer apresentam taxas elevadas de recidiva. Os fármacos utilizados para essa malignidade ainda se mostram ineficazes, além de apresentarem muitos efeitos adversos (Plotkin e Wen, 2003). Há ainda a dificuldade de ultrapassar a barreira hemato encefálica (BHE) e os baixos tempos de meia-vida desses fármacos resultam no uso de altas doses terapêuticas, contribuindo para a toxicidade.

Glioblastomas são tumores que possuem áreas hipóxicas (Persano *et al.*, 2011; Hardee e Zagzag, 2012). Microambientes hipóxicos contribuem para a progressão do câncer, promovem a sobrevivência celular, motilidade e angiogênese (Keith e Simon, 2007).

Além disso, evidências sugerem que a hipóxia induz a desdiferenciação de células tumorais maduras para células-tronco tumorais (CTT), responsáveis pelo crescimento tumoral, pela resistência a radio e quimioterapia e pela alta taxa de recidiva nesses tipos de câncer (Soeda *et al.*, 2009; Persano *et al.*, 2013).

Visto que a hipóxia contribui para a malignidade tumoral e resistência aos tratamentos e que estudos com linhagens celulares geralmente não abordam esse aspecto de tumores sólidos, um de nossos objetivos foi o desenvolvimento de um modelo *in vitro* de ambiente hipóxico que se aproximasse da realidade *in vivo*, para avaliarmos possíveis adaptações desenvolvidas pelas células de glioma de rato C6. Os resultados descritos no Capítulo I mostram que a hipóxia aumentou os níveis proteicos de nestina e CD133, e a presença desses marcadores, conforme já descrito na literatura, ocorre no núcleo de tumores sólidos. Observamos também alterações morfológicas nas células que se assemelham às características de CTT.

Além disso, analisamos o período de reoxigenação. Durante esse processo observamos aumento dos níveis protéicos de GFAP, o que se assemelha com a periferia de tumores *in vivo* (Persano *et al.*, 2011).

Estudos demonstram que o núcleo tumoral hipóxico de glioblastomas *in vivo* apresenta resistência à temozolomida, que é o principal fármaco utilizado no tratamento dessa malignidade (Stupp *et al.*, 2005). Dessa forma, recriar o microambiente hipóxico *in vitro*, tentando aproximar algumas características presentes nos tumores sólidos, poderá contribuir para estudos futuros de novos fármacos. Neste trabalho, modificamos as condições no ambiente tumoral e analisamos qual seriam as respostas desse tumor heterogêneo frente a essas modificações.

A seguir avaliamos o potencial terapêutico e a citotoxicidade da DOX *in vitro,* os resultados são apresentados no Capítulo II. A DOX, apesar de ser um anti-hipertensivo utilizado na clínica, possui características na sua estrutura química que a torna uma molécula semelhante a vários fármacos antitumorais já em uso, bem como a outros que ainda estão em desenvolvimento.

A DOX apresentou baixa toxicidade em culturas primárias de astrócitos e culturas organotípicas de hipocampo, modelos de célula e tecido não tumoral, respectivamente. O fármaco induziu morte celular apoptótica e necrótica em células de glioma de rato C6 nas concentrações de 150 e 180 µM e morte celular apoptótica nas concentrações de 50 e 75 µM em células de glioma humano (U138-MG). Essas diferenças de concentrações podem ser explicadas pelas diferentes espécies bem como pelas diferenças nas mutações que cada linhagem possui (Vogelbaum *et al.*, 1999).

Alterações gênicas são frequentes nos glioblastomas e resultam em desregulação de vias de sinalização intracelulares levando à resistência a morte celular e aumento de proliferação (Rasheed *et al.*, 1999; Maher *et al.*, 2001; Wechsler-Reya e Scott, 2001; Ghosh *et al.*, 2005). O mecanismo de ação dadoxazosina *in vitro* pode estar associado a via da PI3K/Akt. A via da Ras/PI3k/Akt encontra-se mutada em 88% dos GB. A sobrevida média de pacientes com GB que tem ativa a via da PI3K (n = 42/56) e Akt (37/56) é de 11 meses em comparação com pacientes com níveis mais baixos de ativação de PI3K e Akt (40 meses). A DOX foi capaz de induzir a diminuição da fosforilação da $\text{Akt}_{\text{Ser473}}$ e diminuição da fosforilação da GSK-$3\beta_{\text{Ser-9}}$. Quando tratamos as células com o LY294002 (inibidor de PI3K), ocorre um efeito similar ao causado por doxazosina em relação à diminuição na fosforilação da GSK-$3\beta_{\text{Ser-9}}$.

A proteína supressora tumoral p53 apresenta-se mutada em 87% dos glioblastomas. Conforme demonstrado ainda no Capítulo II, o tratamento com DOX induziu aumento da fosforilação da proteína p53 e promoveu parada no ciclo celular em G0/G1 em ambas as linhagens. A DOX também promoveu a diminuição do índice mitótico e ativação de caspase-3 clivada.

Estes resultados sugerem que o mecanismo da ação da DOX possui certa especificidade ao tecido canceroso, viabilizando uma possível avaliação *in vivo* do fármaco. A toxicidade é um problema associado a vários fármacos, principalmente quimioterápicos (Plotkin e Wen, 2003). Além disso, o mecanismo de ação da DOX pode estar associado à inibição da via da PI3K/Akt.

As mitocôndrias são organelas que possuem papel fundamental na regulação de vários processos celulares. Muitos desses processos estão desregulados nos gliomas, dentre eles: a morte celular por apoptose (via intrínseca), a proliferação celular, o metabolismo energético e o equilíbrio de espécies reativas de oxigênio (Ordys *et al.*, 2010). A sinalização celular mitocôndria-núcleo muitas vezes encontra-se comprometida no câncer. No Capítulo III demonstramos que a DOX induziu aumento de PGC-1α e de TFAM, com consequente aumento na biogênese mitocontrial ao mesmo tempo em que foi capaz de promover a morte celular apoptótica. O PGC-1α pode estar relacionado com neuroproteção, já que no nosso estudo anterior a concentração que induziu morte nas células cancerosas não foi tóxica para as células sadias. Por outro lado, há estudos que citam a biogênse mitocondrial como sendo um mecanismo de resistência da célula cancerosa a exposição a fármacos e agentes tóxicos (Vellinga *et al.*, 2015).

O fator de necrose tumoral alfa (TNF-α), uma das citocinas quantificadas nesse estudo, está relacionada com vários eventos celulares como sobrevivência, diferenciação e morte (Christofides *et al.*, 2015). O TNF-α é um promotor endógeno tumoral pois estimula o crescimento, a proliferação, invasão, metástase e angiogênese. A maioria das células do câncer é resistente à citotoxicidade induzida pelo TNF-α o que resulta em promoção tumoral (Balkwill, 2002). A ação dessa citocina é dúbia, mas o balanço da sinalização do TNF-α em induzir sobrevivência e morte celular é determinante na resposta celular. Modular e estudar esse balanço pode ajudar no desenvolvimento de fármacos que são capazes de prevenir/tratar o câncer. Várias pesquisas têm demonstrado que a concentração de TNF-α no plasma aumenta em pacientes com diferentes tipos de câncer (Yoshida *et al.*, 2002; Pfitzenmaier *et al.*, 2003; Michalaki *et al.*, 2004). Alguns estudos mostram que o TNF-α é capaz de promover a tumorigênese e outros demonstram que ele possui efeitos antitumorais em alguns modelos experimentais (Balkwill, 2002).

Como observado em nosso estudo, houve diminuição na secreção de TNF-α após tratamento com doxazosina por 48 h. Como o TNF-α pode agir como antitumoral ou pró-tumoral e sua regulação ainda está em estudo, as diferentes respostas celulares podem ser atribuídas às diferenças entre os organismos, o meio no qual a células está e ainda, na exposição à carcinógenos. As citocinas (TNF-α, IL1-β, IL6) exercem um papel importante como reguladores negativos do PGC-1α. Portanto, o aumento dos níveis do PGC-1α pode estar associado à diminuição na secreção do TNF-α pelas células que receberam tratamento.

No Capítulo IV, caracterizamos a autofluorescência da doxazosina e a partir dessa característica da molécula nós conseguimos mapear a distribuição do fármaco nas células de glioma. O monitoramento do fármaco no ambiente celular pode auxiliar na descoberta do mecanismo de ação do mesmo e/ou de resistência celular. As diferenças de pH dos compartimentos celulares podem protonar e desprotonar a doxazosina e, de acordo com essa característica físico-química, influenciar na fluorescência da mesma (intensidade e mudança de cor) (Chung e Eaton, 2013). Da mesma forma, as diferentes polaridades dos constituintes celulares - tais como lipídeos, proteínas e a molécula do DNA - e a interação do fármaco com essas biomoléculas também podem influenciar na fluorescência (Chung e Eaton, 2013). O estudo mais aprofundado da fluorescência da molécula associado à caracterização fisico-química do ambiente tumoral pode auxiliar no desenvolvimento de novos agentes terapêuticos com marcação fluorescente específica (Garland *et al.*, 2016). Sabe-se, por exemplo, que as células tumorais criam um ambiente mais ácido ao seu redor do que as células não-tumorais (Sinha *et al.*, 2006). Então, sintetizar uma molécula ou partir de um protótipo que tenha sensibilidade a essas mudanças de pH e que induz morte celular em gliomas seria interessante de ser utilizado em estudos farmacológicos *in vivo* e *in vitro*.

Analisando os resultados obtidos de captação celular em 48 h, o aumento da concentração da doxazosina não aumenta proporcionalmente com o aumento da fluorescência, ou seja, ocorre uma saturação da fluorescência (citometria/verde), podendo ser esta devido a um mecanismo de interação com alguma proteína receptora. Como visto no Capítulo II, concentrações crescentes de doxazosina induzem aumento proporcional na morte de linhagens de glioma. No entanto, em relação à fluorescência, percebemos que o aumento da concentração do fármaco não leva a aumento proporcional de células fluorescentes. Dessa forma, as alterações na fluorescência intracelular podem estar relacionadas com as mudanças morfológicas ou com os mecanismos que levaram à morte celular.

Em 24 h podemos observar, também, a presença de vesículas. O fármaco parece estar vesiculado, visto que em 48 h de acordo com a ressonância magnética nuclear de hidrogênio (Capítulo IV, figura 5), não observamos o fármaco íntegro nem biotransformado no meio de cultivo. Em 48h, por outro lado, observamos morte celular por apoptose (cerca de 55% das células) e por necrose (15% das células) na concentração de 180 µM (Capítulo II, figura 3) e o fármaco não se encontra no meio extracelular (Capítulo IV, figura 5).

De acordo com os resultados obtidos no Capítulo I, mantivemos as condições ambientais, ou seja, as mesmas condições experimentais, sem mudanças drásticas de nutrientes, oxigênio, fatores de crescimento e percebemos que, mesmo assim, o tumor se comporta de maneira heterogênea. As células tumorais apresentaram diferenças na captação do fármaco, na resposta fisiológica - se está mais estática ou forma prolongamentos citoplasmáticos (blebs) - e no tempo em que essa resposta ocorre.

No Capítulo V, nós avaliamos se o efeito antiglioma da DOX está relacionado com o EGFR. Alterações gênicas em RTKs são comuns em glioblastomas (McLendon *et al.*, 2008). Uma das mutações mais comuns é a amplificação de EGFR. Além disso, estudos demonstram que o EGFR pode ser expresso em sua forma mutada em glioblastomas (EGFRvIII). Por esses motivos, o EGFR e sua forma mutada são potenciais alvos terapêuticos em glioblastomas (Hatanpaa *et al.*, 2010).

Nós tratamos as células C6 com EGF, o ligante endógeno do EGFR, com o intuito de aumentar a expressão de EGFR nas células. Hayat e colaboradores (2005) demonstraram que ligantes endógenos podem aumentar a expressão de seus receptores. No Capítulo V nós vimos que o tratamento das células C6 com EGF por 48 h aumentou a proliferação celular e a expressão do RNA mensageiro de EGFR. Corroborando nossos resultados, Lund-Johansen e colaboradores (1990) demonstraram que tratamento com EGF induz crescimento, migração e invasão de células de glioma. Além disso, Pedersen e colaboradores (1994) descobriram que a indução de proliferação em células de glioma ocorreu nas linhagens que apresentavam níveis elevados de expressão de EGFR, não em células com baixa expressão do receptor.

Por outro lado, Högnason e colaboradores (2001) descreveram que o tratmento com EGF induziu apoptose em células tumorais que expressam um mutante negativo dominante da Ras e superexpressam EGFR. No entanto, as células de glioma C6 apresentam aumento de expressão de Ras e de EGFR, o que pode explicar os efeitos de indução de proliferação do EGF nessa linhagem.

Em seguida, nós vimos que a DOX diminui a fosforilação de $EGFR_{Tyr1068}$ em células C6 e que o co-tratamento com AG1478 (inibidor de EGFR) potencializou este efeito, demonstrando que esses dois derivados quinazolidínicos podem estar agindo em sinergismo. Além disso, o pré-tratamento com EGF aumentou os níveis de p-EGFR e o tratamento com DOX reverteu essa fosforilação, mas apenas nas concentrações mais elevadas do fármaco.

O EGFRvIII é uma forma truncada do receptor de EGF que está presente em glioblastomas, a qual não possui o domínio extracelular e está constitutivamente ativa (Hataanpa *et al.*, 2010). A expressão aumentada de EGFR que observamos nesse estudo pode ser das duas formas do receptor, visto que os primers utilizados não diferem entre eles. Portanto, esse aumento de expressão pode ter ocorrido para ambos wtEGFR e EGFRvIII. Luwor e colaboradores (2004) demonstraram que o EGFRvIII pode formar heterodímeros com wtEGFR e ativar o receptor. Wiley e colaboradores (1988) descobriram que células que superexpressam EGFR aumentam a ativação do receptor independente de ligante. Nesse contexto, concentrações maiores de DOX foram necessárias para diminuir a fosforilação de EGFR após pré-tratamento com EGF.

Nós também avaliamos a indução de morte celular do co-tratamento da DOX com o AG1478 e do pré-tratamento de células C6 com EGF, seguido de tratamento com DOX ou AG1478. O inibidor de EGFR induziu morte celular por necrose. No Capítulo II nós vimos que a DOX induz principalmente morte celular por apoptose nas células C6 e isso ocorre nas concentrações de 100, 150 e 180 µM. Quando co-tratamos DOX e AG1478, houve morte celular por necrose nas concentrações de DOX de 150 e 180 µM, e apoptose em 180 µM. Esses resultados demonstram que as duas moléculas podem competir pelo mesmo sítio de ligação no EGFR e que foi necessário aumentar a concentração de DOX no co-tratamento para que o fármaco exercesse sua ação.

No Capítulo V nós também demonstramos que o pré-tratamento de células C6 com EGF sensibilizou as células resistentes à indução de morte celular pela DOX e o AG1478. Novamente, isso pode estar relacionado a um aumento da expressão de EGFRvIII pelo pré-tratamento com EGF, visto que o AG1478 tem maior especificidade pela forma mutada do receptor (Sibenaller *et al.*, 2005).

A diminuição da fosforilação de EGFR provocada pelo tratamento com a doxazosina e a inibição da via da PI3K/Akt pelo fármaco mostrado nesse estudo sugerem que o EGFR é um alvo da DOX em células de glioma. Corroborando nossos resultados, Liao e colaboradores (2011) demonstraram que a DOX inibe EGFR em células de câncer de mama.

No Capítulo VI, utilizamos o fármaco na sua forma nanoencapsulada. As vantagens das nanocápsulas são muitas, dentre elas a diminuição da dose, obter efeitos mais vetorizados ao órgão-alvo, bem como aumentar a eficácia do mesmo (Heath e Davis, 2008). Nesse estudo, demonstramos que a DOX nanoencapsulada (DOX-NC) induziu morte celular em linhagem de glioma de rato C6 em concentrações 100 vezes menores do que as que utilizamos para a doxazosina em solução (DOX) conforme descrito no Capítulo II. Nós também analisamos o efeito da DOX-NC em culturas organotípicas de hipocampo e, da mesma maneira que o observado com a DOX, a DOX-NC demonstrou baixa toxicidade, sendo seletiva para células tumorais.

O modelo de cultura celular *in vitro* permite avaliar mecanismos de sinalização celular, bioquímicos, moleculares, análise de alvos farmacológicos e características fisiopatológicas específicas, com alta reprodutibilidade. O microambiente formado permite a integração de sinais que modelam o comportamento fenotípico das células (Freshney, 1986). Porém as culturas não permitem a integração de todos os sinais entre os órgãos e sistemas como ocorre em modelos *in vivo*.

O modelo de implante de células C6 de glioma em cérebro de ratos foi proposto por Takano e colaboradores (Takano *et al.*, 2001) e é adequado para estudos que investigam a biologia do tumor, bem como para novas abordagens terapêuticas no tratamento dos gliomas. Nesse estudo, células C6 foram implantadas no estriado dos animais e, após 10 dias do implante do tumor, as nanocápsulas contendo DOX e na sua forma livre foram administradas por gavagem durante 10 dias consecutivos. Através de análise histopatológica foi possível observar significativa redução do volume tumoral. É importante ressaltar que as nanocápsulas de DOX, além de reduzir o volume tumoral, foram capazes de reduzir as características histopatológicas de malignidade dos tumores (figuras de mitose, neovascularização, hemorragia).

Gliomas apresentam alta taxa proliferativa e presença de neovascularizações, o que geralmente resulta em arquitetura tecidual defeituosa. Fármacos nanoencapsulados demonstram maior acessibilidade ao tecido tumoral do que o fármaco livre, pois os poros presentes na vasculatura tumoral acumulam 10 a 100 vezes mais nanofármaco do que o fármaco livre. Além disso, Béduneau e colaboradores (Béduneau *et al.*, 2007) demonstraram que nanopartículas são endocitadas pelas células, o que permite que elas evitem os mecanismos de resistência à captação de fármacos nos tumores.

A fim de confirmar o grau de malignidade das células remanescentes após os tratamentos, procedeu-se a análise das proteínas CD133 e pEGFR *in vitro* e *in vivo*. Em gliomas, CD133 é utilizado como marcador de células-tronco tumorais e para enriquecimento dessa subpopulação (Singh *et al.*, 2003). Células tumorais expressando CD133 influenciam o crescimento tumoral a longo prazo e o aumento da expressão desse antígeno está correlacionado com sobrevivência de pacientes com glioma (Zeppernick *et al.*, 2008). Nesse estudo, demonstramos que a DOX-NC diminuiu os níveis proteicos de CD133 em células C6 e ambos tratamentos (DOX-NC e DOX) diminuíram as células CD133-positivas *in vivo*.

A via de sinalização do EGFR está muito ativa em gliomas e estudos pré-clínicos e clínicos sugerem que essa via aumentada leva a resistência à radioterapia (Wong *et al.*, 1987; Wong *et al.*, 1992; Lammering *et al.*, 2001). Ainda, foi demonstrado que a expressão de EGFR aumenta malignidade tumoral e diminui a sobrevivência de pacientes (Chakravarti *et al.*, 2004). Além disso, a via do EGFR em tumores está associada alterações em fatores de transcrição, apoptose e angiogênese (Feldkamp *et al.*, 1999).

No Capítulo II, demonstramos que a DOX diminuiu a ativação de cinases presentes na cascata de sinalização de EGFR em células de glioma. Por outro lado, no Capítulo VI evidenciamos que o tratamento com DOX-NC e DOX diminuiu a fosforilação de EGFR e a imunorreatividade ao EGFR *in vitro* e *in vivo*, respectivamente. Hui e colaboradores (Hui *et al.*, 2008) comprovaram que a DOX inibe a sinalização de EGFR e induz apoptose em células de câncer de mama, o que está de acordo com nossos achados. Os resultados descritos no Capítulo VI demonstram que a DOX apresenta efeito antitumoral *in vivo* e que sua ação *in vitro* e *in vivo* foi potencializada pela nanoencapsulação do fármaco. Assim, confirmamos o potencial antitumoral da DOX e da nanotecnologia aplicada à farmacologia para o desenvolvimento de novas estratégias terapêuticas para o tratamento de gliomas.

Os nossos estudos estão baseados na fisiopatologia do tumor frente a mudanças de condições experimentais. Primeiramente, avaliamos o tumor em mudanças no ambiente (hipóxia, nutrientes e reoxigenação) mimetizando o ambiente hipóxico *in vitro* para que se aproximasse do ambiente *in vivo*. Estudamos a exposição do tumor a um agente químico, a DOX (Figura 8). Utilizamos diferentes modelos experimentais a fim de observar se os efeitos se confirmavam tano *in vitro* como *in vivo*. Observamos a captação do fármaco *in vitro*, a fim de utilizar a fluorescência intrínseca da DOX como aliada para observação da distribuição do fármaco nas células.

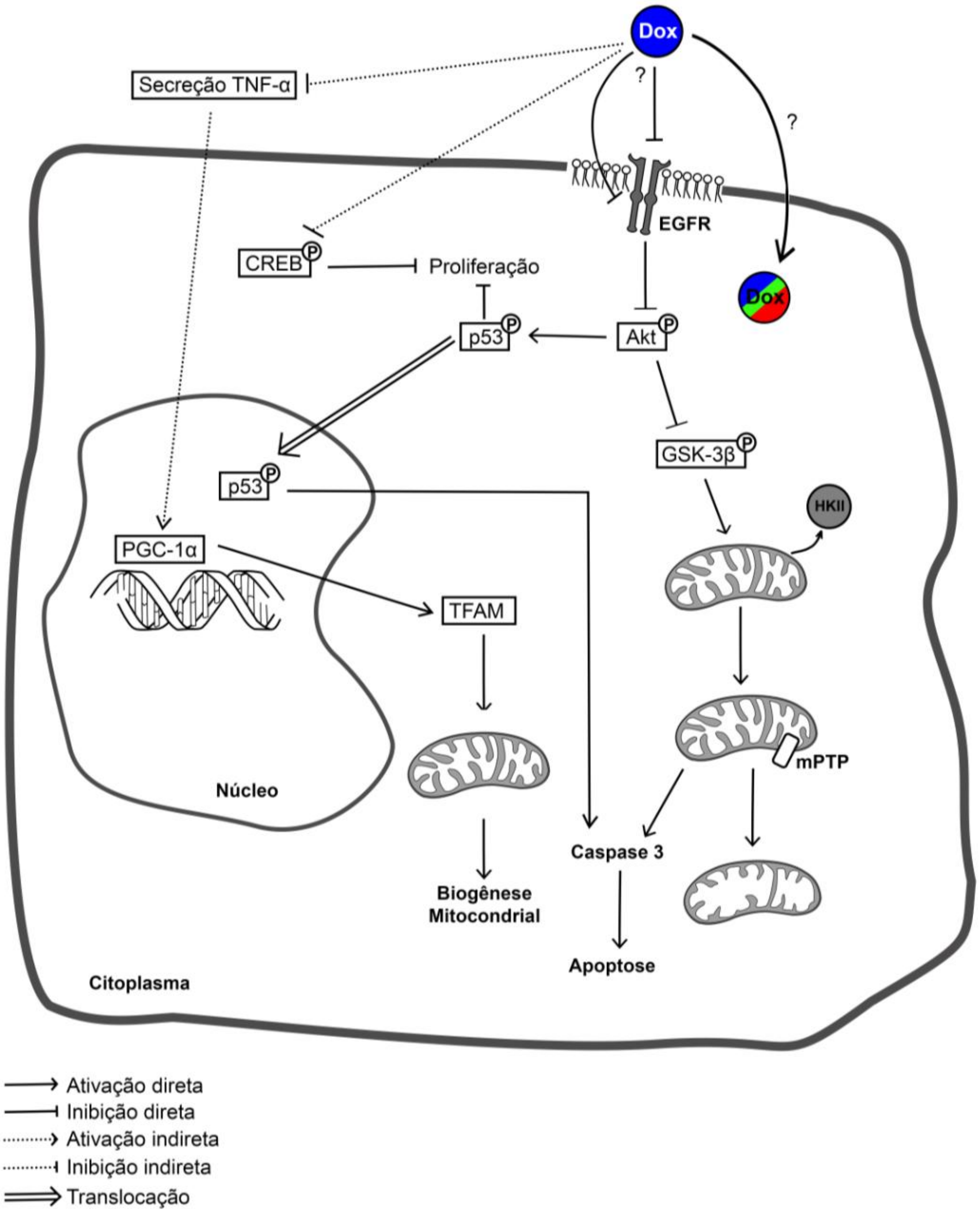
Dox
Secreção TNF-α
?
?
EGFR
CREB P
Proliferação
p53 P
Akt P
Dox
GSK-3β P
p53 P
HKII
PGC-1α
TFAM
mPTP
Núcleo
Caspase 3
Biogênese Mitocondrial
Apoptose
Citoplasma
Ativação direta
Inibição direta
Ativação indireta
Inibição indireta
Translocação

Figura 8: Representação esquemática dos efeitos da doxazosina em células de glioma. A doxazosina apresenta autofluorescência azul em solução hidroalcóolica e o fármaco é captado de forma heterogênea por células de glioma, apresentando fluorescência azul, verde e vermelho no meio intracelular. A doxazosina induz morte celular por apoptose e parada do ciclo celular via inibição da via do EGFR/PI3K/Akt e ativação de GSK-3β e p53. GSK-3β pode estar agindo na mitocôndria pela indução da abertura do poro de transição mitocondrial (mPTP), induzindo morte celular por apoptose. A doxazosina também diminui a fosforilação de CREB e a secreção de TNF-α, o que pode ter contribuído para a inibição da proliferação e aumento de PGC-1α, respectivamente. PGC-1α induziu a transcrição de TFAM, o qual induziu biogênese mitocondrial.

Também alteramos as propriedades físico-químicas da molécula, nanoencapsulando o fármaco. O objetivo das nanocápsulas é melhorar a distribuição e a biodisponibilidade do fármaco, para ter efeitos mais pronunciados, com relação à vetorização, diminuição da dose terapêutica e, consequentemente, da toxicidade, além de adequação da posologia, melhorando a qualidade de vida do paciente.

Enfim, conhecer como ocorrem os mecanismos de resistência aos fármacos, estudar as características da fisiopatologia da doença, investigar como as células se adaptam a determinados ambientes mudando o modelo de estudo, aproximar com mais veracidade da patologia, se certificar da neurototoxicidade, e, se for o caso, alterar as características físico-químicas do fármaco, tornam possível a investigação de novos agentes terapêuticos que se aproximam da realidade *in vivo*.

10. CONCLUSÕES

Esta tese apresentou os resultados obtidos no estudo dos efeitos da doxazosina em modelos *in vitro* e *in vivo* de glioma. Como importantes contribuições para o tema de pesquisa desenvolvido nesta tese destacam-se:

- O desenvolvimento de um modelo para mimetizar o microambiente hipóxico *in vitro* e o envolvimento da hipóxia e reoxigenação na desdiferenciação/diferenciação de células de glioma (Capítulo I);

- O efeito antitumoral da doxazosina em linhagens de glioma humano e de rato e a seletividade que o fármaco demonstrou pelas células tumorais, visto que causou baixa neurotoxicidade em cultura primária de astrócitos e em cultura organotípica de hipocampo (Capítulo II);

- A capacidade da doxazosina em reduzir a atividade da via da PI3K/Akt, os níveis de p-EGFR e p-CREB e de TNF-α secretados pelas células de glioma; assim como ativar as proteínas GSK-3β, p53, TFAM e PGC-1α e induzir biogênese mitocondrial e apoptose em linhagens de glioma (Capítulos II, III e V);

- A sensibilização das células de glioma ao tratamento com doxazosina por meio de pré-tratamento com EGF (Capítulo V);

- A caracterização da autofluorescência da doxazosina e a utilização dessa característica da molécula para analisar os padrões de captação e distribuição celular do fármaco em células de glioma (Capítulo IV), descrito por nós pela primeira vez;

- O efeito antitumoral da doxazosina nanoencapsulada e diminuição de CD133 e da fosforilação de EGFR em células de glioma; além de sua baixa neurotoxicidade em culturas organotípicas de hipocampo (Capítulo V);

- A regressão tumoral e diminuição dos marcadores de malignidade CD133 e pEGFR em modelo de implantação de glioma *in vivo* provocada pela doxazosina na sua forma livre e nanoencapsulada (Capítulo V).

A sequência de trabalhos apresentados nesta tese permitiu aprofundar o conhecimento sobre o potencial antitumoral da doxazosina e sua neurotoxicidade e toxicidade sistêmica, sobre a fisiopatologia de gliomas frente a alterações no microambiente tumoral, sobre características físico-químicas da doxazosina e o uso de propriedades da molécula para estudar os mecanismos de ação desse fármaco em gliomas.

11. PERSPECTIVAS

Como continuação desse trabalho, pretende-se seguir com os seguintes objetivos:

- Mimetizar o microambiente hipóxico e tratar as células com DOX;
- Analisar morte celular, a marcação com CD133, nestina e GFAP associadas com a captação do fármaco;
- Marcar vesículas e observar se elas se co-localizam com o fármaco (co-localização/confocal);
- Sintetizar derivados da DOX e testá-los em gliomas.

12. REFERÊNCIAS BIBLIOGRÁFICAS

AGARWALA, S. S. et al. Temozolomide for the treatment of brain metastases associated with metastatic melanoma: a phase II study. **Journal of Clinical Oncology,** v. 22, n. 11, p. 2101-2107, 2004. ISSN 0732-183X.

ALBERTS, B. et al. **Molecular Biology of the Cell**. 6th. Garland Science Taylor & Francis Group, 2014.

BACHELDER, R. E.; WENDT, M. A.; MERCURIO, A. M. Vascular endothelial growth factor promotes breast carcinoma invasion in an autocrine manner by regulating the chemokine receptor CXCR4. **Cancer research,** v. 62, n. 24, p. 7203-7206, 2002. ISSN 0008-5472.

BALKWILL, F. Tumor necrosis factor or tumor promoting factor? **Cytokine and Growth Factor Reviews,** v. 13, n. 2, p. 135-141, 2002. ISSN 1359-6101.

BAO, S. et al. Glioma stem cells promote radioresistance by preferential activation of the DNA damage response. N**ature,** v. 444, n. 7120, p. 756-760, 2006. ISSN 0028-0836.

BÉDUNEAU, A.; SAULNIER, P.; BENOIT, J.-P. Active targeting of brain tumors using nanocarriers. **Biomaterials,** v. 28, n. 33, p. 4947-4967, 2007. ISSN 0142-9612.

BRAT, D. J.; VAN MEIR, E. G. Glomeruloid microvascular proliferation orchestrated by VPF/VEGF. **The American journal of pathology,** v. 158, n. 3, p. 789-796, 2001. ISSN 0002-9440.

BRENNER, D.; MAK, T. W. Mitochondrial cell death effectors. **Current opinion in cell biology,** v. 21, n. 6, p. 871-877, 2009. ISSN 0955-0674.

BRUNTON, L. L.; CHABNER, B.; KNOLLMANN, B. C. **Goodman & Gilman's the pharmacological basis of therapeutics**. McGraw-Hill Medical New York, 2011.

CADIOLI, L. P.; SALLA, L. D. Nanotecnologia: um estudo sobre seu histórico, definição e principais aplicações desta inovadora tecnologia. **Revista de Ciências Exatas e Tecnologia,** v. 1, n. 1, p. 98-105, 2015. ISSN 2178-6895.

CASTEDO, M. et al. Cell death by mitotic catastrophe: a molecular definition. **Oncogene,** v. 23, n. 16, p. 2825-2837, 2004. ISSN 0950-9232.

CHAKRAVARTI, A. et al. The prognostic significance of phosphatidylinositol 3-kinase pathway activation in human gliomas. **Journal of Clinical Oncology,** v. 22, n. 10, p. 1926-1933, 2004. ISSN 0732-183X.

CHEN, T. C. et al. Soluble TNF-α receptors are constitutively shed and downregulate adhesion molecule expression in malignant gliomas. **Journal of Neuropathology & Experimental Neurology,** v. 56, n. 5, p. 541-550, 1997. ISSN 0022-3069.

CHILIN, A. et al. Exploring epidermal growth factor receptor (EGFR) inhibitor features: the role of fused dioxygenated rings on the quinazoline scaffold. **Journal of medicinal chemistry,** v. 53, n. 4, p. 1862-1866, 2010. ISSN 0022-2623.

CHRISTOFIDES, A.; KOSMOPOULOS, M.; PIPERI, C. Pathophysiological mechanisms regulated by cytokines in gliomas. **Cytokine,** v. 71, n. 2, p. 377-384, 2015. ISSN 1043-4666.

CHUNG, H. S.; EATON, W. A. Single-molecule fluorescence probes dynamics of barrier crossing. **nature,** v. 502, n. 7473, p. 685-688, 2013. ISSN 0028-0836.

DANDY, W. E. Removal of right cerebral hemisphere for certain tumors with hemiplegia: Preliminary report. **Journal of the American Medical Association,** v. 90, n. 11, p. 823-825, 1928. ISSN 0002-9955.

DAVIS, M. E. Glioblastoma: Overview of Disease and Treatment. **Clinical journal of oncology nursing,** v. 20, n. 5, p. S2, 2016. ISSN 1538-067X.

DIRKS, P. B. Cancer: stem cells and brain tumours. **nature,** v. 444, n. 7120, p. 687-688, 2006. ISSN 0028-0836.

DOLECEK, T. A. et al. CBTRUS statistical report: primary brain and central nervous system tumors diagnosed in the United States in 2005–2009. **Neuro-oncology,** v. 14, n. suppl 5, p. v1-v49, 2012. ISSN 1522-8517.

ECKLEY, M.; WARGO, K. A. A review of glioblastoma multiforme. **US Pharm,** v. 35, n. 5, p. 3-10, 2010.

ERAMO, A. et al. Chemotherapy resistance of glioblastoma stem cells. **Cell Death & Differentiation,** v. 13, n. 7, p. 1238-1241, 2006. ISSN 1350-9047.

ETRYCH, T. et al. Fluorescence optical imaging in anticancer drug delivery. **Journal of Controlled Release,** v. 226, p. 168-181, 2016. ISSN 0168-3659.

FARRELL, C. J.; PLOTKIN, S. R. Genetic causes of brain tumors: neurofibromatosis, tuberous sclerosis, von Hippel-Lindau, and other syndromes. **Neurologic clinics,** v. 25, n. 4, p. 925-946, 2007. ISSN 0733-8619.

FELDKAMP, M. M. et al. Expression of activated epidermal growth factor receptors, Ras-guanosine triphosphate, and mitogen-activated protein kinase in human glioblastoma multiforme specimens. **Neurosurgery,** v. 45, n. 6, p. 1442, 1999. ISSN 0148-396X.

FRESHNEY, R. I. **Animal cell culture: a practical approach**. IRL press Oxford:, 1986.

FULLER, G. N. et al. Molecular Classification of Human Diffuse Gliomas by Multidimensional Scaling Analysis of Gene Expression Profiles Parallels Morphology-Based Classification, Correlates with Survival, and Reveals Clinically-Relevant Novel Glioma Subsets. **Brain pathology,** v. 12, n. 1, p. 108-116, 2002. ISSN 1750-3639.

FULLER, G. N. et al. Reactivation of insulin-like growth factor binding protein 2 expression in glioblastoma multiforme a revelation by parallel gene expression profiling. **Cancer research,** v. 59, n. 17, p. 4228-4232, 1999. ISSN 0008-5472.

FURNARI, F. B. et al. Heterogeneity of epidermal growth factor receptor signalling networks in glioblastoma. **Nature reviews. Cancer,** v. 15, n. 5, p. 302, 2015.

GARLAND, M.; YIM, J. J.; BOGYO, M. A bright future for precision medicine: Advances in fluorescent chemical probe design and their clinical application. **Cell Chem Biol,** v. 23, p. 122-136, 2016.

GARRETT, T. P. et al. Crystal structure of a truncated epidermal growth factor receptor extracellular domain bound to transforming growth factor α. **Cell,** v. 110, n. 6, p. 763-773, 2002. ISSN 0092-8674.

GESBERT, F. et al. BCR/ABL regulates expression of the cyclin-dependent kinase inhibitor p27Kip1 through the phosphatidylinositol 3-Kinase/AKT pathway. **Journal of Biological Chemistry,** v. 275, n. 50, p. 39223-39230, 2000. ISSN 0021-9258.

GHOSH, M. K. et al. PI3K-AKT pathway negatively controls EGFR-dependent DNA-binding activity of Stat3 in glioblastoma multiforme cells. **Oncogene,** v. 24, n. 49, p. 7290-7300, 2005. ISSN 0950-9232.

GOLDSTEIN, D. M.; GRAY, N. S.; ZARRINKAR, P. P. High-throughput kinase profiling as a platform for drug discovery. **Nature reviews Drug discovery,** v. 7, n. 5, p. 391-397, 2008. ISSN 1474-1776.

GRIVICICH, I.; REGNER, A.; ROCHA, A. B. D. Morte celular por apoptose. **Revista brasileira de cancerologia,** v. 53, n. 3, p. 335-343, 2007.

GUHA, A. et al. Proliferation of human malignant astrocytomas is dependent on Ras activation. **Oncogene,** v. 15, n. 23, 1997. ISSN 0950-9232.

GUICCIARDI, M. E.; GORES, G. J. Life and death by death receptors. **The FASEB Journal,** v. 23, n. 6, p. 1625-1637, 2009. ISSN 0892-6638.

HAMERLIK, P. et al. Autocrine VEGF–VEGFR2–Neuropilin-1 signaling promotes glioma stem-like cell viability and tumor growth. **The Journal of experimental medicine,** v. 209, n. 3, p. 507-520, 2012. ISSN 0022-1007.

HARDEE, M. E.; ZAGZAG, D. Mechanisms of glioma-associated neovascularization. **The American journal of pathology,** v. 181, n. 4, p. 1126-1141, 2012. ISSN 0002-9440.

HATANPAA, K. J. et al. Epidermal growth factor receptor in glioma: signal transduction, neuropathology, imaging, and radioresistance. **Neoplasia,** v. 12, n. 9, p. 675-684, 2010. ISSN 1476-5586.

HEATH, J. R.; DAVIS, M. E. Nanotechnology and cancer. **Annu. Rev. Med.,** v. 59, p. 251-265, 2008. ISSN 0066-4219.

HOCK, M. B.; KRALLI, A. Transcriptional control of mitochondrial biogenesis and function. **Annual review of physiology,** v. 71, p. 177-203, 2009. ISSN 0066-4278.

HOLLAND, E. C. Glioblastoma multiforme: the terminator. **Proceedings of the National Academy of Sciences,** v. 97, n. 12, p. 6242-6244, 2000. ISSN 0027-8424.

HUI, H.; FERNANDO, M. A.; HEANEY, A. P. The α 1-adrenergic receptor antagonist doxazosin inhibits EGFR and NF-κB signalling to induce breast cancer cell apoptosis. **European Journal of Cancer,** v. 44, n. 1, p. 160-166, 2008. ISSN 0959-8049.

HUSE, J. T.; HOLLAND, E.; DEANGELIS, L. M. Glioblastoma: molecular analysis and clinical implications. **Annual review of medicine,** v. 64, p. 59-70, 2013. ISSN 0066-4219.

HUSE, J. T.; PHILLIPS, H. S.; BRENNAN, C. W. Molecular subclassification of diffuse gliomas: seeing order in the chaos. **Glia,** v. 59, n. 8, p. 1190-1199, 2011. ISSN 1098-1136.

ILLIA, G. S. **Que És La Nanotecnología**. 1st. Paidós, 2015.

INSTITUTE, N. C. Division of Cancer Control & Population Sciences. 2016. Disponível em: < https://epi.grants.cancer.gov/ >. Acesso em: 17/11/2016.

JACKSON, R. J. et al. Limitations of stereotactic biopsy in the initial management of gliomas. **Neuro-oncology,** v. 3, n. 3, p. 193-200, 2001. ISSN 1522-8517.

JAKUBOVICZ, D. E.; GRINSTEIN, S.; KLIP, A. Cell swelling following recovery from acidification in C6 glioma cells: an *in vitro* model of postischemic brain edema. **Brain research,** v. 435, n. 1-2, p. 138-146, 1987. ISSN 0006-8993.

JORDAN, C. T.; GUZMAN, M. L.; NOBLE, M. Cancer stem cells. **New England Journal of Medicine,** v. 355, n. 12, p. 1253-1261, 2006. ISSN 0028-4793.

JOSEPH, J. V. et al. Hypoxia enhances migration and invasion in glioblastoma by promoting a mesenchymal shift mediated by the HIF1α–ZEB1 axis. **Cancer letters,** v. 359, n. 1, p. 107-116, 2015. ISSN 0304-3835.

JUAN-ALBARRACÍN, J. et al. Automated glioblastoma segmentation based on a multiparametric structured unsupervised classification. **PloS one,** v. 10, n. 5, p. e0125143, 2015. ISSN 1932-6203.

KANG, C. et al. Delivery of Nanoparticles for Treatment of Brain Tumor. **Current Drug Metabolism,** v. 17, n. 8, p. 745-754, 2016. ISSN 1389-2002.

KAUR, B. et al. Hypoxia and the hypoxia-inducible-factor pathway in glioma growth and angiogenesis. **Neuro-oncology,** v. 7, n. 2, p. 134-153, 2005. ISSN 1522-8517.

KAYE, B. et al. The metabolism and kinetics of doxazosin in man, mouse, rat and dog. **British journal of clinical pharmacology,** v. 21, n. S1, p. 19S-25S, 1986. ISSN 1365-2125.

KEITH, B.; SIMON, M. C. Hypoxia-inducible factors, stem cells, and cancer. **Cell,** v. 129, n. 3, p. 465-472, 2007. ISSN 0092-8674.

KIEBISH, M. A. et al. Brain mitochondrial lipid abnormalities in mice susceptible to spontaneous gliomas. **Lipids,** v. 43, n. 10, p. 951-959, 2008. ISSN 0024-4201.

KNIZETOVA, P. et al. Autocrine regulation of glioblastoma cell-cycle progression, viability and radioresistance through the VEGF-VEGFR2 (KDR) interplay. **Cell cycle,** v. 7, n. 16, p. 2553-2561, 2008. ISSN 1538-4101.

KOFF, J. L.; RAMACHANDIRAN, S.; BERNAL-MIZRACHI, L. A time to kill: targeting apoptosis in cancer. **International journal of molecular sciences,** v. 16, n. 2, p. 2942-2955, 2015.

KRAKSTAD, C.; CHEKENYA, M. Survival signalling and apoptosis resistance in glioblastomas: opportunities for targeted therapeutics. **Molecular cancer,** v. 9, n. 1, p. 1, 2010. ISSN 1476-4598.

LAMMERING, G. et al. Epidermal growth factor receptor as a genetic therapy target for carcinoma cell radiosensitization. **Journal of the National Cancer Institute,** v. 93, n. 12, p. 921-929, 2001. ISSN 0027-8874.

LEMASTERS, J. J. et al. The mitochondrial permeability transition in toxic, hypoxic and reperfusion injury. In: (Ed.). **Detection of Mitochondrial Diseases**: Springer, 1997. p.159-165.

LEMASTERS, J. J. et al. Mitochondrial dysfunction in the pathogenesis of necrotic and apoptotic cell death. **Journal of bioenergetics and biomembranes,** v. 31, n. 4, p. 305-319, 1999. ISSN 0145-479X.

LIAO, C. H. et al. Anti-angiogenic effects and mechanism of prazosin. **The Prostate,** v. 71, n. 9, p. 976-984, 2011. ISSN 1097-0045.

LIMA, F. R. et al. Glioblastoma: therapeutic challenges, what lies ahead. **Biochimica et Biophysica Acta (BBA)-Reviews on Cancer,** v. 1826, n. 2, p. 338-349, 2012. ISSN 0304-419X.

LOUIS, D. N. et al. The 2016 World Health Organization Classification of Tumors of the Central Nervous System: a summary. **Acta Neuropathol**, v. 131, p. 803-820, 2016.

MACKENZIE, D. A classification of the tumours of the glioma group on a histogenetic basis with a correlated study of prognosis. **Canadian Medical Association journal,** v. 16, n. 7, p. 872, 1926.

MAHER, E. A. et al. Malignant glioma: genetics and biology of a grave matter. **Genes & development,** v. 15, n. 11, p. 1311-1333, 2001. ISSN 0890-9369.

MALUMBRES, M.; BARBACID, M. RAS oncogenes: the first 30 years. **Nature reviews cancer,** v. 3, n. 6, p. 459-465, 2003. ISSN 1474-175X.

MCLENDON, R. et al. Comprehensive genomic characterization defines human glioblastoma genes and core pathways. Nature, v. 455, n. 7216, p. 1061-1068, 2008. ISSN 0028-0836.

MICHALAKI, V. et al. Serum levels of IL-6 and TNF-α correlate with clinicopathological features and patient survival in patients with prostate cancer. **British journal of cancer,** v. 90, n. 12, p. 2312-2316, 2004. ISSN 0007-0920.

MOODIE, S. A. et al. Complexes of Ras-GTF with Raf-1 and mitogen-activated protein kinase kinase. **Science,** v. 260, n. 5114, p. 1658-1662, 1993. ISSN 0036-8075.

NELSON, D. L.; COX, M. M. **Lehninger Principles of Biochemistry**. 6th. W. H. Freeman, 2012.

OGISO, H. et al. Crystal structure of the complex of human epidermal growth factor and receptor extracellular domains. **Cell,** v. 110, n. 6, p. 775-787, 2002. ISSN 0092-8674.

OKADA, H.; MAK, T. W. Pathways of apoptotic and non-apoptotic death in tumour cells. **Nature reviews cancer,** v. 4, n. 8, p. 592-603, 2004. ISSN 1474-175X.

OLIVEIRA, A. N. D. **Determinação da toxicidade *in vitro* e *in vivo* de compostos quinazolínicos e identificação do ácido homovanílico por espectrometria de ressonância magnética nuclear de hidrogênio (^{1}H)**. 2009. Dissertação de Mestrado Unicamp

ORDYS, B. B. et al. The role of mitochondria in glioma pathophysiology. **Molecular neurobiology,** v. 42, n. 1, p. 64-75, 2010. ISSN 0893-7648.

OSTROM, Q. T. et al. CBTRUS statistical report: Primary brain and central nervous system tumors diagnosed in the United States in 2008-2012. **Neuro-oncology,** v. 17, n. suppl 4, p. iv1-iv62, 2015. ISSN 1522-8517.

PARSONS, D. W. et al. An integrated genomic analysis of human glioblastoma multiforme. **Science,** v. 321, n. 5897, p. 1807-1812, 2008. ISSN 0036-8075.

PERSANO, L. et al. Glioblastoma cancer stem cells: role of the microenvironment and therapeutic targeting. **Biochemical pharmacology,** v. 85, n. 5, p. 612-622, 2013. ISSN 0006-2952.

PERSANO, L. et al . The three-layer concentric model of glioblastoma: cancer stem cells, microenvironmental regulation, and therapeutic implications. **The Scientific World Journal,** v. 11, p. 1829-1841, 2011.

PETTY, A. et al. A small molecule agonist of EphA2 receptor tyrosine kinase inhibits tumor cell migration in vitro and prostate cancer metastasis *in vivo*. **PloS one,** v. 7, n. 8, p. e42120, 2012. ISSN 1932-6203.

PFITZENMAIER, J. et al. Elevation of cytokine levels in cachectic patients with prostate carcinoma. **Cancer,** v. 97, n. 5, p. 1211-1216, 2003. ISSN 1097-0142.

PLOTKIN, S. R.; WEN, P. Y. Neurologic complications of cancer therapy. **Neurologic clinics,** v. 21, n. 1, p. 279-318, 2003. ISSN 0733-8619.

RASHEED, B. A. et al. Molecular pathogenesis of malignant gliomas. **Current opinion in oncology,** v. 11, n. 3, p. 162, 1999. ISSN 1040-8746.

RIEMENSCHNEIDER, M. J. et al. Molecular diagnostics of gliomas: state of the art. **Acta neuropathologica,** v. 120, n. 5, p. 567-584, 2010. ISSN 0001-6322.

ROY, S. et al. Recurrent Glioblastoma: Where we stand. **South Asian journal of cancer,** v. 4, n. 4, p. 163, 2015.

SALLINEN, S.-L. et al. Identification of differentially expressed genes in human gliomas by DNA microarray and tissue chip techniques. **Cancer research,** v. 60, n. 23, p. 6617-6622, 2000. ISSN 0008-5472.

SANAI, N.; BERGER, M. S. Glioma extent of resection and its impact on patient outcome. **Neurosurgery,** v. 62, n. 4, p. 753-766, 2008. ISSN 0148-396X.

SANAI, N.; MIRZADEH, Z.; BERGER, M. S. Functional outcome after language mapping for glioma resection. **New England Journal of Medicine,** v. 358, n. 1, p. 18-27, 2008. ISSN 0028-4793.

SCARPULLA, R. C. Transcriptional paradigms in mammalian mitochondrial biogenesis and function. **Physiological reviews,** v. 88, n. 2, p. 611-638, 2008. ISSN 0031-9333.

SCHLAME, M.; RUA, D.; GREENBERG, M. L. The biosynthesis and functional role of cardiolipin. **Progress in lipid research,** v. 39, n. 3, p. 257-288, 2000. ISSN 0163-7827.

SCOTT, J. et al. Long-term glioblastoma multiforme survivors: a population-based study. **Canadian Journal of Neurological Sciences/Journal Canadien des Sciences Neurologiques,** v. 25, n. 03, p. 197-201, 1998. ISSN 2057-0155.

SHAI, R. et al. Gene expression profiling identifies molecular subtypes of gliomas. **Oncogene,** v. 22, n. 31, p. 4918-4923, 2003. ISSN 0950-9232.

SINGH, S. K. et al. Identification of a cancer stem cell in human brain tumors. **Cancer research,** v. 63, n. 18, p. 5821-5828, 2003. ISSN 0008-5472.

SINHA, R. et al. Nanotechnology in cancer therapeutics: bioconjugated nanoparticles for drug delivery. **Molecular cancer therapeutics,** v. 5, n. 8, p. 1909-1917, 2006. ISSN 1535-7163.

SMALLEY, M.; ASHWORTH, A. Stem cells and breast cancer: a field in transit. **Nature reviews cancer,** v. 3, n. 11, p. 832-844, 2003. ISSN 1474-175X.

SOEDA, A. et al. Hypoxia promotes expansion of the CD133-positive glioma stem cells through activation of HIF-1α. **Oncogene,** v. 28, n. 45, p. 3949-3959, 2009. ISSN 0950-9232.

SÖZERI, O. et al. Activation of the c-Raf protein kinase by protein kinase C phosphorylation. **Oncogene,** v. 7, n. 11, p. 2259-2262, 1992. ISSN 0950-9232.

STILES, C. D.; ROWITCH, D. H. Glioma stem cells: a midterm exam. **Neuron,** v. 58, n. 6, p. 832-846, 2008. ISSN 0896-6273.

STUPP, R. et al. Radiotherapy plus concomitant and adjuvant temozolomide for glioblastoma. **New England Journal of Medicine,** v. 352, n. 10, p. 987-996, 2005. ISSN 0028-4793.

STURGILL, T. W. et al. Insulin-stimulated MAP-2 kinase phosphorylates and activates ribosomal protein S6 kinase II. 1988.

TAKANO, T. et al. Glutamate release promotes growth of malignant gliomas. **Nature medicine,** v. 7, n. 9, p. 1010-1015, 2001.

TANWAR, M. K.; GILBERT, M. R.; HOLLAND, E. C. Gene expression microarray analysis reveals YKL-40 to be a potential serum marker for malignant character in human glioma. **Cancer research,** v. 62, n. 15, p. 4364-4368, 2002. ISSN 0008-5472.

TEBBUTT, N.; PEDERSEN, M. W.; JOHNS, T. G. Targeting the ERBB family in cancer: couples therapy. **Nature reviews cancer,** v. 13, n. 9, p. 663-673, 2013. ISSN 1474-175X.

THAKKAR, J. P. et al. Epidemiologic and molecular prognostic review of glioblastoma. **Cancer Epidemiology Biomarkers & Prevention,** v. 23, n. 10, p. 1985-1996, 2014. ISSN 1055-9965.

VALEUR, B.; BERBERAN-SANTOS, M. N. **Molecular fluorescence: principles and applications**. John Wiley & Sons, 2012. ISBN 3527328378.

VAN MEIR, E. G. et al. Exciting new advances in neuro-oncology: the avenue to a cure for malignant glioma. **CA: a cancer journal for clinicians,** v. 60, n. 3, p. 166-193, 2010. ISSN 1542-4863.

VELLINGA, T. T. et al. SIRT1/PGC1α-dependent increase in oxidative phosphorylation supports chemotherapy resistance of colon cancer. **Clinical cancer research,** v. 21, n. 12, p. 2870-2879, 2015. ISSN 1078-0432.

VENTURA-CLAPIER, R.; GARNIER, A.; VEKSLER, V. Transcriptional control of mitochondrial biogenesis: the central role of PGC-1α. **Cardiovascular research,** v. 79, n. 2, p. 208-217, 2008. ISSN 0008-6363.

VISVADER, J. E.; LINDEMAN, G. J. Cancer stem cells in solid tumours: accumulating evidence and unresolved questions. **Nature reviews cancer,** v. 8, n. 10, p. 755-768, 2008. ISSN 1474-175X.

VOGELBAUM, M. A. et al. Overexpression of bax in human glioma cell lines. **Journal of neurosurgery,** v. 91, n. 3, p. 483-489, 1999. ISSN 0022-3085.

WECHSLER-REYA, R.; SCOTT, M. P. The developmental biology of brain tumors. **Annual review of neuroscience,** v. 24, n. 1, p. 385-428, 2001. ISSN 0147-006X.

WEINSTEIN, J. N. et al. The cancer genome atlas pan-cancer analysis project. **Nature genetics,** v. 45, n. 10, p. 1113-1120, 2013. ISSN 1061-4036.

WICK, A. et al. Bevacizumab does not increase the risk of remote relapse in malignant glioma. **Annals of neurology,** v. 69, n. 3, p. 586-592, 2011. ISSN 1531-8249.

WICK, W. et al. Pathway inhibition: emerging molecular targets for treating glioblastoma. **Neuro-oncology,** v. 13, n. 6, p. 566-579, 2011. ISSN 1522-8517.

WIRSCHING, H.-G.; WELLER, M. The Role of Molecular Diagnostics in the Management of Patients with Gliomas. **Current treatment options in oncology,** v. 17, n. 10, p. 51, 2016. ISSN 1527-2729.

WONG, A. J. et al. Increased expression of the epidermal growth factor receptor gene in malignant gliomas is invariably associated with gene amplification. **Proceedings of the National Academy of Sciences,** v. 84, n. 19, p. 6899-6903, 1987. ISSN 0027-8424.

WONG, A. J. et al. Structural alterations of the epidermal growth factor receptor gene in human gliomas. **Proceedings of the National Academy of Sciences,** v. 89, n. 7, p. 2965-2969, 1992. ISSN 0027-8424.

WYKRETOWICZ, A.; GUZIK, P.; WYSOCKI, H. Doxazosin in the current treatment of hypertension. **Expert opinion on pharmacotherapy,** v. 9, n. 4, p. 625-633, 2008. ISSN 1465-6566.

YADAVA PHD, N. Oxidative phosphorylation-dependent regulation of cancer cell apoptosis in response to anticancer agents. 2015.

YEWALE, C. et al. Epidermal growth factor receptor targeting in cancer: a review of trends and strategies. **Biomaterials,** v. 34, n. 34, p. 8690-8707, 2013. ISSN 0142-9612.

YOSHIDA, N. et al. Interleukin-6, tumour necrosis factor α and interleukin-1β in patients with renal cell carcinoma. **British journal of cancer,** v. 86, n. 9, p. 1396-1400, 2002. ISSN 0007-0920.

ZEPPERNICK, F. et al. Stem cell marker CD133 affects clinical outcome in glioma patients. **Clinical cancer research,** v. 14, n. 1, p. 123-129, 2008. ISSN 1078-0432.

13. ANEXO I

Lista de Figuras

Figura 1. Classificação histológica dos tumores primários do SNC.

Figura 2. Algoritmo de classificação de gliomas difusos de acordo com características histológicas e moleculares.

Figura 3. Estrutura química da doxazosina [4-4-amino-6,7-dimetoxiquinazolina-2-il)-piperazina]1-il-(2,3-diidro-1,4-benzodioxina-3-il).

Figura 4. Características do microambiente hipóxico em glioblastoma.

Figura 5. Alterações no DNA e as mudanças no número de cópias nas vias de sinalização: (a) receptor tirosina-quinase (RTK), RAS, e fosfoinositol-3-quinase (PI3K), (b) supressor de tumoral p53, e (c) supressor de tumores retinoblastoma (Rb).

Figura 6. Estrutura química da doxazosina [4-4-amino-6,7-dimetoxiquinazolina-2-il)-piperazina]1-il-(2,3-diidro-1,4-benzodioxina-3-il).

Figura 7. Desenho esquemático da composição de uma nanocápsula com mesilato de doxazosina.

Figura 8: Representação esquemática dos efeitos da doxazosina em células de glioma.

Tabela 1. Classificação dos gliomas segundo os graus de malignidade.

Tabela 2. Principais características de glioblastomas IDH-selvagem e IDH-mutado.

1. ANEXO II

Normas de formatação de artigos da revista Oncotarget

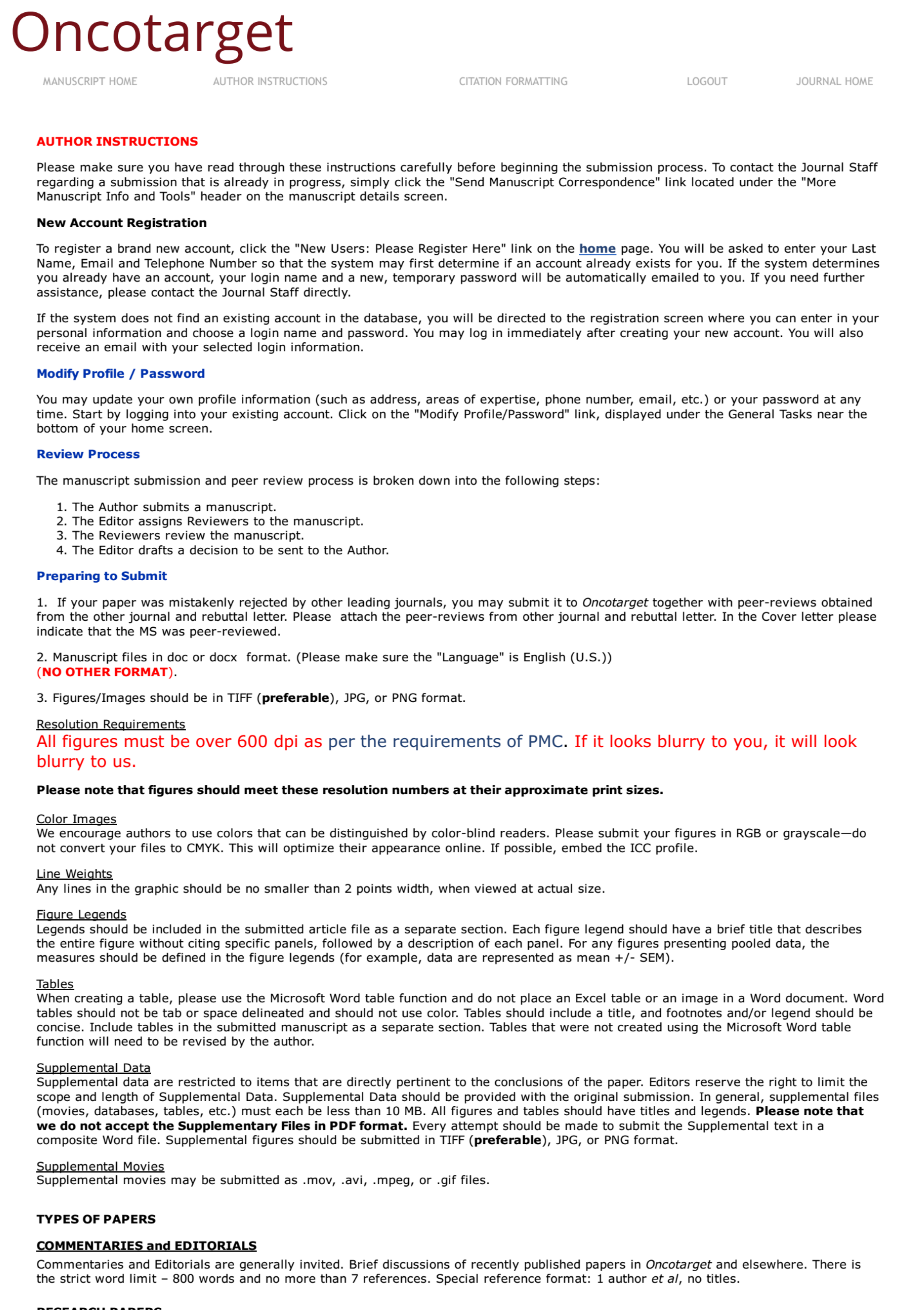

Oncotarget

MANUSCRIPT HOME AUTHOR INSTRUCTIONS CITATION FORMATTING LOGOUT JOURNAL HOME

AUTHOR INSTRUCTIONS

Please make sure you have read through these instructions carefully before beginning the submission process. To contact the Journal Staff regarding a submission that is already in progress, simply click the "Send Manuscript Correspondence" link located under the "More Manuscript Info and Tools" header on the manuscript details screen.

New Account Registration

To register a brand new account, click the "New Users: Please Register Here" link on the **home** page. You will be asked to enter your Last Name, Email and Telephone Number so that the system may first determine if an account already exists for you. If the system determines you already have an account, your login name and a new, temporary password will be automatically emailed to you. If you need further assistance, please contact the Journal Staff directly.

If the system does not find an existing account in the database, you will be directed to the registration screen where you can enter in your personal information and choose a login name and password. You may log in immediately after creating your new account. You will also receive an email with your selected login information.

Modify Profile / Password

You may update your own profile information (such as address, areas of expertise, phone number, email, etc.) or your password at any time. Start by logging into your existing account. Click on the "Modify Profile/Password" link, displayed under the General Tasks near the bottom of your home screen.

Review Process

The manuscript submission and peer review process is broken down into the following steps:

1. The Author submits a manuscript.
2. The Editor assigns Reviewers to the manuscript.
3. The Reviewers review the manuscript.
4. The Editor drafts a decision to be sent to the Author.

Preparing to Submit

1. If your paper was mistakenly rejected by other leading journals, you may submit it to *Oncotarget* together with peer-reviews obtained from the other journal and rebuttal letter. Please attach the peer-reviews from other journal and rebuttal letter. In the Cover letter please indicate that the MS was peer-reviewed.

2. Manuscript files in doc or docx format. (Please make sure the "Language" is English (U.S.))
(**NO OTHER FORMAT**).

3. Figures/Images should be in TIFF (**preferable**), JPG, or PNG format.

Resolution Requirements
All figures must be over 600 dpi as per the requirements of PMC. If it looks blurry to you, it will look blurry to us.

Please note that figures should meet these resolution numbers at their approximate print sizes.

Color Images
We encourage authors to use colors that can be distinguished by color-blind readers. Please submit your figures in RGB or grayscale—do not convert your files to CMYK. This will optimize their appearance online. If possible, embed the ICC profile.

Line Weights
Any lines in the graphic should be no smaller than 2 points width, when viewed at actual size.

Figure Legends
Legends should be included in the submitted article file as a separate section. Each figure legend should have a brief title that describes the entire figure without citing specific panels, followed by a description of each panel. For any figures presenting pooled data, the measures should be defined in the figure legends (for example, data are represented as mean +/- SEM).

Tables
When creating a table, please use the Microsoft Word table function and do not place an Excel table or an image in a Word document. Word tables should not be tab or space delineated and should not use color. Tables should include a title, and footnotes and/or legend should be concise. Include tables in the submitted manuscript as a separate section. Tables that were not created using the Microsoft Word table function will need to be revised by the author.

Supplemental Data
Supplemental data are restricted to items that are directly pertinent to the conclusions of the paper. Editors reserve the right to limit the scope and length of Supplemental Data. Supplemental Data should be provided with the original submission. In general, supplemental files (movies, databases, tables, etc.) must each be less than 10 MB. All figures and tables should have titles and legends. **Please note that we do not accept the Supplementary Files in PDF format.** Every attempt should be made to submit the Supplemental text in a composite Word file. Supplemental figures should be submitted in TIFF (**preferable**), JPG, or PNG format.

Supplemental Movies
Supplemental movies may be submitted as .mov, .avi, .mpeg, or .gif files.

TYPES OF PAPERS

COMMENTARIES and EDITORIALS

Commentaries and Editorials are generally invited. Brief discussions of recently published papers in *Oncotarget* and elsewhere. There is the strict word limit – 800 words and no more than 7 references. Special reference format: 1 author *et al*, no titles.

RESEARCH PAPERS

There is no a word limit for any section of the paper, except an abstract (not more than 200 words); no reference limit. Any number of pages and references. Up to 14 figures.

Research papers should contain the following sections in this order: Title, Authors, Affiliations, Contact Information, Keywords (5), Abstract, Introduction, Results, Discussion, Methods or Materials and Methods, Abbreviations, Author Contributions, Acknowledgments, Conflicts of Interest, Funding, References

Please do not provide a running title or the amount of words.

RESEARCH PERSPECTIVES

Topical discussions of recent scientific advances. May contain clarifications, new interpretations. May include both published and unpublished original data to clarify the point. Any number of figures. Must include abstract and keywords. Should be well referenced, with a minimal number of references above 70. There is no upper limit on the number of references.

REVIEWS

Authors may suggest a Review on a broad topic of general interest. Should be well referenced, with a minimal number of references above 90. Reviews should include 1-6 figures, diagrams or cartoons.

MEETING REPORTS

Reports of conferences and symposia in cancer research and related fields of study. Reports should ideally be submitted within 3 months of the meeting.

REFERENCES

See Citation Formatting. Authors are strongly encouraged to use an automated reference manager such as Thomson Reuters EndNote, Zotero, or Mendeley. Follow the links to download output styles for Oncotarget.

PUBLICATION FEES

To provide open access, *Oncotarget* uses a business model in which expenses — including those of peer review, journal production, and online hosting and archiving — are recovered by charging a journal-specific publication fee to the authors or research sponsors for each article they publish.

Updated on 01/20/2017: A **publication fee** of **$3,400 (USD)** applies to Research Papers (in any specialty), Reviews, and Case Reports. A reduced fee of $1900 (USD) applies to Research Perspectives. There are no additional charges based on color, length, figures, or other elements.

Discretionary **Discounts** may be available on a case-by-case basis, see below for further information.

For papers submitted before **February 5, 2017,** the publication fee is $2,850 (USD).

In comparison: *Nature Communications* fees $5,200, *Cell Reports fees* $5,000

There is no fee for Editorials, invited Research Perspectives, and News.

Oncotarget provides various fee support programs.

We offer publication fees discounts for papers whose corresponding authors are based in HINARI countries (the world's lowest income countries as defined by the World Bank).

Discretionary discounts will be considered on a case-by-case basis, and may be granted in cases of financial need. All applications for discretionary discounts should be made prior to, or at the point of manuscript submission; requests made after acceptance or during the review process will not be considered. Authors supported by the Libraries' Fund for Open Access Journals will receive a partial discount.

To request a discount please contact us at payment@oncotarget.com. Please do not include requests for financial support in cover letters.

Before submitting a manuscript, please gather the following information:

- All Authors
  - First and Last Names
  - Postal Addresses
  - Work Telephone Numbers (for Corresponding Author only)
  - E-mail addresses
- Title (you can copy and paste this from your manuscript)
- Abstract (you can copy and paste this from your manuscript)
- Manuscript files in Word (Please make sure the "Language" is "English (U.S.)" via Tools->Language->Set Language) or WordPerfect format.
- Cover Letter, including job title and institution for EVERY Author listed on the manuscript

Submission Process

The four steps of the submission process are: Files, Manuscript Information, Validate, and Submit. The four steps each contain sub-steps that can be accessed by clicking on their respective tabs. Navigating through this "Tab View" will save any entered information each time a new tab is clicked (or the boxes "Save and Continue" and "Next" are clicked). Each step and sub-step is listed below:

1. **Files**
   - **Upload Files**
     A screen asking for the actual file locations (via an open file dialog) will appear. After completing this screen, your files will be sent to be converted to PDF for the peer review process.
   - **Remove Files**
     Allows the user to remove previously uploaded files.
   - **Replace Files**
     Allows the user to replace any previously submitted files with another file.
   - **File Type**
     This tab prompts the user to choose the "file type" that corresponds to the upload document. Though the file types can vary from journal to journal, the five basic types of files are, Author Cover Letter, Article File, Figure, Table, Supplemental Material.
   - **File Description**
     When uploading a file type labeled "Figure", "Table", or "Supplemental Material" it is required to give a brief description of the content that is included in the file.
   - **File Order**

This tab allows to user to rearrange files to be displayed at the author's discretion. This tab also gives the option to merge PDF files into a single PDF file to display to the Editor and Reviewers. Upon completion the user must check the checkbox indicating completion of the ordering and selection process.

2. **Manuscript Information**
   - **Title, Abstract**
     It is required for the user to provide a Title for the manuscript as well as an Abstract. The Title and Abstract all have word or character limits.
   - **Authors**
     This tab prompts the user to submit General Information about the author. The fields marked with an asterisk (*) are required, and need to be completed to continue the submission process.
   - **Keywords & Subject Areas**
     A screen where the author provides at subject areas of the manuscript from the list provided. If needed, the author can provide keywords for the manuscript by typing it in any boxes that might be provided.
   - **Detailed Information**
     This screen asks for more detailed information regarding the manuscript. Though the questions in this tab may vary from journal to journal, typical questions include "Conflict of Interest" and "Dual Publication".
   - **Author Review Suggestions**
     This screen allows the user to provide "suggested reviewers" to include for the revision process. The author can also provide reviewers to exclude from the revision process.

3. **Validate**
   - **Approve Files**
     The screen allows the user to verify that the manuscript has been uploaded and converted to the PDF format correctly.
   - **Approve Manuscript**
     This screen provides the user with all the information gathered from the submission process. It will provide a summary of all of the data entered so far, with the option to change any of those items.

4. **Submit**
   This screen is the final step of the submission process. The system will check to make sure everything is completed before the manuscript is submitted. If the manuscript is ready for submission, then there will be text that reads: "Your manuscript is ready to be submitted. Click the link below to finalize your submission." Otherwise, it will ask that you modify your submission to fulfill all of the submission requirements.

Submitting Revisions

If you have been asked to revise your manuscript and you are ready to resubmit it, log on to the submission system and, on your author home page, click the "Revise Manuscript" link of the manuscript you wish to resubmit. You will be asked to review the information you originally submitted to confirm its accuracy. If any of the original files have been revised, replace them. Include only the final version of each file in your revision submission.

In your rebuttal letter, please be sure to provide a point-by-point reply to the reviewers' comments as well as a listing of all the changes made, including any changes to authorship, noting the page numbers on which the individual changes appear. When you have successfully resubmitted your manuscript, you will receive acknowledgment via email. The revised version of your manuscript may undergo another review if the original submission required extensive changes or if the authors' responses to the criticisms entail rebuttal rather than revision. A decision as to whether or not the manuscript will be sent back out for review is made at the discretion of the Editors.

Getting Help

- **Context-Sensitive Help**
  If you need additional help, you can click on the help signs spread throughout the system. A help dialog will pop up with context-sensitive help.
- **Contact Journal Staff**
  You may contact the Journal Staff at any time by clicking the "Send Manuscript Correspondence" link under the "More Manuscript Info and Tools" header on the manuscript details screen.
- **Login Help**
  If you have forgotten or do not know your login name or password, simply click the "Unknown/Forgotten Password" link on the home page. You will be asked to enter either your Login Name or your First and Last Name. If a single account can be found in the database, the system will automatically and instantly send you an email with your login name and a new, temporary password. If a single account cannot be identified from the information provided, you will need to contact the Journal Staff to reset your password for you.

Manuscript Status

After you approve your manuscript, the submission process is complete. You can get the status of your manuscript via:

1. Logging into the system with your password.
2. Clicking on the link represented by your manuscript tracking number and abbreviated title.
3. Clicking on the "Check Status" link at the bottom of the displayed page.

This procedure will display detailed tracking information about where your manuscript is in the submission/peer review process.

Starting

The manuscript submission process starts by pressing the "Submit Manuscript" link on your "Home" page after you have logged into the system. Please make sure you have gathered all the required manuscript information listed above **BEFORE** starting the submission process.

Please press HOME to continue.

MANUSCRIPT HOME HELP FOR AUTHORS CITATION FORMATTING REVIEWER INSTRUCTIONS LOGOUT

Licensed under Patent #US 7,620,555B1